

# **Investigation of bacterial hydrogenase functions using an operon deletion technology in *Escherichia coli***

**A thesis submitted in fulfilment of the requirements for the degree of**

**Doctor of Philosophy in Engineering**

By

**Chandra Shekhar**

**Supervisor: Prof. Dr. Toshinari Maeda**



**March 2021**

**Kyushu Institute of Technology**

**Graduate School of Life Science and Systems Engineering**

**Department of Biological Functions Engineering**



## ABSTRACT

Hydrogen metabolism is among the most ancient and widespread metabolic trait of microbial life. *Escherichia coli* (*E. coli*) is one of the most studied microorganisms for hydrogen metabolism as well as other metabolic phenomena. The four hydrogenase isozymes, hydrogenase 1 (Hyd-1), hydrogenase 2 (Hyd-2), hydrogenase 3 (Hyd-3), and hydrogenase 4 (Hyd-4), play key roles in hydrogen metabolism by catalyzing the reversible reaction of hydrogen to protons and electrons ( $2\text{H}^+ + 2\text{e}^- \rightleftharpoons \text{H}_2(\text{g})$ ). A comparison of the identity between large hydrogenase subunits indicates that either Hyd-1 and Hyd-2 or Hyd-3 and Hyd-4 have a similar homology that was supposed to be a potent reason for inconsistent reports regarding the functions of hydrogenases. Hydrogenases are important integral membrane proteins; therefore, they directly influence microbial membrane physiology. Apart from hydrogen metabolism, hydrogenases were hypothesized to have an essential role in other metabolic activities related to survival in the stressed condition.

Hence, the purpose of my Ph. D. study is to investigate the absolute as well as other parallel roles of hydrogenases in hydrogen and associated metabolisms of *E. coli*. Two types of hydrogenase operon mutants were mainly constructed and employed in the study: (1) operon mutants devoid of only one hydrogenase operon and containing other three in the genome and (2) operon mutants devoid of three hydrogenase operons and possessing solely one hydrogenase operon in the genome. During the study, all single genes encoding large subunit gene deletion mutants along with a quadruple operon mutant devoid of all four hydrogenase operons were employed for their comparative analysis.

Using single operon deleted mutants, along with the hydrogen production and uptake activities, hydrogenases were found to have crucial roles in growth, glucose metabolism, energy, redox balance, and pH homeostasis of the cell. The two hydrogenases, Hyd-2 and Hyd-3 were specifically confirmed to possess solely hydrogen productive capabilities, whereas all

four have uptake activity. The four single hydrogenase operon mutants were further employed to investigate their roles in persistence and acid resistance mechanisms under oxygen-deprived (micro-aerobic) states along with anaerobic conditions. All the hydrogenases were identified as having remarkable regulating functions in cellular viabilities. However, the roles of energy (ATP) and metabolism (NADH) were found crucial in hydrogenase-mediated cell survival and glucose metabolic phenomenon. Moreover, persistence and acid resistance studies demonstrated the ROS-scavenging and intracellular pH homeostasis activities, respectively, of hydrogenases. Hydrogenases are pivotal in the maintenance of proton gradient across the membrane and quinone pool, therefore, in  $\text{NAD}^+$  reduction activity and ATP synthesis, hydrogenases are found to play significant roles in the cell. Global transcriptomic analysis demonstrated possible regulating roles of the hydrogenases in diverse and critical metabolic activities. The comprehensive genomic connectivity of the hydrogenases further indicates their roles in bacterial healthy metabolism and survival.

Apart from the work with hydrogenases, hydrogen metabolism was further investigated by the random genomic deletion approach, where we designed a new genetic engineering approach by which genomic insertion-deletions can be performed randomly and easily using NNN-extension primer-based PCR products. The approach not only showed efficient and accurate but also successfully demonstrates causing multiple deletions at the same time in the bacterial genome. The study demonstrated that hydrogen metabolism in the bacteria is not an essential metabolic activity since growth and productivity were not affected in random and multiple genomic deletion clones.

Taken together, all the findings of this study contribute to understanding microbial hydrogen metabolism and its various roles in bacterial physiology, survival, and adaptation to adverse environmental conditions.

## CONTENTS

Content	Page
Front page	1
Abstract	3
Table of contents	7
List of Figures	13
List of Tables	15
List of Abbreviations	17



## TABLE OF CONTENTS

ABSTRACT.....	3
CONTENTS.....	5
LIST OF FIGURES .....	13
LIST OF TABLES .....	15
LIST OF ABBREVIATIONS.....	17
CHAPTER 1 .....	19
INTRODUCTION AND LITERATURE REVIEW .....	19
1.1. Escherichia coli and Hydrogen metabolism.....	19
1.2. Hydrogen metabolism: Glucose and Glycerol Metabolic Pathways.....	19
1.3. Hydrogenases: Mechanism of Functioning of Hydrogenases.....	21
1.4. The Parallel Roles of Hydrogenases .....	23
1.4.1 Persistence against antibiotics .....	23
1.4.2. Resistance against acid .....	24
1.5. Research outline and Objectives .....	26
1.5.1. Outline.....	26
1.5.2. Objectives .....	28
CHAPTER 2 .....	29
INVESTIGATION OF THE GLUCOSE METABOLISM BY THE DELETION OF THE OPERONS OF HYDROGENASE IN ESCHERICHIA COLI .....	29
2.1. Introduction .....	29
2.2. Materials and Methods .....	33
2.2.1. Bacterial strains, media, and growth conditions.....	33
2.2.2. E. coli hydrogenase operon mutants.....	35
2.2.3. Mutant verification of each hydrogenase operon and large subunit gene mutant ..	37
2.2.4. Specific growth rates and pH measurement .....	41
2.2.5. Fermentation and hydrogen assessment .....	42
2.2.6. Fermentation assays with formate and pyruvate .....	42
2.2.7. Glucose assay .....	42
2.2.8. ATP assay .....	43
2.2.9. NADH assay .....	43
2.2.10. Total RNA extraction and quantitative reverse transcription-PCR (qRT-PCR) ..	44
2.2.11. DNA library preparation and high-throughput sequencing.....	45
2.2.12. RNA Seq data analysis .....	45

2.2.13. Statistical analysis.....	46
2.3. Results .....	46
2.3.1. Hydrogen productivity by the hydrogenase operon mutants.....	46
2.3.2. Growths and change in pH in the cultures of hydrogenase operon mutants .....	48
2.3.4. Glucose consumption by hydrogenase operon mutants .....	50
2.3.5. Total intracellular ATP levels in hydrogenase operon mutants .....	52
2.3.6. Intracellular NADH levels in hydrogenase operon mutants.....	53
2.3.7. Downregulation of glucose metabolism-associated genes .....	55
2.3.8. Transcriptomic analysis of hydrogenase operon mutants.....	57
2.4. Discussion .....	58
2.5. Conclusion.....	63
CHAPTER 3 .....	65
INVESTIGATION OF THE ABSOLUTE ROLE OF EACH HYDROGENASE OPERON IN HYDROGEN METABOLISM BY CONSTRUCTING THE ESCHERICHIA COLI STRAINS POSSESSING ONLY A SINGLE HYDROGENASE OPERON IN THE GENOME .....	65
3.1. Introduction .....	65
3.2. Materials and Methods .....	69
3.2.1. Bacterial strains, media, and growth conditions.....	69
3.2.2. Making hydrogenase operons-deletion mutants .....	73
3.2.3. Verification of hydrogenase operon deletion .....	74
3.2.4. Fermentation and hydrogen assessment .....	77
3.2.5. Hydrogen production and growth rates estimation of single-gene and operon- deletion mutants of hydrogenases.....	78
3.2.6. Construction of pBR322/hybOABCDEFGF and pBR322/hycABCDEFGFHI and hydrogen productivity complementation assay .....	78
3.2.7. Hydrogen uptake assays .....	80
3.2.8. pH-vibration fermentation: Hydrogen assessment at low alkaline pH under glucose metabolism.....	81
3.3. Results .....	81
3.3.1. The ideal multiple hydrogenase operon-deletion mutants.....	81
3.3.2. A comparative functional evaluation of single-gene and operon-deletion mutants of hydrogenases (Hydrogen productivity and specific growth rates) .....	82
3.3.3. The absolute role of hydrogenases in hydrogen production.....	84
3.3.4. Effects of multiple hydrogenase operon deletions on bacterial growth .....	85

3.3.5. pH-vibration fermentation: Hydrogen production by Hyd-2 .....	86
3.3.6. Complementation of hydrogen productivity from hyb and hyc operons.....	87
3.3.7. All the hydrogenases are solely able to have hydrogen uptake activity .....	88
3.4. Discussion .....	89
3.5. Conclusion.....	94
CHAPTER 4 .....	95
INVESTIGATION OF THE ROLE OF HYDROGENASES IN THE PERSISTENCE OF ESCHERICHIA COLI.....	95
4.1. Introduction .....	95
4.2. Materials and Methods .....	97
4.2.1. Bacterial strains, media, and growth conditions.....	97
4.2.2. Persister assay.....	99
4.2.3. Dissolved-Oxygen Measurements .....	99
4.2.4. Total RNA extraction and quantitative reverse transcription PCR (qRT-PCR).....	99
4.2.5. Reactive oxygen species assay .....	100
4.2.6. DNA library preparation and high-throughput sequencing.....	101
4.2.7. Transcriptomic (RNA Seq) data analysis .....	101
4.3. Results .....	102
4.3.1. Cultural growths and dissolved oxygen concentrations .....	102
4.3.2. Cellular viabilities in persistence.....	104
4.3.3. Hydrogenase expressions in persisters .....	106
4.3.4. Altered ROS levels in persisters .....	107
4.3.5. KEGG pathway enrichment analyses .....	109
4.3.6. Gene ontology (GO) enrichment analyses.....	110
4.4. Discussion .....	117
4.5. Conclusion.....	121
CHAPTER 5 .....	123
ELUCIDATING THE SIGNIFICANCE OF HYDROGENASES IN CELLULAR VIABILITY AND ACID RESISTANCE OF ESCHERICHIA COLI.....	123
5.1. Introduction .....	123
5.2. Materials and Methods .....	125
5.2.1. Bacterial strains and media.....	125
5.2.2. The hydrogenase operon and gadE mutants .....	126
5.2.3. Acid resistance assay .....	127

5.2.4. Total RNA extraction and quantitative reverse transcription PCR (qRT-PCR)...	127
5.2.5. DNA library preparation and high-throughput sequencing .....	127
5.2.6. RNA Seq data analysis .....	128
5.2.7 Dissolved-Oxygen measurements .....	128
5.2.8. Intracellular pH measurement .....	128
5.2.9. Statistical analysis.....	129
5.3. Results .....	129
5.3.1. Oxygen-deprived state of the mutant cultures .....	129
5.3.2. Elevated hydrogenase expressions .....	131
5.3.3. Viabilities of the hydrogenase operon mutants in acid resistance.....	132
5.3.4. The Effect of extracellular pH (pHex) on intracellular pH (pHi).....	133
5.3.5. Affected acid resistance systems in the acid-resistant cells .....	134
5.4. Discussion .....	136
5.5. Conclusion.....	140
CHAPTER 6 .....	141
INVESTIGATION OF THE HYDROGEN METABOLISM BY A NEW APPROACH OF RANDOM GENOMIC DELETIONS USING AMBIGUOUS SEQUENCES IN THE ESCHERICHIA COLI GENOME.....	141
6.1. Introduction .....	141
6.1. Materials and Methods .....	144
6.2.1. Bacterial strains, media, and growth conditions.....	144
6.2.2. Designing the primers for test gene deletion and random genomic deletion .....	145
6.2.3. Preparation of PCR product and genomic deletions.....	147
6.2.4. Evaluation of the accuracy of the primers: mutation verification .....	148
6.2.5. Evaluation of the efficiency of the primers: phenotype verification .....	149
6.2.6. Total RNA extraction and quantitative reverse transcription-PCR (qRT-PCR) ..	150
6.2.7. Phenotypic evaluations of random genomic deletion mutants: Hydrogen productivity and growth.....	150
6.3. Results .....	151
6.3.1. Determining the effective minimum length of homology extension to generate gene deletion mutants:.....	151
6.3.2. Evaluating the efficiency and accuracy of the homology extension: .....	155
6.3.3. Genomic deletions using randomly targeting primers and confirmation: .....	155
6.3.4. Estimating the number of insertions in a single genome:.....	157

6.3.5. Evaluation of the phenotype of the multiple random insertions containing mutants:	158
6.4. Discussion .....	160
6.5. Conclusion.....	164
CHAPTER 7 .....	167
CONCLUDING REMARKS AND SUGGESTIONS FOR THE FUTURE.....	167
REFERENCES .....	169
PUBLICATION AND CONFERENCE ATTENDED.....	203
Publication.....	203
Seminar and symposium presented .....	203
ACKNOWLEDGEMENT .....	205



## LIST OF FIGURES

<b>Figure 1. 1</b> The glucose and glycerol-associated hydrogen metabolic pathways. ....	20
<b>Figure 1. 2</b> The four hydrogenases of <i>E. coli</i> . ....	21
<b>Figure 1. 3</b> Illustration of the research outline and its associations to the various fields. ....	27
<b>Figure 2. 1</b> Controversies in hydrogen production with glucose and glycerol. ....	31
<b>Figure 2. 2</b> Large subunit protein sequence homology between each hydrogenase. ....	31
<b>Figure 2. 3</b> Targeted locations (indicated by arrows) of the operon for their deletions. ....	35
<b>Figure 2. 4</b> Verification of hydrogenase mutants (operon and single-gene mutants for Hyd-1, Hyd-2, Hyd-3, and Hyd-4). ....	38
<b>Figure 2. 5</b> Hydrogen production; operon deletion vs single gene deletion. ....	48
<b>Figure 2. 6</b> Rate of growth and changes of pH during the growth of the hydrogenase mutants. ....	50
<b>Figure 2. 7</b> Glucose consumption by hydrogenase operon mutants investigated by monitoring glucose concentration in the cultures of the strains at different time intervals. ....	51
<b>Figure 2. 8</b> Energy and redox balance assessment of hydrogenase operon mutants. ....	54
<b>Figure 2. 9</b> Transcriptional analysis of glucose metabolism-associated genes in <i>hyb</i> operon mutant. ....	55
<b>Figure 2. 10</b> KEGG enrichment pathway analysis to investigate the most significant metabolic pathways affected by the deletion of <i>hyb</i> operon. ....	57
<b>Figure 3. 1</b> Glucose and glycerol metabolic pathways in <i>E. coli</i> . ....	67
<b>Figure 3. 2</b> Illustration of the methodology employed for constructing multiple operon deletion mutants. ....	73
<b>Figure 3. 3</b> The PCR verification of multiple hydrogenase operon deletions. ....	75
<b>Figure 3. 4</b> The final structure of the cloning vector containing <i>hyb</i> (a) and <i>hyc</i> (b). ....	79
<b>Figure 3. 5</b> The strain quadruple operon mutant ( $\Delta hya hyb hyc hyf$ ) possessing vector (pBR322) containing cloned <i>hyb</i> and <i>hyc</i> operons. ....	80
<b>Figure 3. 6</b> Effect of single operon deletion and single-gene deletion of <i>E. coli</i> hydrogenases on hydrogen production (a) and specific growth rate (b). ....	83
<b>Figure 3. 7</b> Hydrogen production of 4 triple hydrogenase operon mutants (possessing only the single hydrogenase in the genome of <i>E. coli</i> ) from glucose (a) or glycerol (b) as a carbon source. ....	84
<b>Figure 3. 8</b> Growth curve and pH change during the hydrogen fermentation using glucose (a and c) and glycerol (b and d). ....	86
<b>Figure 3. 9</b> pH-vibration fermentation to assess hydrogen productivity. ....	87
<b>Figure 3. 10</b> Complementation of hydrogen production for the quadruple hydrogenase operon mutant ( $\Delta Hyd-1234$ ) (indicated as ‘None’) by cloning <i>hyb</i> or <i>hyc</i> operon into pBR322 cloning vector. ....	88
<b>Figure 3. 11</b> Hydrogen uptake activity of 4 triple hydrogenase operon mutants (possessing only the single hydrogenase in the genome of <i>E. coli</i> ). ....	88

<b>Figure 3. 12</b> A comparison of specific growth rates between triple operon and triple single-gene deletion mutants. ....	91
---	----

<b>Figure 4. 1</b> The growth profile of the strains and cultural dissolved oxygen concentrations (below). ....	103
<b>Figure 4. 2</b> Cell viabilities of hydrogenase operon mutants in persistence.....	105
<b>Figure 4. 3</b> Hydrogenase expressions in persisters. ....	106
<b>Figure 4. 4</b> ROS quantification in persistence. ....	109
<b>Figure 4. 5</b> Affected metabolisms in initial cells and persisters. ....	110
<b>Figure 4. 6</b> GO enrichment analysis of differentially expressed genes from initial cells and persisters of the <b>hya</b> operon mutant for biological processes (a), cellular components (b), and molecular functions (c). ....	112
<b>Figure 4. 7</b> GO enrichment analysis of differentially expressed genes from initial cells and persisters of the <b>hyb</b> operon mutant for biological processes (a), cellular components (b), and molecular functions (c). ....	113
<b>Figure 4. 8</b> GO enrichment analysis of differentially expressed genes from initial cells and persisters of the <b>hyc</b> operon mutant for biological processes (a), cellular components (b), and molecular functions (c). ....	115
<b>Figure 4. 9</b> GO enrichment analysis of differentially expressed genes from initial cells and persisters of the <b>hyf</b> operon mutant for biological processes (a), cellular components (b), and molecular functions (c). ....	116

<b>Figure 5. 1</b> Growth and dissolved oxygen (DO) concentrations of the hydrogenase mutants. ....	130
<b>Figure 5. 2</b> Elevated hydrogenase expressions in the acid-resistant hydrogenase mutant cells. ....	131
<b>Figure 5. 3</b> Influenced cellular viability of the hydrogenase operon mutants at low pH.....	133
<b>Figure 5. 4</b> The hydrogenase operon mutants are not able to maintain their internal pH when external pH changes. ....	134
<b>Figure 5. 5</b> Downregulated expression of the genes associated with acid resistance systems. ....	135

<b>Figure 6. 1</b> Illustration of the random genomic deletion strategy. ....	143
<b>Figure 6. 2</b> Determining the effective minimum length of homology extension to generate gene deletion mutants. ....	152
<b>Figure 6. 3</b> Evaluating the efficiency and accuracy of the homology extension. ....	153
<b>Figure 6. 4</b> Genomic deletions using randomly targeting primers and confirmation. ....	157
<b>Figure 6. 5:</b> Estimation of the number of insertions in a single genome. ....	158
<b>Figure 6. 6</b> Evaluation of the phenotype of the multiple random insertions containing mutants. ....	159

## LIST OF TABLES

Table 2. 1 <i>E. coli</i> strains and plasmids used in the study .....	34
Table 2. 2 Primary function of each gene of every hydrogenase operon in <i>E. coli</i> .....	36
Table 2. 3 List of primers used in the study .....	39
Table 3. 1 The strains and plasmids used in this study .....	70
Table 3. 2 List of primers used in this study .....	76
Table 4. 1 <i>E. coli</i> strains used in this study .....	98
Table 4. 2 List of primers used in qRT-PCR.....	100
Table 5. 1 <i>E. coli</i> strains used in this study .....	125
Table 5. 2 List of primers used in this study .....	126
Table 6. 1 <i>E. coli</i> strains, mutants, and plasmids used in this study .....	144
Table 6. 2 List of primers used in this study .....	145



## LIST OF ABBREVIATIONS

---

<i>Escherichia coli</i>	<i>E. coli</i>
Parent strain	PS
Hydrogen	H <sub>2</sub>
Hydrogenase 1	Hyd-1
Hydrogenase 2	Hyd-2
Hydrogenase 3	Hyd-3
Hydrogenase 4	Hyd-4
Formate hydrogen lyase	FHL
Formate dehydrogenase H	Fdh-H
Luria-Bertani	LB
Polymerase chain reaction	PCR
Deoxyribonucleic acid	DNA
Optical density	OD
Gas chromatography	GC
Adenosine triphosphate	ATP
Quantitative real time PCR	qRT-PCR
Nicotinamide adenine dinucleotide	NAD
Reduced nicotinamide adenine dinucleotide	NADH
Oxidized nicotinamide adenine dinucleotide	NAD <sup>+</sup>
Flavin adenine dinucleotide	FADH
Ribonucleic acid	RNA
National Center for Biotechnology Information	NCBI
Short Reads Archive	SRA
Estimated Degree of Gene Expression in Prokaryotes	EDGE-pro

Lactate dehydrogenase	LDH
Phosphoenolpyruvate	PEP
FLP recombinase recognition target	FRT
Methylviologen	MV
Electron transport chains	ETC
Reactive oxygen species	ROS
Hydroxyl radicals	OH•

---

# CHAPTER 1

## INTRODUCTION AND LITERATURE REVIEW

### 1.1. *Escherichia coli* and Hydrogen metabolism

*Escherichia coli* (*E. coli*) is one of the most studied microorganisms in the world, as not only its whole genome sequence but also its annotated genes, operons, and other genomic regions are available, and the metabolic pathways are well-characterized (Goodall, 2018). In addition, advanced genetic manipulations allow us to challenge the approaches of genetic engineering, protein engineering, and synthetic biology for industrial applications (Zhao, 2019; Sanchez-Torres, 2009). The *E. coli* KEIO mutant library is a powerful tool that allows to evaluate the importance of each nonlethal gene rapidly and to analyzing bacterial function (Baba, 2006). Isozymes are well known to have the same chemical/catalytic reaction despite their different amino acid sequence (Sawers, 1994). Hydrogenase isozymes of *E. coli* are playing key roles in hydrogen metabolism by catalyzing the reversible reaction of hydrogen to protons and electrons ( $2\text{H}^+ + 2\text{e}^- \rightleftharpoons \text{H}_2 (\text{g})$ ) (Maeda, 2018).

### 1.2. Hydrogen metabolism: Glucose and Glycerol Metabolic Pathways

The hydrogen contributory role of hydrogenases in *E. coli* seems dissimilar to glucose or glycerol as a carbon source (Sawers, 1986; Juanita, 2009; Mirzoyan, 2018; Trchounian, 2012) because of their separate anaerobic metabolism (Fig. 1.1). Glycerol is converted to metabolites through the 1,3-propanediol pathway, whereas the glycolytic pathway is used for glucose (Trchounian, 2012). Therefore, hydrogen metabolism is different when glycerol is used as a carbon source due to the repression or the expression of some genes, which are highly dependent on the presence of glucose (Sawers, 1986; Vardar-Schara, 2008; Trchounian, 2012). Moreover, the transport mechanism of  $\text{H}^+$  in glycerol is also different from that of glucose (Juanita, 2009; Trchounian, 2012). Along with the carbon source, external pH is also one of the influencing factors for the activity of hydrogenases (Petrosyan, 2020; Trchounian, 2012;

Sinha, 2011). Although the metabolic function seems similar during the glycerol and glucose metabolisms at a low external pH, hydrogen production from glycerol can be altered at a slightly alkaline pH condition (Petrosyan, 2020; Trchounian, 2012). Moreover, Fdh-H activity is lowered by the change from pH 7.5 to pH 6.0 (Petrosyan, 2020; Axley, 1990).

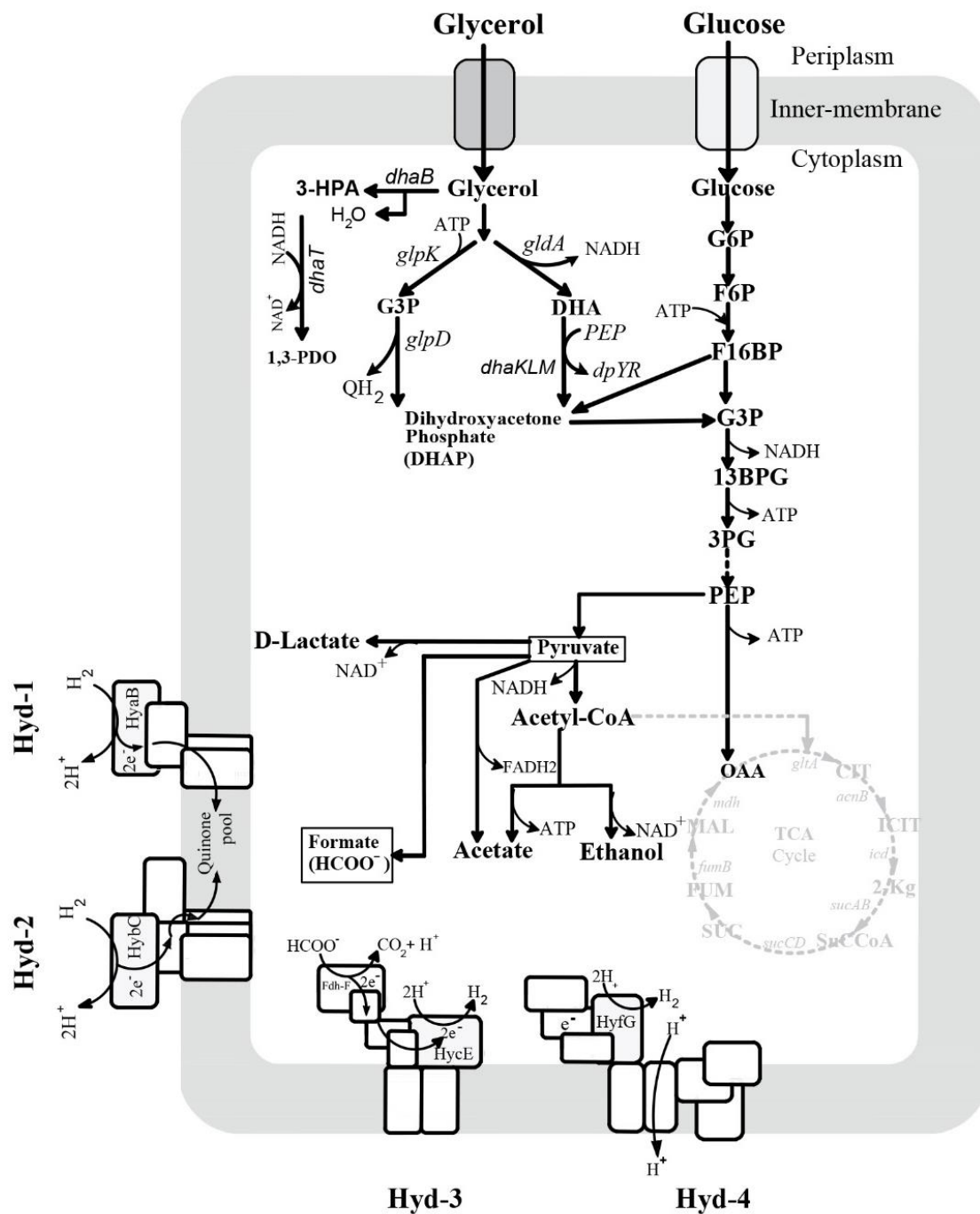


**Figure 1. 1** The glucose and glycerol-associated hydrogen metabolic pathways.

### 1.3. Hydrogenases: Mechanism of Functioning of Hydrogenases

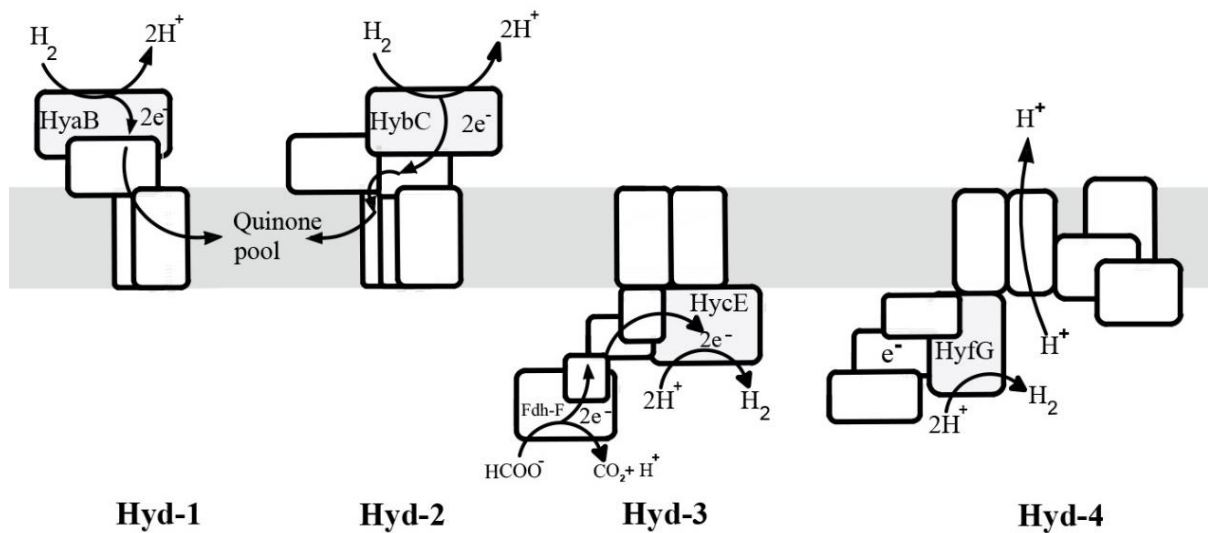


**Figure 1. 2** The four hydrogenases of *E. coli*.

The four hydrogenases of *E. coli* (Fig. 1.2) are encoded by different operons such as hydrogenase 1 (Hyd-1) encoded by *hyaABCDE* operon, hydrogenase 2 (Hyd-2) encoded by *hybOABCDEFG* operon, hydrogenase 3 (Hyd-3) encoded by *hycABCDEFGH* operon, and hydrogenase 4 (Hyd-4) encoded by *hyfABCDEFGH* operon (Richard, 1999; Maeda, 2008; Andrews, 1997).

**Hydrogenase 1:** Hyd-1 is tolerant to oxygen (Lukey, 2010) and is coexpressed with a cytochrome oxidase (Brondsted, 1996), which suggests its physiological role is most likely to operate at the anaerobic/aerobic switch when *E. coli* is transitioning from an anaerobic to an aerobic environment. Hyd-1 is maximally expressed under anaerobic conditions at the stationary phase (Sawers, 1994) and is predominantly a respiratory, hydrogen-oxidizing enzyme (Volbeda, 2013).

**Hydrogenase 2:** Hyd-2 is expressed maximally under anaerobic respiratory conditions, especially in an exponential growth phase where it couples hydrogen oxidation to the generation of a transmembrane electrochemical gradient (Pinske, 2015). Previous reports which are validated by our recent work on hydrogenases demonstrated that Hyd-2 as a reversible

[NiFe]-hydrogenase that can operate as a redox pressure release valve to maintain the redox balance of the cell (Pinske, 2015). This further allows the oxidation of reduced quinol to be coupled to hydrogen production (Pinske, 2015; Trchounian, 2013). That signifies Hyd-2 as the major respiratory ‘uptake’ hydrogenase in *E. coli* (Ballantine, 1985).

**Hydrogenase 3:** Hyd-3 is expressed under anaerobic fermentative conditions (i.e., in the absence of all exogenous respiratory electron acceptors). Being a component of the formate hydrogenlyase (FHL) complex (Bohm, 1990), Hyd-3 connects formate oxidation to proton reduction and is responsible for most of the sustained hydrogen production. Based on the sequence identity, most of the components of Hyd-3 have equivalents in the respiratory NADH dehydrogenase Complex I (Efremov, 2012; Marreiros, 2013). Based on this evolutionary link with Complex I, in some other life forms, Hyd-3 activity in the membrane could be associated with proton (or other ions) translocation and thus energy conservation (Batista, 2013; Nitschke, 2009). However, this has never been shown for *E. coli*. Moreover, *E. coli* Hyd-3/FHL could be an energy-conserving system (Sargent, 2016).

**Hydrogenase 4:** Hyd-4 is also considered silent hydrogenase in *E. coli* since the *hyf* operon is not normally transcribed and therefore not possible to measure-related hydrogenase activity (Andrews, 1997; Self, 2004; Skibinski, 2002). Therefore, detection of Hyd-4 activity is still a challenge (Skibinski, 2002). Hyd-4 is closely related to Hyd-3 and, consequently, evolutionarily links to Complex I (Andrews, 1997). This report is further supported by the structural arrangement in the membrane domain of Hyd-4, which indicate it's more closely related to Complex I, than that of Hyd-3. Hyd-4 is, therefore, more likely to be coupled in the generation of the transmembrane electrochemical gradient (Marreiros, 2013; Moparthi, 2011). Although genetic analysis suggests that the Hyd-4 may be able to transduce free energy released during the formate hydrogenlyase reaction to the generation of a transmembrane ion gradient (Batista,

2013; Marreiros, 2013), the physiological or biochemical role of Hyd-4 is not fully understood (Sargent, 2016).

## **1.4. The Parallel Roles of Hydrogenases**

### **1.4.1 Persistence against antibiotics**

Persisters are the multidrug-tolerant phenotypic variants of the wild type that have entered a nongrowing dormant state that protects them from the lethal action of antibiotics (Wood, 2016; Wood, 2013). Unlike resistant mutants, persister cells do not proliferate in the presence of the antibiotics, but on the removal of the antibiotic, the cells can give rise to a sensitive population similar to the original one (Keren, 2004). This indicates the non-inherited nature of persistence (Maisonneuve, 2014); however, another view conceives that bacterial persistence is a programmed phenomenon with a genetic basis that has evolved to allow organisms to survive sudden environmental insults (Wilmaerts, 2019). Moreover, toxin/antitoxin systems, the stringent response, and SOS response are also involved in the generation of persisters (Fernández-García, 2016; Nguyen, 2011; Dorr, 2009). Recent reports characterized two physiological features of persisters; reduced metabolism and reduced energy level indicating the critical roles of ATP and NADH (Allison, 2011; Kohanski, 2007; Maisonneuve, 2014; Shan, 2017; Harms, 2019). It has been recently shown that a decrease in ATP facilitates the drug tolerance of persisters since most bactericidal antibiotics act by corrupting energy-dependent targets (Shan, 2017). Furthermore, the elevated PMF generated by the oxidation of NADH facilitates the uptake of antibiotics that lead to cell death (Allison, 2011) through the damages caused by superoxide ions originated by the activities of the antibiotics. (Kohanski, 2007).

Mycobacterial hydrogenases are found differentially expressed and active during growth and persistence, which suggests that hydrogen oxidation is important for microbial existence in a non-replicative, persistent state (Cordero, 2019). For *S. Typhimurium*, the use of

molecular hydrogen by uptake hydrogenases is essential for its virulence (Benoit, 2019). Moreover, the pathogenic *Helicobacter* species *H. pylori* and *H. hepaticus* can respire hydrogen through a respiratory [NiFe]-hydrogenase, whereas a mutant hydrogenase strain of *H. pylori* is much less efficient in its colonization in mice (Olson, 2002). These reports indicate a pivotal role of hydrogenases in bacterial virulence and viability. Highly purified bidirectional hydrogenase of *Clostridium pasteurianum* could rapidly reduce several 2-, 4- and 5-nitroimidazole compounds via an electron carrier-coupled mechanism, indicating hydrogenase mediated survivability (Church, 1990). It was hypothesized before that endogenous or exogenous hydrogen can reduce the killing effect by neutralizing cytotoxic hydroxyl radicals (OH•) since a bactericidal treatment induces bacterial death via OH• (Kohanski, 2007). Interestingly, hydrogen selectively could reduce the OH•, the most cytotoxic of reactive oxygen species (ROS), and effectively protected cells, and thus can be used as an effective antioxidant therapy (Ohsawa, 2007). Therefore, hydrogen metabolism in the bacteria could be assumed to effectively reduce the susceptibility to antibiotics and facilitate antibiotic tolerance to enhance bacterial survival (Nie, 2012). All the mentioned reports here further strengthen our hypothesis.

#### **1.4.2. Resistance against acid**

Acid resistance in enteric bacteria such as *E. coli* is one important example of such an adaptation (Zhao, 2010). The extraordinary ability of *E. coli* to survive and resist extreme acidic stress makes it a model for this study (Foster, 2004). Along with well-studied *E. coli* strains (such as O157:H7 and K-12) (King, 2010; Hayes, 2006; Maurer, 2004, Jeong, 2008), other strains such as *Salmonella enterica* (Spector, 2012), and *Shigella flexneri* (McNorton, 2012), *Helicobacter pylori* (Ansari, 2017) and most popularly known lactic acid bacteria (Tsakalidou, 2011) are well known to be highly resistant to low pH and can survive in acidic conditions of the mammalian stomach as well, which can decrease rapidly to an approximate pH of 2.0 (Kanjee, 2013). Hydrogenases are complex metalloenzymes that catalyze the reversible

conversion between H<sub>2</sub> and protons (Maeda, 2018). Several previous reports are indicating their potent roles in bacterial survival in an acidic environment (Hayes, 2006; McNorton, 2012; Ansari, 2017; Noguchi, 2010; Tsakalidou, 2011). Besides *E. coli*, *Helicobacter pylori* and *Shigella flexneri* are also well-recognized masters of surviving gastric acidity, where the roles of hydrogenases are found crucial for their survival under acidic conditions (Bhattacharyya, 2000; McNorton, 2012).

The basis of action of the acid resistance mechanism is the direct consumption of intracellular protons to counteract acid stress (Kanjee, 2013). Besides the amino acid-based decarboxylase acid resistance mechanisms, the other major class identified is the hydrogen-gas-producing formate hydrogen lyase (FHL) complex in *E. coli* (Kanjee, 2013). Hydrogenases in *E. coli* have been suggested to reduce cytoplasmic acidic ambience and contribute to its acid resistance systems (Hayes, 2006; Noguchi, 2010; Lutz, 1991). HypA in *E. coli* and *Helicobacter pylori* is involved in the maturation of nickel-dependent hydrogenases. The transcriptional regulation of *hypA* was found to be pH-dependent, showing upregulation at acidic pH, indicating that the HypA metallochaperone in *Aeromonas* might play a role in acid tolerance (Fernández-Bravo, 2019). Several hydrogenases of *E. coli* respond to pH and oxygen level since, under oxygen limitation, each hydrogenase operon showed higher expression in acid than in base (Rossmann; 1991; Hayes, 2006). Hydrogenase activity may be important at low pH for its contribution to the expulsion of excess protons from the cytoplasm (Lutz, 1991; Trchounian, 2012). The importance of hydrogenase expression in pH-related stress was confirmed by the loss of acid resistance in a strain defective for *hyp*. A *hypF* strain lacking all hydrogenase activity showed a loss of extreme-acid resistance. Thus, hydrogenase activity by one or more of the hydrogenase systems was necessary for stationary-phase acid resistance (Hayes, 2006). Microorganisms developed various effective mechanisms to survive the acidic environment. Different organisms employ a variety of strategies, which may include (1) actively expelling

protons out of the cell; (2) sequestering the intracellular protons via biochemical reactions that either consumes protons or generate ammonia; (3) repairing or preventing acid damage in macromolecules; and (4) modifying the proton permeability of the cellular membrane (Lund, 2014). The proteins embedded in the membranes will be exposed to the detrimental effect of acidic pH due to their cellular location. For example, the domains of inner membrane proteins which are in the periplasm will be exposed to the low pH of the periplasm if the external medium is acidified (Martinez, 2012). Since hydrogenases are membrane-bound protein complexes and involved in hydrogen metabolism (oxidation of hydrogen to proton and reduction vice versa) (Vardar-Schara, 2008), they seem to be the most influencing factor to all these four mechanisms underlying acid tolerance.

## **1.5. Research outline and Objectives**

### **1.5.1. Outline**

Broadly, this study has two main objectives: (1) To investigate hydrogen metabolism by elucidating the absolute function of hydrogenases and random genomic deletions in *E. coli*; (2) To investigate the roles of hydrogenases in associated physiological phenomenon that facilitates the bacterial survival such as persistence and acid resistance. To achieve these two goals, we designed two approaches: targeted deletions of hydrogenase operons and random genomic deletions from *E. coli* genome.

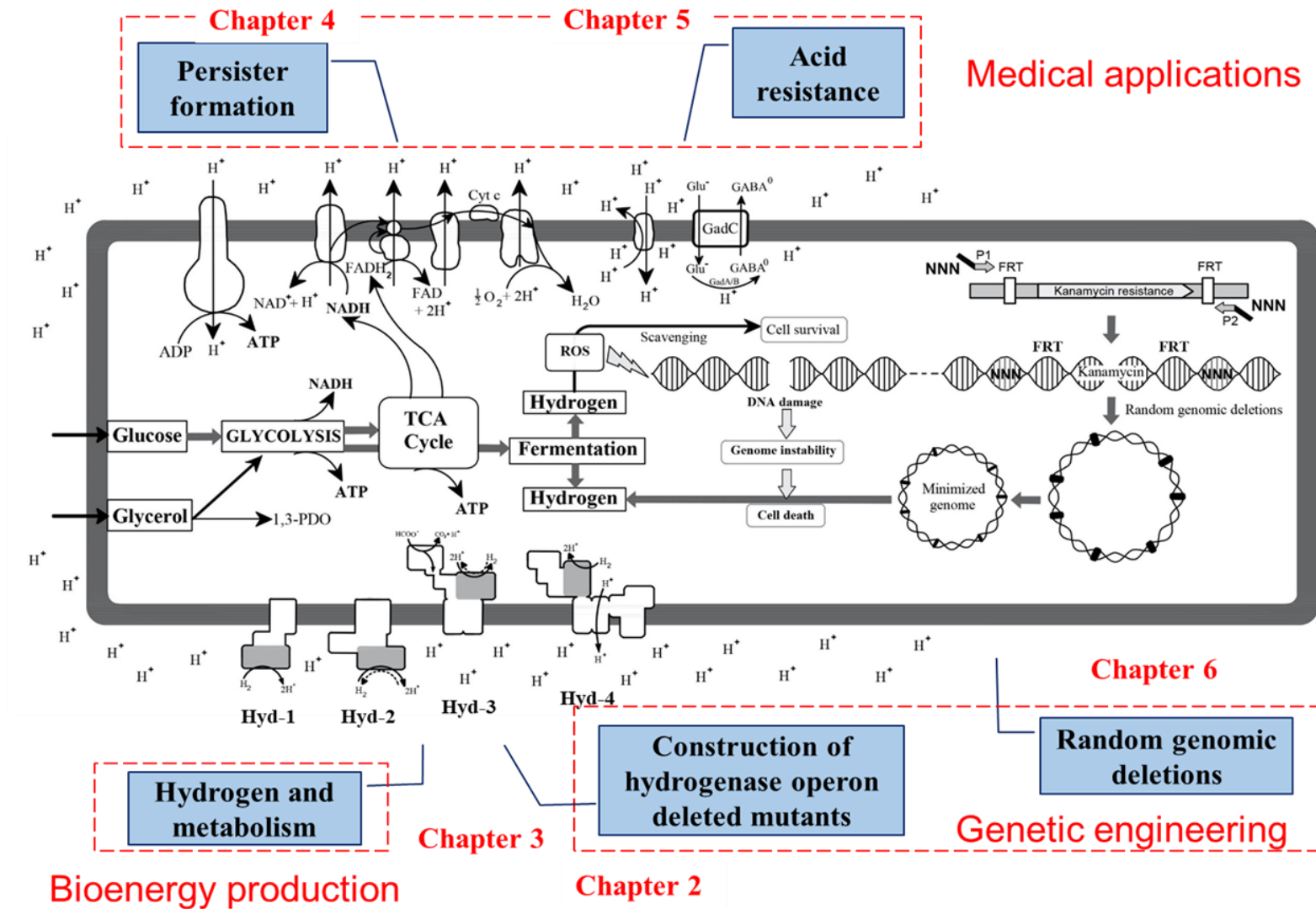


**Figure 1. 3** Illustration of the research outline and its associations to the various fields.

### 1.5.2. Objectives

The objectives of this study are:

1. To investigate the absolute functions of hydrogenases through targeted hydrogenase operons deletion technology [**study 1 and 2**].
2. To investigate the role of hydrogenases in the bacterial survival mechanisms in resistance to antibiotics and acids [**study 3 and 4**].
3. To investigate the effects on/and essentiality of hydrogen metabolism for bacterial survival by random genomic deletion technology [**study 5**].

The research as a whole is dedicated to investigating the functions of bacterial hydrogenases and hydrogen metabolism and consists of genomic deletions, which can be either targeted hydrogenase operon deletions or random genomic deletions from the *E. coli* genome. The study plan is designed in such a way that, along with addressing the controversies associated with hydrogenase functions reported by the previous studies (**study 1 and 2**), some additional essential metabolic functions of hydrogenases required for bacterial survival can also be elucidated (**study 3 and 4**). The single hydrogenase operon deletion mutants uncover the roles of hydrogenases in hydrogen and glucose metabolism, growth, antibiotic persistence, and acid resistance (studies 1, 3, and 4). On the other hand, constructed strains possessing only a single hydrogenase operon in the genome (deletion of the other three) demonstrated their absolute roles in hydrogen metabolism (study 2). This study also takes one more fundamental question into consideration; Is hydrogen metabolism an essential or non-essential metabolic phenomenon (**study 5**)? Therefore, clones constructed by random genomic deletions were found best suitable to answer this question. Overall, this research successfully demonstrates the significance of hydrogen metabolism in bacteria.

## CHAPTER 2

# INVESTIGATION OF THE GLUCOSE METABOLISM BY THE DELETION OF THE OPERONS OF HYDROGENASE IN *ESCHERICHIA COLI*

### 2.1. Introduction

*Escherichia coli* (*E. coli*) is one of the most studied microorganisms because not only its entire genome has been sequenced but also the annotated genes, operons, and other genomic regions, and well-characterized metabolic pathways are currently available (Goodall, 2018). In addition, progress in advanced genetic manipulation supported the creation of powerful tools such as the *E. coli* KEIO mutant library that allows for evaluating the importance of each nonlethal gene rapidly and to construct of novel industrially important strains (Baba, 2006). Thus, basic techniques and tools for deleting target genes (Datsenko, 2000) or random regions (Shekhar, 2022) in *E. coli* could be useful for metabolic engineering and lead to the generation of novel strains, for example, a quadruple mutant defective in *hyaB*, *hybC*, *hycA*, and *fdoG* genes (Maeda, 2008a); a septuple mutant defective in *hyaB*, *hybC*, *hycA*, *fdoG*, *ldhA*, *frdC*, and *aceE* genes (Maeda, 2007); or another septuple mutant defective in *frdC*, *ldhA*, *fdoG*, *ppc*, *narG*, *mgsA*, and *hycA* genes (Tran, 2014) capable of producing hydrogen from a formate, glucose, or glycerol.

*E. coli* has four hydrogenases, hydrogenase 1 (Hyd-1) (Sawers, 1986), hydrogenase 2 (Hyd-2) (Ballantine, 1986), hydrogenase 3 (Hyd-3) (Sawers, 1985), and hydrogenase 4 (Hyd-4) (Andrews, 1997), which play key roles in hydrogen metabolism (Sargent, 2016). Hyd-1 is encoded by *hyaABCDEF*, Hyd-2 by *hybOABCDEFGH*, Hyd-3 by *hycABCDEFGH*, and Hyd-4 by *hyfABCDEFGHIJ* (Shekhar, 2021). Regarding the function of Hyd-1, Hyd-2, Hyd-3, or Hyd-4, it has been reported that Hyd-1 and Hyd-2 have hydrogen-uptake activity (Maeda, 2018), and Hyd-3 has hydrogen production activity via the catalysis of formate by formate hydrogen

lyase (FHL) consisting of Hyd-3 and formate dehydrogenase-H (Fdh-H encoded by *fdhF*) (Sanchez-Torres, 2009). The fermentative route of hydrogen production starts with the conversion of glucose to pyruvate and NADH through glycolysis. In *E. coli*, pyruvate is then converted to acetyl-CoA and formate, which is further catalyzed by pyruvate formate lyase (PFL) (Leonhartsberger, 2002; Vardar-Schara, 2008). Hydrogen is produced from formate by the FHL complex in *E. coli* under anaerobic conditions by the hydrogenase activity of Hyd-3 (Trchounian, 2012). Evolved hydrogen is consumed through the hydrogen-uptake activity of all the hydrogenases (Shekhar, 2021). The hydrogenases, Hyd-1, and Hyd-2 oxidize hydrogen and contribute electrons to the quinone pool (Sargent 2016; Trchounian, 2012). Hyd-1 is predominantly a respiratory, hydrogen-oxidizing enzyme (King, 1999). Hyd-2 can operate as a redox pressure release valve, allowing the oxidation of reduced quinol to be coupled with hydrogen production (Menon, 1994). Hyd-3 is a component of the FHL complex, which connects formate oxidation to proton reduction and is responsible for the majority of sustained hydrogen production by *E. coli* (Maeda, 2008b; Trchounian, 2013). Hyd-4 is closely related to Hyd-3 (Sargent, 2016). Some studies suggest that this isoenzyme may be able to transduce the free energy released during the FHL reaction to the generation of a transmembrane ion gradient (Trchounian, 2012; Trchounian, 2013). However, there are some inconsistent reports regarding the hydrogenase functions; for example, Hyd-4 can produce or consume hydrogen (Mirzoyan, 2017), and glucose concentration may influence the activity of Hyd-4 (Trchounian, 2014), whereas the function of Hyd-4 is also considered to be silent (Self, 2004; Mirzoyan, 2018) or a fossil (Sargent, 2016) (Fig. 2.1). Recent studies have shown the clear activity of Hyd-4 in the absence of Hyd-1, Hyd-2 and Hyd-3 large subunits (Trchounian, 2021) and complete operons (Shekhar, 2021). In addition, although *E. coli* is a facultative microbe capable of metabolizing a wide range of organic carbon sources, the growth rate, and hydrogen production are different under different fermentation conditions using glucose or glycerol (Maeda, 2007; Trchounian,

2013). Such differences in the functions of Hyd-1, Hyd-2, Hyd-3, and Hyd-4 may be due to the differences in pH value, type of buffer, and/or nutrient conditions (Trchounian, 2012).

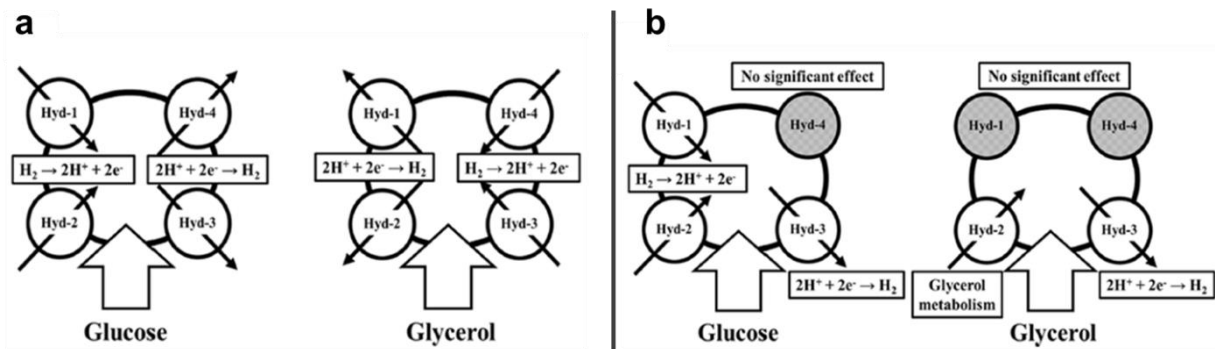
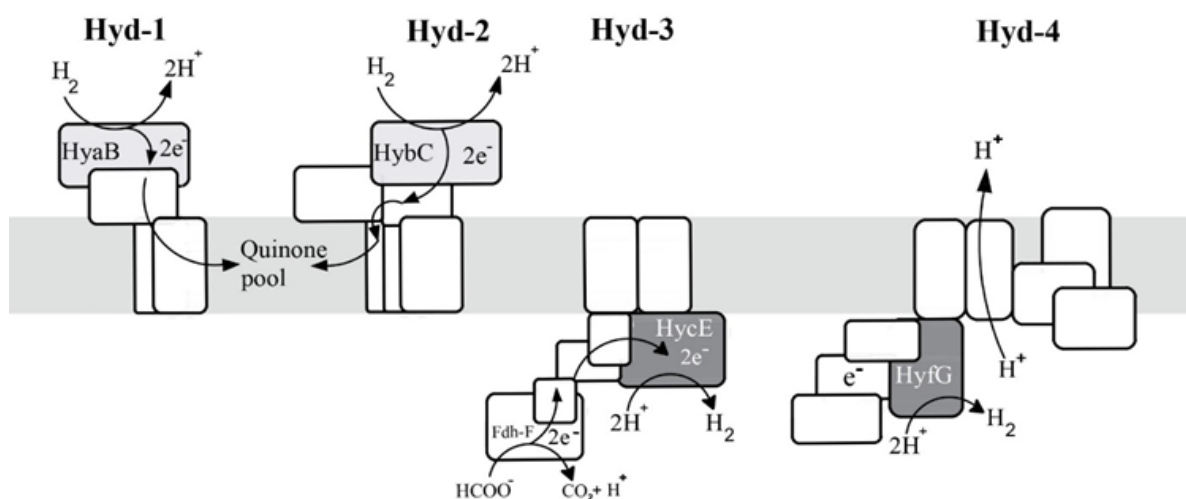


**Figure 2. 1** Controversies in hydrogen production with glucose and glycerol.

As reported by two research groups: Armenian group (a) and Maeda (Wood) group (b) (Maeda, 2018).

A comparison of the identity between large hydrogenase subunits derived from Hyd-1, Hyd-2, Hyd-3, and Hyd-4 indicates that either Hyd-1 and Hyd-2 or Hyd-3 and Hyd-4 have a similar homology that may be associated with their function or activity in hydrogen metabolism (Sargent, 2016; Vardar-Schara, 2008; Trchounian, 2012). We speculated that the resemblance of four hydrogenases might influence the functions related to hydrogen metabolism, due to partial complementation by another hydrogenase homolog that may occur in each single-gene mutation for *E. coli* hydrogenases, as pointed out by some previous reports on hydrogenases (Blokesch, 2006; Trchounian, 2012; Menon, 1994; Redwood, 2008) (Fig. 2.2; table and figure). For example, as *hyf* expression resembles to that of the *hyc* operon (Skibinski, 2002) and *hya* is similar to *hyb* (Vardar-Schara, 2008) due to significant sequence similarity among their respective large subunit genes, a cross-talk was suggested that can partially complement *hyaB* and *hyfG* gene functions in the *hyaB* and *hyfG* mutants by *hybC* and *hycE* genes, respectively (Trchounian, 2012). Therefore, we hypothesized that the inconsistent reports regarding the functions of *E. coli* hydrogenases might be due to partial complementation of the genes.

**Figure 2. 2** Large subunit protein sequence homology between each hydrogenase (below).



Large subunit	Hyd-1 ( <i>hyaB</i> )	Hyd-2 ( <i>hybC</i> )	Hyd-3 ( <i>hycE</i> )	Hyd-4 ( <i>hyfG</i> )
Hyd-1 ( <i>hyaB</i> )	-	<b>40.7%</b>	13.9%	11.9%
Hyd-2 ( <i>hybC</i> )	<b>40.7%</b>	-	13.8%	11.0%
Hyd-3 ( <i>hycE</i> )	13.9%	13.8%	-	<b>69.8%</b>
Hyd-4 ( <i>hyfG</i> )	11.9%	11.0%	<b>69.8%</b>	-

In this study, four-hydrogenase operon-deletion mutants ( $\Deltahya$ ,  $\Deltahyb$ ,  $\Deltahyc$ , and  $\Deltahyf$ ) of *E. coli* have been constructed to minimize the partial complementation (Fig. 2.2). Initially, the phenotypic differences were analyzed and compared between hydrogenase operon and their respective single-gene deletion mutants ( $\DeltahyaB$ ,  $\DeltahybC$ ,  $\DeltahycE$ , and  $\DeltahyfG$ ). Among the four hydrogenases of *E. coli*, Hyd-2 was found crucial for glucose metabolism under both anaerobic and aerobic conditions. Next in the study, some more aspects of metabolism such as ATP, [NADH]/[NAD<sup>+</sup>] redox ratio, glucose metabolism associated gene expressions, and transcriptome were also investigated to formulate a probable mechanism. Among the hydrogenases, Hyd-2 was found significant in the regulation of glucose metabolism which influences not only hydrogen metabolism but also the growth, energy, and redox balance homeostasis of *E. coli*.

## 2.2. Materials and Methods

### 2.2.1. Bacterial strains, media, and growth conditions

*E. coli* K-12 BW25113 strain was used as the parent strain (abbreviated as PS) in the study and all the constructed hydrogenase operon mutants are listed in Table 2.1. The strains were initially streaked from  $-70^{\circ}\text{C}$  glycerol stocks on Luria-Bertani (LB) agar plates and a single colony was used to inoculate to grow at  $37^{\circ}\text{C}$  for overnight. Mutants were grown in the presence of kanamycin ( $50\text{ }\mu\text{g/mL}$ ). A fresh culture was prepared in a 250 mL flask (Iwaki, Japan) containing 50 mL LB at  $37^{\circ}\text{C}$  and 120 rpm using a bioshaker (BR-180LF, Taitec). All experiments were conducted using at least three biological replicates. The glucose medium used was LB-based media containing 10 g/L Bacto Tryptone, 5 g/L yeast extract, and 5 g/L NaCl, with 100 mM glucose (Maeda et al. 2007; Penfold et al. 2003). Cell growth was measured based on cell turbidity at  $\text{OD}_{600}$  by UV/VIS spectrophotometer (JASCO V-530). Total protein for *E. coli* was found 0.22 mg/OD per mL (Protein assay kit, Sigma Diagnostics, St. Louis, MO, USA) (Sanchez-Torres, 2013). Cell amounts were determined based on cell turbidity at  $\text{OD}_{600}$  using the relationship of 0.22 mg/mL/ $\text{OD}_{600}$ . The alkaline (pH 7.5) media was mainly used for the assays since the maximal expression of the *hyb* operon has been reported at alkaline pH (King et al. 1999) and to maintain uniformity in the overall investigation. The final concentrations of each antibiotic used in LB-ampicillin, LB-chloramphenicol, and LB-kanamycin media or plates were  $50\text{ }\mu\text{g/mL}$  ampicillin,  $30\text{ }\mu\text{g/mL}$  chloramphenicol, and  $50\text{ }\mu\text{g/mL}$  kanamycin, respectively. Carbenicillin ( $10\text{ }\mu\text{g/mL}$ ) was used in the place of ampicillin whenever necessary. Chemicals were purchased from Wako Pure Chemical Industries Ltd. (Osaka, Japan), Dojindo Molecular Technologies, Inc. (Kumamoto, Japan), Sigma-Aldrich Co. LLC (Tokyo, Japan), and Nacalai Tesque, Inc. (Kyoto, Japan).

**Table 2. 1 *E. coli* strains and plasmids used in the study.**

Strains/plasmids	Genotype/relevant characteristics	Reference
<i>E. coli</i> BW25113	F $\Delta$ ( <i>araD-araB</i> )567 $\Delta$ lacZ4787 (::rrnB-3) $\lambda$ - <i>rph-I</i> $\Delta$ ( <i>rhaD-rhaB</i> ) 568 <i>hsdR</i> 514; parental strain for the Keio collection	Yale Coli Genetic Stock Center
pKD4	PCR template containing FRT-kanamycin-FRT cassette	Yale Coli Genetic Stock Center
pKD46	Red recombinase expression system	Yale Coli Genetic Stock Center
<i>E. coli</i> BW25113 $\Delta^a$ <i>hyaA-F</i> <sup>c</sup> :: <sup>b</sup> <i>Kan</i> <sup>d</sup>	Hyd-1 operon deleted mutant	This study
<i>E. coli</i> BW25113 $\Delta$ <i>hybO-F</i> :: <i>Kan</i>	Hyd-2 operon deleted mutant	This study
<i>E. coli</i> BW25113 $\Delta$ <i>hycA-I</i> :: <i>Kan</i>	Hyd-3 operon deleted mutant	This study
<i>E. coli</i> BW25113 $\Delta$ <i>hyfA-R</i> :: <i>Kan</i>	Hyd-4 operon deleted mutant	This study
<i>E. coli</i> BW25113 $\Delta$ <i>hyaB</i> :: <i>Kan</i>	Hyd-1 large subunit gene deleted mutant	(Sanchez-Torres et al. 2013)
<i>E. coli</i> BW25113 $\Delta$ <i>hybC</i> :: <i>Kan</i>	Hyd-2 large subunit gene deleted mutant	(Sanchez-Torres et al. 2013)
<i>E. coli</i> BW25113 $\Delta$ <i>hycE</i> :: <i>Kan</i>	Hyd-3 large subunit gene deleted mutant	(Sanchez-Torres et al. 2013)
<i>E. coli</i> BW25113 $\Delta$ <i>hyfG</i> :: <i>Kan</i>	Hyd-4 large subunit gene deleted mutant	(Sanchez-Torres et al. 2013)
<i>E. coli</i> JW2965 $\Delta$ <i>hybO</i> :: <i>Kan</i>	Hyd-2 subunit gene deleted mutant	(Baba et al. 2006)
<i>E. coli</i> JW2964 $\Delta$ <i>hybA</i> :: <i>Kan</i>	Hyd-2 subunit gene deleted mutant	(Baba et al. 2006)
<i>E. coli</i> JW5494 $\Delta$ <i>hybB</i> :: <i>Kan</i>	Hyd-2 subunit gene deleted mutant	(Baba et al. 2006)
<i>E. coli</i> JW2961 $\Delta$ <i>hybD</i> :: <i>Kan</i>	Hyd-2 subunit gene deleted mutant	(Baba et al. 2006)
<i>E. coli</i> JW2960 $\Delta$ <i>hybE</i> :: <i>Kan</i>	Hyd-2 subunit gene deleted mutant	(Baba et al. 2006)
<i>E. coli</i> JW5493 $\Delta$ <i>hybF</i> :: <i>Kan</i>	Hyd-2 subunit gene deleted mutant	(Baba et al. 2006)
<i>E. coli</i> JW2958 $\Delta$ <i>hybG</i> :: <i>Kan</i>	Hyd-2 subunit gene deleted mutant	(Baba et al. 2006)

a and b:  $\Delta$  and :: represents “deletion” and “replaced by gene,” respectively.

c: A-F, O-F, A-I, and A-R represents the “from and to” deleted segment of *hya*, *hyb*, *hyc*, and *hyf* operons, respectively.

d: *Kan* denotes the kanamycin resistance gene.

### 2.2.2. *E. coli* hydrogenase operon mutants

Each hydrogenase operon mutant was constructed by the one-step inactivation method explained by Datsenko and Wanner (Datsenko, 2000). The 1.4 kb polymerase chain reaction (PCR) product to delete the target hydrogenase operon was prepared using a 70-nt-long primer set that included 50-nucleotide homology extensions and 20-nucleotide priming sequences (FRT-flanked kanamycin resistance cassette) for pKD4, and a template DNA. The remaining procedures were also conducted according to the original literature (Baba, 2006; Datsenko, 2000) (Fig. 6.3). Electroporation was performed in a 0.1 cm cuvette at 1.8 V and 200 ohms according to the manufacturer's instructions (Bio-Rad) using 50  $\mu$ L of the electrocompetent cells and 100 ng of the purified PCR product. The shocked cells were added to 1 mL LB medium and incubated for 1 h at 37°C, and then, one-half of this was spread onto an LB agar plate containing kanamycin to select kanamycin-resistant transformants (mutants). The primary function or feature of each subunit protein of every hydrogenase is mentioned in Table 2.2.

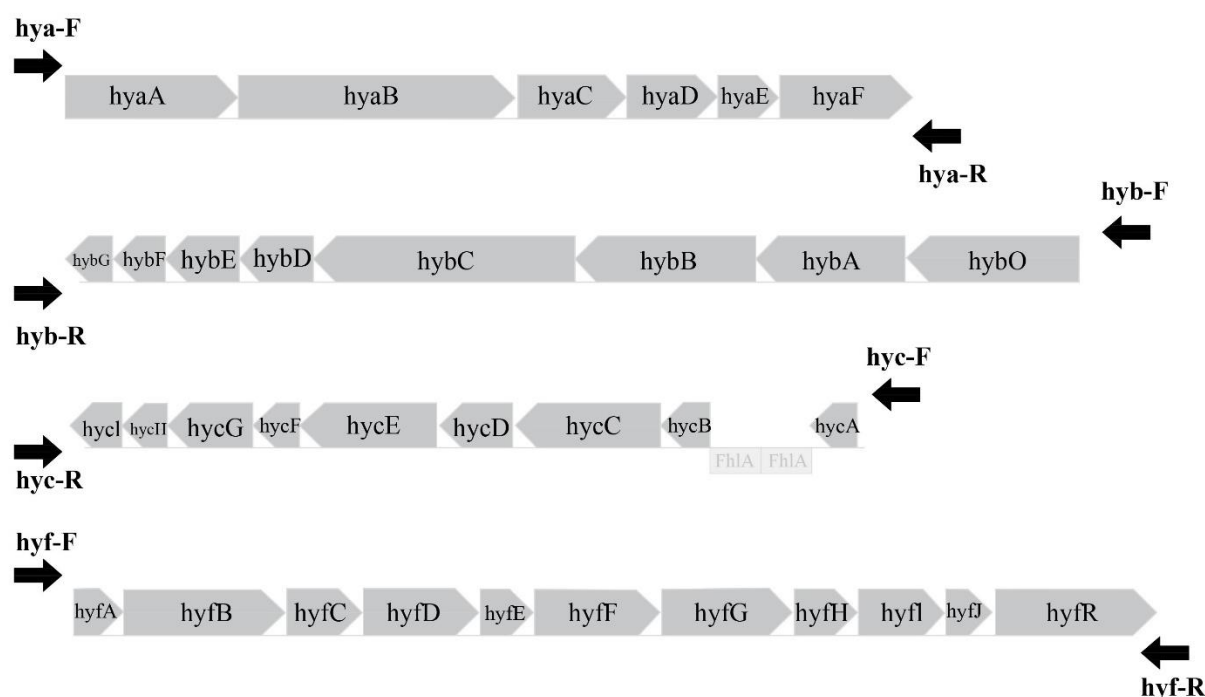


**Figure 2. 3** Targeted locations (indicated by arrows) of the operon for their deletions. The 70-nt long primer set that includes 50-nt homology extensions was designed for targeted deletions of hydrogenase operons using the method explained by Datsenko and Wanner (Datsenko, 2000). The exact location of the 50-nt homology extensions in the forward and

reverse primers is shown as a black arrow at the two ends of each hydrogenase operon. The complete sequences of the oligos are provided in Table 2.3.

**Table 2. 2 Primary function of each gene of every hydrogenase operon in *E. coli***

Operon	Gene	Function/characteristics of the gene product	Reference
<i>hyaABCDEF</i> (Hydrogenase 1)	<i>hyaA</i>	Hyd-1 small subunit	(Karp, 1996)
	<i>hyaB</i>	Hyd-1 large subunit	(Karp, 1996)
	<i>hyaC</i>	Hyd-1 cytochrome b subunit	(Karp, 1996)
	<i>hyaD</i>	Putative Hyd-1 maturation protease HyaD	(Karp, 1996)
	<i>hyaE</i>	Putative HyaA chaperone	(Karp, 1996)
	<i>hyaF</i>	Protein involved in nickel incorporation into Hyd-1 proteins	(Karp, 1996)
<i>hybOABCDEFG</i> (Hydrogenase 2)	<i>hybO</i>	Hyd-2 small subunit	(Karp, 1996)
	<i>hybA</i>	Hyd-2 iron-sulfur protein	(Karp, 1996)
	<i>hybB</i>	Hyd-2 membrane subunit	(Karp, 1996)
	<i>hybC</i>	Hyd-2 large subunit	(Karp, 1996)
	<i>hybD</i>	Hyd-2 maturation protease	(Karp, 1996)
	<i>hybE</i>	Hyd-2-specific chaperone	(Karp, 1996)
	<i>hybF</i>	Hyd-2 maturation protein HybF	(Karp, 1996)
	<i>hybG</i>	Hyd-2 accessory protein	(Karp, 1996)
<i>hycABCDEFGHI</i> (Hydrogenase 3)	<i>hycA</i>	Regulator of the transcriptional regulator FhlA	(Karp, 1996)
	<i>hycB</i>	Formate hydrogenlyase subunit HycB, Fe-S subunit HycB	(Karp, 1996)
	<i>hycC</i>	Formate hydrogenlyase subunit HycC	(Karp, 1996)
	<i>hycD</i>	Formate hydrogenlyase subunit HycD	(Karp, 1996)
	<i>hycE</i>	Formate hydrogenlyase subunit HycE, Hyd-3 large subunit	(Karp, 1996)
	<i>hycF</i>	Formate hydrogenlyase subunit HycF, Fe-S subunit HycF	(Karp, 1996)
	<i>hycG</i>	Formate hydrogenlyase subunit HycG	(Karp, 1996)
	<i>hycH</i>	Formate hydrogenlyase assembly protein	(Karp, 1996)
<i>hyfABCDEFGH</i> (Hydrogenase 4)	<i>hyfI</i>	Hyd-3 maturation protease	(Karp, 1996)
	<i>hyfA</i>	Hyd-4 component A	(Karp, 1996)
	<i>hyfB</i>	Hyd-4 component B	(Karp, 1996)
	<i>hyfC</i>	Hyd-4 component C	(Karp, 1996)

<i>hyfD</i>	Hyd-4 component D	(Karp, 1996)
<i>hyfE</i>	Hyd-4 component E	(Karp, 1996)
<i>hyfF</i>	Hyd-4 component F	(Karp, 1996)
<i>hyfG</i>	Hyd-4 catalytic subunit HyfG, Hyd-4 large subunit	(Karp, 1996)
<i>hyfH</i>	Hyd-4 component H	(Karp, 1996)
<i>hyfI</i>	Hyd-4 catalytic subunit HyfI, Hyd-4 small subunit	(Karp, 1996)
<i>hyfJ</i>	Putative Hyd-4 assembly protein	(Karp, 1996)
<i>hyfR</i>	DNA-binding transcriptional activator HyfR	(Karp, 1996)

---

### 2.2.3. Mutant verification of each hydrogenase operon and large subunit gene mutant

Three PCRs were performed to evaluate the structure of all hydrogenase operons and their corresponding large subunit gene deletion mutant's loci separately, as explained previously (Baba, 2006; Datsenko, 2000; Shekhar, 2022) (Fig. 2.4). Two specific primers for the kanamycin gene (k1 and k2) were used to confirm the insertion into the target operon and large subunit locations. Two reactions were performed using upstream and downstream region-specific primers with k1 or k2 to ensure the presence of both new junction fragments. The third reaction was carried out with the flanking upstream and downstream specific primers only to verify the simultaneous loss of the parental fragment and the gain of the new mutant-specific fragment. A fresh colony of each mutant was suspended in 20  $\mu$ L water, from which 2  $\mu$ L was used in the PCR mixture after boiling the cells at 100°C for 5 min. PCR was carried out using Quick Taq® HS DyeMix reagent (Toyobo Co., Ltd.). The PCR mixture consisted of 12.5  $\mu$ L of 2 $\times$  Quick Taq® HS DyeMix buffer and 0.75  $\mu$ L of each primer (20 mM). The total volume was adjusted up to 25  $\mu$ L by sterilized water, and the products were amplified for 30 cycles (initial denaturation at 95°C for 2 min, denaturation at 95°C for 30 s, annealing at 54°C for 30 s, elongation at 68°C for 1 min, and a final extension at 68°C for 10 min). Control colonies were always also tested. All the primers used in this study are listed in Table 2.2. Moreover, the deletion of operon from the genome was further confirmed by assessing the expressions of all

hydrogenase's large subunit genes in each operon deleted mutant using qRT-PCR (explained below).

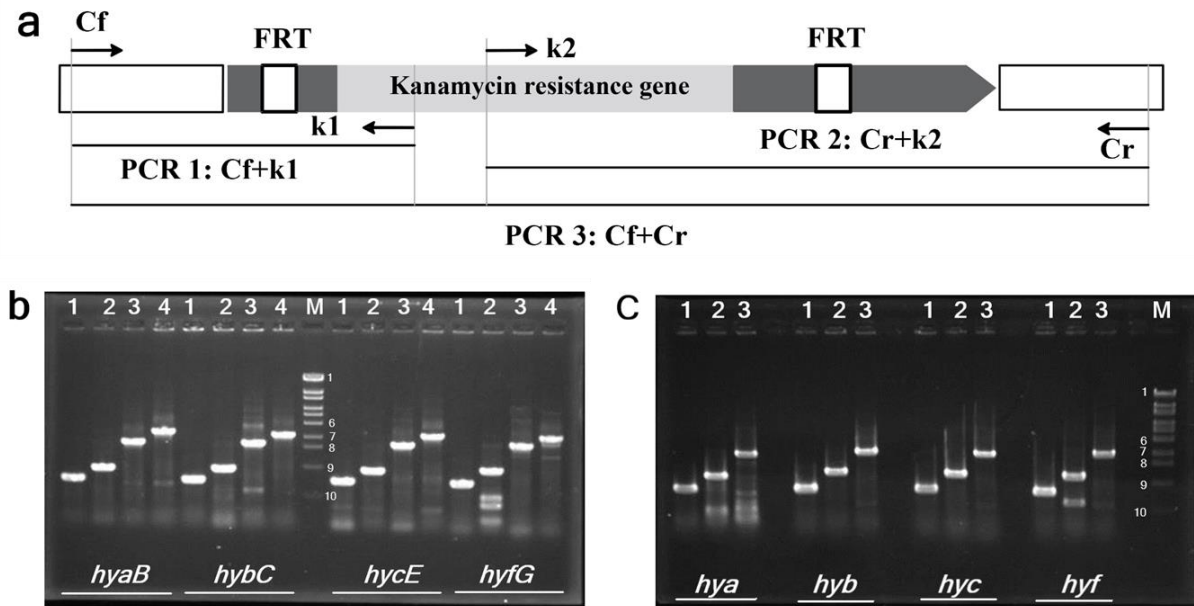


**Figure 2. 4** Verification of hydrogenase mutants (operon and single-gene mutants for Hyd-1, Hyd-2, Hyd-3, and Hyd-4).

(a) Primer locations and three PCRs to confirm each mutant: Cf, the forward primer specific for upstream locus; Cr, the reverse primer specific for downstream locus; k1, kanamycin resistance gene-specific reverse primer (Baba, 2006); k2, kanamycin resistance gene-specific forward primer (Baba, 2006). The following three PCRs were performed: PCR 1, Cf + k1 (to confirm the insertion of kanamycin resistance gene in place of the targeted gene or operon); PCR 2, k2 + Cr (to confirm the insertion of kanamycin resistance gene in place of the targeted gene or operon); PCR 3, Cf + Cr (to confirm the complete deletion of the targeted gene or operon and/or the insertion of a kanamycin resistance gene at that place) (Baba, 2006). (b) PCR products for mutants in which each single-gene corresponding to the large subunit of hydrogenases was deleted. Lane 1, Cf + k1 (for mutant); lane 2, k2 + Cr (for mutant); lane 3, Cf + Cr (for mutant); lane 4, Cf + Cr (for parent strain); lane M, marker 6 (OneSTEP; Nippon Gene, Japan). (c) PCR products for mutants in which the operon of hydrogenases was deleted. Lane 1, Cf + k1 (for mutant); lane 2, k2 + Cr (for mutant); lane 3, Cf + Cr (for mutant); lane M, marker 6 (OneSTEP; Nippon Gene). The amplified fragments in three PCR reactions are nearly 0.6, 0.8, and 1.5kbp, respectively. In the fourth lane in (b), the band indicates the nearly 1.7kbp amplified large subunit gene fragment of each hydrogenase from the parent strain. The

numbered bands as 1, 6, 7, 8, 9, and 10 on the marker lane (M) indicate 19.33, 2.69, 1.88, 1.49, 0.93, and 0.42kbp sizes, respectively.

**Table 2. 3 List of primers used in the study**

Primer	Significance	Sequence (5'-3')	Reference
<b>Primers used in the making and confirmation of operon mutants</b>			
k1	To confirm the presence of kanamycin resistance gene	CAGTCATAGCCGAATAGCCT	(Datsenko, 2000)
k2	To confirm the presence of kanamycin resistance gene	CGGTGCCCTGAATGAACTGC	
<i>Hya-F<sup>a</sup></i>		CATAAGCGCCCGGTGTCCTGCCGGTGTC GCAAGGAGGAGAGACGTGCGATGTGTA	This study
<i>Hya-R<sup>b</sup></i>	To delete <i>hya</i> operon	GGCTGGAGCTGCTTC ATTCGCCGATTGCGATATTCATAAGACT GAAAGCGATACTTACCGTCTTTCATATG AATATCCTCCTTAG	
<i>Hyb-F</i>		TGCGATTGAGGCAAAATATATGCCAGGT CTTCGCAACGGAATAACTATAAGTGTAG	This study
<i>Hyb-R</i>	To delete <i>hyb</i> operon	GCTGGAGCTGCTTC ATGCCTGATGCGACGCTGCCGCGTCTTA TCAGGCCTACGAAAGCTAATCACATATG AATATCCTCCTTAG	
<i>Hyc-F</i>		GCACAAAAAATGCTTAAAGCTGGCATCT CTGTAAACGGGTAACCTGACAGTGTAG	This study
<i>Hyc-R</i>	To delete <i>hyc</i> operon	GCTGGAGCTGCTTC GCTGGTTACCCCCATCAAGAACATCCCT GTCCTGATTCCTTAATGAAAAACATATG AATATCCTCCTTAG	
<i>Hyf-F</i>	To delete <i>hyf</i> operon	CTTTATGCAATATGAAATGCAATGTTTC ATATCATTTTCAAGGAGCCGACGTGTAG GCTGGAGCTGCTTC	This study

<i>Hyf</i> -R		TGCAAGTCGAAAGAGAGTTTGTCTCTCA TGCATACTCCTGCAAAAGCAGACATATG AATATCCTCCTTAG	
<i>Hya</i> -Fc <sup>c</sup>	To confirm <i>hya</i>	ACAATACTTTCTGGCGACGTG	This study
<i>Hya</i> -Rc <sup>d</sup>	operon deletion	AAAAGTGATACAGCGCGGTC	
<i>Hyb</i> -Fc	To confirm <i>hyb</i>	CACTAATGCTTCTTCCCTTCGT	This study
<i>Hyb</i> -Rc	operon deletion	GACGCCAGTGATTTTCGAGAC	
<i>Hyc</i> -Fc	To confirm <i>hyc</i>	TGTTGATTATCCCTGCGGTG	This study
<i>Hyc</i> -Rc	operon deletion	AGTGATTGCCAGTAATGGGGA	
<i>Hyf</i> -Fc	To confirm <i>hyf</i>	TCACATTCTCGCTTTCCT	This study
<i>Hyf</i> -Rc	operon deletion	ATCCGATCGCCATAAACACG	
<b>Primers used in the confirmation of large subunit gene deleted mutants</b>			
<i>hyaB</i> -Fc	To confirm large	CATTCCACCGCCGATACCGTCG	(Sanchez-
<i>hyaB</i> -Rc	subunit gene	GTATCCGGTGACCATCAACACC	Torres, 2013)
	deletion of Hyd-1		
<i>hybC</i> -Fc	To confirm large	TCCCGACCTGGGAAGAACTG	(Sanchez-
<i>hybC</i> -Rc	subunit gene	GTGCCGCCATCGAGGATCTC	Torres, 2013)
	deletion of Hyd-2		
<i>hycE</i> -Fc	To confirm large	GTGGTCGGCGTCCTGGTTATCG	(Sanchez-
<i>hycE</i> -Rc	subunit gene	CTGCTCTGGCTTACCACGGAAG	Torres, 2013)
	deletion of Hyd-3		
<i>hyfG</i> -Fc	To confirm large	ACCTGTCATCAGGATCCTGG	(Sanchez-
<i>hyfG</i> -Rc	subunit gene	ACAGGCGCAGGCACCGCAGG	Torres, 2013)
	deletion of Hyd-4		
<b>Primers used in qRT-PCR</b>			
<i>ptsG</i> -RT <sup>e</sup> -F	Glucose-specific	GGTTTTCCACGGCGACATTCC	This study
<i>ptsG</i> -RT-R	PTS enzyme	GCGCGGTTTTCTGGTTTAGCA	
	IIBC component		
<i>ldhA</i> -RT-F	LDH, converting	GCTAACTTCTCTCTGGAAGGTCTG	(Yusoff,
<i>ldhA</i> -RT-R	pyruvate to	GACATACTCCACACCGAGTTCC	2012)
	lactate		
<i>crp</i> -RT-F	DNA-binding	CGAAAACCGCCTGTGAAGT	This study
<i>crp</i> -RT-R	transcriptional	GACGACGCGCCATCTGTG	
	dual-regulator		
	CRP		
<i>pykA</i> -RT-F		CCTCTCCAACAATAAAGGTATC	This study

<i>pykA</i> -RT-R	Pyruvate kinase II, converts PEP to pyruvate	GGTAATCTACGCCAATCAAC	
<i>ppc</i> -RT-F	PEP carboxylase,	GTGTGGCATGGGTATTATC	This study
<i>ppc</i> -RT-R	overexpression of <i>ppc</i> improves growth yield on glucose	CTCTCCTGACGGATATCAA	
<i>pflB</i> -RT-F	Encodes pyruvate formate-lyase	TGTTTCAGTACCTGGGTAAA	This study
<i>pflB</i> -RT-R		CCATAAGCACCAACGATAC	
<i>rrsG</i> -F	Housekeeping gene for	TATTGCACAATGGGCGCAAG	(Yusoff,
<i>rrsG</i> -R	expression data	ACTTAACAAACCGCCTGCGT	2012)
<i>hycE</i> -RT-F	Positive control	ATCAGCTGACTGTCACCGTAAAG	(Yusoff,
<i>hycE</i> -RT-R		GTAATCCAACACTTAGTGCCCTTC	2012)

a and b: F and R represent forward and reverse primers, respectively.

c and d: Fc and Rc represent forward and reverse primers, respectively, used for mutation confirmation.

e: RT denotes primers used in RT-PCR.

#### 2.2.4. Specific growth rates and pH measurement

Three independent fresh cultures were prepared to have OD less than 0.05 using overnight aerobically grown strains. The cell turbidity of the strains was recorded at 600 nm wavelength at 30 min intervals on growing aerobically at 37°C. Only the values belonging to the exponential part (0.05-0.8) of the growth curve were taken to calculate the specific growth rate (Donner, 2017). Specific growth rates ( $\mu$ ) in terms of slopes were determined from the ln vs OD plots of each mutant (Donner, 2017). Along with aerobic cultures, separate anaerobic cultures of the strains were also prepared to grow under the same conditions as mentioned below (without using glucose), and cell turbidity was monitored at 600 nm during growth. To monitor the change in pH, 200  $\mu$ l cultural sample was provided to calibrate pH meter (Horiba, LAQUAtwin pH11) at 2 h and 12 h incubation times during the fermentation process.

### 2.2.5. Fermentation and hydrogen assessment

The overnight aerobic culture was adjusted to OD<sub>600</sub> of 0.05 in fresh LB medium (25 mL) in the crimp top vial (65 mL) supplemented with 100 mM glucose (Maeda, 2007) inside the anaerobic system (Forma Anaerobic System 1025, Thermo Scientific). The cultures were sparged with nitrogen for 5 min to remove oxygen after sealing the vials with rubber and an aluminum cap. These culture vials were then incubated at 37°C, 120 rpm. The amount of hydrogen generated in the flask headspace was measured by gas chromatography (GC) using a 6890 gas chromatograph equipped with an AT 19095P-NS5 column (Agilent Technologies, Inc., Santa Clara, CA) as described previously (Sanchez-Torres, 2013). The amount of hydrogen generated was calculated using the following equation (Shekhar, 2021):

Hydrogen production (μmol) =

Peak area × Standard hydrogen curve × 65,000 μL (headspace)/100 μL (injection)

### 2.2.6. Fermentation assays with formate and pyruvate

The fresh cultures with adjusted OD<sub>600</sub> to 0.05 in LB medium (10 mL) were prepared from the overnight aerobic cultures, as explained above. The cultures were supplemented with sodium formate (20 mM) or sodium pyruvic acid (20 mM) similar to the glucose above. All vials were sealed, sparged with nitrogen, and incubated at 37°C, 120 rpm. Three independent *E. coli* cultures were assayed to estimate hydrogen production after 24 h of incubation.

### 2.2.7. Glucose assay

*In vitro* assay for the quantitative determination of glucose in culture was performed using a Glucose C2 kit (Wako, code no. 437-90902) with slight modifications from the manufacturer's instructions. In brief, the supernatant was collected (13 krpm/1 min) from 1 mL of 24 h anaerobically grown culture (37°C, 120 rpm), as explained above for the assay. The Colour reagent (1.5 mL) provided with the kit was mixed with 100 μL of the 10 × diluted

supernatants and incubated at 37°C for 4 min. Aerobic cultures of the strains were prepared for comparative analysis. Absorbance was monitored at 505 nm wavelength.

#### **2.2.8. ATP assay**

Intracellular ATP concentrations were determined by using a bioluminescent ATP assay kit (FLAA/Sigma), with some modifications from the manufacturer's instructions. Briefly, the pellet was collected from 1 mL (8000 rpm/2 min/4°C) anaerobically grown culture. The cells were washed twice with pre-chilled PBS (1 ×) and resuspended in 1mL pre-chilled PBS (1 ×). The cell resuspension was neutralized (pH ≈7.8) using a 5 M NaOH solution followed by cellular lysis by trichloroacetic acid (final concentration 1%). 100 µL of ATP Assay Mix solution was added to the wells. Swirled and allowed to stand at room temperature (RT) for ~3 min. Rapidly added 100 µL of sample to the reaction wells of 96-well plate. Swirled briskly to mix and immediately measured the amount of light produced using a luminometer (Thermo Scientific VARIOSKAN FLASH 5250040). Each assay run included a blank sample and ATP standard sample to remove the noise values. All samples were prepared and analyzed in triplicates.

#### **2.2.9. NADH assay**

NADH levels were measured according to the manufacturer's instructions of the assay kit (Abcam, ab65348). In brief, the pellet was collected from 1mL of anaerobically 24 h grown culture by centrifugation at 4000 rpm, 4°C for 10 min. Cells were washed with ice-cold phosphate buffer solution (PBS) and then extracted with 400 µL of NADH/NAD Extraction Buffer by two freeze/ thaw cycles of 20 min at – 70 °C followed by 10 min at RT. To remove any insoluble material, the extraction was centrifuged for 5 min, 4°C at top speed after a short vortex of 10 sec. To measure total NAD (sum of NAD<sup>+</sup> and NADH), 50 µL of each sample supernatant was mixed with 100 µL Reaction Mix (containing NAD cycling buffer and NAD Cycling Enzyme Mix) and incubated at RT for 5 min to convert NAD<sup>+</sup> to NADH, followed by

the addition of 10  $\mu$ L NADH developer buffer and 2 h incubation at RT. To measure NADH, NAD<sup>+</sup> from 200  $\mu$ L of each extracted sample was decomposed by incubation at 60°C for 30 min before measurement. OD values at 450 nm wavelength were then recorded using a microplate reader (Thermo Scientific VARIOSKAN FLASH 5250040).

#### **2.2.10. Total RNA extraction and quantitative reverse transcription-PCR (qRT-PCR)**

Anaerobic cultures of the parent strain and *hyb* operon mutants were prepared in LB medium supplemented with glucose as explained above. The cultures incubated for 24 h were used for collecting cell pellets for RNA extraction using 100  $\mu$ L RNALater Solution (Applied Biosystems, Foster City, CA) in 2 mL screw-cap tubes after centrifugation at 13krpm for 1 min. The tubes containing cell pellets were immersed in 100 mL dissolved dry ice in ethanol (95%) for 10 s and stored at  $-70^{\circ}\text{C}$  before RNA extraction. Total RNA was extracted using a bead beater model 3011b (Wakenyaku Co. Ltd., Japan) and the RNeasy Mini Kit (Qiagen, Inc., Valencia, CA) as explained previously (Shekhar, 2022). StepOne Real-Time PCR System and Power SYBR Green® RNA-to-CT™ 1-Step Kit (Applied Biosystems) were used for the transcription analysis of the seven-glucose metabolism-associated targeted genes (*ptsG*, *crp*, *ppc*, *pykA*, *ldhA*, *pflB*, and *hycE*). Housekeeping gene *rrsG* (16S rRNA) and *hycE* were used to normalize the expression data and as a positive control, respectively. RNA extracted from the parent strain was used as the reference template. All the primers used for this transcription analysis are listed in Table 2. Three technical replicate samples were performed. The expression of the listed genes was analyzed using 50 ng total RNA, and the collected data were analyzed through the relative quantification for qRT-PCR ( $2^{-\Delta\Delta\text{CT}}$ ) (Pfaffl 2001). Additionally, the qRT-PCR was employed to assess the activity of each hydrogenase large subunit gene in all the operon mutants. However, the data submitted, and the results demonstrated the complete loss of activity of each hydrogenase expression in the respective operon mutant.

### **2.2.11. DNA library preparation and high-throughput sequencing**

The DNA library preparation was performed using the Nextera XT DNA Library Prep Kit (Illumina), following the manufacturer's recommended protocol. Briefly, the cDNA was subjected to simultaneous fragmentation and tagmentation to cleave the DNA by the Nextera transposase enzyme. The cleaved DNA was further subjected to PCR amplification for barcoding the samples with a dual adapter index with a unique barcode sequence (Nextera XT Index kit) to differentiate each sample. Then, the PCR products were purified using Agencourt AMPure XP beads (Beckman Coulter Inc., CA, USA) and normalized using the Nextera XT Library Normalization Beads before pooling all the samples. The normalized and pooled samples were loaded in a 600-cycle V3 MiSeq reagent cartridge kit (Illumina) for sequencing in the Illumina MiSeq sequencer. Sequencing was performed for 301, 8, 8, and 301 cycles for forward, index 1, index 2, and reverse reads, respectively. The raw sequence data has been deposited in the National Center for Biotechnology Information (NCBI) under the Short Reads Archive (SRA) accession number PRJNA625150.

### **2.2.12. RNA Seq data analysis**

Raw reads were subjected to quality assessment to determine whether they were qualified for mapping by fastQC (Andrews, 2020) and trimmed using cutadapt tool (Martin, 2011) based on the Phred score quality cutoff  $\geq 30$ . The trimmed good-quality reads were mapped with the reference genome of *E. coli* str. K-12 substr. MG1655 [NCBI Reference Sequence: NC\_000913.3]. The mapping tool EDGE-pro v1.0.1 (Estimated Degree of Gene Expression in Prokaryotes) (Magoc, 2012) was employed to map on the reference genome since it uses the bowtie2 tool (Langmead, 2012) and is designed especially for prokaryote genomes. Moreover, the count of reads and a final abundance matrix were prepared using EDGE-pro. The differential gene expression analysis was done by using the edgeR tool (Robinson, 2010). The functional annotations were retrieved from UniProt and NCBI databases.

### 2.2.13. Statistical analysis

Statistical significance was evaluated with the Student t-test or ANOVA and Tukey's test. P values of <0.05, <0.01, and <0.001 were considered significant (\*), very significant (\*\*), and highly significant (\*\*\*) respectively. For transcriptomic analysis, significant genes were filtered with p-value  $\leq 0.05$ . Upregulated and downregulated genes were filtered using fold change  $\geq 0.8$  and  $\leq -0.8$ , respectively.

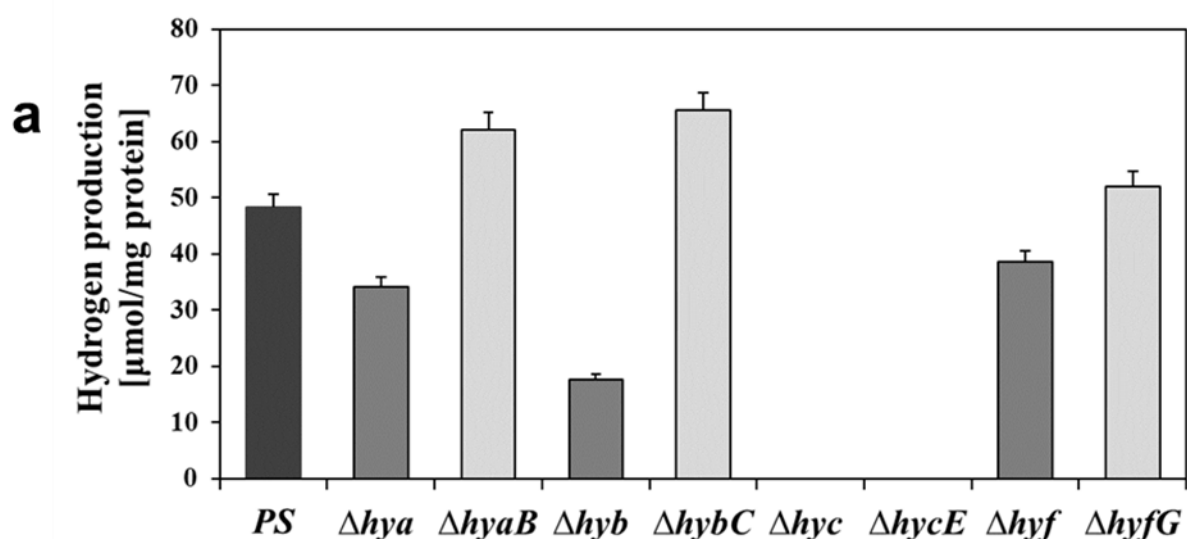
## 2.3. Results

### 2.3.1. Hydrogen productivity by the hydrogenase operon mutants

To evaluate the hydrogen production from the four *E. coli* hydrogenases operon mutants ( $\Deltahya$ ,  $\Deltahyb$ ,  $\Deltahyc$ , and  $\Deltahyf$ ), their corresponding single-gene deletion mutants (gene encoding the large subunit;  $\DeltahyaB$ ,  $\DeltahybC$ ,  $\DeltahycE$ , and  $\DeltahyfG$ ) were used as reference strains, since, as to date, in various studies mostly mutants of single-gene of hydrogenases were used. The hydrogen production from glucose was examined using all eight mutants. Glucose as a substrate has been commonly used in hydrogen metabolism investigations with various concentration ranges (Trchounian, 2014; Yoshida, 2006; Penfold, 2003). For example, 5 - 180 mM (Yoshida, 2006) and 3 - 200 mM (Penfold, 2003) using *E. coli* strains. Importantly, Penfold et al. reported the highest rate of hydrogen evolution occurrence at 100 mM concentration. Maeda et al. used 111- and 100-mM concentrations for hydrogen assays employing single gene mutants of hydrogenases with same *E. coli* strain (Maeda, 2007). Furthermore, operon mutants of hydrogenases showed significant hydrogen productivity at 100 mM than other tested concentrations (10 mM) in this study (data not shown). As a result, contrary to single-gene mutations, operon deletion reduced hydrogen production. Unlike  $\DeltahyaB$ ,  $\DeltahybC$ , and  $\DeltahyfG$  mutants that produce more or nearly the same amount of hydrogen as the parent strain,  $\Deltahya$ ,  $\Deltahyb$ , and  $\Deltahyf$  mutants showed relatively low hydrogen production (Fig. 2.5a). Both *hyaB* and *hybC* are involved in hydrogen uptake; therefore, their deletion indicated increased hydrogen

production (Maeda, 2007). As mentioned earlier about the silent nature of *hyfG*, its deletion did not show any significant change in hydrogen production (Self, 2004). In particular, *hyb* operon mutant had notably low hydrogen production compared to the other mutants and parent strains. The slight increase in hydrogen production by  $\Delta hya$  (relative to  $\Delta hyb$ ) and decrease by  $\Delta hyb$  probably is due to hydrogen scavenging and reversible (bidirectional, i.e., possessing both hydrogen-producing and uptaking activities) nature of Hyd-1 and Hyd-2, respectively (Trchounian, 2012). Whereas, as expected, *hyc* operon mutant and  $\Delta hycE$  mutant did not produce hydrogen (Maeda, 2008b), indicating their most crucial role in hydrogen synthesis.

Pyruvate and formate are the essential intermediates in the hydrogen metabolism of *E. coli* (Vardar-Schara, 2008), therefore, they are used as substrates to examine the hydrogen production of *hyb* operon mutant. As a result, this mutant was found able to produce hydrogen from both of these substrates (Fig. 2.5b), with a higher yield than the parent strain. This ability to metabolize these substrates but not glucose indicated the affected glucose metabolism in *hyb* operon mutant.



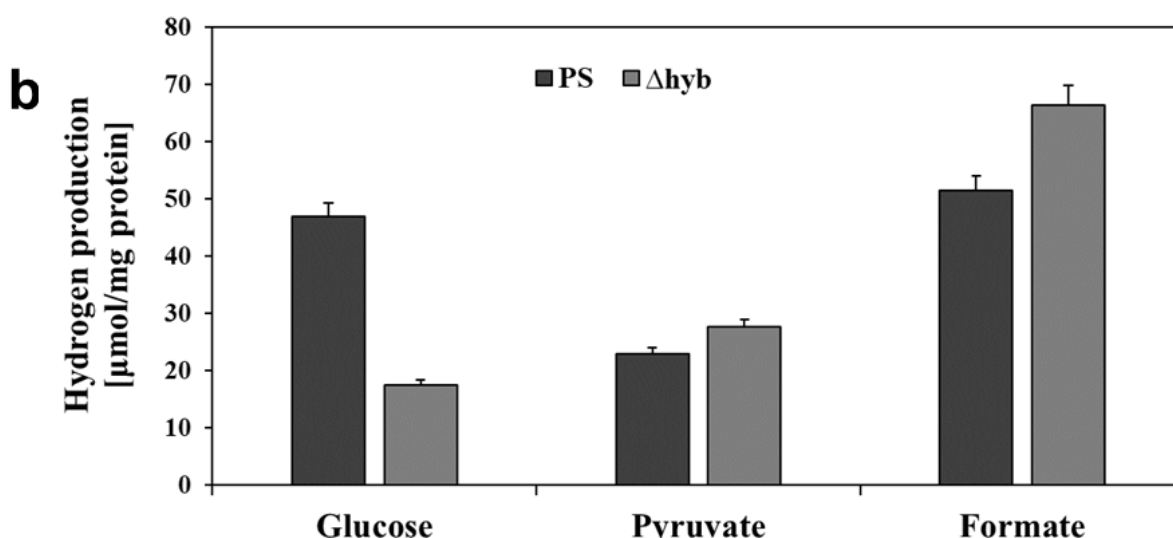


**Figure 2. 5** Hydrogen production; operon deletion vs single gene deletion.

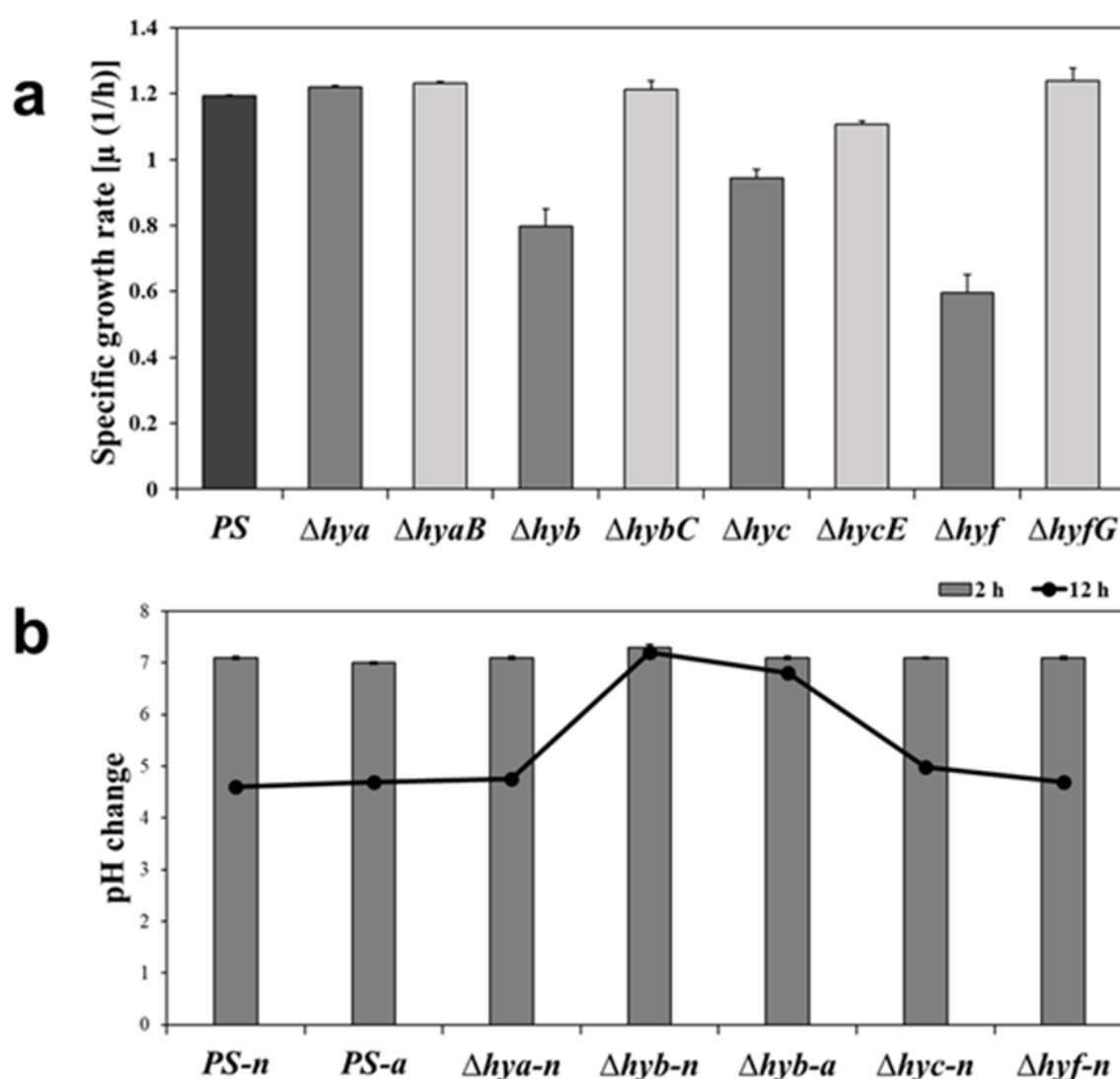
(a) Hydrogen production in four hydrogenase operons deletion mutants in comparison to their respective single-gene deletion mutants in the presence of glucose. (b) The reduced production of hydrogen in *hyb* operon mutant was further evaluated with pyruvate and formate as substrates. Hydrogen yield is shown here measured after 24 h growth under anaerobic fermentation. The pH of the medium was adjusted to 7.5. Data is obtained from triplicates from two independent biological samples. Error bars represent stdev.

### 2.3.2. Growths and change in pH in the cultures of hydrogenase operon mutants

Under anaerobic conditions, a significantly reduced growth was found in *hyb* operon-deletion mutant only (data not shown). Whereas, in the case of aerobic conditions, *hyb* and *hyf* operon mutants showed significantly reduced growth rates compared to the other strains including their large subunit gene deletion mutants ( $\Delta hybC$  and  $\Delta hyfG$ , respectively) (Fig. 2.6a). *hyc* and *hycE* mutants also showed slightly slower growth than the parent strain under both aerobic and anaerobic conditions. *hya* operon mutant along with its respective large subunit gene deletion mutants ( $\Delta hyaB$ ) did not show any alteration in the growth rate. Since *hyb* operon mutant was found to be unique in later studies and commonly found to affect growth both aerobically and anaerobically, each single gene mutant of *hyb* ( $\Delta hybO$ ,  $\Delta hybA$ ,  $\Delta hybB$ ,  $\Delta hybC$ ,  $\Delta hybD$ ,  $\Delta hybE$ ,  $\Delta hybF$ , and  $\Delta hybG$ ) was examined further to evaluate whether any of the mutants was related to the growth defect as observed in *hyb* operon mutant. However, no single mutant of *hyb* showed stagnation of growth (Fig. 2.6c), which indicated that the growth defect

arose due to the deletion of the entire operon. The reduced growth might be associated with its ability to release the excess reducing equivalent in the form of hydrogen (Szenk, 2017; Singh, 2009).

In addition, the pH change of the culture was monitored during the growth of all the strains under anaerobic conditions and *hyb* operon mutant along with parent strain under aerobic conditions. Interestingly, the pH of the culture of *hyb* operon mutant was found almost unchanged throughout the growth (Fig. 2.6). A slightly altered pH from the culture of *hyc* mutants was also observed as compared to other strains. The stable pH of the media of the bacteria reveals its weakened metabolism (Russell, 1997), so *hyb* operon mutant could be inferred similarly.



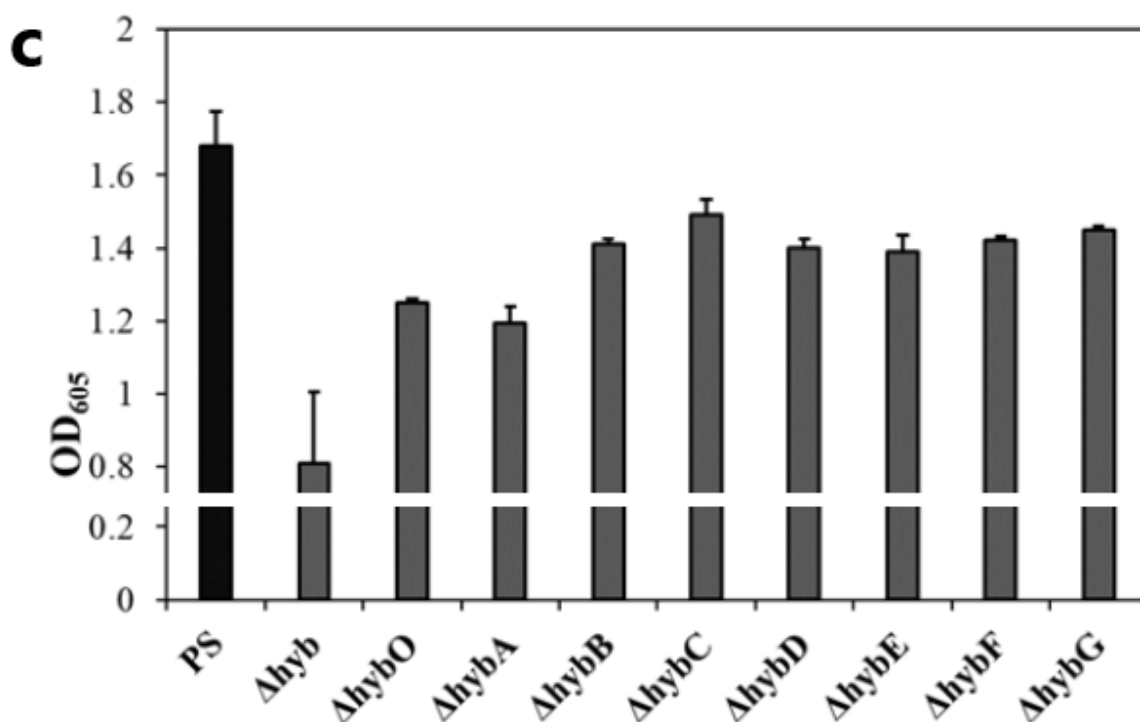


**Figure 2. 6** Rate of growth and changes of pH during the growth of the hydrogenase mutants. (a) Specific growth rates of the operon deletion mutants in comparison with single-gene deletion mutants. Growth rates were calculated by using OD<sub>600</sub> values of the exponential phase (less than 0.8) only. (b) pH changes of the cultures of operon mutants under anaerobic conditions (PS: parent strain and  $\Deltahya$ ,  $\Deltahyb$ ,  $\Deltahyc$ , or  $\Deltahyf$ : the operon deletion mutant of hydrogenase 1, hydrogenase 2, hydrogenase 3, or hydrogenase 4). The parent strain and *hyb* operon mutant were also evaluated for any change in the pH under aerobic conditions. Data obtained from aerobic and anaerobic conditions were represented with “a” and “n”, respectively. (c) Growth of each single gene mutant of *hyb* operon in comparison with *hyb* operon mutant and parent strain. Turbidity representing bacterial growth was determined by obtaining the absorbance of the different mutant cultures at 605 nm (Patel, 2022). The data presented here is the mean of the three independent cultures, and error bars represent stdev.

#### 2.3.4. Glucose consumption by hydrogenase operon mutants

Glycolysis is the primary metabolic pathway, where the substrate is converted to pyruvate, a central molecule of microbial fermentation (Pandey, 2013). Based on the decreased hydrogen production by *hyb* operon mutant in glucose medium and its non-consumption is a suspected outcome of reduced growth. We assayed the glucose consumption-ability of this mutant in comparison with other strains. In this regard, the glucose concentration in the cultures of the strains was monitored under aerobic conditions and anaerobic fermentation. Interestingly,

compared to the other strains, *hyb* operon mutant was unable to consume glucose under both conditions (Fig. 2.7a and b).

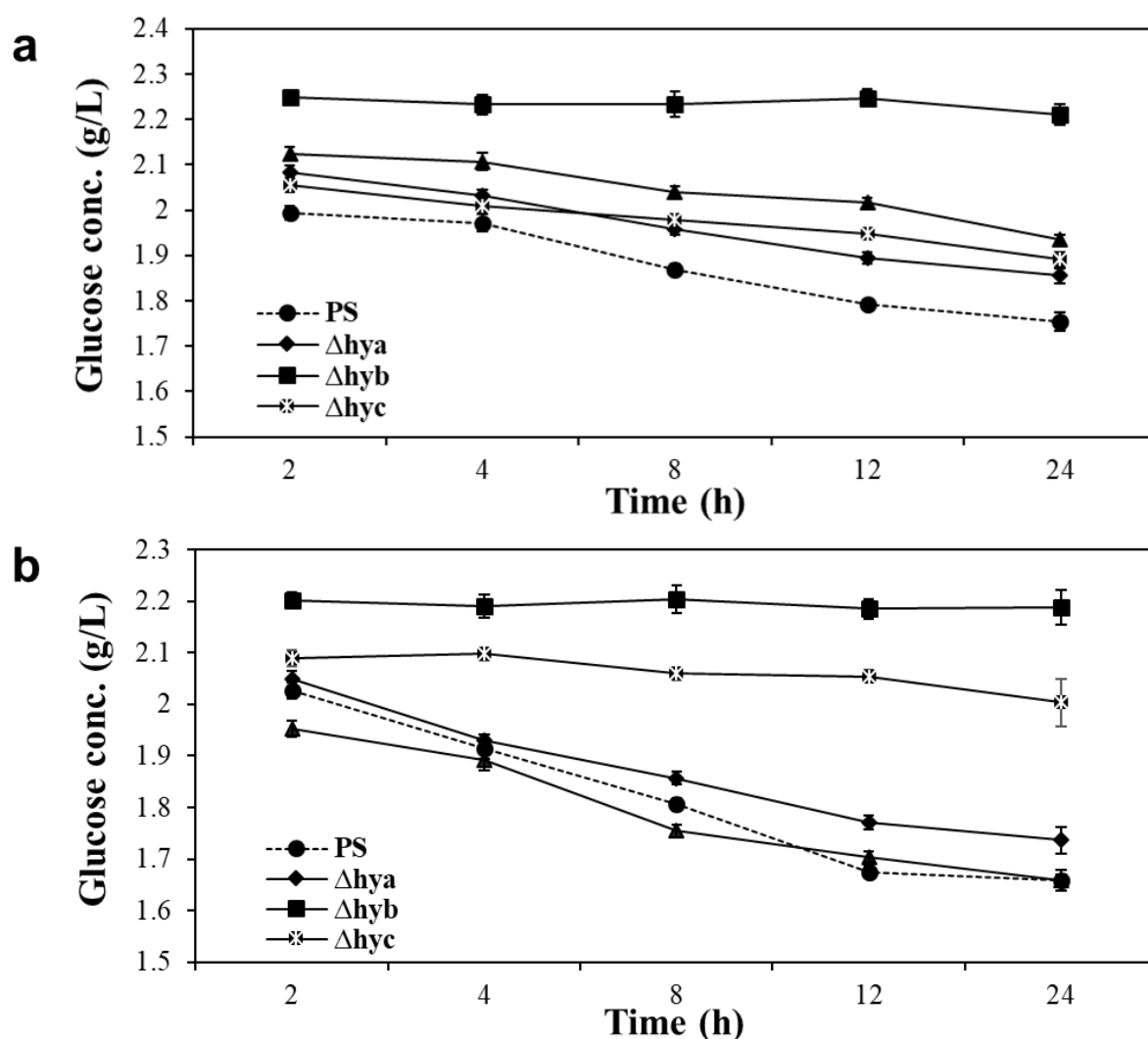


**Figure 2. 7** Glucose consumption by hydrogenase operon mutants investigated by monitoring glucose concentration in the cultures of the strains at different time intervals.

(a) Glucose concentrations in the cultures under aerobic conditions. (b) Glucose concentrations in the cultures under anaerobic conditions. Parent strain (closed circle) is represented by a dashed line, whereas *hya* mutant (closed diamond), *hyb* mutant (closed square), *hyc* mutant (closed cross), and *hyf* mutants (closed triangle) are represented by solid lines. Data is the mean of three independent cultures; error bars indicate stdev.

No glucose consumption may lead to reduced hydrogen production by this mutant. The single-gene mutant of *hyb* operon ( $\Delta hybC$ ) was previously reported to have reduced glycerol consumption and also cell growth, which suggests that glycerol utilization is directly related to

biomass production (Sanchez-Torres, 2013). In the same way, probably correlate with glucose consumption and low growth. The survival of *hyb* mutant without consuming the glucose is probably due to the preferential utilization of other carbon sources, such as tryptone present in the LB medium. In addition, a slightly reduced glucose consumption was also observed from *hyc* mutants under anaerobic conditions compared to other strains, which is similar to *hyb* mutants (Fig. 2.7b). However, the glucose consumption inability seemed more significant in the case of *hyb* mutants, since first, *hyb* is found common in non-consumption of glucose under both the conditions and second, at the beginning of fermentation, *hyc* mutant could consume glucose, as its level is lower than *hyb* mutant. In addition, after 12 h of fermentation, glucose concentration was found slightly lowered, which further indicates its consumption by *hyc* mutant, although it is slow and low.

### **2.3.5. Total intracellular ATP levels in hydrogenase operon mutants**

The [Ni-Fe] hydrogenases play a key role in energy metabolism (Pandey, 2013). Since the FOF1-ATPase maintains the proton-motive force across the membrane of the cells, hydrogenase activity is reported to be dependent on the active FOF1-ATPase during glycerol as well as glucose fermentation (Trchounian, 2012). Therefore, hydrogenases are crucial in oxidizing hydrogen to recycle electrons, protons, and ATP for energy metabolism (Szenk, 2017; Singh, 2009; Pandey, 2013). Based on these, the regulation of ATP, and therefore, the reason for altered intracellular ATP content was hypothesized by the inactivation of hydrogenases. As a result of the ATP quantification assay, all the mutants except for *hya* operon mutant were observed with decreased intracellular ATP in comparison with the parent strain in which *hyb* mutant was noticed with relatively reduced ATP levels (Fig. 2.8a). Hydrogenases, based on their different competencies toward hydrogen metabolism, are expected to impart non-identical gradients across the membrane (Hallenbeck, 2014). Therefore, deletions of hydrogenase operons can influence ATP metabolism, and thus a distinct ATP synthesis activity could be

observed (Pandey, 2013). Specifically, Hyd-2 and Hyd-3, since both of these were noted as significant in hydrogen uptake and synthesis activities, and therefore most crucial in maintaining membrane gradient were found with considerably lowered ATP levels (Fig. 2.8a), indicating their regulating roles to FOF1-ATPase. However, the dependence of the activities of the Hyd-1 (and Hyd-2) on the FOF1-ATP synthase for glucose fermentation has been elucidated (Trchounian et al. 2011), our study showed slight contradictions in the case of Hyd-1, since the deletion of *hya* operon did not cause any change in intracellular ATP levels. Noticeably, Hyd-1 mutant did not show any significant alteration in phenotype from all the assays of this study indicating its phenotypic resemblance to PS. As mentioned earlier, glucose concentration might be an influencing factor for hydrogenase activity, especially Hyd-4, as its activity depends on glucose concentration (Trchounian, 2014; Trchounian, 2014). Moreover, recently Vanyan et al., showed that the relationship or metabolic cross-talk between hydrogenases, proton, ATPase, and potassium transport depends on glucose concentration, where low glucose concentration was found crucial for this activity (Vanyan, 2022). Therefore, the glucose concentration used in this study may act as a determining parameter by which four hydrogenases are governing differently.

### **2.3.6. Intracellular NADH levels in hydrogenase operon mutants**

Glucose metabolism generates excess electrons, which must be disposed of for continued growth and metabolic activity of the cells (Pandey, 2013). Hydrogenases, since also act as electron valves, are involved in the quinone pool, where these electrons are used for  $\text{NAD}^+$  reduction (Hallenbeck, 2002). The protons, on the other hand, are transferred between metabolic intermediates through these redox reactions by dehydrogenases (Srikanth, 2010). The need for redox balancing during metabolism is what drives hydrogen production by hydrogenases (Bommer, 2019). Since during the fermentation of glucose, NADH is involved as the principal, reducing equivalent, therefore decided to examine the cultures of hydrogenase

operon mutants. As a result, from all the strains, *hyb* operon mutant was found with a significantly low level of NADH (Fig. 2.8b). In contrast to *hyb*, *hya* operon mutant showed elevated levels of NADH, indicating an antagonistic role of Hyd-1 to that of Hyd-2. Hyd-3 and Hyd-4 seemed to have similar participation in redox balance, which might be because of their homologous nature to each other (Vardar-Schara, 2008).

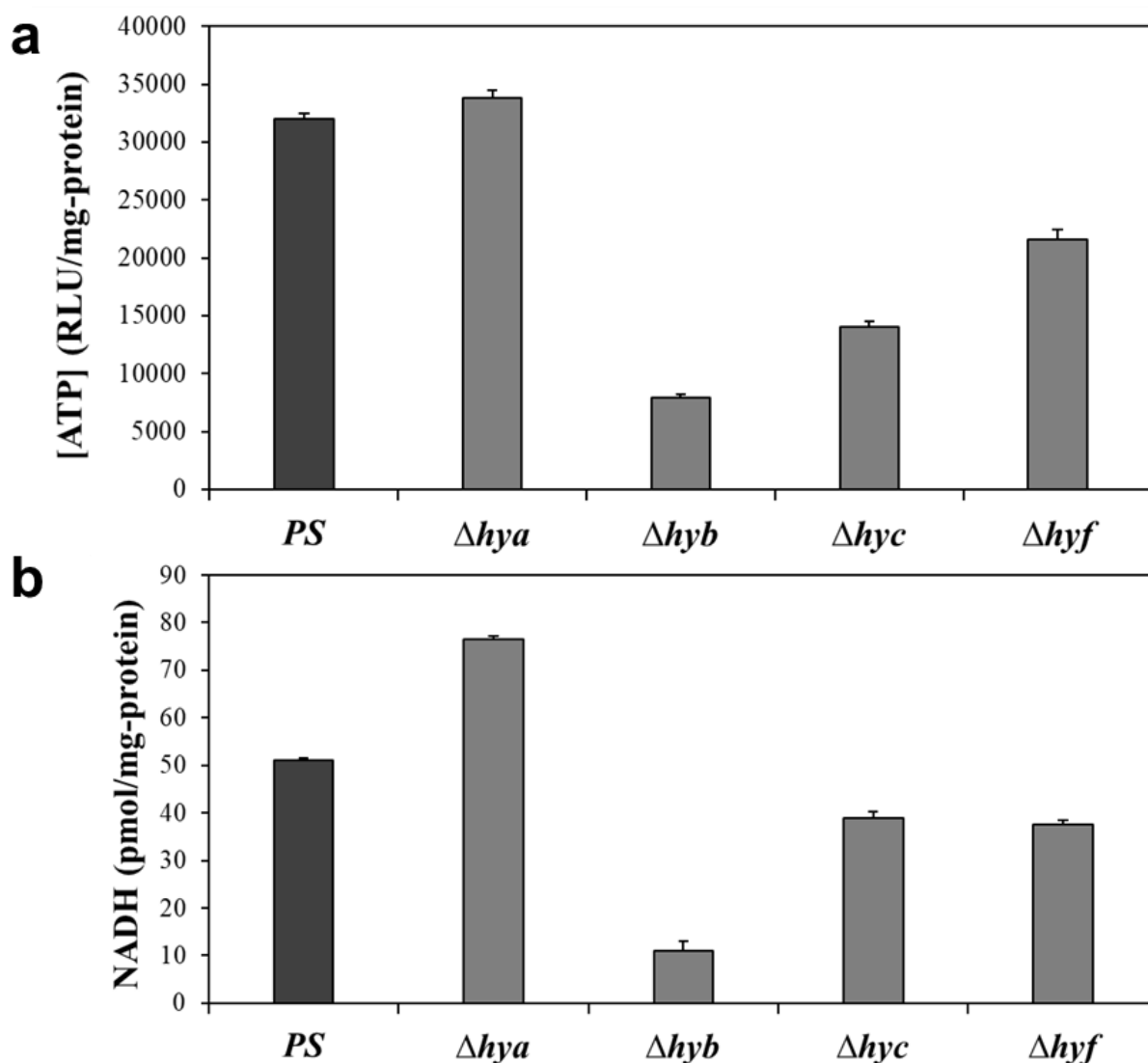


**Figure 2. 8** Energy and redox balance assessment of hydrogenase operon mutants. (a) Quantification of the total ATP from cultures of strains grown for 24h under anaerobic conditions. (b) Quantification of the NADH from cultures of strains grown for 24 h under anaerobic conditions. N = 5, error bars represent stdev.

### 2.3.7. Downregulation of glucose metabolism-associated genes

Most facultative anaerobes produce hydrogen by the breakdown of glucose into subsequent metabolites during glycolysis. Moreover, glucose fermentation conditions are critically crucial for the activity of hydrogenases. Glucose produces pyruvate via the glycolytic pathway to regenerate ATP. Several steps and genes involved therein of glycolysis are reported to be crucial for glucose metabolism and biomass generation in *E. coli*. Some key genes (*ptsG*, *crp*, *ppc*, *pykA*, *ldhA*, *pflB*, and *hycE*) are crucial for glucose metabolism, and therefore, for hydrogen production (Pandey, 2013) were selected, and their expression was evaluated by qRT-PCR. Fig. 2.9a shows the genes and their functioning branch in glucose metabolism. The *rrsG* (16S rRNA) and *hycE* mutants (large subunit gene of *hyc*) were taken as housekeeping and positive controls, respectively, for this study (Trchounian, 2014). The expression level of these genes was monitored from the parent strain and *hyb* operon mutant. As a result, all genes were found with downregulated expressions in *hyb* operon mutant (Fig. 2.9b).

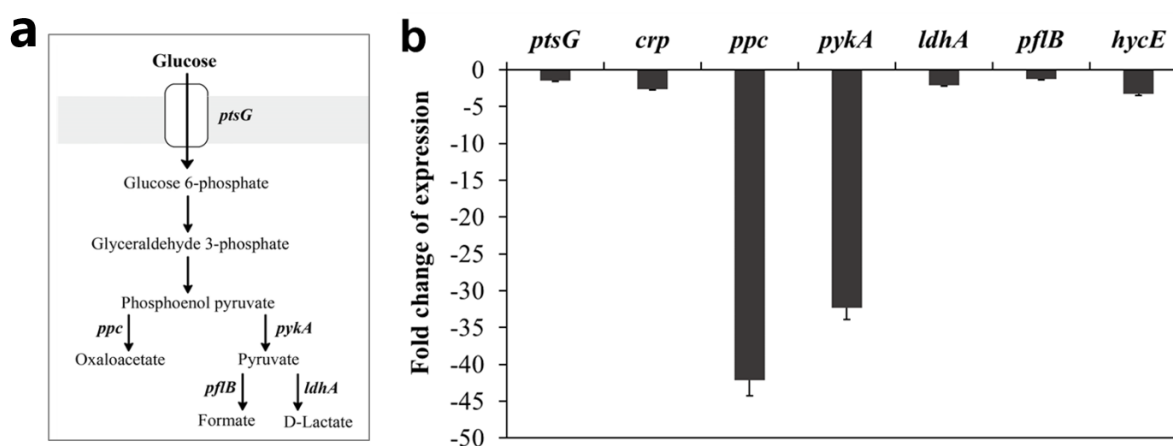


**Figure 2. 9** Transcriptional analysis of glucose metabolism-associated genes in *hyb* operon mutant.

(a) Metabolic pathway of glucose and seven tested genes (*ptsG*, *crp*, *ppc*, *pykA*, *ldhA*, *pflB*, and *hycE*). (b) The expression level of these genes was evaluated by qRT-PCR. The RNA used for this analysis was extracted from the *E. coli* cultures incubated for 24 h anaerobically. N = 5, error bars represent stdev.

The *ptsG* gene contributes to the bacterial phosphotransferase system and mediates the

uptake and phosphorylation of glucose. In the absence of glucose, *ptsG* expression is repressed by the action of a transcription factor (Mlc) that controls the entry of glucose into glycolysis (Plumbridge, 2002). Post-transcriptionally, *ptsG* levels were regulated by the glycolytic flux (Kargeti, 2017). The *crp* is a global regulator of genes for carbon source utilization (Kargeti, 2017). A *crp* single deletion mutant showed affected growth and biomass under anaerobic conditions (Shimada, 2011). LdhA is a soluble NAD-linked lactate dehydrogenase (LDH) that is specific for the production of D-lactate. The enzyme although present under aerobic conditions but is induced when *E. coli* is grown on a variety of sugars under anaerobic conditions (Jiang, 2001). The *pflB* gene encodes pyruvate formate-lyase protein, and its expression was regulated by carbon metabolism, which indicates glycolysis functions act as an inducer of *pflB* gene expression *pflB* (Rasmussen, 1991). As mentioned, all the genes were functionally influencing glucose metabolism, the impaired glucose metabolism in *hyb* operon mutant seems a contributory phenomenon where several metabolic steps appear to be associated. Notably, the expression of *ppc* and *pykA* was remarkably found lower than that of the other genes. *ppc* encodes phosphoenolpyruvate (PEP) carboxylase that converts PEP into oxaloacetate (Millard, 1996). The overexpression of *ppc* improved the growth yield on glucose during fermentation (Millard, 1996). A mutant for the *ppc* gene grew slower along with less glucose consumption when compared to the parent strain (Morita, 2003). A *ppc* mutant exhibited PEP accumulation along with allosteric inhibition of some glycolytic enzymes, which in turn affects the activity of other enzymes (Morita, 2003). For example, the accumulation of glucose 6-phosphate and fructose 6-phosphate was found responsible for *ptsG* mRNA degradation, which further influenced glycolytic flux and led to slower growth and lowered glucose uptake rate (Malcovati, 1969). The *pykA* gene encodes for pyruvate kinase II, which converts PEP into pyruvate and is reported to be important in the control of metabolic flux in glycolysis (Siddiquee, 2004). Additionally, pyruvate kinase is an allosteric enzyme, catalyzing

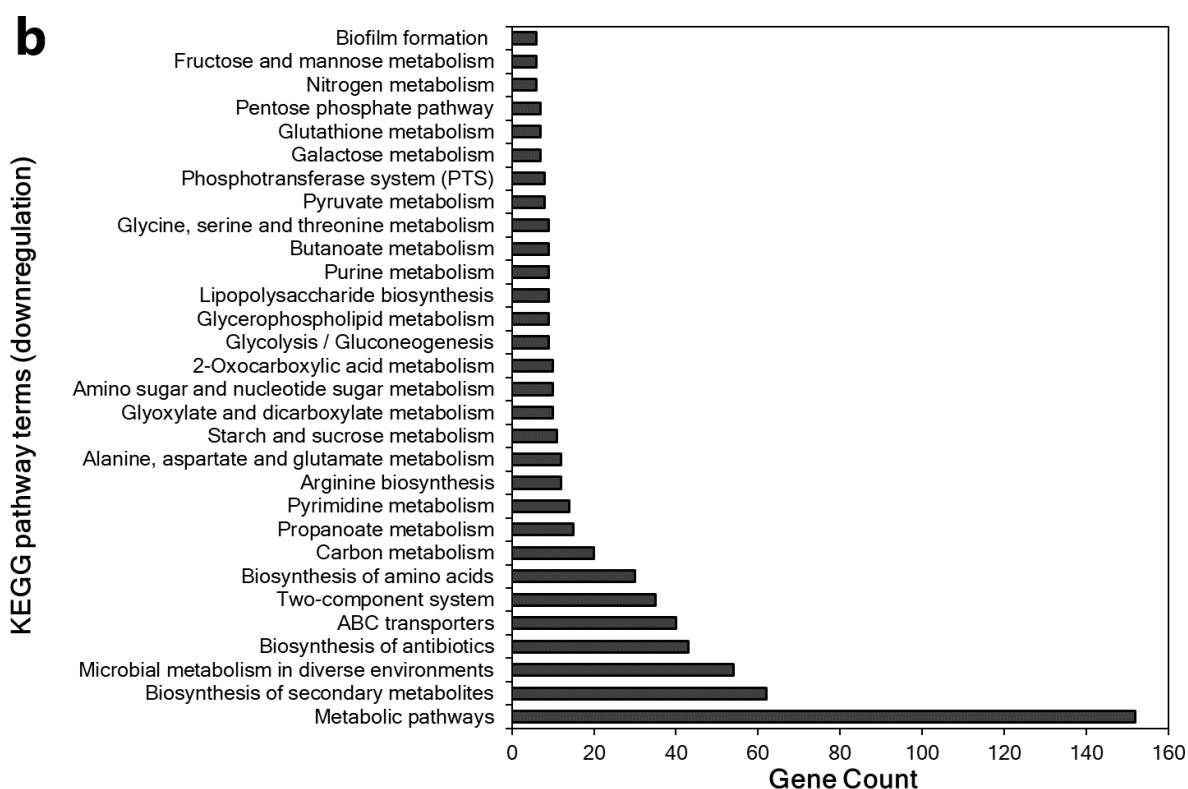
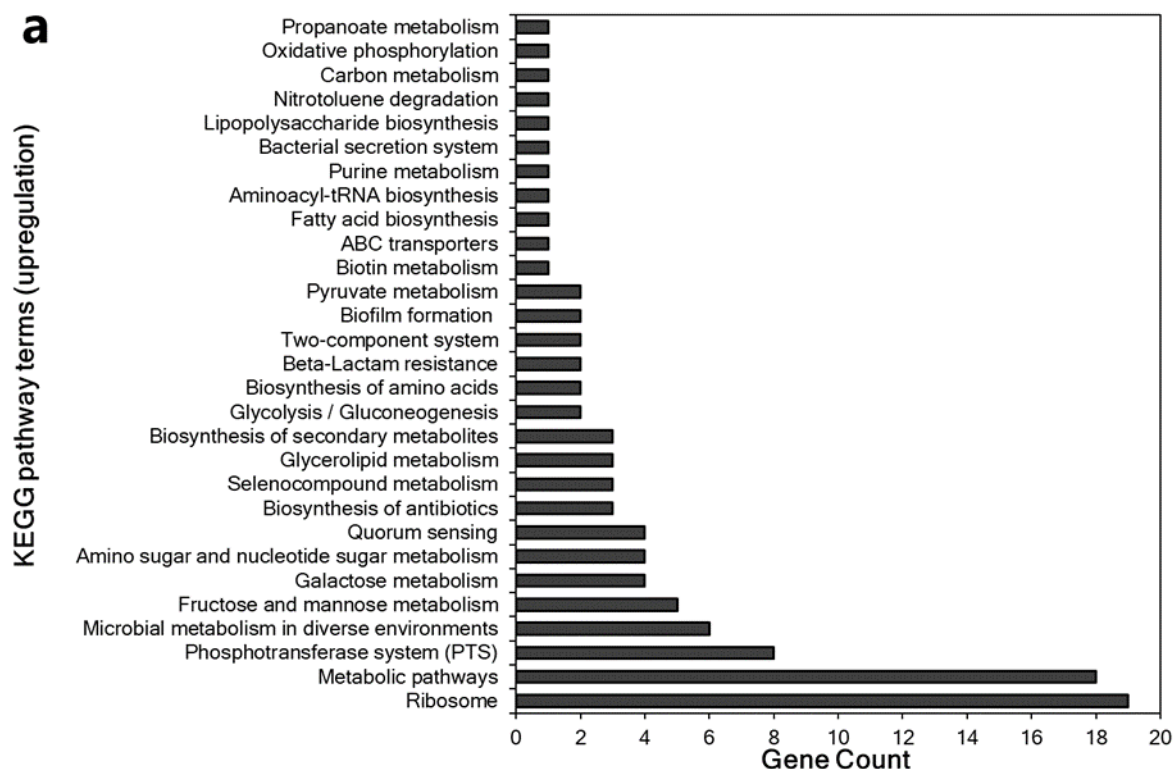
one of the two substrate-level phosphorylation steps that generate ATP in glycolysis (Malcovati, 1969). This makes *pykA* essential to our study. The critical repression of the two genes is one of the strong factors that lead to glucose deficiency in *hyb* operon mutant evidenced by previous reports, where their inactivation caused reduced growth and glucose metabolic activity, as mentioned above (Morita, 2003; Malcovati, 1969).

### 2.3.8. Transcriptomic analysis of hydrogenase operon mutants

Omics technologies can be effectively used to study cellular metabolism. In particular, transcriptomics can identify global changes in the metabolites that are directly related to cellular phenotypes (Kim, 2016). The transcriptomes of the mutants were assessed to evaluate the global transcriptional changes within the mutant cells. The KEGG pathway analysis was used to interpret the biological pathway-based information obtained from the transcriptome of the *hyb* operon mutant. Both the upregulated and downregulated pathways were evaluated and mapped (Fig. 2.10a and b). As a result, in comparison with upregulation, downregulation was found more affected as the downregulated pathways were detected with a higher gene count. The more affected metabolic pathways (specifically glycolysis), biosynthesis of secondary metabolites, transporters, and associated metabolisms such as carbon, may demonstrate the regulatory influences of Hyd-2 on them.

**Figure 2. 10** KEGG enrichment pathway analysis to investigate the most significant metabolic pathways affected by the deletion of *hyb* operon (below).

Top 30 pathways (based on the number of associated genes with that metabolic pathway) all those upregulated (a) and downregulated (b) are shown in the figure. The pathway analysis was performed using the transcriptomic data. The raw sequence data is available at NCBI under the SRA accession number PRJNA625150.



## 2.4. Discussion

However, there are a few reports investigating the whole operon of Hyd-1 (Menon,

1991; Laurinavichene, 2002), Hyd-2 (Laurinavichene, 2002), Hyd-3 (Sauter, 1992), and Hyd-4 (Andrews, 1997) available, extensive information on hydrogen metabolism results from the studies where mostly mutants of single-gene of hydrogenases were considered. As we hypothesized, mutational analysis by considering whole hydrogenase operon may not only help to understand their distinct functions in hydrogen metabolism but also provide an approach to minimize the probable partial complementation among them, as discussed earlier. In this study, therefore, four hydrogenase operon deletion mutants ( $\Deltahya$ ,  $\Deltahyb$ ,  $\Deltahyc$ , and  $\Deltahyf$ ) of *E. coli* were constructed to evaluate hydrogen metabolism in comparison to their respective single-gene deletion (gene encoding the large subunit) mutants ( $\DeltahyaB$ ,  $\DeltahybC$ ,  $\DeltahycE$ , and  $\DeltahyfG$ ) using glucose as the substrate. Since *hyb* operon mutant was found distinct from other operon mutants, the discussion here would be mainly focused on that. Significant low hydrogen production was found from *hyb* operon mutant compared to the other mutants, including its respective single-gene deletion mutants ( $\DeltahybC$ ) (Fig. 2.5a). This reduced hydrogen production probably is due to the bidirectional (possessing both hydrogen-producing and uptaking activities) nature of Hyd-2 (Sanchez-Torres, 2013). However, single-gene deletion did not cause a reduction in hydrogen production except *hycE*, in contrast to this, operon deletion reduced this production. The significance of this result lies in the fact that operon deletion causes more influential phenotypic effects than single gene deletions. Our study provides first-hand data where operon deletion was compared with its respective key single gene deletion. No hydrogen was detected from *hyc* operon and  $\DeltahycE$  mutants, which further confirms that the hydrogen synthesis in *E. coli* is mainly contributed by Hyd-3 activity under anaerobic fermentation of glucose (Maeda, 2008a). *E. coli* converts glucose into pyruvate, which is then converted into formate and lactate. After that, formate is converted to hydrogen and carbon dioxide by the FHL system (Trchounian, 2014). Various studies showed significantly improved hydrogen metabolism in *E. coli* using pyruvate and formate (Maeda, 2018; Vardar-Schara,

2008; Trchounian, 2012). Despite low hydrogen production from glucose, a comparatively increased hydrogen was detected from *hyb* mutants in the presence of pyruvate and formate than the parent strain (Fig. 2.5b). This was the first evidence indicating defective glucose metabolism that arose due to deletion of hydrogenase operon (*hyb* here) since this operon mutant was capable of metabolizing both formate and pyruvate, but not the glucose.

Second, remarkable altered phenotypic variation among operon deletion mutants in comparison with their respective single gene mutants was observed from their growth patterns measured under aerobic conditions, since significantly reduced growth rates were shown by operon deletion mutants (except *hya*) (Fig. 2.6a). However, the *hyf* operon mutant showed the lowest, *hyb* operon mutant was observed with notable reduced growth under aerobic conditions. Mirzoyan et al. (Mirzoyan, 2018) demonstrated that in *E. coli* mainly Hyd-4 (relatively more than Hyd-3) affects cell growth when lactose was used as a substrate, indicating its considerable role in growth. However, Hyd-4 enzyme is a subject for separate study and needs further deeper investigation, since limited information is available about this hydrogenase which might be due to its not transcribing nature at normal growth conditions (Trchounian, 2012). Whereas, in the case of anaerobic conditions, only *hyb* operon mutant was again found to exhibit significantly reduced growth compared to other mutants, including its single-gene mutant ( $\Delta hybC$ ) and parent strain (data not shown). It was interesting to find that this growth defect of *hyb* operon mutant was not observed in any other mutant of *hyb* ( $\Delta hybO$ ,  $\Delta hybA$ ,  $\Delta hybB$ ,  $\Delta hybC$ ,  $\Delta hybD$ ,  $\Delta hybE$ ,  $\Delta hybF$ , and  $\Delta hybG$ ) (Fig. 2.6c). This indicated that the critical growth defect was triggered by deleting the entire operon rather than every single gene of *hyb*. The ability of Hyd-2 to release excess reducing equivalent in the form of hydrogen (Szenk, 2017; Singh, 2009) appears to be affected which may have caused this reduced growth by the deletion of *hyb* operon.

Importantly, *hyb* operon mutant was found not able to consume glucose under both

aerobic and anaerobic conditions (Fig. 2.7a and b). This non-consumption of glucose defect of *hyb* could provide clear evidence of impaired glucose metabolism, which was unique to this mutant. Interestingly, the observed unchanged pH of the media of this mutant under similar conditions (Fig. 2.6b) could be explained only if there is some metabolic defect, as under healthy glucose metabolism; basically, the produced organic acids maintain the pH of the culture low (Russell, 1997). However, this glucose consumption deficiency of the *hyb* operon mutant may not be correlated to the growth defect, as reported earlier that there are separate metabolic pathways in *E. coli* for biomass and energy production (Carlson, 2004). Previously, it was reported that *hybC* deletion caused decreased hydrogen synthesis activity, growth rate, and glycerol consumption during glycerol metabolism (Sanchez-Torres, 2013; Trchounian, 2009). In this work, we could show that Hyd-2 activity is crucial and essential to have optimum biomass, hydrogen production, and glucose metabolism. It was reported previously that the inability of the cell to maintain internal pH showed decreased hydrogen production (Bowles et al. 1985), which may result in lowering the intracellular level of ATP, therefore inhibiting glucose uptake (Pandey, 2013; Nath, 2006). These reports support our findings coupled with Hyd-2.

Hydrogen production appears to be a necessary metabolic response to maintain redox balance (Pandey, 2013). The cellular redox generated during glucose metabolism helps in the establishment of a proton motive force across the membrane (Szenk, 2017). Released from the glycolysis pathway, the significant role of NADH (the reduced form of  $\text{NAD}^+$ ) is to supply electrons to the electron transport chain, which drives the production of ATP (Szenk, 2017). This recycling of reduced equivalent NADH to regenerate  $\text{NAD}^+$  is thus crucial for glycolysis to run during fermentation (Pandey, 2013). Therefore, these cofactors (ATP and NADH) play critical roles in a large number of bacterial cellular reactions and hold the potential to serve as targets for altering cellular metabolism (Holm, 2010). The significantly reduced level of total

ATP in *hyb* operon mutant (Fig. 2.8a) indicates the regulation of FOF1-ATPase by Hyd-2 through influencing the electron transport chain and proton motive force across the membrane. Since hydrogenases influence the gradients or proton motive forces across the membrane, therefore, their deletions may cause a distinct effect on ATP synthesis as suggested previously (Sapra, 2003), specifically Hyd-2 and Hyd-3, since both of these are noted as significant in hydrogen uptake and synthesis activities in *E. coli* (Shekhar, 2021). Since hydrogenases also act as electron valves, are involved in the quinone pool, where electrons are used for  $\text{NAD}^+$  reduction (Hallenbeck, 2002) indicating a need for redox balancing of metabolism is what drives hydrogen production by hydrogenases. The *hyb* operon mutant was found with a significantly low level of NADH, indicating a severely affected redox ratio (Fig. 2.8b). It has been previously reported that a slow glycolytic rate is by itself expected to limit the reduction of  $\text{NAD}^+$  to NADH in glycolysis (Christensen, 2014). The role of Hyd-2 is found crucial in maintaining  $[\text{NADH}]/[\text{NAD}^+]$  redox ratio and therefore the continuation of glycolysis during the fermentative process of *E. coli*. As reported previously, *E. coli* strains expressing NADH oxidase to lower cellular NADH concentrations and expressing F1F0-ATP synthase to hydrolyze ATP showed an increased glycolytic flux; furthermore, the overexpression of both their genes appeared to restore the redox or energy balance, respectively (Singh, 2009; Holm, 2010; Payot, 1998). Thus, Hyd-2 appeared to influence the activities of NADH oxidase and F1F0-ATP synthase in glucose metabolism. Hyd-2 provides electrons to the quinone pool of the electron transport chain in the membrane (Szenk, 2017; Pandey, 2013). These electrons are taken by fumarate and reduced to succinate by fumarate reductase, the step where NADH is oxidized to  $\text{NAD}^+$  (Pandey, 2013; Zhang, 2009). In this way, deletion of *hyb* operon sounds affects the level of ATP and NAD in the cell and therefore glucose metabolism (Szenk, 2017; Singh, 2009; Pandey, 2013).

The expression levels of all the glucose metabolism associated tested genes, namely,

*ptsG*, *crp*, *ldhA*, *pflB*, *ppc*, *pykA*, and *hycE* in *hyb* operon mutant, were detected to decreased (Fig. 2.9a and b). This reduction in the expression of these genes indicates their Hyd-2 mediated regulation and thus resulted in the impairment of glucose metabolism overall. Remarkably, the two genes, *ppc*, and *pykA*, were found significantly more crucial than other genes since their consequential lessen expression. Both of these genes have been reported previously for their essential functions in glucose metabolism and growth (Millard, 1996; Morita, 2003; Malcovati, 1969; Siddiquee, 2004). In brief, the glucose consumption capability of a *ppc* gene inactivated mutant was found compromised along with slower growth than the parent strain (Morita, 2003). Moreover, PEP accumulation along with allosteric inhibition of some glycolytic enzymes was characteristically found in this mutant, which in turn also affects the activity of other enzymes and influences the glycolytic flux, and led to slower growth and lower glucose uptake rate (Malcovati, 1969). In the case of *pykA* gene, this gene was also reported to control the metabolic flux in glycolysis and ATP generation (Malcovati, 1969; Siddiquee, 2004). Furthermore, the more down-regulated KEGG pathways terms associated with *E. coli* metabolisms (specifically glycolysis) point to a regulatory or influencing role of Hyd-2 on the metabolism (Fig. 2.10a and b). This may indicate the involvement of Hyd-2 in the regulation of other (than ATP and NAD) cellular metabolic activities in *E. coli*, further investigation, therefore, is advisable. So, in this view, the appeared defect in glucose metabolism by the deletion of *hyb* operon seems to be a dysfunction that emerged as a collective phenotypic variation in *E. coli* where ATP and NADH are involved as crucial factors.

## 2.5. Conclusion

In conclusion, more influential phenotypic effects could be evaluated from operon deletion in comparison to their respective single gene deletions, since in the study, hydrogen metabolism and growth were found most affected phenotypes that emerged due to whole operon deletions. Among all four hydrogenases of *E. coli*, Hyd-2 is marked crucial for growth and

glucose metabolism along with hydrogen production. The hydrogenases appeared significant in the maintenance of proton gradient across the membrane which might be by reducing protons released through metabolism to hydrogen. Since, as reported, hydrogenase acts as an electron valve and is involved in the quinone pool, where electrons are used for  $\text{NAD}^+$  reduction activity and their functioning are dependent on the FOF1-ATPase activity; hydrogenases were expected to contribute dissimilar gradients and therefore shown a distinct effect on ATP synthesis and NADH content in the cell. Hyd-2 as its bidirectional nature and efficiency in both hydrogen uptake and synthesis activities seemed most crucial for the gradient generation across the membrane, therefore, influencing ATP and NADH most. A significantly decreased expression of *ppc* and *pykA*, indicates their regulation by Hyd-2 and consequently, glucose consumption. Therefore, the key role of Hyd-2 is not only hydrogen metabolism but also energy and redox balance maintenance in *E. coli* cells. Whereas global transcriptomic analysis indicates the plausible roles of Hyd-2 in other metabolic pathways of *E. coli* which are encouraged to be researched further.

## CHAPTER 3

# INVESTIGATION OF THE ABSOLUTE ROLE OF EACH HYDROGENASE OPERON IN HYDROGEN METABOLISM BY CONSTRUCTING THE *ESCHERICHIA COLI* STRAINS POSSESSING ONLY A SINGLE HYDROGENASE OPERON IN THE GENOME

### 3.1. Introduction

Isozymes are well known to have the same chemical/catalytic reaction despite of their different amino acid sequence (Ballantine, 1985). For example, the three isoforms of carnitine palmitoyltransferase 1 that catalyze the formation of acylcarnitine in mammals and the two isozymes that contribute to the pyruvate kinase activity in *Vibrio cholera* (Hada, 2014; Guerrero-Mendiola, 2017). Furthermore, the generation and analysis of genetically modified mice have revealed the unexpectedly diverse physiological functions of 13 Phospholipase C (PLC) isozymes in mammals (Nakamura, 2017). Interestingly, all the PLC isozymes can catalyze the same reaction; however, each PLC isozyme has unique physiological functions also (Nakamura, 2017). Hydrogenases have been reported for their isozymatic nature, which indicates their activity based on cross interaction between them (Bagyinka, 2014).

*Escherichia coli* (*E. coli*) has 4 hydrogenase isozymes (NiFe-type) which catalyze the reversible reaction of hydrogen to protons and electrons ( $2\text{H}^+ + 2\text{e}^- \rightleftharpoons \text{H}_2$ ) (Maeda, 2018). These hydrogenases are encoded by different operons: hydrogenase 1 (Hyd-1) encoded by *hyaABCDEF* operon, hydrogenase 2 (Hyd-2) encoded by *hybOABCDEFG* operon, hydrogenase 3 (Hyd-3) encoded by *hycABCDEFGH* operon, and hydrogenase 4 (Hyd-4) encoded by *hyfABCDEFGH* operon (Maeda, 2018; Dubini, 2002). Hyd-1 and Hyd-2 are the membranes associated with hydrogen-oxidizing isozymes (Sawers, 1986). Along with the tremendous efficiency as a biocatalyst for hydrogen fuel (Kim, 2012), hydrogenases have been proposed to serve the hydrogen recycling function, indicating their crucial role in facilitating

redox balance (Sawers, 1986; Juanita, 2009). Although both of them operate preferentially under different conditions, on the level of gene expression and enzyme activity, a metabolic cross-talk between them has been proposed (Ballantine, 1985; Blokesch, 2001). The large and small subunits of both Hyd-1 (*hyaB*) and Hyd-2 (*hybC*) share sequence homology, which is a probable cause of that cross-talk (Vardar-Schara, 2008). Hyd-3 has hydrogen production activity via the catalysis by the formate hydrogen lyase (FHL) complex where it works together with formate dehydrogenase-H (Fdh-H encoded by *fdhF*) (Maeda, 2007; Maeda, 2008). Like Hyd-1 and Hyd-2, Hyd-3 also operates in a reverse direction having a significant hydrogen uptake activity (Maeda, 2007). Hyd-4 was found to produce and consume hydrogen by the influence of glucose concentration (Mirzoyan, 2017; Trchounian, 2014; Petrosyan, 2020; Mirzoyan, 2018a; Mirzoyan, 2018b), whereas the function of Hyd-4 is also considered silent (Sawers, 1986; Self, 2004). The Hyd-4 operon (*hyfABCDEFGHIRfocB*) codes for a hydrogenase resembling the FHL complex (Andrews, 1997). Nine genes of *hyf* operon encode subunits that are homologous to seven Hyd-3 subunits, whereas the expression patterns of the *hyc* and *hyf* operons differ considerably (Andrews, 1997). Despite a relatively good understanding of the catalytic mechanism, the role of hydrogenases in hydrogen metabolism has still not been completely understood because of some inconsistent reports regarding their functions in *E. coli* (Sawers, 1986; Trchounian, 2012).

In particular, the hydrogen contributory role of hydrogenases in *E. coli* seems dissimilar to glucose or glycerol as a carbon source (Sawers, 1986; Juanita, 2009; Mirzoyan, 2018a; Trchounian, 2012) because of their separate anaerobic metabolism (Fig. 3.1).

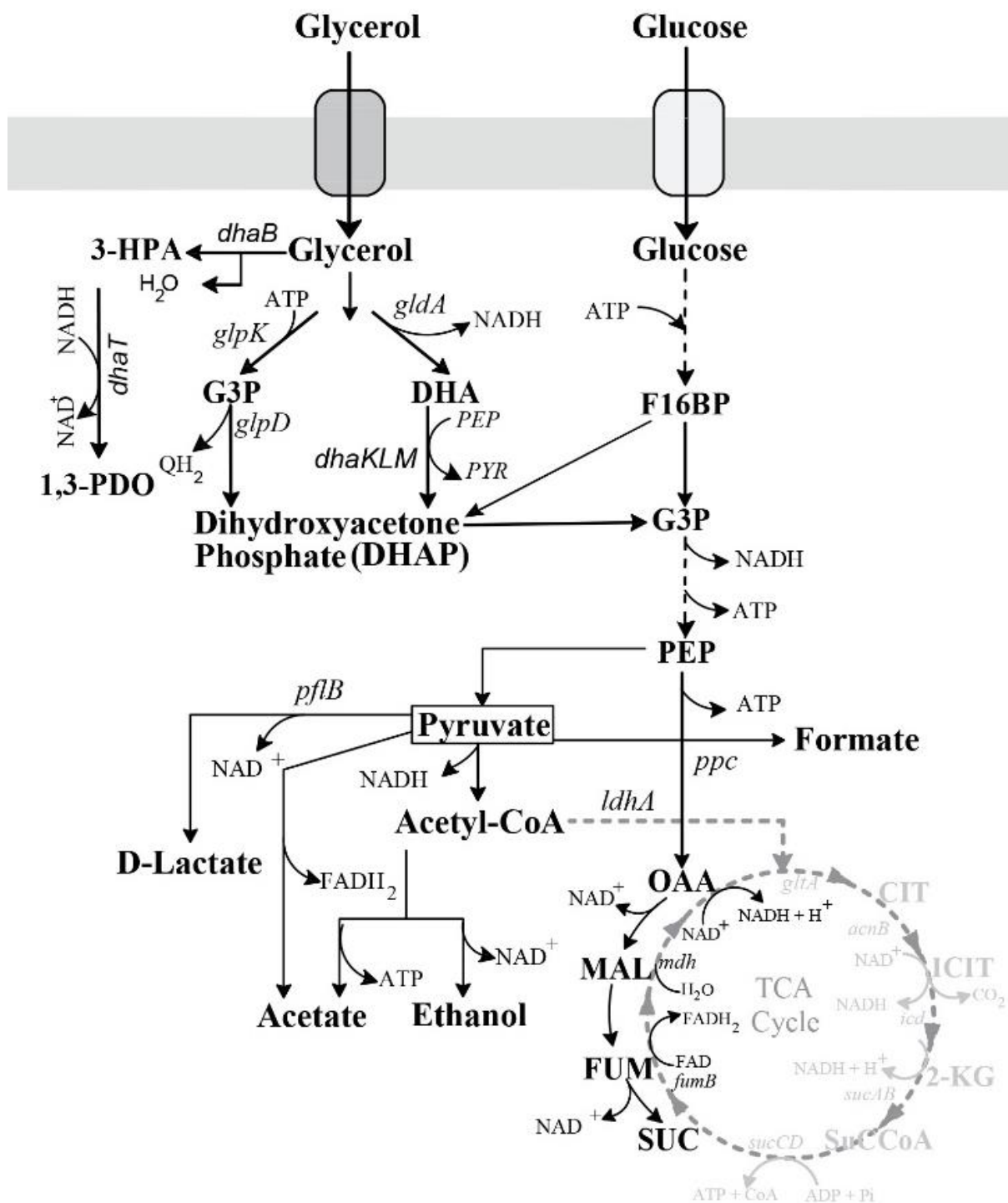


**Figure 3. 1** Glucose and glycerol metabolic pathways in *E. coli*.

Glycerol is converted to metabolites through the 1,3-propanediol pathway, whereas the glycolytic pathway is used for glucose (Trchounian, 2012). Therefore, hydrogen metabolism is different when glycerol is used as a carbon source due to the repression or the expression of

Chandra SHEKHAR (Maeda Lab.)

some genes, which are highly dependent on the presence of glucose (Sawers, 1986; Vardar-Schara, 2008; Trchounian, 2012). Moreover, the transport mechanism of  $H^+$  in glycerol is also different from that of glucose (Juanita, 2009; Trchounian, 2012). Along with the carbon source, external pH is also one of the influencing factors for the activity of hydrogenases (Petrosyan, 2020; Mirzoyan, 2018b; Trchounian, 2012; Sinha, 2011). Although the metabolic function seems similar during the glycerol and glucose metabolisms at a low external pH, hydrogen production from glycerol can be altered at a slightly alkaline pH condition (Petrosyan, 2020; Trchounian, 2012). Moreover, Fdh-H activity is lowered by the change from pH 7.5 to pH 6.0 (Petrosyan, 2020; Mirzoyan, 2018b; Axley, 1990).

From the 4-hydrogenase isozymes in *E. coli*, Hyd-1 is similar to Hyd-2, and Hyd-3 is similar to Hyd-4, the detailed functions are still disputable to consider because the purification of each hydrogenase is technically difficult to verify the activity of each hydrogenase isozyme one-by-one (Vardar-Schara, 2008; Petrosyan, 2020; Mirzoyan, 2018a). On the other hand, the functional analyses using mutants could be one of the powerful approaches to understanding the functions of the 4-hydrogenase isozymes; however, the mutant in which only a single gene could be inactivated was used for its functional analysis to date. This approach still leaves a big question about how the remaining active genes in each operon will influence the functions of hydrogen metabolism.

In this study, several hydrogenase operon-deletion mutants have been constructed: four triple operon-deletion mutants having only the single hydrogenase in the genome (by deleting the other 3 hydrogenases) and one quadruple operon-deletion mutant, which is devoid of all hydrogenases (by deleting all 4 hydrogenase operons) to evaluate a clear *in-vivo* function of each hydrogenase in *E. coli*. In the work, the hydrogen production of each solely present hydrogenase could be assessed without the interference of other hydrogenases. Furthermore, the growth and hydrogen uptake capabilities of the absolute hydrogenases were analyzed. Our

study reconfirmed that Hyd-3 is a principal hydrogen producer and Hyd-2 is also important in hydrogen synthesis. Our study also confirms the hydrogen uptake abilities of all the hydrogenases of *E. coli*. The hydrogenase operon-deletion mutants constructed in this study may provide a good tool for further research of hydrogenases.

## **3.2. Materials and Methods**

### **3.2.1. Bacterial strains, media, and growth conditions**

The strains and mutants of this study are listed in Table 3.1. *E. coli* K-12 BW25113 (parent strain, abbreviated as PS) and all the mutants were initially streaked from -70 °C glycerol stocks on Luria-Bertani (LB) agar plates (with kanamycin, 50 µg/mL, in case of mutants) (Sambrook, 1989). Fresh cultures were prepared by inoculating every single colony in 250 mL flask (Iwaki, Japan) containing 50 mL of LB with kanamycin for mutant or without kanamycin for parent strain at 37 °C with shaking at 120 rpm using bio-shaker (BR-180LF, Taitec). All experiments were conducted by taking the samples at least in triplicates. The glucose medium used was LB-based media containing 10 g/L Bacto Tryptone, 5 g/L yeast extract, and 5 g/L NaCl, with 2.25% glucose (Maeda, 2007; Yasin, 2013). Glycerol minimal medium used was supplemented with 10 g/L glycerol, 0.172 mg/L NiCl<sub>2</sub>, and 0.02 mg/L Na<sub>2</sub>SeO<sub>3</sub> (Trchounian, 2013). The alkaline (pH 7.5) media was mainly used for the assays; however, acidic media (pH 6.5) was also employed for comparative analysis whenever required. For transduction work, bottom plates, as well as LB plates, consisted of tryptone 10 g/L, yeast extract 1 g/L, NaCl 8 g/L, and agar 10 g/L, whereas the top agar media contain tryptone 10 g/L, yeast extract 1 g/L, NaCl 8 g/L, and agar 8 g/L. Both of them were added with 1 M CaCl<sub>2</sub> (final concentration: 2 mM) and 50% glucose (final concentration: 0.1%) after autoclave. The final concentrations of each antibiotic used in LB-Ampicillin, LB-Chloramphenicol, LB-Kanamycin media or plates were 50 µg/mL of ampicillin, 30 µg/mL of chloramphenicol, and 50 µg/mL of kanamycin, respectively. Carbenicillin (10 µg/mL) was also used in place of ampicillin

whenever necessary. Cell growth was monitored at 600 nm with a UV/VIS spectrophotometer (JASCO V-530) using at least two independent cultures for each strain. The total cell protein values were quantified based on optical density (OD) and total proteins in parent strain (Protein assay kit, Sigma Diagnostics, St. Louis, MO, USA), 0.22 mg/OD/mL. Chemicals were purchased from Wako Pure Chemical Industries, Ltd. (Osaka, Japan), Dojindo Molecular Technologies, Inc. (Kumamoto, Japan), Sigma Al-rich Co. Llc (Tokyo, Japan), and Nacalai Tesque, Inc (Kyoto, Japan).

**Table 3. 1 The strains and plasmids used in this study**

Strain/plasmid	Genotype/relevant characteristics	Reference
<i>E. coli</i> BW25113	F <sup>-</sup> Δ( <i>araD-araB</i> )567Δ <i>lacZ</i> 4787 (::rrnB-3)λ <sup>-</sup> <i>rph-1</i> Δ( <i>rhaD-rhaB</i> ) 568 <i>hsdR</i> 514; parental strain for the Keio collection.	Yale Coli Genetic Stock center
pKD4	PCR template containing FRT-kanamycin-FRT cassette	Yale Coli Genetic Stock Center
pKD46	Red recombinase expression system	Yale Coli Genetic Stock Center
pCP20	Amp <sup>R</sup> and Cm <sup>R</sup> plasmid; thermal induction of FLP synthesis	(Datsenko, 2000)
pBR322	Amp <sup>R</sup> and Tet <sup>R</sup> cloning vector	(Bolivar, 1977)
pBR322- <i>hyb</i>	pBR322 vector containing <i>hyb</i> operon	This study
pBR322- <i>hyc</i>	pBR322 vector containing <i>hyc</i> operon	This study
<i>E. coli</i> BW25113 Δ <sup>a</sup> <i>hyaA-F</i> :: <sup>b</sup> <i>kan</i> <sup>d</sup>	Hyd-1 operon deleted mutant, kan <sup>+e</sup>	This study
<i>E. coli</i> BW25113 Δ <i>hybO-F</i> :: <i>kan</i>	Hyd-2 operon deleted mutant, kan <sup>+</sup>	This study

<i>E. coli</i> BW25113 $\Delta hycA-I::kan$	Hyd-3 operon deleted mutant, kan <sup>+</sup>	This study
<i>E. coli</i> BW25113 $\Delta hyfA-R::kan$	Hyd-4 operon deleted mutant, kan <sup>+</sup>	This study
<i>E. coli</i> BW25113 $\Delta fdhF::kan$	<i>fdhF</i> gene deleted mutant, kan <sup>+</sup>	(Yasin, 2013)
<i>E. coli</i> BW25113 $\Delta hyaA-F \Delta kan$	Hyd-1 operon deleted mutant, kan <sup>-f</sup>	This study
<i>E. coli</i> BW25113 $\Delta hybO-F \Delta kan$	Hyd-2 operon deleted mutant, kan <sup>-</sup>	This study
<i>E. coli</i> BW25113 $\Delta hycA-I \Delta kan$	Hyd-3 operon deleted mutant, kan <sup>-</sup>	This study
<i>E. coli</i> BW25113 $\Delta hyfA-R \Delta kan$	Hyd-4 operon deleted mutant, kan <sup>-</sup>	This study
<i>E. coli</i> BW25113 $\Delta hya \Delta hyb::kan$	Hyd-1 and Hyd-2 operons deleted mutant, kan <sup>+</sup>	This study
<i>E. coli</i> BW25113 $\Delta hya \Delta hyc::kan$	Hyd-1 and Hyd-3 operons deleted mutant, kan <sup>+</sup>	This study
<i>E. coli</i> BW25113 $\Delta hya \Delta hyf::kan$	Hyd-1 and Hyd-4 operons deleted mutant, kan <sup>+</sup>	This study
<i>E. coli</i> BW25113 $\Delta hyb \Delta hyc::kan$	Hyd-2 and Hyd-3 operons deleted mutant, kan <sup>+</sup>	This study
<i>E. coli</i> BW25113 $\Delta hyb \Delta hyf::kan$	Hyd-2 and Hyd-4 operons deleted mutant, kan <sup>+</sup>	This study
<i>E. coli</i> BW25113 $\Delta hyc \Delta hyf::kan$	Hyd-3 and Hyd-4 operons deleted mutant, kan <sup>+</sup>	This study
<i>E. coli</i> BW25113 $\Delta hya \Delta hyb \Delta kan$	Hyd-1 and Hyd-2 operons deleted mutant, kan <sup>-</sup>	This study
<i>E. coli</i> BW25113 $\Delta hya \Delta hyc \Delta kan$	Hyd-1 and Hyd-3 operons deleted mutant, kan <sup>-</sup>	This study
<i>E. coli</i> BW25113 $\Delta hya \Delta hyf \Delta kan$	Hyd-1 and Hyd-4 operons deleted mutant, kan <sup>-</sup>	This study

<i>E. coli</i> BW25113 $\Delta hyb \Delta hyc \Delta kan$	Hyd-2 and Hyd-3 operons deleted mutant, kan <sup>-</sup>	This study
<i>E. coli</i> BW25113 $\Delta hyb \Delta hyf \Delta kan$	Hyd-2 and Hyd-4 operons deleted mutant, kan <sup>-</sup>	This study
<i>E. coli</i> BW25113 $\Delta hyc \Delta hyf \Delta kan$	Hyd-3 and Hyd-4 operons deleted mutant, kan <sup>-</sup>	This study
<i>E. coli</i> BW25113 $\Delta hya \Delta hyb \Delta hyc::kan$	Hyd-1, Hyd-2 and Hyd-3 operons deleted mutant, kan <sup>+</sup>	This study
<i>E. coli</i> BW25113 $\Delta hyaB \Delta hybC \Delta hycE::kan$	Large subunit genes of Hyd-1, Hyd-2 and Hyd-3 operons deleted mutant, kan <sup>+</sup>	(Maeda, 2007)
<i>E. coli</i> BW25113 $\Delta hya \Delta hyb \Delta hyf::kan$	Hyd-1, Hyd-2 and Hyd-4 operons deleted mutant, kan <sup>+</sup>	This study
<i>E. coli</i> BW25113 $\Delta hya \Delta hyc \Delta hyf::kan$	Hyd-1, Hyd-3 and Hyd-4 operons deleted mutant, kan <sup>+</sup>	This study
<i>E. coli</i> BW25113 $\Delta hya \Delta hyc \Delta hyf::kan$	Hyd-1, Hyd-3 and Hyd-4 operons deleted mutant, kan <sup>+</sup>	This study
<i>E. coli</i> BW25113 $\Delta hya \Delta hyc \Delta hyf \Delta kan$	Hyd-1, Hyd-3 and Hyd-4 operons deleted mutant, kan <sup>-</sup>	This study
<i>E. coli</i> BW25113 $\Delta hya \Delta hyc \Delta hyf \Delta fdhF::kan$	Hyd-1, Hyd-3 and Hyd-4 operons and <i>fdhF</i> gene deleted mutant, kan <sup>+</sup>	This study
<i>E. coli</i> BW25113 $\Delta hya \Delta hyb \Delta hyc \Delta hyf::kan$	Hyd-1, Hyd-2, Hyd-3, and Hyd-4 operons deleted mutant, kan <sup>+</sup>	This study

---

a and b:  $\Delta$  and  $::$  represents “deletion” and “replaced by gene,” respectively.

c: A-F, O-F, A-I, and A-R represents the “from and to” deleted segment of *hya*, *hyb*, *hyc*, and *hyf* operons, respectively.

d: *kan* denotes kanamycin resistance gene.

e: kan<sup>+</sup> denotes ‘with’ kanamycin resistance gene

f: kan<sup>-</sup> denotes ‘without’ kanamycin resistance gene

### 3.2.2. Making hydrogenase operons-deletion mutants

Four mutants in each single hydrogenase operon were constructed according to the method reported by Datsenko and Wanner, 2000 (Datsenko, 2000). In brief, each 1.4 kb PCR product to delete the target hydrogenase operon was prepared by using a 70-nt-length primer set that included 50-nt homology extensions and 20-nt priming sequences (FRT-flanked kanamycin resistance cassette) for pKD4, which was used as a template DNA. Electroporation was done through 0.1 cm cuvette at 1.8 kV and 200 ohm according to the manufacturer's instructions (Bio-Rad) by using 50  $\mu$ L of electrocompetent cells (containing pKD46) and 100 ng of the purified PCR product. The shocked cells were added to 1 mL LB, incubated for 1 h at 37 °C, and then one-half was spread onto agar containing kanamycin to select kanamycin-resistant transformants (mutants).

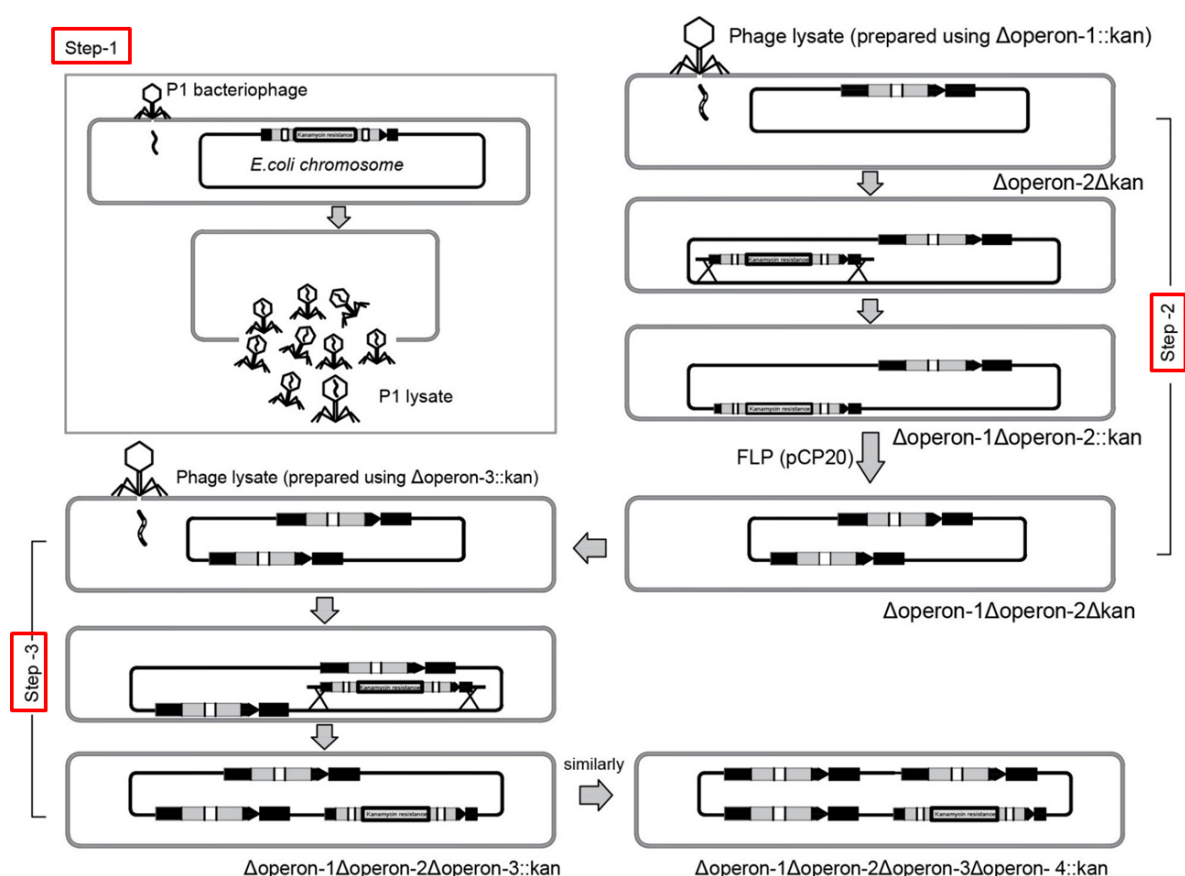
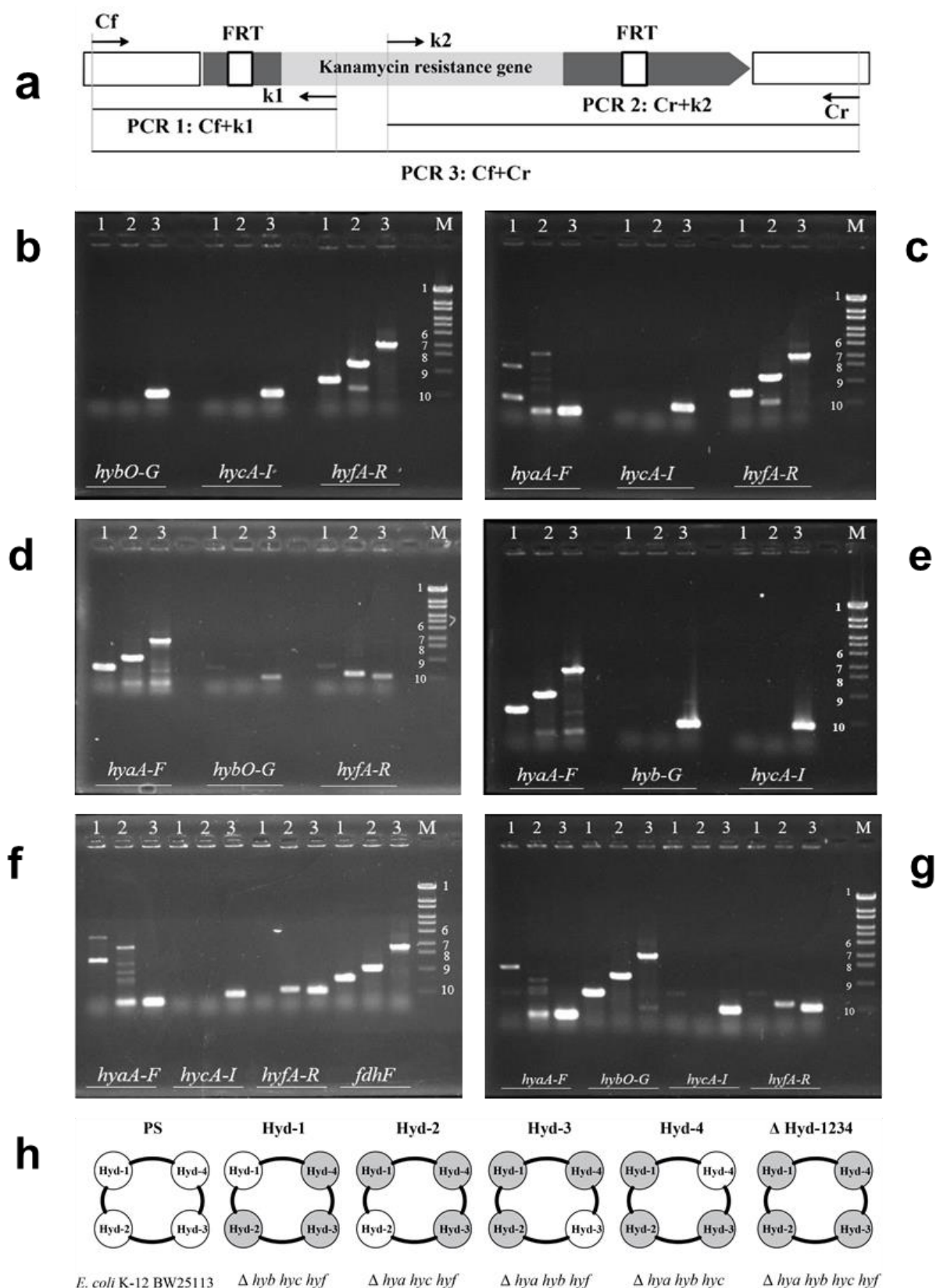


**Figure 3. 2** Illustration of the methodology employed for constructing multiple operon deletion mutants.

Once all the single hydrogenase operon deleted (operon replaced by FRT-flanked kanamycin resistance cassette) mutants were constructed and verified, their kanamycin resistance gene was eliminated as described previously by expressing the FLP recombinase protein from pCP20, as an FLP recognition target that is excised by FLP recombinase flanks each kanamycin resistance gene (Cherepanov, 1995). The sequential rounds of P1 transduction were performed to introduce multiple hydrogenase operon deletions into a single strain (Maeda, 2007; Windle, 1986) (Fig. 3.2). All the strains constructed during repeated rounds of P1 transduction are listed in Table 3.1.

### **3.2.3. Verification of hydrogenase operon deletion**

Three PCR reactions were conducted to evaluate the structure of all the hydrogenase operon mutants, as previously explained (Datsenko, 2000) (Fig. 3.3). Two specific primers for the kanamycin-resistant gene (k1 and k2) were used to confirm the insertion to the target hydrogenase operon location. Two reactions were performed by using upstream and downstream region-specific primers of a targeted operon with k1 or k2 to confirm for both new junction fragments. The third reaction was carried out with the flanking upstream and downstream region-specific primers only to verify simultaneous loss of the parental operon fragment and gain of the new mutant-specific fragment. A fresh colony of each mutant was suspended in 20  $\mu$ L water, from which 2  $\mu$ L was used in the PCR mixture after boiling the cells at 100 °C for 5 min. The PCR reaction was carried out using Quick Taq® HS DyeMix reagent (TOYOBO CO., Ltd.). The PCR reaction mixture consists of 12.5  $\mu$ L 2X Quick Taq® HS DyeMix buffer, 0.75  $\mu$ L each primer (20 mM). The total volume was adjusted up to 25  $\mu$ L by sterilized water, and the products were amplified for 30 cycles (initial denaturation at 95 °C for 2 min, denaturation at 95 °C for 30 sec, annealing at 54 °C for 30 sec, elongation at 68 °C for 1 min and a final extension at 68 °C for 10 min). Control colonies were also tested side-by-side. All primers used in this study are listed in Table 3.2.



primer (Datsenko, 2000). The three PCRs were performed: PCR 1, Cf + k1 (to confirm the insertion of kanamycin resistance gene in place of a targeted operon); PCR 2, k2 + Cr (to confirm the insertion of kanamycin resistance gene in place of a targeted operon); PCR 3, Cf + Cr (to confirm the complete deletion of targeted operon and/or the insertion of a kanamycin resistance gene at that place) (Datsenko, 2000). (b-g) Three PCR reactions using each triple hydrogenase operon deleted mutant. Lane 1, Cf + k1; lane 2, k2 + Cr; lane 3, Cf + Cr; lane M, marker 6 (OneSTEP; Nippon Gene, Japan). From B to G;  $\Delta hyb hyc hyf$ ,  $\Delta hya hyc hyf$ ,  $\Delta hya hyb hyf$ ,  $\Delta hya hyb hyc$ ,  $\Delta hya hyc hyf \Delta fdhF$ , and  $\Delta hya hyb hyc hyf$ , respectively. The numbered bands as 1, 6, 7, 8, 9, and 10 on the marker lane (M) indicate 19.33, 2.69, 1.88, 1.49, 0.93, and 0.42 kbp sizes, respectively.

**Table 3. 2 List of primers used in this study**

Primer	Significance	Sequence (5'-3')	Reference
<b>Primers used in making the mutants</b>			
<i>Hya-F</i>	To delete	CATAAGCGCCCGGTGTCCTGCCGGTGTCTCGCAAGGA	This study
	Hyd-1 operon	GGAGAGACGTGCGATGTGTAGGCTGGAGCTGCTTC	
<i>Hya-R</i>		ATTCGCCGATTGCGATATTCATAAGACTGAAAGCG ATACTTACCGTCTTTCATATGAATATCCTCCTTAG	
<i>Hyb-F</i>	To delete	TGCGATTGAGGCAAAATATATGCCAGGTCTTCGCA	This study
	Hyd-2 operon	ACGGAATAACTATAAGTGTAGGCTGGAGCTGCTTC	
<i>Hyb-R</i>		ATGCCTGATGCGACGCTGCCGCGTCTTATCAGGCCT ACGAAAGCTAATCACATATGAATATCCTCCTTAG	
<i>Hyc-F</i>	To delete	GCACAAAAAATGCTTAAAGCTGGCATCTCTGTAA	This study
	Hyd-3 operon	ACGGGTAACCTGACAGTGTAGGCTGGAGCTGCTTC	
<i>Hyc-R</i>		GCTGGTTCACCCCATCAAGAACATCCCTGTCCTGAT TCCTTAATGAAAAACATATGAATATCCTCCTTAG	
<i>Hyf-F</i>	To delete	CTTTATGCAATATGAAATGCAATGTTTCATATCATT	This study
	Hyd-4 operon	TTCAAGGAGCCGACGTGTAGGCTGGAGCTGCTTC	
<i>Hyf-R</i>		CGCGCAAGAATAATCTTCAGCCCGACGAACTGTTT CGCCGGGCTGATTTTCATATGAATATCCTCCTTAG	
<b>Primers used in confirmation of the mutation</b>			
k1	Confirmation of kanamycin resistance gene	CAGTCATAGCCGAATAGCCT	(Datsenko , 2000)
k2	Confirmation of kanamycin	CGGTGCCCTGAATGAACTGC	

	resistance		
	gene		
<i>Hya</i> -Fc	To confirm	ACAATACTTTCTGGCGACGTG	This study
<i>Hya</i> -Rc	Hyd-1 operon deletion	AAAAGTGATACAGCGCGGTC	
<i>Hyb</i> -Fc	To confirm	CACTAATGCTTCTTCCCTTCGT	This study
<i>Hyb</i> -Rc	Hyd-2 operon deletion	GACGCCAGTGATTTCGAGAC	
<i>Hyc</i> -Fc	To confirm	TGTTGATTATCCCTGCGGTG	This study
<i>Hyc</i> -Rc	Hyd-3 operon deletion	AGTGATTGCCAGTAATGGGGA	
<i>Hyf</i> -Fc	To confirm	TCACATTCTCGCTTTCCCCT	This study
<i>Hyf</i> -Rc	Hyd-4 operon deletion	ATCCGATCGCCATAAACACG	
<i>fdhF</i> -Fc	To confirm	GTCACGCGGTATTTTCGTTTC	This study
<i>fdhF</i> -Rc	the <i>fdhF</i> mutation	GGCCTCTGCTGCCTTTAAATA	
<b>Primers used in cloning of <i>hyb</i> and <i>hyc</i> operons</b>			
Hyb-F-		ATGCTTCTTCCCTTCGTTTTAGCGCCCCGCCGCAGT	This study
hybOp	Cloning <i>hyb</i>	ATCATGATATCGAT	
Hyb-R-	operon	AATGCCTGATGCGAGCTCGCCGCGTCTTATCAGGC	
SacI		CTACGAAAGCTAATC	
Hyc-F-		TTAATAACAATAAATTAAGTTGGCACAAAAAAT	This study
hycAp	Cloning <i>hyc</i>	GCTTAAAGCTGGCAT	
Hyc-R-	operon	TTAGCATTTGGGAGCTCAGCTGGTTCACCCCATCAA	
SacI		GAACATCCCTGTCC	

\*Fc and Rc represent forward, and reverse primers used for mutation confirmation respectively.

### 3.2.4. Fermentation and hydrogen assessment

The overnight aerobic culture was adjusted to OD<sub>600</sub> of 0.05 in fresh LB medium (25 mL) in the crimp-top vial (65 mL) supplemented with glucose (2.25%) inside the anaerobic system (Forma anaerobic system 1025, Thermo Scientific). The cultures were sparged for 5 min with nitrogen to remove oxygen after the vials were sealed with rubber and an aluminium cap. Three separate cultures were prepared and assayed for their hydrogen productivity after

the incubation at 37 °C, 120 rpm. The amount of hydrogen generated in the headspace was measured by gas chromatography (GC) using a 6890 gas chromatograph equipped with an AT 19095P-NS5 column (Agilent Technologies Inc., Santa Clara, CA). Total protein was calculated as 0.22 mg/mL/OD<sub>600</sub>.

The amount of hydrogen generated was calculated by using the following equation (Taifor, 2017):

Hydrogen production (μmol) =

Peak area × Standard hydrogen curve × 65,000 μL (headspace)/100 μL (injection)

For the growth analysis, cell turbidity was measured at 600 nm wavelength during the growth at different time durations. Moreover, change in pH was also monitored from all the anaerobic cultures using at least three separate cultures.

### **3.2.5. Hydrogen production and growth rates estimation of single-gene and operon-deletion mutants of hydrogenases**

The hydrogen productivity of all eight mutants was examined using the medium of pH 6.5 supplemented with glucose as substrate, as mentioned above. For the specific growth rates, three independent fresh cultures were prepared to have OD less than 0.05 using overnight aerobically grown strains. The cell turbidity of the strains was recorded at 600 nm at the interval of 30 min on growing aerobically at 37 °C. Only the values belonging to the exponential part of growth were taken to calculate the specific growth rate (μ) (Laffly, 2010).

### **3.2.6. Construction of pBR322/*hybOABCDEFGF* and pBR322/*hycABCDEFGHI* and hydrogen productivity complementation assay**

Construction of each recombinant vector containing *hyb* or *hyc* operon and complementation was performed as explained previously (Maeda, 2007; Laffly, 2010). pBR322 was used as a cloning vector (Bolivar, 1977). In brief, *E. coli* BW25113 genomic DNA was obtained using DNeasy UltraClean Microbial Kit (Qiagen). The 6746bp and 8005bp

chromosomal DNA fragments encoding *hybOABCDEFG* and *hycABCDEFGHI* respectively were amplified using Phusion High-Fidelity DNA polymerase (New England BioLabs) with the phosphorylated primers mentioned in Table 3.2 with 30 cycles and 68°C annealing on a thermal cycler (Bio-Rad). Forward and reverse primers to amplify the operon were designed to contain the native promoter and *SacI* restriction site, respectively. The PCR product was then purified with QIAquick PCR purification kit (Qiagen) and cloned into the *EcoRV* site of pBR322. The resulting recombinant plasmids (11,107 bp with *hyb* and 12,366 bp with *hyc*) were extracted using QIAprep spin miniprep kit (Qiagen) and verified by sequence-specific restriction enzyme digestions and sequencing (Fig. 3.4).

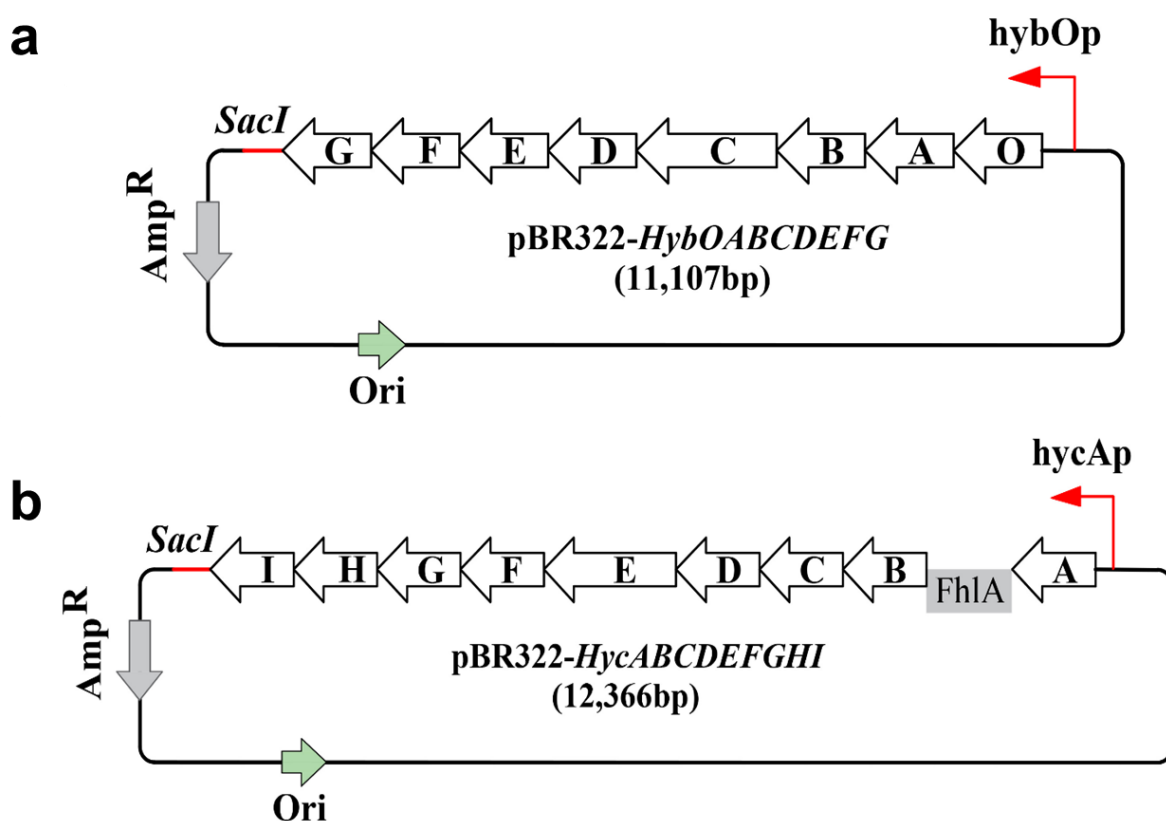


**Figure 3. 4** The final structure of the cloning vector containing *hyb* (a) and *hyc* (b). *Amp<sup>R</sup>* indicates ampicillin resistance gene. *SacI* restriction site and native promoters of *hyb* and *hyc* (*hybOp* and *hycAp*, respectively) are indicated in red.

The verified plasmids containing *hyb* or *hyc* operon were electroporated into the quadruple operon mutant ( $\Delta hya$  *hyb* *hyc* *hyf*) as mentioned above (Fig. 3.5). The successful transformants were selected from LB- ampicillin agar plates. The parent strain and quadruple

mutants containing the empty vector, pBR322 (the plasmid without cloning each operon) were also prepared for comparative evaluation. Single colonies were used to prepare overnight aerobic cultures, which were used for anaerobic fermentation using glucose or glycerol as a substrate in the medium at pH 7.5. Hydrogen production was evaluated as mentioned above.

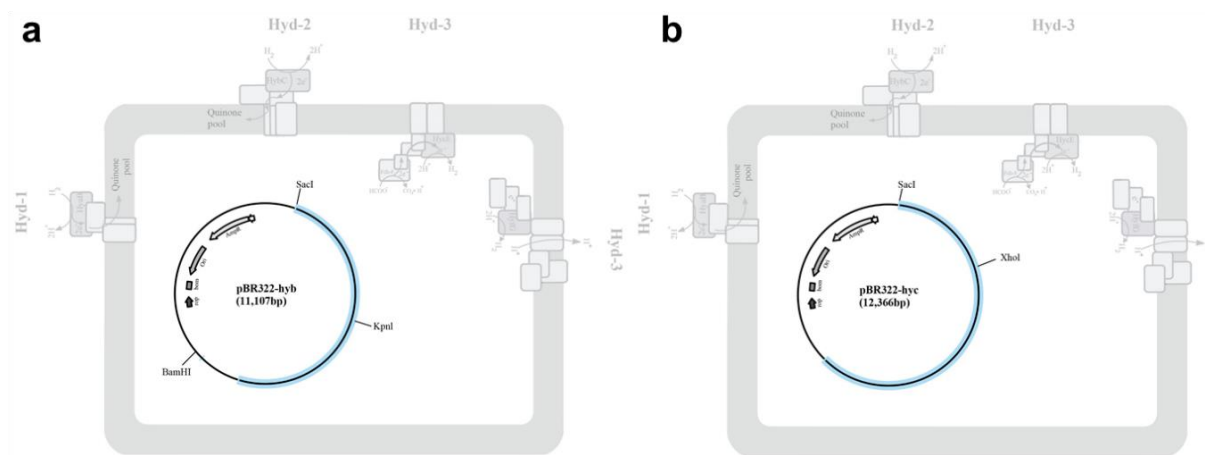


**Figure 3.5** The strain quadruple operon mutant ( $\Delta hya\ hyb\ hyc\ hyf$ ) possessing vector (pBR322) containing cloned *hyb* and *hyc* operons.

### 3.2.7. Hydrogen uptake assays

Hydrogen uptake activity was measured as the increase in absorbance as oxidized methyl viologen (MV) ( $\epsilon_{604} = 13.9\text{ mM}^{-1}\text{ cm}^{-1}$ ) is reduced [ $MV^{+2} + 1/2H_2 \rightarrow MV^{+1} + H^+$ ] as reported previously (Maeda, 2007). Three independent cell cultures were prepared for the hydrogen assay. After 6 h of anaerobic incubation, the cell pellets from 1.5 mL were resuspended with 1 mL Tris buffer (50 mM, pH 8.0). Oxidized MV ( $MV^{+2}$ , colorless) solution (1 mL, 0.8 mM in 50 mM Tris buffer, pH 8), was poured into cuvettes that were sealed with stoppers and sparged with pure hydrogen gas for 3 min. The cell suspensions (0.5 mL) were mixed into the cuvettes, and the change in absorbance (604 nm) during 20 min was monitored. For the calculations, the following formula was used:

$$\text{Total protein} = 0.5\text{ mL} \times OD600 \times 0.22\text{ mg protein/mL}$$

### Hydrogen uptake

$$= \frac{1 \text{ mol } H_2}{2 \text{ mol } MV +} \times \frac{\text{Abs min}^{-1}}{13.9 \text{ mM}^{-1} \text{ cm}^{-1} \times 1 \text{ cm}} \times 1.5 \text{ mL} \times \frac{1000 \text{ nmol}}{\mu\text{mol}} \times \frac{1}{\text{mg protein}}$$

Hydrogen uptake ability was also assayed using GC, as explained previously (Maeda, 2007). The cultures (10 mL) were prepared for the hydrogen assay and incubated at 37 °C with shaking at 120 rpm for 6 h. The pellets were collected from 5 mL culture of each strain and resuspended in 10 mL phosphate buffer (100 mM, pH 7.5) in the vials, which were then sparged with hydrogen for 3 min after sealing. The cells were then incubated at 37 °C with shaking at 120 rpm. The amount of hydrogen in the headspace was monitored at different time intervals.

### 3.2.8. pH-vibration fermentation: Hydrogen assessment at low alkaline pH under glucose metabolism

Hydrogen was assessed from the cultures of three strains, namely, PS, *Δhya hyc hyf*, and *Δhya hyc hyf ΔfdhF* as mentioned above. The pH was monitored and adjusted to ~7.5 using 25% aqueous ammonia, each time after 6 h, 12 h, 24 h, 48 h, and 72 h (Bolivar, 1977). Hydrogen was measured altogether. LB media of pH 7.5, both supplemented with glucose, was used to grow the strains. Three separate cultures were prepared and assayed.

## 3.3. Results

### 3.3.1. The ideal multiple hydrogenase operon-deletion mutants

To study the function of a gene, the observation of the resulting phenotype after knock-out mutagenesis is one of the most commonly utilized approaches (Maeda, 2009). The targeted gene deletions followed by their sequential mobilization into a single strain using P1 phage produced a collection of hydrogenase operon deleted mutants where the four hydrogenases of *E. coli* are removed in different combinations (Table 3.1, Fig. 3.2). The operon mutants devoid of three and all four hydrogenases were evaluated to study their absolute function in hydrogen metabolism. The multiple hydrogenase operon-deletion mutants constructed for this study are recommended for further research on hydrogenases.

### 3.3.2. A comparative functional evaluation of single-gene and operon-deletion mutants of hydrogenases (Hydrogen productivity and specific growth rates)

First, hydrogen productivity of 4 single operon-deletion mutants ( $\Deltahya$ ,  $\Deltahyb$ ,  $\Deltahyc$ , and  $\Deltahyf$ ) and 4 single-gene mutants devoid of each gene encoding the large subunit ( $\DeltahyaB$ ,  $\DeltahybC$ ,  $\DeltahycE$ , and  $\DeltahyfG$ ) for *E. coli* hydrogenases were compared. Contrary to three single-gene mutations ( $\DeltahyaB$ ,  $\DeltahybC$ , and somehow  $\DeltahyfG$ ) which showed more hydrogen production, the hydrogen productivity of three operon-deletion mutants ( $\Deltahya$ ,  $\Deltahyb$ , and  $\Deltahyf$  mutants) was lower than that of the parent strain (Fig. 3.6a). In particular, *hyb* operon mutant had significantly lower hydrogen production than the other mutants and parent strain. On the other hand, as expected, *hyc* operon mutant and  $\DeltahycE$  mutant did not produce hydrogen (Maeda, 2008), again confirming that Hyd-3 has a crucial role in hydrogen synthesis.

Next, using the same mutants, specific growth rates were compared in an aerobic condition. As a result, both *hyb* and *hyf* operon mutants showed significantly reduced growth rates, whereas their single-gene mutants ( $\DeltahybC$  and  $\DeltahyfG$ ) indicated the same specific growth rate as the parent strain (Fig. 3.6b). In addition, *hyc* and *hycE* mutants also showed slightly lower growth than the parent strain, whereas *hya* operon mutant along with its respective large subunit gene mutant ( $\DeltahyaB$ ) showed the same growth as the parent strain. The individual growth rates of single-gene (large subunit) mutants showed a similar trend as mentioned in a previous report (Mirzoyan, 2018a).

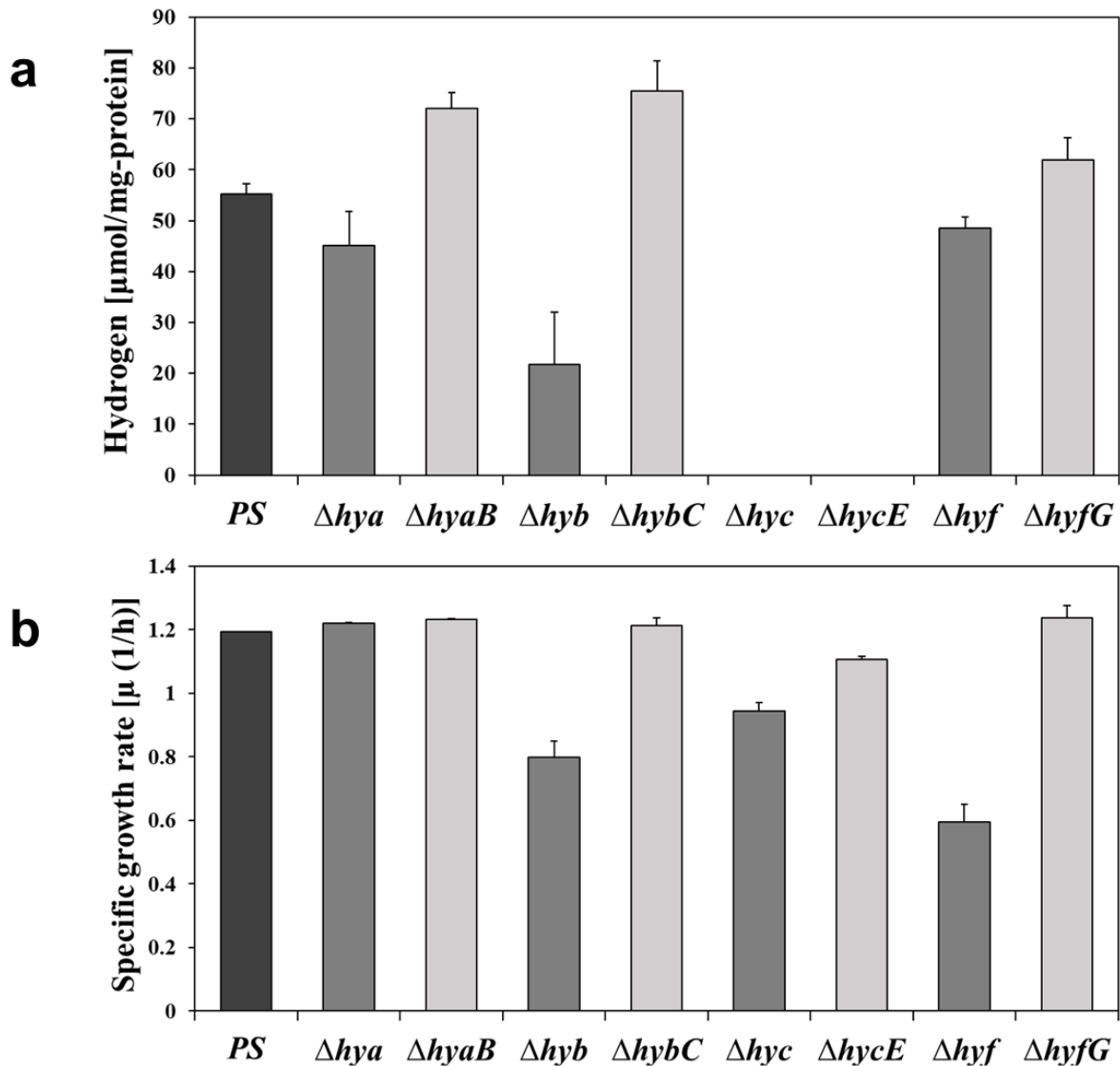


**Figure 3. 6** Effect of single operon deletion and single-gene deletion of *E. coli* hydrogenases on hydrogen production (a) and specific growth rate (b).

Hydrogen production was assayed at 24 hours by using an LB medium supplemented with 2.25% glucose (pH 6.5). On the other hand, specific growth rates were analyzed under aerobic conditions with LB medium. The strains tested were BW25113 (PS),  $\Delta hya$  (operon-deletion mutant for hydrogenase 1),  $\Delta hyaB$  (single-gene deletion mutant for the large subunit of hydrogenase 1),  $\Delta hyb$  (operon-deletion mutant for hydrogenase 2),  $\Delta hybC$  (single-gene deletion mutant for the large subunit of hydrogenase 2),  $\Delta hyc$  (operon-deletion mutant for hydrogenase 3),  $\Delta hycE$  (single-gene deletion mutant for the large subunit of hydrogenase 3), and  $\Delta hyf$  (operon-deletion mutant for hydrogenase 4),  $\Delta hyfG$  (single-gene deletion mutant for the large subunit of hydrogenase 4). The data indicated here is from the replicates of two independent duplicates. Error bars represent stdev.

Thus, the phenotypic differences between operon and single-gene deletions motivated us to construct four ideal hydrogenase operon mutants ( $\Delta hyb hyc hyf$ ,  $\Delta hya hyc hyf$ ,  $\Delta hya hyb$

*hyf*, and  $\Delta hya\ hyb\ hyc$ ) possessing only the single intact hydrogenase in the genome of *E. coli*; thereby, a clear *in-vivo* function of each hydrogenase can be investigated.

### 3.3.3. The absolute role of hydrogenases in hydrogen production

To evaluate the hydrogen productivity by the four *E. coli* hydrogenases (Hyd-1, Hyd-2, Hyd-3, and Hyd-4), 4 triple hydrogenase operon-deletion mutants were used and compared with the parent strain along with a quadruple hydrogenase operon mutant devoid of all four hydrogenases. Under glucose metabolism, Hyd-3 was reconfirmed to be the main hydrogenase that is essential to the production of hydrogen gas (Fig. 3.7a).

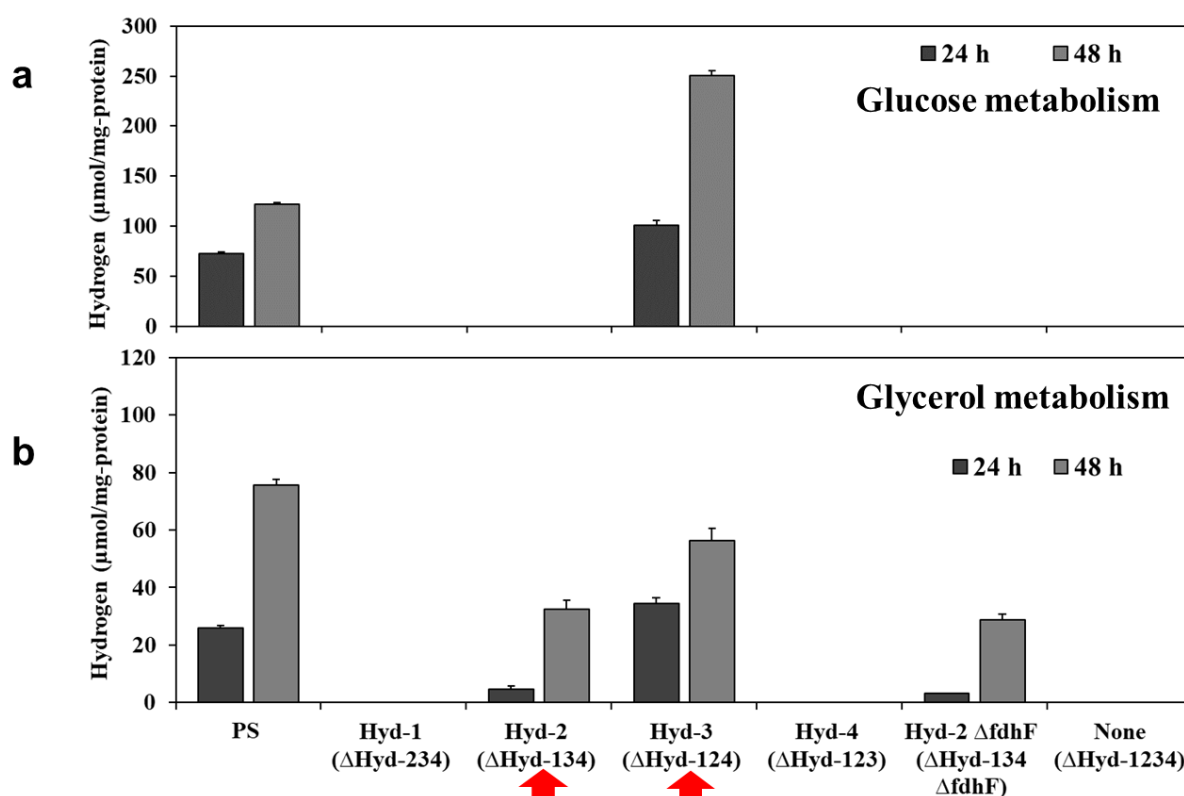


**Figure 3. 7** Hydrogen production of 4 triple hydrogenase operon mutants (possessing only the single hydrogenase in the genome of *E. coli*) from glucose (a) or glycerol (b) as a carbon source.

Hydrogen production was assayed under anaerobic conditions at 24 and 48 hours by using an LB medium supplemented with 2.25% glucose or 10 g/L glycerol. The strains tested were BW25113 (PS), Hyd-1 ( $\Delta$ Hyd-234), which has only hydrogenase 1 (the other 3 hydrogenase operons were deleted), Hyd-2 ( $\Delta$ Hyd-134), which has only hydrogenase 2, Hyd-2 ( $\Delta$ Hyd-134), which has only the hydrogenase 2, Hyd-3 ( $\Delta$ Hyd-124) which has only the hydrogenase 3, Hyd-4 ( $\Delta$ Hyd-123) which has only the hydrogenase 4, Hyd-2  $\Delta$ fdhF (*fdhF* gene was further deleted for Hyd-2 strain), and None ( $\Delta$ Hyd-1234) which is the quadruple operon mutant devoid of all four hydrogenase operons. Data are from triplicates of two independent replicates; error bars indicate stdev.

The hydrogen productivity of Hyd-3 from glucose was higher than the parent strain. Under glycerol metabolism, together with Hyd-3, Hyd-2 was also found to be able to produce hydrogen (Fig. 3.7b). However, their productivities were lower than the parent strain. To verify that formate dehydrogenase-H (*fdhF*), which is a component of the FHL complex, is required for the production of hydrogen gas by Hyd-2 ( $\Delta hya hyc hyf$ ), a new quadruple mutant ( $\Delta hya hyc hyf \Delta fdhF$ ) was constructed (Fig. 3.3f) and tested to evaluate the performance of hydrogen productivity. Interestingly, almost the same amount of hydrogen was observed with or without the FdhF protein (Fig. 3.7b). This result confirms that the hydrogen produced was due to the function of Hyd-2 itself. However, no hydrogen was produced when glucose was used in this quadruple mutant ( $\Delta hya hyc hyf \Delta fdhF$ ). Besides, hydrogen was not detected from Hyd-1 and Hyd-4 under both glucose and glycerol as a carbon source as shown in Fig. 3.7. In addition, no hydrogen production was recorded in another quadruple mutant ( $\Delta hya hyb hyc hyf$ ) where all four hydrogenase operons were deleted (Fig. 3.7).

### **3.3.4. Effects of multiple hydrogenase operon deletions on bacterial growth**

Anaerobic growth of the strains having solely either Hyd-1, Hyd-2, or Hyd-4 was lower than the parent strain in the presence of glucose (Fig. 3.8a). However, one operon mutant having only Hyd-3 showed similar growth to the parent strain. In the presence of glycerol as a carbon source, the growth of all the mutants decreased when compared to the parent strain (Fig. 3.8b). The growth of Hyd-2 was slightly lower than that of the parent strain, whereas Hyd-1 and Hyd-4 showed the lowest growth among the strains tested. The change of pH during the anaerobic fermentation using glucose or glycerol was also monitored with time. As shown in Fig. 3.8c, in all the strains tested (parent strain, Hyd-1, Hyd-2, Hyd-3, and Hyd-4), pH values were lowered within 12 h from pH 7.5 to around pH 4.5, although the pace of pH change in the parent strain was slower than the other strains when glucose was a carbon source. Under

glycerol metabolism, a significant pH change was not observed in the other strains except Hyd-2, which showed a gradual decrease of pH with time (Fig. 3.8d).

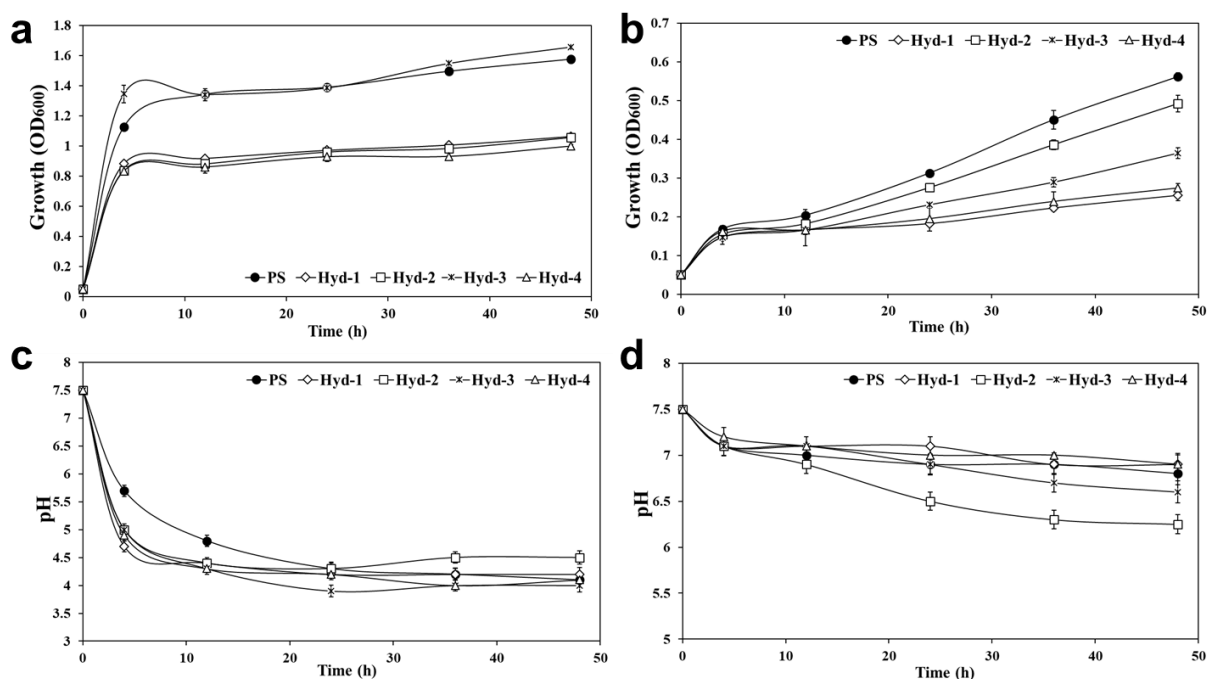


**Figure 3. 8** Growth curve and pH change during the hydrogen fermentation using glucose (a and c) and glycerol (b and d).

Anaerobic growth using glucose (a) or glycerol (b) was monitored with time, and pH under hydrogen fermentation using glucose (c) or glycerol (d) as a carbon source was also checked with time. The strains tested were BW25113 (PS) (closed circle), Hyd-1 (intact hydrogenase 1 is only present in the genome) (open diamond), Hyd-2 (intact hydrogenase 2 is only present in the genome) (open square), Hyd-3 (intact hydrogenase 3 is only present in the genome) (open cross), and Hyd-4 (intact hydrogenase 4 is only present in the genome) (open triangle). Data are the mean of three independent cultures; error bars indicate stdev.

### 3.3.5. pH-vibration fermentation: Hydrogen production by Hyd-2

Since Hyd-2 was able to produce hydrogen from glycerol, a rapid pH decrease in glucose was hypothesized as a possible reason that no hydrogen production was observed in Hyd-2 strain (Mirzoyan, 2018b). Therefore, a pH-vibration fermentation was conducted: pH value of the culture containing glucose media was adjusted to around pH 7.5 at 4 h, 12 h, 24 h, 48 h, and 72 h by using 25% aqueous ammonia, which can be utilized as a nitrogen source by bacteria (Bolivar, 1977). As a result, Hyd-2 was able to produce hydrogen when the pH vibration fermentation was conducted (Fig. 3.9). Although hydrogen production was very low,

both the Hyd-2 strains with or without the *fdhF* gene showed the same amount of hydrogen. The results clarified that hydrogen production by Hyd-2 is observed from not only glycerol but also glucose.

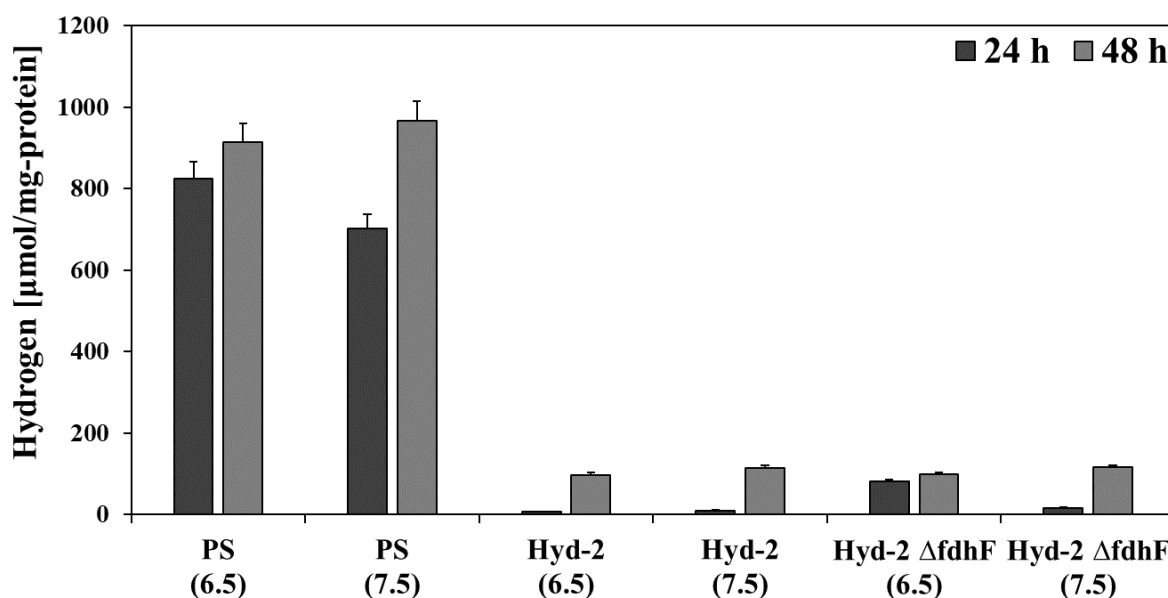


**Figure 3. 9** pH-vibration fermentation to assess hydrogen productivity.

pH-vibration fermentation at low alkaline pH (~7.5) from *hyb* ( $\Delta$ *hya hyc hyf*), *hyb* $\Delta$ *fdhF* ( $\Delta$ *hya hyc hyf*  $\Delta$ *fdhF*), and parent strains to assess their hydrogen productivity using glucose. The pH of the culture was adjusted to near alkaline each time after 12h during the fermentation. Data are the mean of three independent cultures; error bars are standard deviation.

### 3.3.6. Complementation of hydrogen productivity from *hyb* and *hyc* operons

The function of Hyd-2 or Hyd-3 in hydrogen metabolism was further confirmed by the complementation of each plasmid possessing *hyb* or *hyc* operon for the quadruple mutant devoid of all 4 hydrogenases. During the 48-h anaerobic fermentation using glucose, hydrogen production from glucose was only observed in the quadruple mutant capable of expressing Hyd-3 whereas the same mutant which has only the empty vector, showed no hydrogen production (Fig. 3.10). On the other hand, when glycerol was used as a substrate, hydrogen production was certainly recorded in two quadruple mutants possessing each hydrogenase (Hyd-2 and Hyd-3) whereas the same quadruple mutant possessing Hyd-2 was not able to produce hydrogen from glucose. Therefore, the pH-vibration fermentation was again conducted using the same

strain. As a result, hydrogen was detected from the quadruple mutant possessing Hyd-2: the productivity of hydrogen at 48 h was  $66.85 \pm 6.18$  by adjusting pH to around 7.5 at 24 h. Thus, the complementation using these two plasmids demonstrates that Hyd-2 and Hyd-3 have a certain function to produce hydrogen.

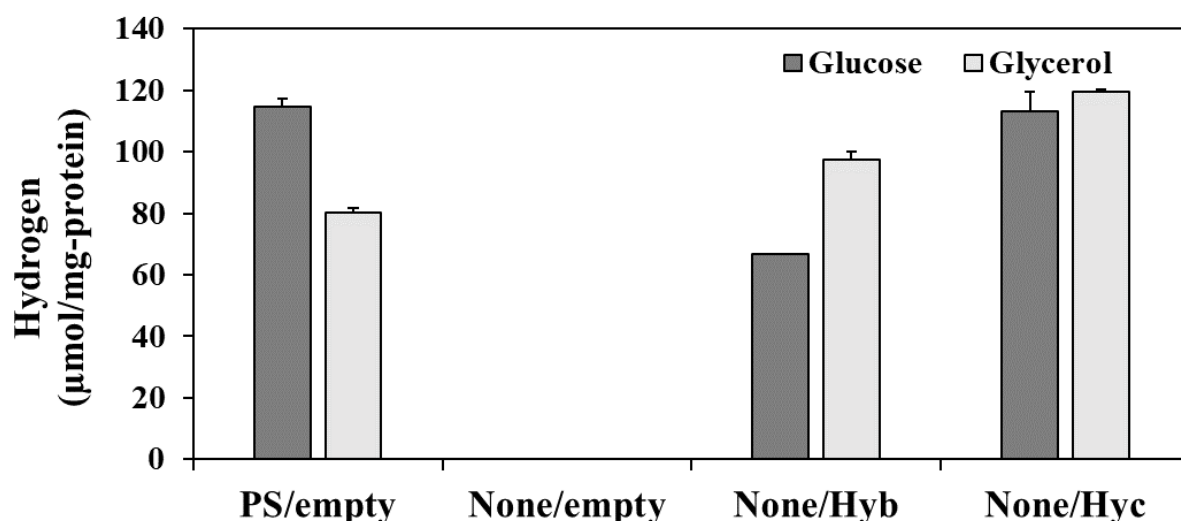


**Figure 3. 10** Complementation of hydrogen production for the quadruple hydrogenase operon mutant ( $\Delta$ Hyd-1234) (indicated as ‘None’) by cloning *hyb* or *hyc* operon into pBR322 cloning vector.

Hydrogen production was assayed under anaerobic conditions at 48 hours by using LB medium supplemented with 2.25% glucose or 10 g/L glycerol. PS/empty indicates the parent strain (BW25113) harboring empty vector pBR322, None/empty indicates the  $\Delta$ Hyd-1234 strain harboring pBR322, None/Hyb indicates the  $\Delta$ Hyd-1234 strain harboring *hyb* operon on pBR322, and None/Hyc indicates the  $\Delta$ Hyd-1234 strain harboring *hyc* operon on pBR322. Data are the mean of three independent cultures; error bars indicate stdev.

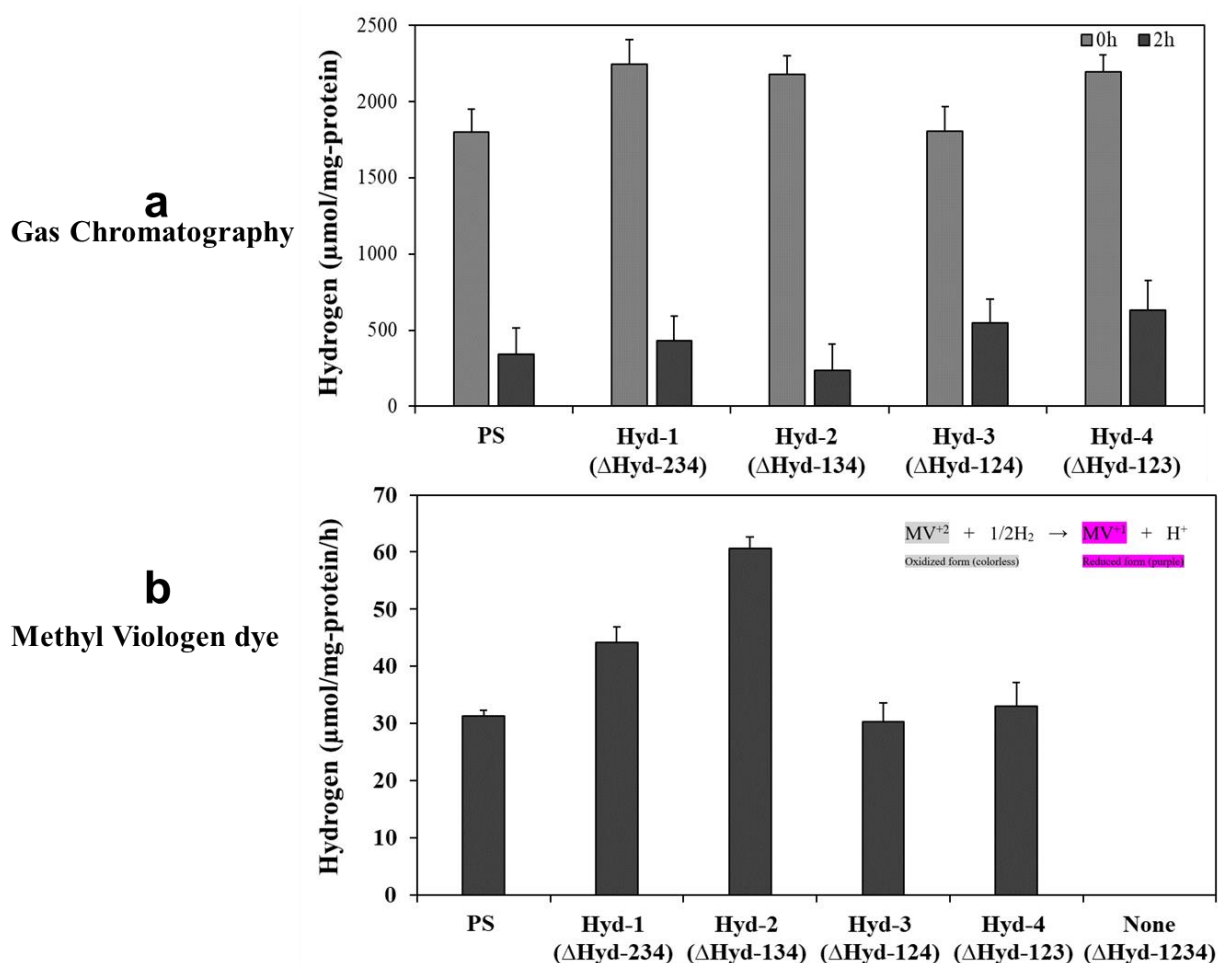
### 3.3.7. All the hydrogenases are solely able to have hydrogen uptake activity

A hydrogen uptake assay was performed to determine if the hydrogenases can have uptake activity of hydrogen. All four hydrogenases were found to have hydrogen uptake activities (Fig. 3.11).

**Figure 3. 11** Hydrogen uptake activity of 4 triple hydrogenase operon mutants (possessing only the single hydrogenase in the genome of *E. coli*) (below).

The assay was conducted by measuring the absorbance derived from a purple product ( $MV_2^+ + 1/2H_2 \rightarrow MV^+ + H^+$ ). The strain tested was PS as the parent strain, BW25113, Hyd-1 (intact hydrogenase 1 is only present in the genome), Hyd-2 (intact hydrogenase 2 is only present in the genome), Hyd-3 (intact hydrogenase 3 is only present in the genome), Hyd-4 (intact

hydrogenase 4 is only present in the genome), and None (quadruple operon mutant devoid of all four hydrogenase operons). Three independent cultures of each strain grown at pH 6.5 were evaluated. Error bars indicate stdev.



From this assay, Hyd-2 was the most significant in hydrogen uptake activity; however, Hyd-1, Hyd-3, and Hyd-4 were also confirmed with this ability. In addition, no hydrogen uptake activity was found in the quadruple operon mutant for hydrogenases ( $\Delta hya\ hyb\ hyc\ hyf$ ). The uptake potentiality of each hydrogenase was further confirmed by using GC to confirm the activity and verify the results (data not shown).

### 3.4. Discussion

The existed sequence homology between the genes of different hydrogenase operons has been suggested to impart partial complementation or cross interaction between them (Maeda, 2018; Vardar-Schara, 2008). Furthermore, based on the level of gene expression and enzyme activity, the possible metabolic cross-talk between the counterparts of the operons has

Chandra SHEKHAR (Maeda Lab.)

been proposed as it can be explained how the activity of one hydrogenase get reduced in the absence of another (Blokesch, 2001; Trchounian, 2012). There are several studies that indicate about the controversies regarding the functions of hydrogenases (Sawers, 1986; Trchounian, 2012). We hypothesized that the origin of these controversies are due to the partial complementation or cross-talk between the hydrogenases. Hence, four triple hydrogenase operon mutants containing only one solely present hydrogenase by deleting the other three and a quadruple operon mutant devoid of all hydrogenase operons in the genome (Fig. 3.2, 3.3, Table 3.1) have been constructed to get rid of cross-talk and to evaluate an absolute function of each hydrogenase without the influence of others.

There is no prior information available about the functional influences of operon deletion with respect to a single gene deletion. Therefore, a comparative evaluation has been done so that the effect of operon deletion on hydrogen metabolism and growth could be investigated in comparison with single-gene deletion since biomass and biohydrogen are considered as essential consequences of the hydrogenase function (Alberts, 2002) (Fig. 3.6a and 3.6b). Hydrogen productivity found nearly the same or increased when a single gene encoding a large subunit of each hydrogenase was deleted from the genome (Fig. 3.6a). However, in the case of operon deletion, reduced productivity found from each operon mutant. This result indicates the phenotypic influences are different from operon deletion in comparison with single gene deletion. The specific growth rates were also found not similar of each operon to their respective single-gene mutant except Hyd-1 (Fig. 3.6b), indicating the regulating role of Hyd-2, Hyd-3, and Hyd-4 on growth. Hyd-2 has been recognized as associated with energy metabolism in *E. coli* (Dubini, 2002), indicating its crucial role in growth. Moreover, triple operons deletions were found more crucial than triple gene deletions for bacterial growth (Fig. 3.12).

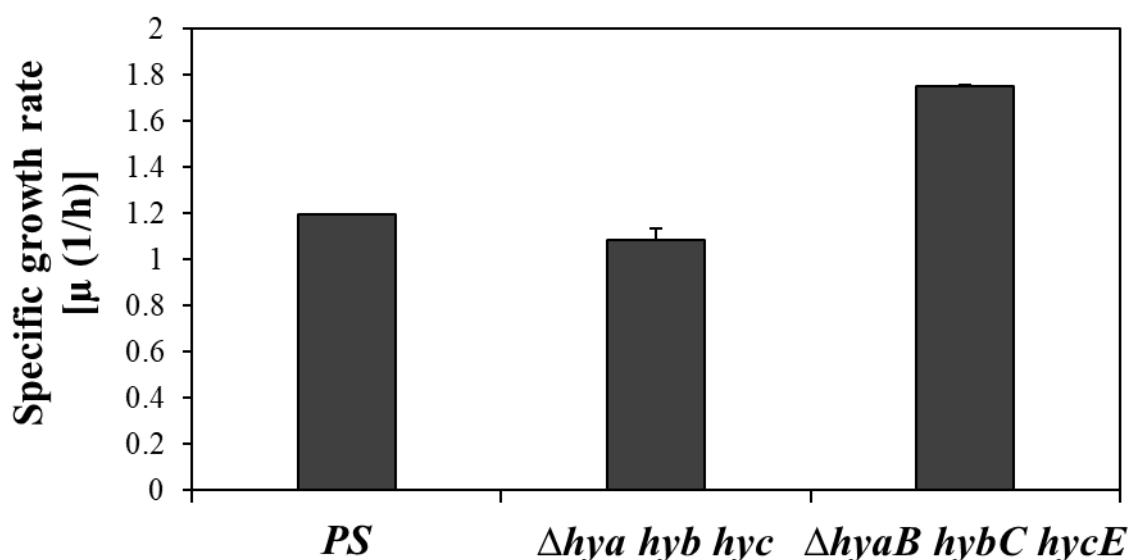


**Figure 3. 12** A comparison of specific growth rates between triple operon and triple single-gene deletion mutants.

Strains were grown under aerobic conditions with LB medium.  $n = 3$ , error bars represent stdev.

Under glucose metabolism, Hyd-3 was found as the sole hydrogen producer (Fig. 3.7a). Although this has been already reported that Hyd-3 is mainly responsible for hydrogen-producing activity by using a mutant of *hycE* (lacking the large subunit gene of Hyd-3) (Maeda, 2007; Petrosyan, 2020; Mirzoyan, 2018a), our study is the further verification of this by the complete removal of other operons (Hyd-1, Hyd-2, and Hyd-4). Slight alkalinity influences the hydrogen productivity compared to slightly acidic conditions by Hyd-3, as hydrogen production was found more at pH 7.5 (data at pH 6.5 not shown) (Petrosyan, 2020, Mirzoyan, 2018a, Trchounian, 2012; Poladyan, 2020). In the absence of other hydrogenases, the high productivity of Hyd-3 than the parent strain indicates more hydrogen uptake or/and hydrogen level regulating (inside the cell) activities by the other hydrogenases (Redwood, 2008), as supported by the uptake activity (Fig. 3.7).

Unlike glucose, under glycerol metabolism, Hyd-2 was also detected for its hydrogen productivity. However, it was comparatively low (Fig. 3.7b). The role of Hyd-2 for hydrogen production from glycerol was confirmed to be important in glycerol metabolism (Trchounian,

2013). Since *fdhF* is associated with hydrogen metabolism as a part of the FHL system (Mirzoyan, 2018a; Trchounian, 2015), its deletion further confirms the absolute ability of Hyd-2 for hydrogen production. Additionally, no remarkable difference in hydrogen generated from Hyd-2 with or without *fdhF* indicates that the function of *fdhF* gene is not required in the hydrogen production by Hyd-2. One noteworthy point of this study is to find the Hyd-1 and Hyd-4 are not solely responsible for hydrogen synthesis with both the substrates, which may indicate their influence by cross-talk of interaction because of sequence homology (Sawers, 1986; Vardar-Schara, 2008).

Under both the glucose and glycerol metabolism, the growth at pH 7.5 is slightly more than at pH 6.5; it might indicate their pH-dependent growth or influencing role and more activity in the alkaline environment (data of pH 6.5 not shown) as suggested previously (Trchounian, 2013; Sinha, 2011). Unlike other strains, the growth of Hyd-2 strain was found like to the parent strain with glycerol (Fig. 3.8b) because of the same reason (Jo, 2015) and the results were supported by an optimum pH of the purified enzyme (King, 1999). At a slightly alkaline pH, the previous report indicates that a different hydrogenase (Hyd-2 but not Hyd-3) is suggested to be mainly involved in hydrogen production (Ballantine, 1986). In addition, Hyd-2 was also reported earlier for hydrogen production under glycerol metabolism at a slightly alkaline pH (Sawers, 1986; Ballantine, 1986) using the large subunit gene *hybC*. Our study further confirms the point from a triple hydrogenase (Hyd-1, Hyd-3, and Hyd-4) operon-deletion mutant ( $\Delta hya hyc hyf$ ) containing solely Hyd-2. As pH plays a crucial role in hydrogen production, the pH change may affect hydrogenase activity and/or metabolic pathways (Petrosyan, 2020; Mirzoyan, 2018b; Trchounian, 2013; Sinha, 2011; Trchounian, 2009). Hyd-2 expression level is affected by the external pH as the maximal expression level could be achieved in an alkaline medium (Jo, 2015), which might be the reason for its different and comparatively decreasing pH under glycerol metabolism. This point further strengthens our

hypothesis that rapidly decreased pH under glucose metabolism makes Hyd-2 disable to produce hydrogen. To verify its functioning ability, pH-vibration fermentation was employed where the pH of the media was adjusted to alkaline (Fig. 3.9). This is important to mention here that adjusting pH to a slight alkaline increased hydrogen productivity by nearly 4-fold from parent strain after 72 h (data not shown). This result further indicates the crucial role of pH in the hydrogenase function and hydrogen metabolism of *E. coli*. The NADH-dependent hydrogenase activity for reduced hydrogen production of Hyd-2 could be correlated since its functional dependency on this cofactor (Fang, 2002). Furthermore, the hydrogen comes up with complementing *hyb* and *hyc* operons in quadruple operon mutant proved a verification of their important role in hydrogen metabolism and pH dependency of Hyd-2 (Fig. 3.10).

Hydrogenases 1, 2, and 3 have been reported for their hydrogen uptake activity (Jo, 2015; King, 1999) during sugar fermentation. Hyd-4 has shown hydrogen uptake property in the presence of glycerol (Zhang, 2009). Many of the previous studies strongly support the cross-talk between Hyd-3 and Hyd-4. For example, like Hyd-3, Hyd-4 is sensitive to osmotic stress at pH 7.5, and pH 6.5 during glucose metabolism (Trchounian, 2012) as indicated in the homology between large subunit genes of Hyd-3 and Hyd-4 (Vardar-Schara, 2008; Petrosyan, 2020; Mirzoyan, 2018a), amino acid sequences of some small subunits of Hyd-3 and Hyd-4 are homologous to components of the electron transport chains (ETC) of bacteria, mitochondria, and plastids (e.g. NADH-ubiquinone-oxidoreductase, complex I) (Zhang, 2009), and protein products of the *hyfD*, *hyfE*, and *hyfF* genes are assumed to give H<sup>+</sup>-translocating activity to Hyd-4 (Mirzoyan, 2017), which was determined with Hyd-3 (Mirzoyan, 2018a; Trchounian, 2011; Bagramyan, 2002). Based on these reports, the hydrogen uptake activity from Hyd-4 under anaerobic fermentation was assumed. Interestingly, like other hydrogenases, Hyd-4 was found to have hydrogen uptake activity (Fig. 3.11). The lacking activity of hydrogen uptake in

quadruple operon mutant indicated that the uptake is the associated phenomenon of hydrogenases.

### **3.5. Conclusion**

From the newly constructed, novel hydrogenase operon mutants, which include four triple hydrogenases, deleted mutants containing only one solely present hydrogenase and a quadruple operon mutant devoid of all hydrogenases from the genome in comparison with the parent strain, the hydrogen metabolism of *E. coli* was investigated. As an absolute function, Hyd-2 and Hyd-3 were confirmed as the hydrogen-producing hydrogenases in *E. coli* and functional with both glucose and glycerol as substrates, although alkaline pH is found crucial for the Hyd-2 activity. In addition, all the hydrogenases are found able for hydrogen uptake activity. The complementation of Hyd-2 and Hyd-3 showed Hyd-3 but not Hyd-2 is more efficient in hydrogen productivity using glucose. However, glycerol is found a more appropriate medium for hydrogen productivity. Hyd-2, with its significant hydrogen uptake activity along with the potential ability of hydrogen production, confirms its noteworthy bi-functional nature. Multiple hydrogenase operon mutants are recommended for further research on hydrogenases.

## CHAPTER 4

# INVESTIGATION OF THE ROLE OF HYDROGENASES IN THE PERSISTENCE OF *ESCHERICHIA COLI*

### 4.1. Introduction

Persisters are the multidrug-tolerant phenotypic variants of the wild type that have entered a nongrowing dormant state to protect from the lethal action of antibiotics (Wood, 2016; Wood, 2013). Along with the non-inherited nature of persistence, another view formulates it as a programmed phenomenon with a genetic basis that has evolved to allow the organisms to survive sudden environmental insults (Maisonneuve, 2014; Wilmaerts, 2019). It has been recently shown that a decrease in adenosine triphosphate (ATP) facilitates the drug tolerance of persisters since most bactericidal antibiotics act by corrupting energy-dependent targets (Shan, 2017). Furthermore, the elevated proton motive force (PMF) generated by the oxidation of nicotinamide adenine dinucleotide (NADH) facilitates the uptake of antibiotics that lead to cell death (Allison, 2011) through the damages caused by superoxide ions originated by the activities of the antibiotics. (Kohanski, 2007). Our hypothesis makes an appearance out of these facts stating that the loss of protein complexes of the membrane, which is supposed to influence energy and metabolism (such as hydrogenases), might have an influential ability on therefore survival against antibiotics.

Hydrogenases are enzymes known for their roles in hydrogen metabolism by catalyzing the reversible reaction of hydrogen to protons and electrons (Maeda, 2018, Shekhar, 2021). The four hydrogenases of *Escherichia coli* (*E. coli*), abbreviated as, Hyd-1, Hyd-2, Hyd-3, and Hyd-4, are encoded by *hyaABCDEF*, *hybOABCDEFGF*, *hycABCDEFGH*, *hyfABCDEFGH* operons respectively (Maeda, 2018). Hyd-1 is coexpressed with a cytochrome oxidase (Brondsted, 1996), which suggests its physiological role is most likely to operate at the anaerobic/aerobic switch. Hyd-2 is popularly known as reversible or bidirectional hydrogenase that can work as

a redox pressure release valve to maintain the redox balance of the cell (Pinske, 2015). Hyd-2 incorporates hydrogen oxidation to the generation of a transmembrane electrochemical gradient (Pinske, 2015). Being a component of the formate hydrogenlyase (FHL) complex, Hyd-3 connects formate oxidation to proton reduction and is responsible for the majority of sustained hydrogen metabolism in *E. coli* (Bohm, 1990). Based on the sequence identity, most of the components of Hyd-3 have equivalents in the respiratory NADH dehydrogenase Complex I (Marreiros, 2013). Based on these evolutionary links with Complex I, Hyd-3 activity to the membrane is supposed to be associated with proton translocation and thus energy conservation. In *E. coli* Hyd-3/FHL could be an energy-conserving system (Batista, 2013). Hyd-4 is closely related to Hyd-3 and consequently, evolutionarily links to Complex I (Andrews, 1997). This report is further supported by the structural arrangement in the membrane domain of Hyd-4, which indicates it's more closely related to Complex I than that of Hyd-3. Hyd-4 is, therefore, more likely to be coupled in the generation of the transmembrane electrochemical gradient (Marreiros, 2013). Genetic analysis suggests that the Hyd-4 may be able to transduce free energy released during the FHL reaction to the generation of a transmembrane ion gradient (Batista, 2013). Mycobacterial hydrogenases were found differentially expressed and active during growth and persistence, which suggests that hydrogen oxidation is important for microbial existence in a non-replicative, persistent state (Cordero, 2019). For *S. Typhimurium*, the use of molecular hydrogen by uptake hydrogenases is essential for its virulence (Benoit, 2019). Moreover, the pathogenic Helicobacter species *H. pylori* and *H. hepaticus* can respire hydrogen through a respiratory [NiFe]-hydrogenase, whereas a mutant hydrogenase strain of *H. pylori* is much less efficient in its colonization in mice (Olson, 2002). These reports indicate the pivotal role of hydrogenases in bacterial virulence and viability. Highly purified bidirectional hydrogenase of *Clostridium pasteurianum* could rapidly reduce several 2-, 4- and 5-nitroimidazole compounds via an electron carrier-coupled mechanism, indicating

hydrogenase mediated survivability (Church, 1990). It was hypothesized before that endogenous or exogenous hydrogen can reduce the killing effect by neutralizing cytotoxic hydroxyl radicals ( $\text{OH}\cdot$ ) since a bactericidal treatment induces bacterial death via  $\text{OH}\cdot$  (Kohanski, 2007). Interestingly, hydrogen selectively could reduce the  $\text{OH}\cdot$ , the most cytotoxic of reactive oxygen species (ROS), and effectively protected cells, and thus can be used as an effective antioxidant therapy (Ohsawa, 2007). A few studies reported that hydrogenases are crucial for bacterial growth inside the gut (Maier, 2014; Olson, 2002), therefore, hydrogenases or hydrogen metabolism in the bacteria could be assumed to effectively reduce the susceptibility to antibiotics and facilitate antibiotic tolerance to enhance bacterial survival (Nie, 2012).

In this study, the four-hydrogenase operon deleted strains of *E. coli* were employed to investigate bacterial persistence. To elucidate a much deeper metabolic influence on persistence by hydrogenases, the transcriptomic dataset was mainly utilized using persister and initial cells. As a result, hydrogenases were found to possess significant influential effects on persistence. This work not only provides hydrogenases' view on persistence but also demonstrates their crucial in bacterial physiology under the influence of antibiotics.

## **4.2. Materials and Methods**

### **4.2.1. Bacterial strains, media, and growth conditions**

*E. coli* K-12 BW25113 was used as the parent strain (abbreviated as PS) in the study. Each hydrogenase operon mutant investigated in this study was constructed in our previous study (Shekhar, 2021) by the one-step inactivation method explained by Datsenko and Wanner (Datsenko, 2000). All the strains including operon mutants employed in this study are listed in Table 4.1. The strains were initially streaked from  $-70^{\circ}\text{C}$  glycerol stocks on Luria-Bertani (LB) (Maeda, 2007) agar plates and a single colony was used to inoculate to grow at  $37^{\circ}\text{C}$  for overnight (in the presence of kanamycin,  $50\text{ }\mu\text{g/mL}$ , in case of mutants). For the persistence and all related assays, ampicillin ( $50\text{ }\mu\text{g/mL}$ ) was mainly employed to get persister (referred to

as ‘antibiotic-treated) cells. A fresh culture was prepared in 250 mL flask (Iwaki, Japan) containing 50 mL LB at 37°C with shaking at 180 rpm using a bioshaker (BR-180LF, Taitec). All experiments were conducted using at least three biological replicates. The medium containing 10 g/L Bacto Tryptone, 5 g/L yeast extract, and 5 g/L NaCl was used to grow the strains. The final concentrations of each antibiotic used in LB-ampicillin, LB-chloramphenicol, and LB-kanamycin media or plates were 50 µg/mL ampicillin, 30 µg/mL chloramphenicol, and 50 µg/mL kanamycin, respectively. Carbenicillin (10 µg/mL) was used in place of ampicillin whenever necessary. Chemicals were purchased from Wako Pure Chemical Industries Ltd. (Osaka, Japan), Dojindo Molecular Technologies, Inc. (Kumamoto, Japan), Sigma-Aldrich Co. LLC (Tokyo, Japan), and Nacalai Tesque, Inc. (Kyoto, Japan).

**Table 4. 1 *E. coli* strains used in this study.**

Strains/plasmids	Genotype/relevant characteristics	Reference
<i>E. coli</i> BW25113	F $\Delta$ ( <i>araD-araB</i> )567 $\Delta$ lacZ4787 (::rrnB-3) $\lambda$ <i>rph-1</i> $\Delta$ ( <i>rhaD-rhaB</i> ) 568 <i>hsdR514</i> ; parental strain for the Keio collection	Yale Coli Genetic Stock Center
<i>E. coli</i> BW25113 $\Delta^a$ <i>hyaA</i> - <i>F<sup>c</sup>::<sup>b</sup>kan<sup>d</sup></i>	Hyd-1 operon deleted mutant	(Shekhar, 2020)
<i>E. coli</i> BW25113 $\Delta$ <i>hybO</i> - <i>F::kan</i>	Hyd-2 operon deleted mutant	(Shekhar, 2020)
<i>E. coli</i> BW25113 $\Delta$ <i>hycA</i> - <i>I::kan</i>	Hyd-3 operon deleted mutant	(Shekhar, 2020)
<i>E. coli</i> BW25113 $\Delta$ <i>hyfA</i> - <i>R::kan</i>	Hyd-4 operon deleted mutant	(Shekhar, 2020)
<i>E. coli</i> BW25113 $\Delta$ <i>hyaB::kan</i>	Hyd-1 large subunit gene deleted mutant	(Sanchez-Torres, 2013)
<i>E. coli</i> BW25113 $\Delta$ <i>hybC::kan</i>	Hyd-2 large subunit gene deleted mutant	(Sanchez-Torres, 2013)
<i>E. coli</i> BW25113 $\Delta$ <i>hycE::kan</i>	Hyd-3 large subunit gene deleted mutant	(Sanchez-Torres, 2013)

<i>E. coli</i> BW25113	Hyd-4 large subunit gene deleted	(Sanchez-Torres, 2013)
$\Delta$ hyfG:: <i>kan</i>	mutant	

a and b:  $\Delta$  and :: represents “deletion” and “replaced by gene,” respectively.

c: *A-F*, *O-F*, *A-I*, and *A-R* represents the “from and to” deleted segment of *hya*, *hyb*, *hyc*, and *hyf* operons, respectively.

d: *kan* denotes kanamycin resistance gene.

#### 4.2.2. Persister assay

The persister assay was performed as per previous explanations with some modifications (Chowdhury, 2016; Wang, 2017). Cultures were grown aerobically at 37 °C with shaking at 180 rpm overnight and then diluted (1:1000) in LB medium. The diluted cultures were incubated until cultures reached the mid-exponential phase ( $OD_{600nm} \approx 0.8$ ) aerobically since this phase is characterized by to increase in the number of persisters more than lag or early exponential phase (Keren, 2003; Wang, 2017) (cells at this stage are termed as initial cells). Cells were then exposed to 50 µg/ml ampicillin, and cultures were incubated for 3 hrs at 37 °C with shaking at 180 rpm (persister cells). To measure cell viability, samples were taken before and after antibiotic treatment (initial cells and persisters), washed and serially diluted in 0.85% (w/v) NaCl solution, plated on LB agar, and grown overnight at 37°C to determine CFU/mL. Experiments were performed with at least two independent cultures.

#### 4.2.3. Dissolved-Oxygen Measurements

Dissolved oxygen (DO) levels within culture flasks were determined using a dissolved oxygen sensor of Custom (DO-1000PE) according to the manufacturer’s instructions. The 50 ml cultures of initial and treated cell populations were prepared as above and used to monitor DO before and after ampicillin treatment at different growth levels. The oxygen sensor was calibrated to media at 37 °C. All measurements were obtained from three separate cultures.

#### 4.2.4. Total RNA extraction and quantitative reverse transcription PCR (qRT-PCR)

The initial cells and persister populations were grown as explained above and removed from the cultures to collect the pellets for RNA extraction using 100 µl RNALater solution (Applied Biosystems Foster City, CA) in 2 ml screw-cap tubes after centrifugation at 13000

rpm, 1 min. The tubes containing cell pellets were immersed in 100 ml of dissolved dry ice in ethanol (95%) for 10 s and stored at -70°C before RNA extraction. Total RNA was extracted using a bead beater model 3011b (Wakenyaku Co. Ltd., Japan) and the RNeasy Mini Kit (Qiagen, Inc., Valencia, CA) as explained in (Mustapha, 2018). A StepOne Real-Time PCR system and Power SYBR green® RNA-to C<sub>T</sub><sup>™</sup> 1- Step kit (Applied Biosystems, Foster City, CA) were used for the transcription analysis of the expression of four hydrogenases in each hydrogenase operon mutant. Housekeeping gene *rrsG* (16S rRNA) was used to normalize the expression data. RNA extracted from the PS was used as the reference template. All the primers used for this transcription analysis are listed in Table 4.2. Two technical replicates of the samples were performed. The expression of the listed genes was analyzed using 50 ng of total RNA and the collected data was analyzed through relative quantification for qRT-PCR ( $2^{-\Delta\Delta C_T}$ ) (Pfaffl, 2001).

**Table 4. 2 List of primers used in qRT-PCR**

Primer	Significance	Sequence (5'-3')	Reference
<i>hyaB</i> -F	Expressing large subunit	CACGGCGGACTTCATTAACA	This study
<i>hyaB</i> -R	gene of Hyd-1	CCGTAGCTGAGAACGCATTTAT	
<i>hybC</i> -F	Expressing large subunit	CAAACGTAGCGACTTTGTTGAG	This study
<i>hybC</i> -R	gene of Hyd-2	GGTAGTTCACCGCACCTTTA	
<i>hycE</i> -F	Expressing large subunit	CCATTCTGCTGGAGGTAGAAC	This study
<i>hycE</i> -R	gene of Hyd-3	ACGCGGAAGAACTGCATAA	
<i>hyfG</i> -F	Expressing large subunit	CTGCATATCACCTCCGATGAA	This study
<i>hyfG</i> -R	gene of Hyd-4	TGCCGCGATGGACATAAA	
<i>rrsG</i> -F	Housekeeping gene for	TATTGCACAATGGGCGCAAG	(Sanchez-Torres, 2013)
<i>rrsG</i> -R	expression data	ACTTAACAAACCGCCTGCGT	

F and R represent forward and reverse primers, respectively.

#### 4.2.5. Reactive oxygen species assay

For the ROS measurements, we used the Molecular Probes<sup>™</sup> Carboxy-H<sub>2</sub>DCFDA kit (Invitrogen #C400) according to the manufacturer's instructions and previously described

(Wang, 2017). In brief, the initial cells and persister populations were grown at 37°C/180 rpm and removed from the cultures as explained above to estimate the ROS levels. The 1mL cultures of each strain were washed twice with pre-warmed PBS (1×) buffer (pH 7.4). After a short incubation at 37°C, the cells were further resuspended in 1 ml 25μM carboxy-H<sub>2</sub>DCFDA reconstituted with PBS buffer and incubated for 30 minutes at 37°C, in the dark. 200μl of the supernatant and cells transferred into 96-well plate separately to record fluorescence at 492/525 nm and optical density at 600 nm respectively using a microplate reader (Thermo Scientific VARIOSKAN FLASH 5250040).

#### **4.2.6. DNA library preparation and high-throughput sequencing**

The DNA library preparation was performed using the Nextera XT DNA Library Prep Kit (Illumina), following the manufacturer's recommended protocol. Briefly, the cDNA was subjected to simultaneous fragmentation and tagmentation to cleave the DNA by Nextera transposome enzyme. The cleaved DNA was subjected to PCR amplification for barcoding the samples with a dual adapter index with a unique barcode sequence (Nextera XT Index kit) to differentiate each sample. Then, the PCR products were purified using Agencourt AMPure XP beads (Beckman Coulter Inc., CA, USA) and normalized using the Nextera XT Library Normalization Beads before pooling all the samples. The normalized and pooled sample was loaded in a 600-cycle V3 MiSeq reagent cartridge kit (Illumina) for sequencing in the Illumina MiSeq sequencer. Sequencing was performed for 301, 8, 8, and 301 cycles for forward, index 1, index 2, and reverse reads, respectively. The raw sequence data has been deposited in the National Center for Biotechnology Information (NCBI) under the Short Reads Archive (SRA) accession number PRJNA671558.

#### **4.2.7. Transcriptomic (RNA Seq) data analysis**

FASTQ formatted raw reads were subjected to quality assessment to determine whether the raw reads were qualified for mapping by fastQC (Andrews, 2010) and trimmed using

cutadapt tool (Martin, 2011) based on the Phred score quality cutoff  $\geq 30$ . The trimmed good-quality reads were mapped to the reference genome of *Escherichia coli* str. K-12 substr. MG1655 [NCBI Reference Sequence: NC\_000913.3]. The software Rockhopper (McClure, 2013) was employed to map on the reference genome, as explained previously (Liu, 2020; McClure, 2013). Gene expression was normalized by calculating Reads per Kilobase per Million Mapped Reads (RPKM) (Liu, 2020). The differential gene expression analysis was done by using the edgeR tool (Robinson, 2010), and significant genes were filtered with a p-value  $\leq 0.05$ . Upregulated and downregulated genes were filtered with fold change  $\geq 0.8$  and  $\leq -0.8$ , respectively. The significantly altered metabolic pathways were obtained through KEGG (Kyoto Encyclopedia of Genes and Genomes) (Kanehisa, 2000) and gene ontology (GO) (Young, 2010) pathway enrichment analysis with the threshold of p-value  $< 0.05$ . The functional annotations were retrieved from UniProt, David, EcoCyc, and NCBI databases.

### **4.3. Results**

#### **4.3.1. Cultural growths and dissolved oxygen concentrations**

Since persister level increases during growth (Keren, 2004; Lewis, 2019), it is important to evaluate the growth of the strains in the presence and absence of the antibiotic. The growth of each hydrogenase operon mutant was monitored during the persister assay. A control group of the same strains was simultaneously monitored where no antibiotic was supplemented. As result, relatively reduced growth of the mutants was observed compared to the PS, specifically, *hyb* and *hyf* mutants (Figure 4.1a).

Furthermore, the concentration of the DO in the cultures was monitored at different time points during the growth (Figure 4.1b). As a result, the oxygen level found dropped to near zero, which might indicate an oxygen-deprived state (referred to as a micro-aerobic state, Shan, 2012) at their mid-exponential phase. This was the point where antibiotic was added to the cultures. Oxygen consumption rate was observed dissimilar among all the mutants, where *hyf* mutant

found slower and *hyb* mutant found relatively faster. As reported, the survival of persisters requires a small (20%) drop in DO saturation, and at high DO concentration levels, the persister population is killed over time (Grant, 2012). The cultural conditions, in this study, indicating nearly zero or zero oxygen concentrations, may indicate the presence of that subpopulation that is susceptible to acting as a persister population.

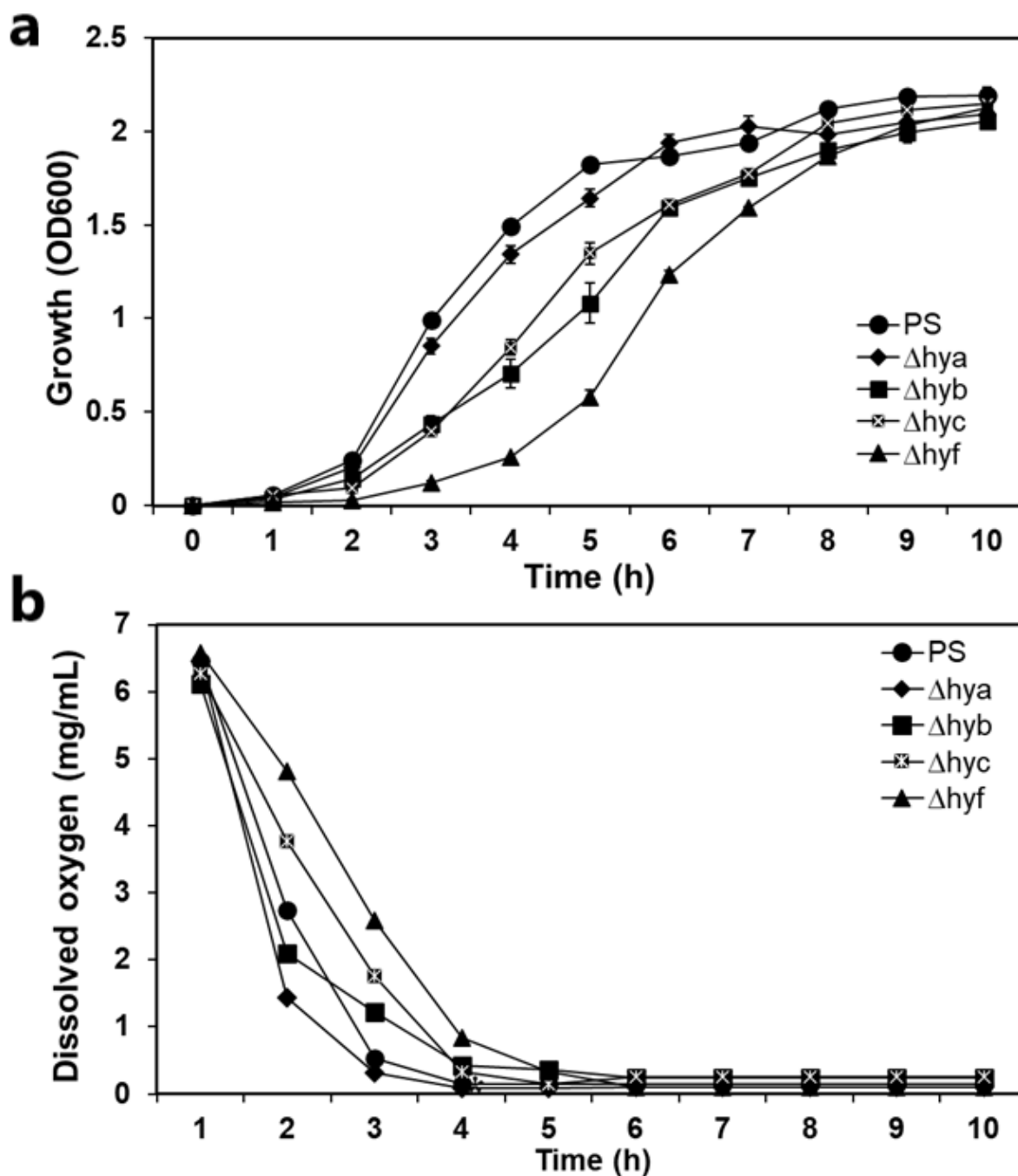


**Figure 4. 1** The growth profile of the strains and cultural dissolved oxygen concentrations (below).

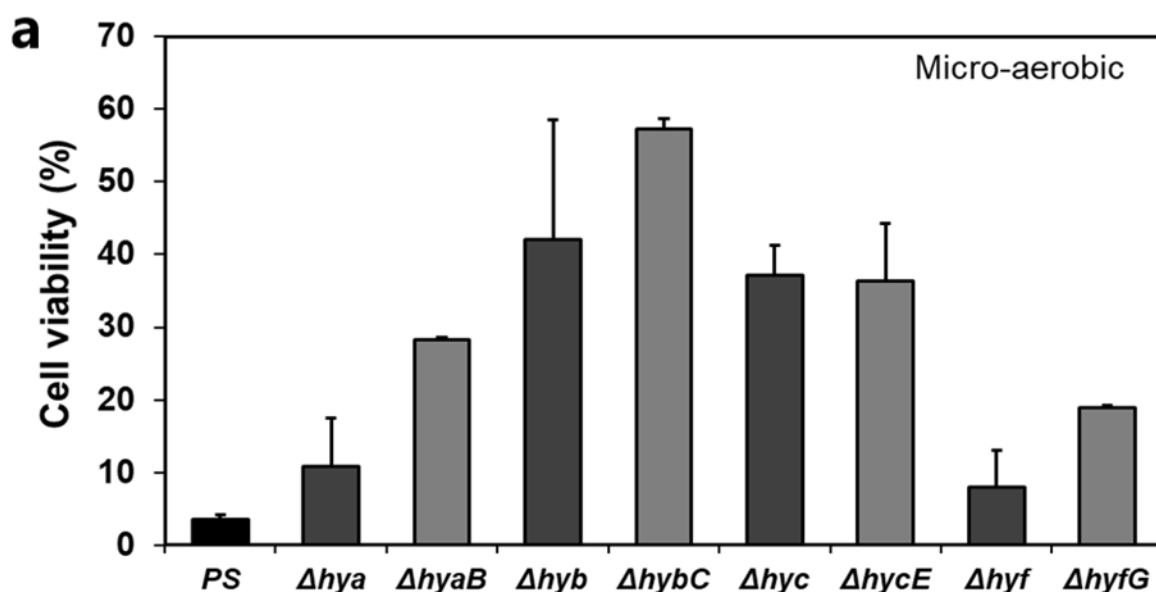
- (a) Growth curves of the operon mutants and comparison with the PS. (b) DO concentrations in the cultures of the strains at different time points of the growth. Data represent the average of three replicates. The error bars indicate the standard deviation.

### 4.3.2. Cellular viabilities in persistence

To evaluate the hydrogenase-mediated cell viability during the persistence, the colony-forming unit (cfu) of the four hydrogenase mutants was estimated by counting the colonies obtained from initial cells and persister populations, as:

$$\text{Cellular viability} = \frac{\text{cfu/mL obtained from persisters}}{\text{cfu/mL obtained from initial cells}}$$

Along with the operon mutants, their respective large subunit gene deleted mutants were also included in the study for comparative analysis and to predict the impact of operon deletion over a single gene deletion in persistence.



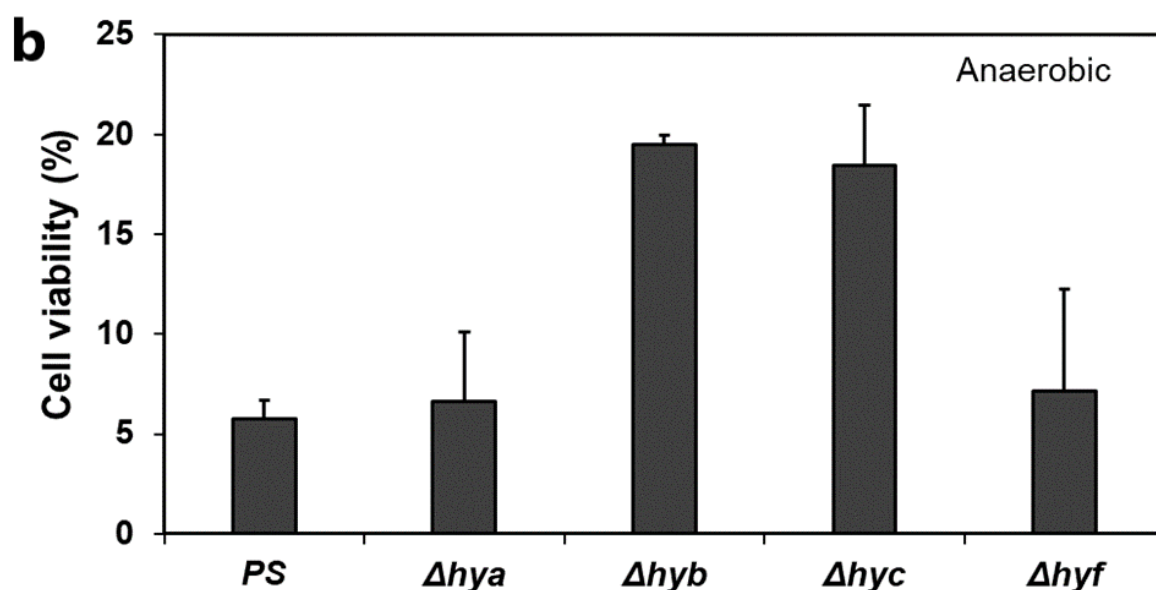


**Figure 4. 2** Cell viabilities of hydrogenase operon mutants in persistence.

The cellular viability of all the strains in persistence under micro-aerobic (oxygen deprived) conditions (a) and of the operon mutants under anaerobic conditions (b). Cell viability was calculated by dividing the cfu/mL obtained from the persisters by the cfu/mL obtained from the initial cells. Data are the mean of three independent assays: error bars indicating stdev.

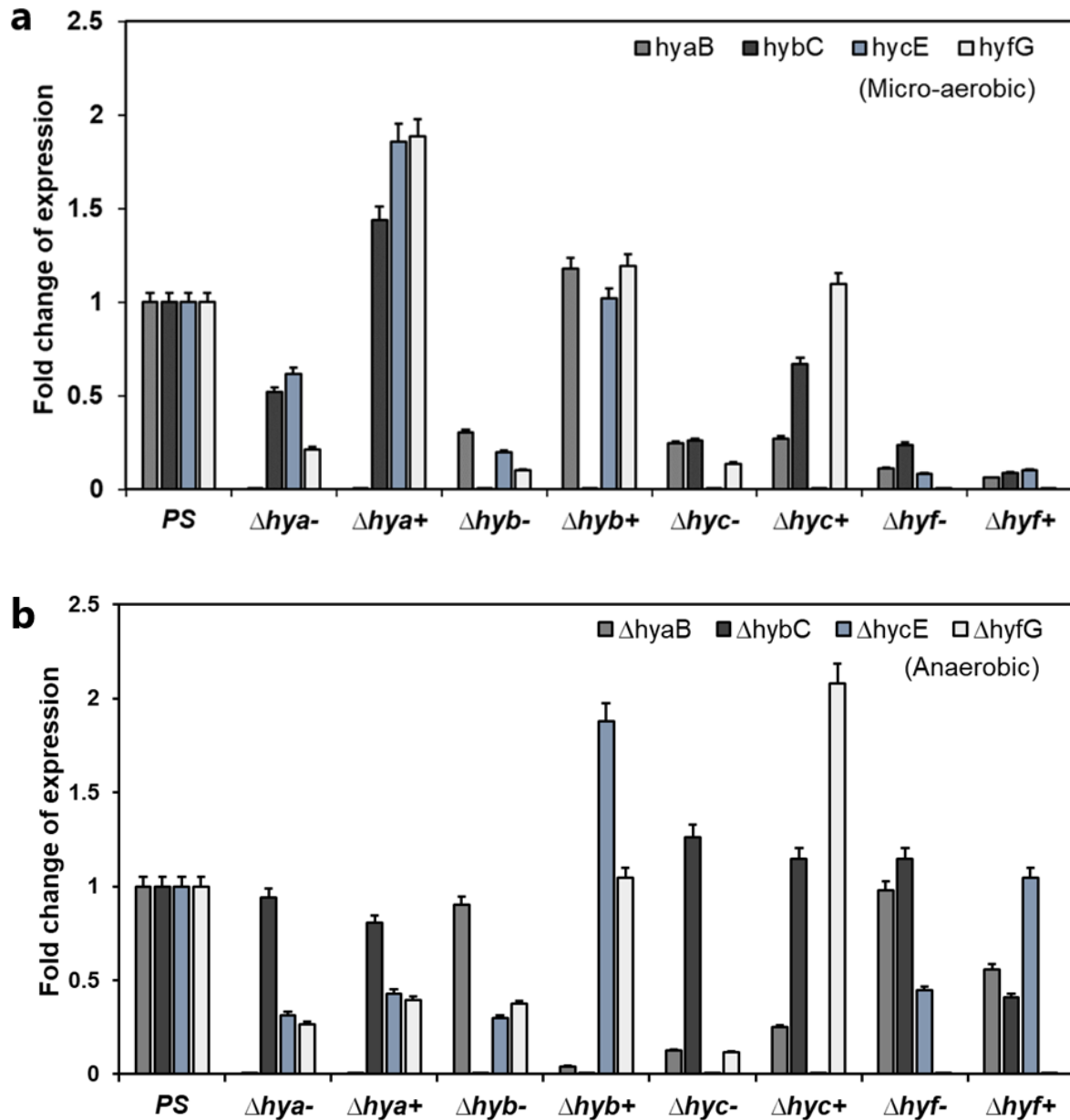
As a result, the cellular viability of the mutants was found to increase of all the hydrogenase mutants compared to the PS (Figure 4.2a). However, no significant change was observed in the number of viable cells from the initial cells of all the mutants, the cell viability was found comparatively more in the case of gene mutants than operon mutants. This may be indicating that operon mutations are more deleterious than gene one, which is supported by our previous study (chapter 3) (Shekhar, 2021). From both types of deletions, *hyb* and *hyc* were found significant for bacterial survival since the viabilities were 20- and 18-fold increased respectively compared to PS. Along with their viabilities under micro-aerobic (oxygen-deprived conditions, mentioned below) conditions, *hyb* and *hyc* operon mutations were also found significant under anaerobic conditions (Figure 4.2b). The increment in viabilities from *hya*, and *hyf* deletions was lower than in other mutants. Importantly, cellular viabilities recorded from anaerobic conditions were lower than micro-aerobic ones (Figure 4.2a and 4.2b).

### 4.3.3. Hydrogenase expressions in persisters

The test conditions of the initial cell and persisters were micro-aerobic (oxygen-deprived) and anaerobic (Figure 4.1 and 4.2). Hydrogenase functions were mainly reported from anaerobic conditions (Maeda, 2018; Vardar-Schara, 2008; Trchounian, 2012), however, some reports are indicating their activity under aerobic or micro-aerobic conditions also (Olson, 2002; Cordero, 2019). Therefore, this was interesting to evaluate the expression of hydrogenases in initial and persisters, under both conditions. In this regard, the expression of the gene encoding the large subunit of each hydrogenase was evaluated from each hydrogenase operon mutant. As a result, the expression of hydrogenases was found very relatively low in initial cells (indicated with ‘-’) (Figure 4.3a and b). Interestingly, a relatively elevated hydrogenase expression was found in persisters (indicated with ‘+’) (specifically *hya*, *hyb*, and *hyc*, under micro-aerobic conditions, and *hyb*, and *hyc*, under anaerobic conditions) (Figure 4.3).

**Figure 4. 3** Hydrogenase expressions in persisters (below).

The fold change expression levels of hydrogenase genes encoding large subunit in initial cells (-) and persisters (+) of each hydrogenase operon mutant. The relative expression level was normalized with a housekeeping gene, *rrsG* (16S rRNA). The bars indicate the mean of the triplicates; the error bar indicates STDEV.



However, despite any specific correlation between micro-aerobic and anaerobic expression data, some consistencies can be drawn such as, first, *hyb* and *hyc* mutants are somehow significant since hydrogenase expressions were higher than others, second, *hyf* showed no change in expression. The hydrogenase expressions from *hyb* and *hyc* mutants indicate a very significant association of hydrogenases in persistence.

#### 4.3.4. Altered ROS levels in persisters

Recent studies have suggested that ROS can provide a protective effect against antibiotics by inducing persistence as well as contributing lethality to the antibiotics to kill them

(Dwyer, 2014; Brynildsen, 2013; Kohanski, 2010). The ability of ROS to both protect and kill bacterial cells motivated us to quantify it in all the strains. As result, the ROS was detected relatively unchanged in initial cells but altered in persisters of all the strains (Figure 4.4). In comparison, ROS levels were detected higher in micro-aerobic than anaerobic conditions. Persistence demonstrated a ROS surge in the *hyc*, *hyf* strains under micro-aerobic, and *hyf* under anaerobic conditions, like PS. The *hyb* mutant seems to be able to deal with ROS under micro-aerobic which might be lost under anaerobic conditions. The *hyc* mutant, showed significant but opposite activity to that of *hyb*, under both conditions. As bacterial survival against antibiotics is mediated by the ability to detoxify ROS (Grant, 2012; Lewis, 2019), the decreased level of ROS in persisters of *hya* and *hyb* mutants (under anaerobic conditions) and *hyb* mutant (under micro-aerobic conditions) may indicating their potent ability in this activity. This further justifies the high cellular viability of *hyb* mutant after antibiotic treatment. *hyc* (under anaerobic conditions) and *hyf* mutant (under both conditions) may reflect their association with the ROS-mediated protective effects against antibiotics (Dwyer, 2014; Brynildsen, 2013).

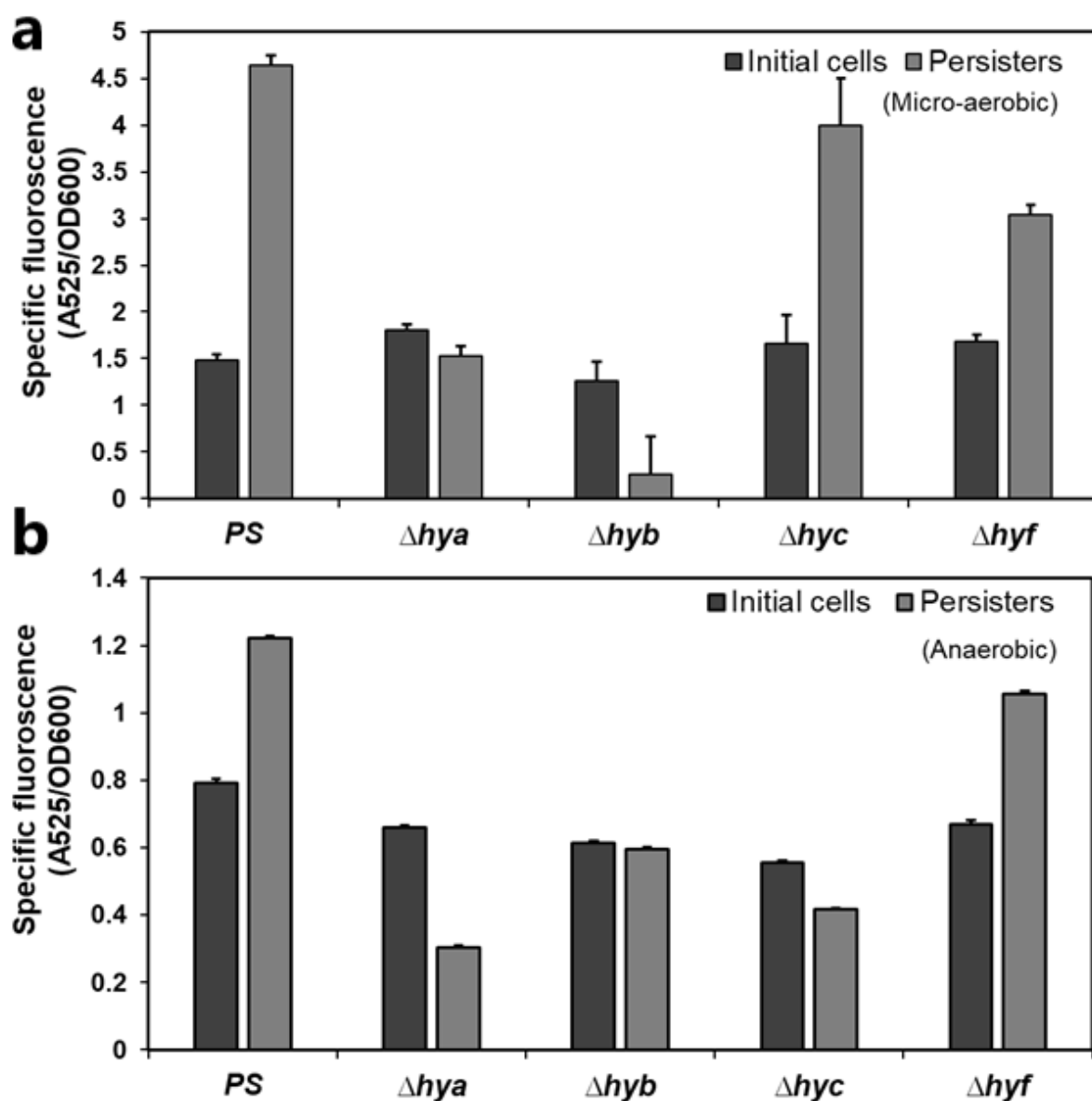


**Figure 4. 4** ROS quantification in persistence.

ROS quantification from cultures of initial cells and persisters. The specific fluorescence is calculated as  $A_{525}/OD_{600}$  from the cultures treated with the general ROS indicator carboxy- $H_2DCFDA$ . Error bars show the standard deviation of the biological triplicates.

#### 4.3.5. KEGG pathway enrichment analyses

As reported, low metabolic activity is the key to the survival of persister cells since in exponentially growing cultures, persisters were significantly more abundant in the least redox-active subpopulation (Wood, 2013; Mehmet, 2015). When only metabolically important pathways were considered, KEGG pathway enrichment analysis showed a supportive result (Fig. 4.5). The persisters of all *hyb*, *hyc*, and *hyc* mutants showed the most altered metabolic

pathways such as amino acid biosynthesis and degradation, carbohydrate biosynthesis and degradation, cell wall biogenesis, energy metabolism, glycolysis, lipid metabolism, metabolic intermediate biosynthesis, oxidative phosphorylation, and TCA cycle compared to initial cells. The *hyc* operon mutant showed relatively more affected metabolism than *hyb* operon mutant. The results may indicate the hydrogenases mediated low metabolism and thus persistence.

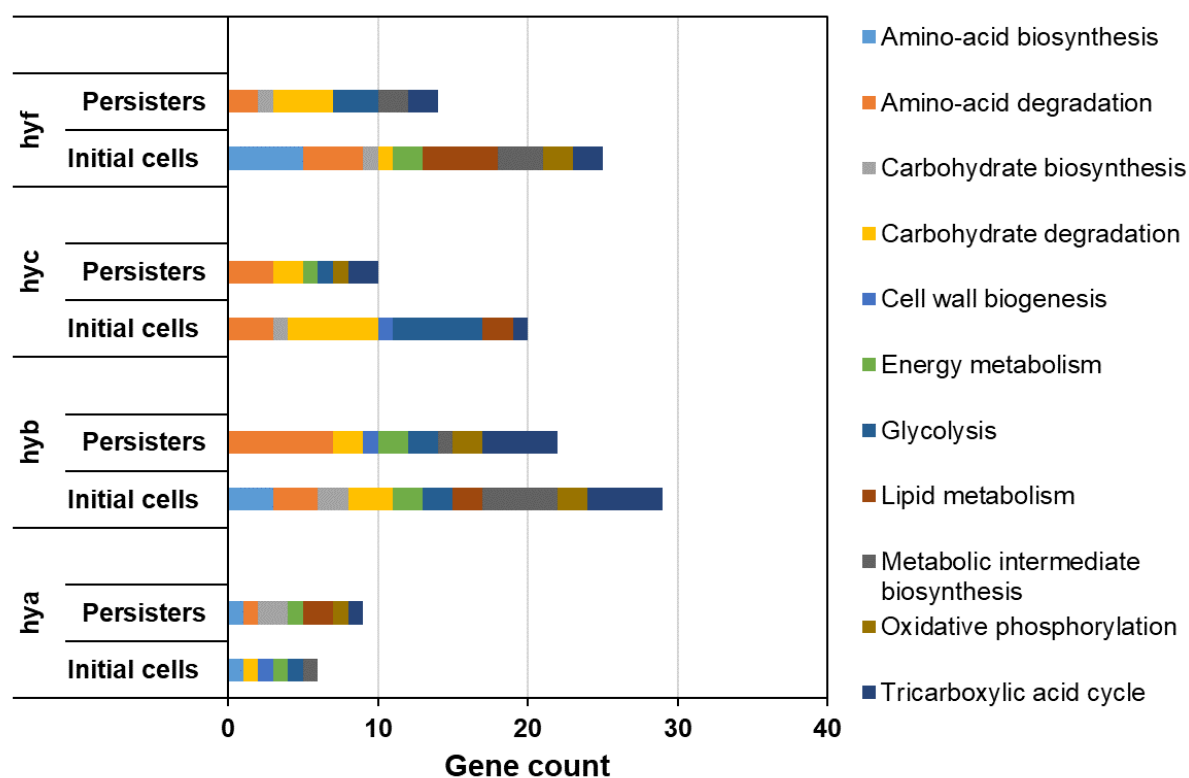
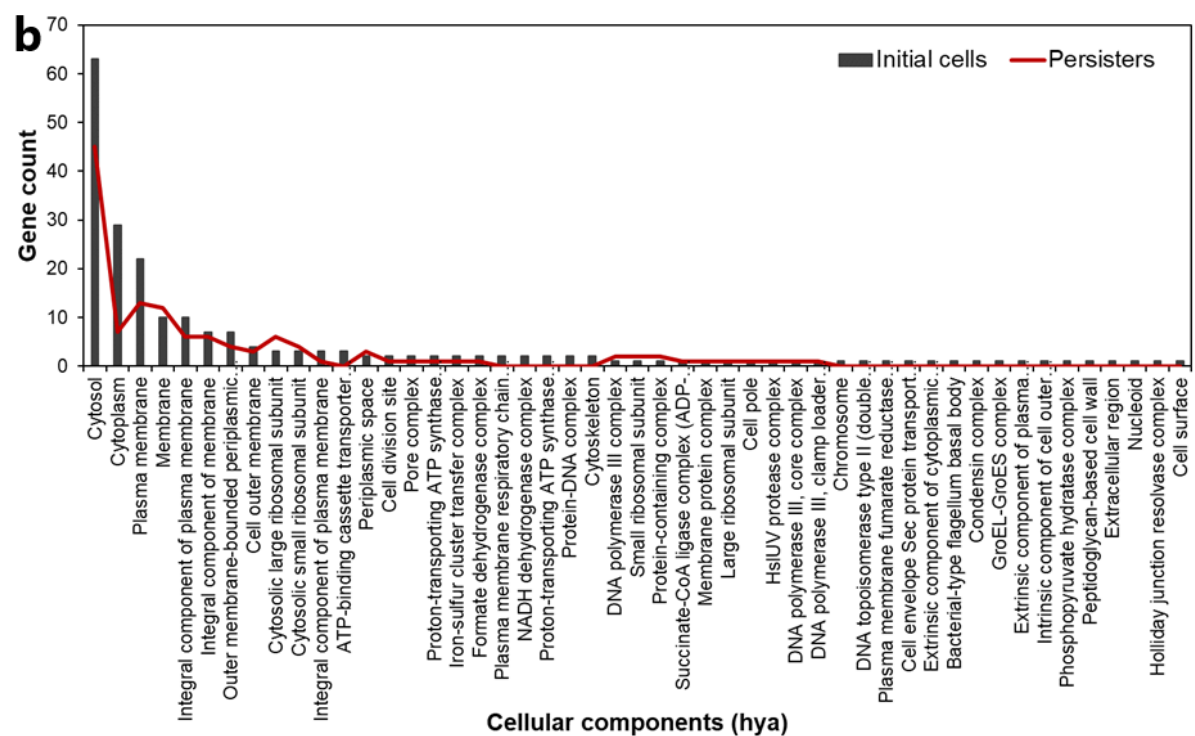
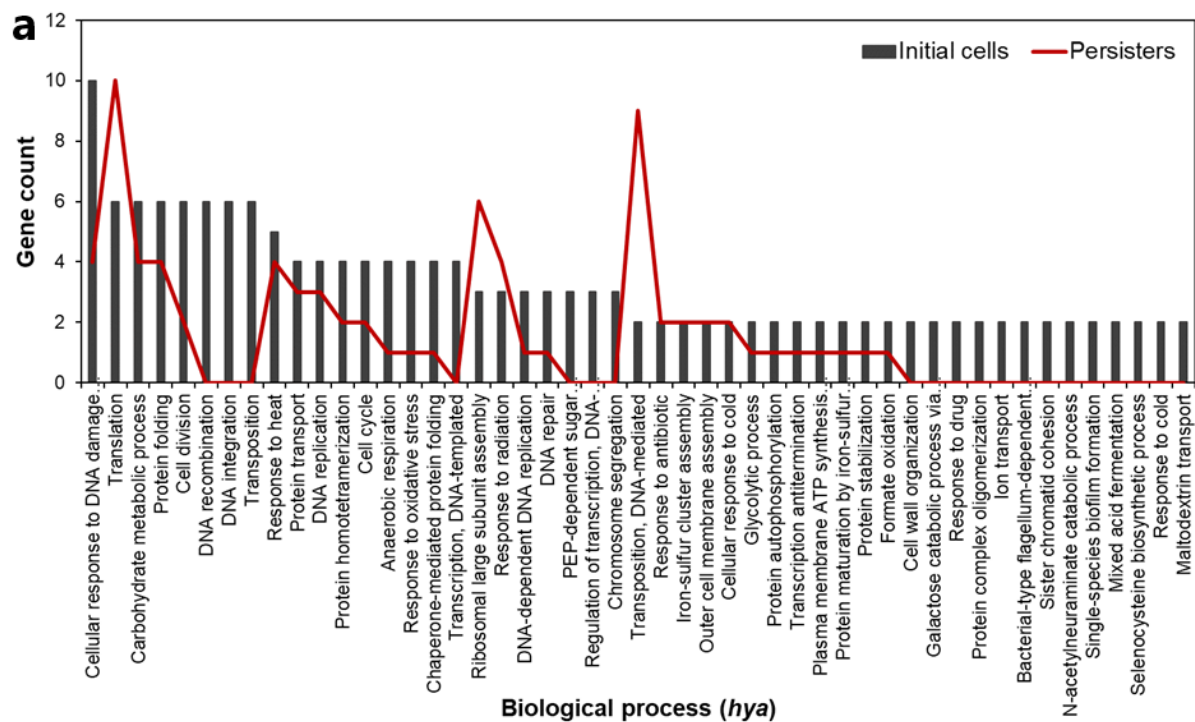


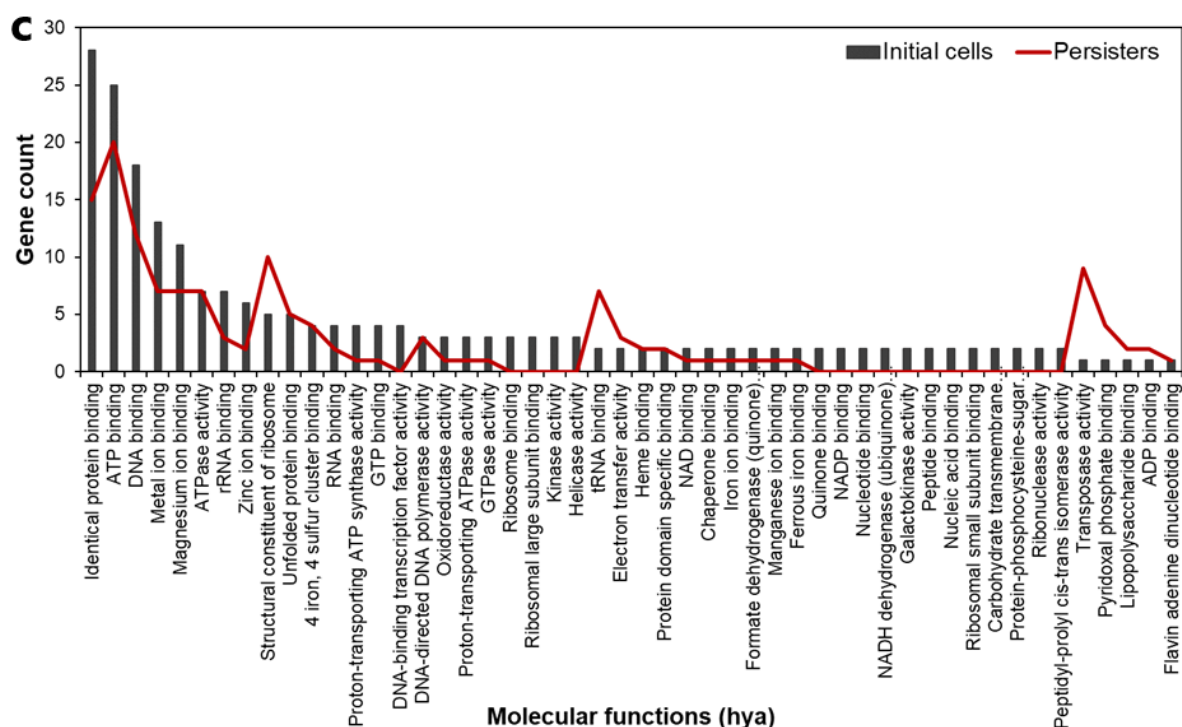
**Figure 4. 5** Affected metabolisms in initial cells and persisters.

The key metabolic pathways in the initial cells and persisters were identified by KEGG pathway enrichment analysis. The data from the mutants were normalized to that of the PS.

#### 4.3.6. Gene ontology (GO) enrichment analyses

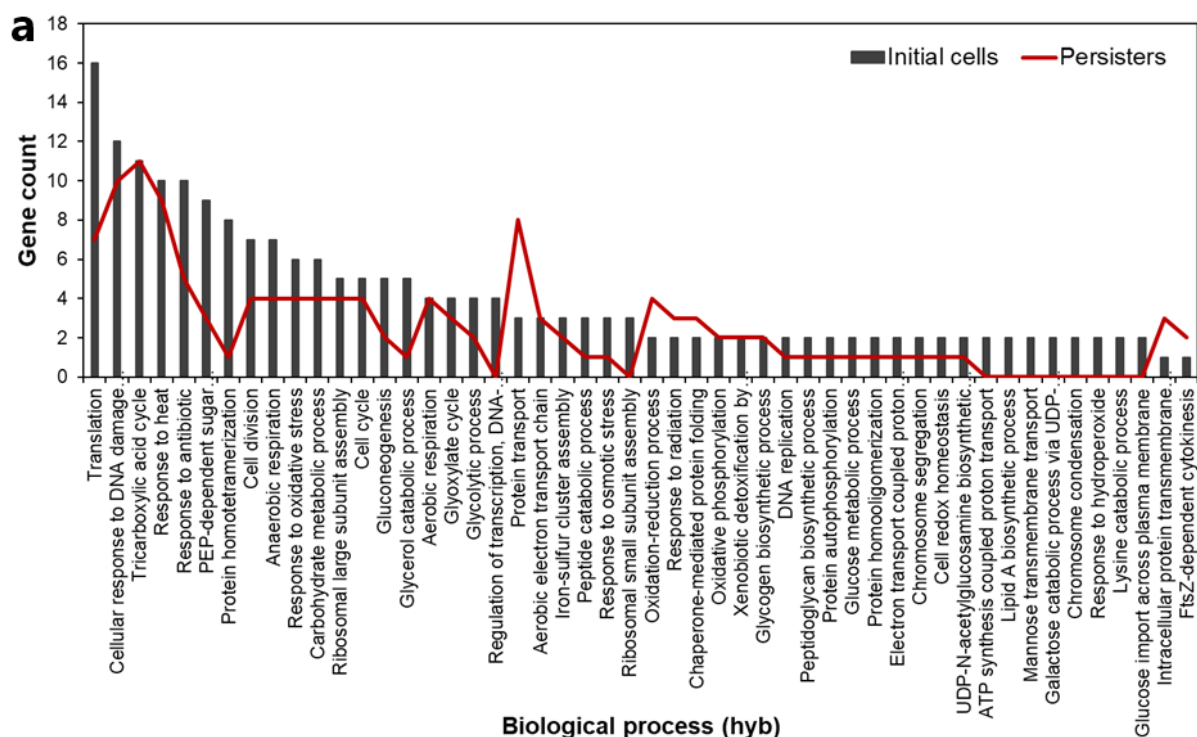
To go deeper into metabolic alterations in persisters, the change in global gene expression was investigated through GO enrichment analyses (Figure 4.6-4.9). The influenced biological processes (BP), cellular components (CC), and molecular functions (MF) were identified using the GO enrichment analysis approach (Young, 2010). The top 50 GO terms ranked in initial cells were chosen to compare in persisters (4.6a-c, 4.7a-c, 4.8a-c, 4.9a-c).

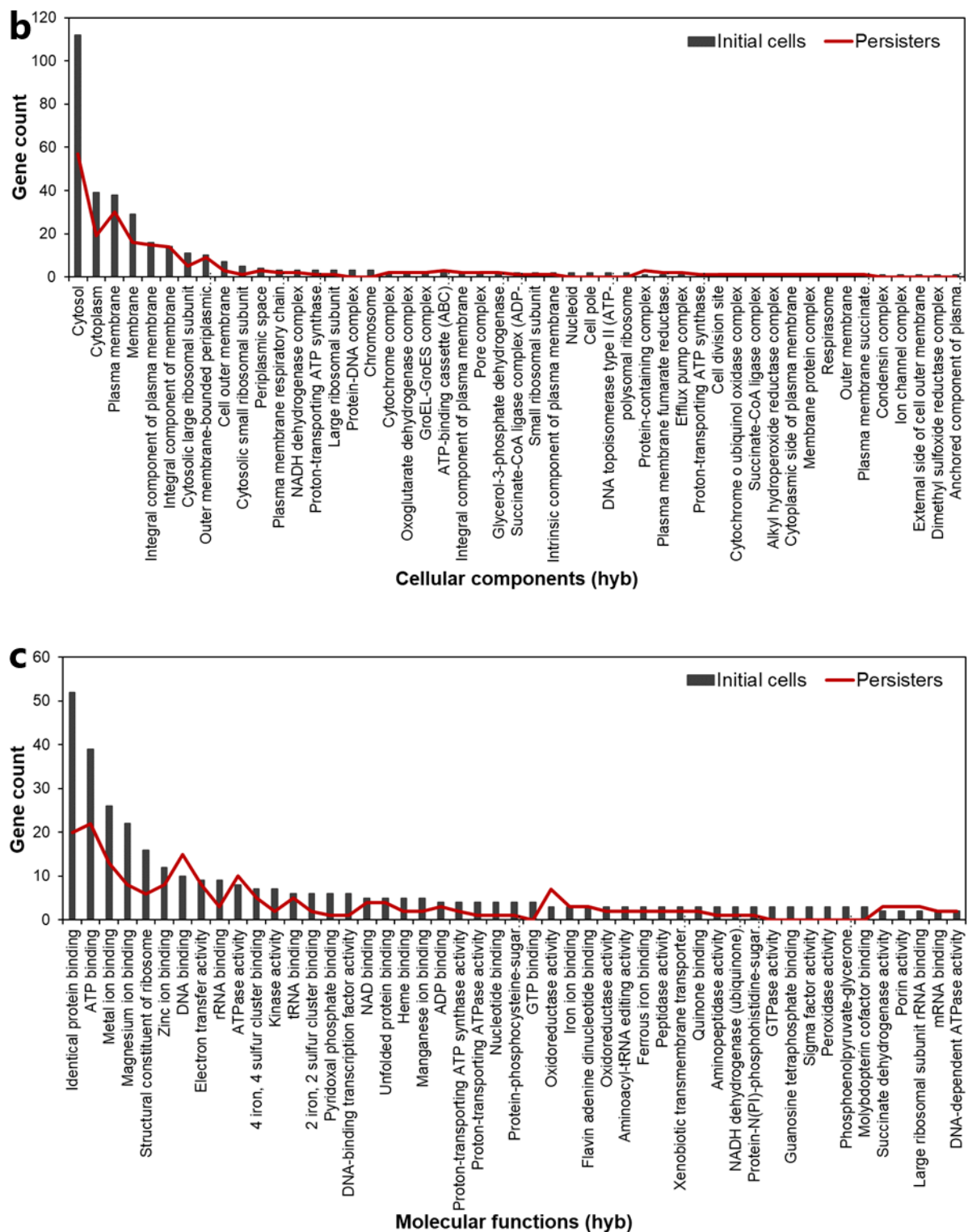




**Figure 4. 6** GO enrichment analysis of differentially expressed genes from initial cells and persisters of the *hya* operon mutant for biological processes (a), cellular components (b), and molecular functions (c).

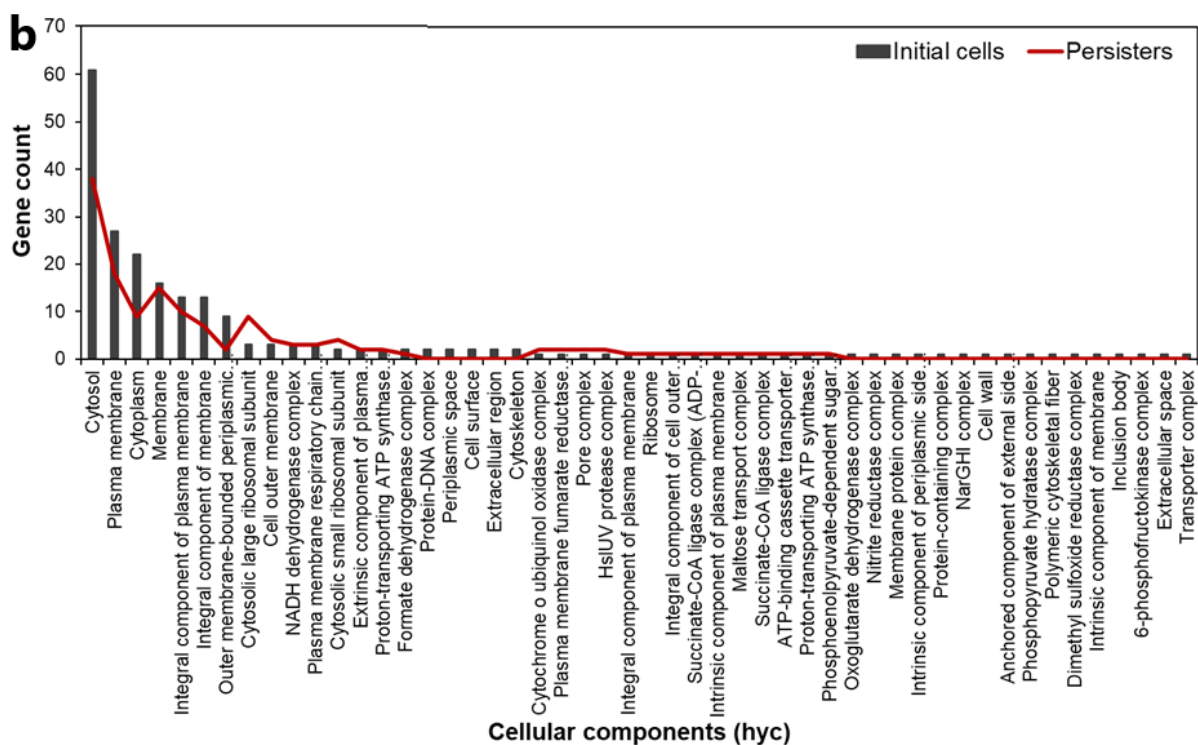
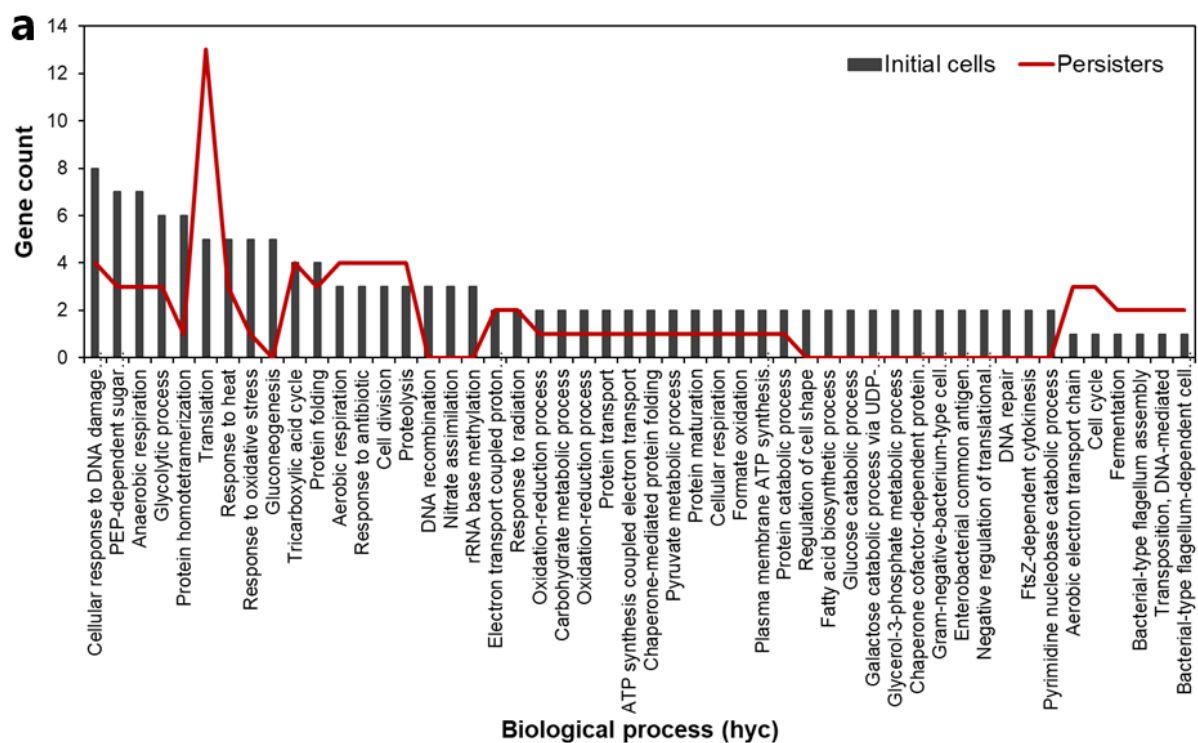
Only the top 50 terms are presented. The data from the mutant strains were normalized with that of the PS.

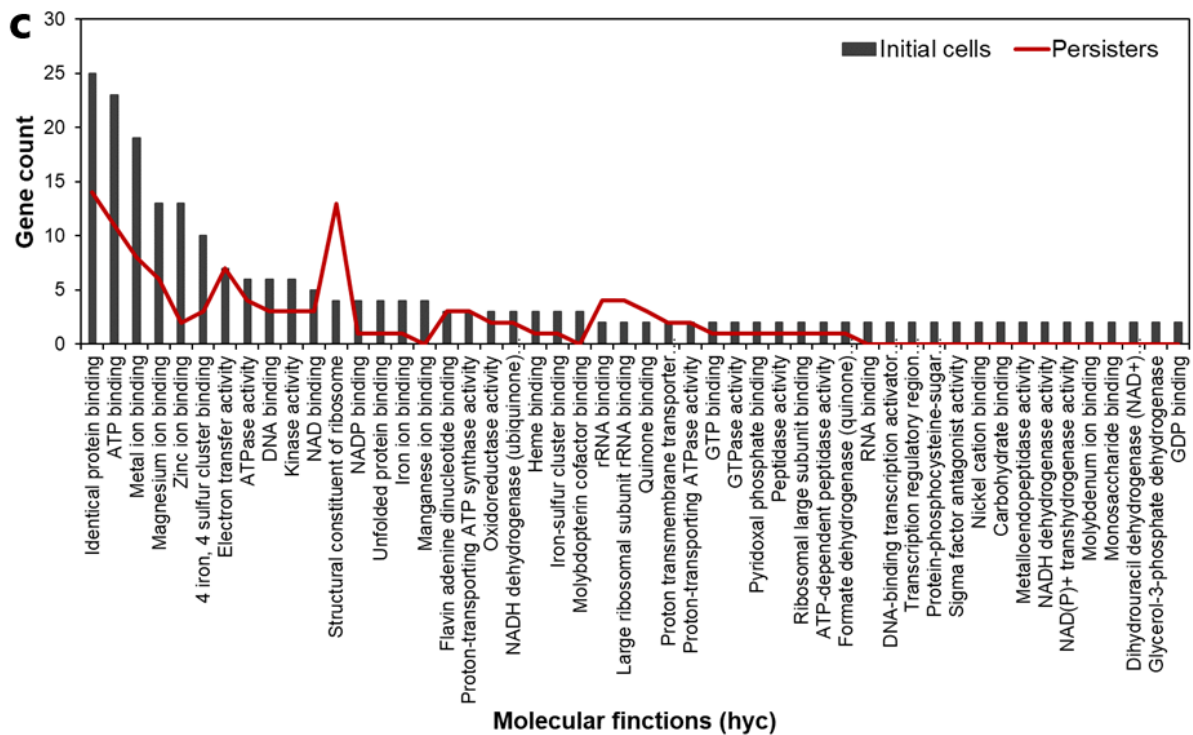




**Figure 4. 7** GO enrichment analysis of differentially expressed genes from initial cells and persisters of the *hyb* operon mutant for biological processes (a), cellular components (b), and molecular functions (c).

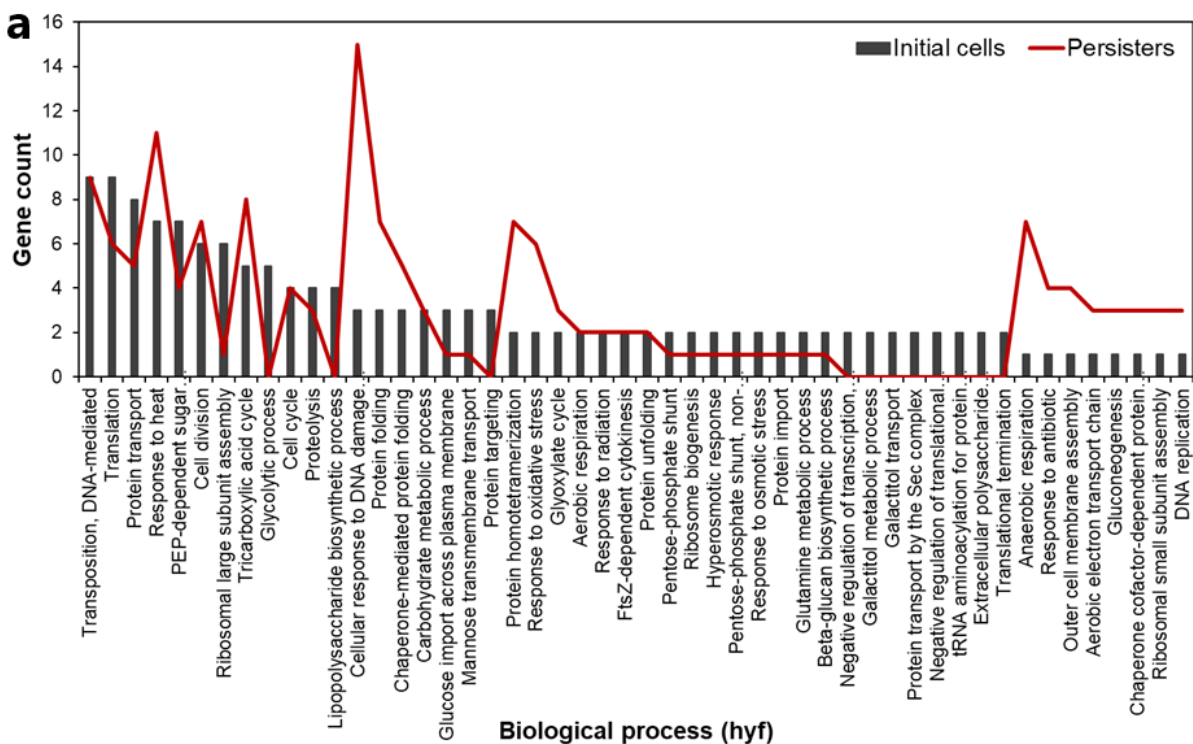
Only top 50 terms are presented. The data from the mutant strains were normalized with that of the PS.





**Figure 4. 8** GO enrichment analysis of differentially expressed genes from initial cells and persisters of the *hyc* operon mutant for biological processes (a), cellular components (b), and molecular functions (c).

Only the top 50 terms are presented. The data from the mutant strains were normalized with that of the PS.



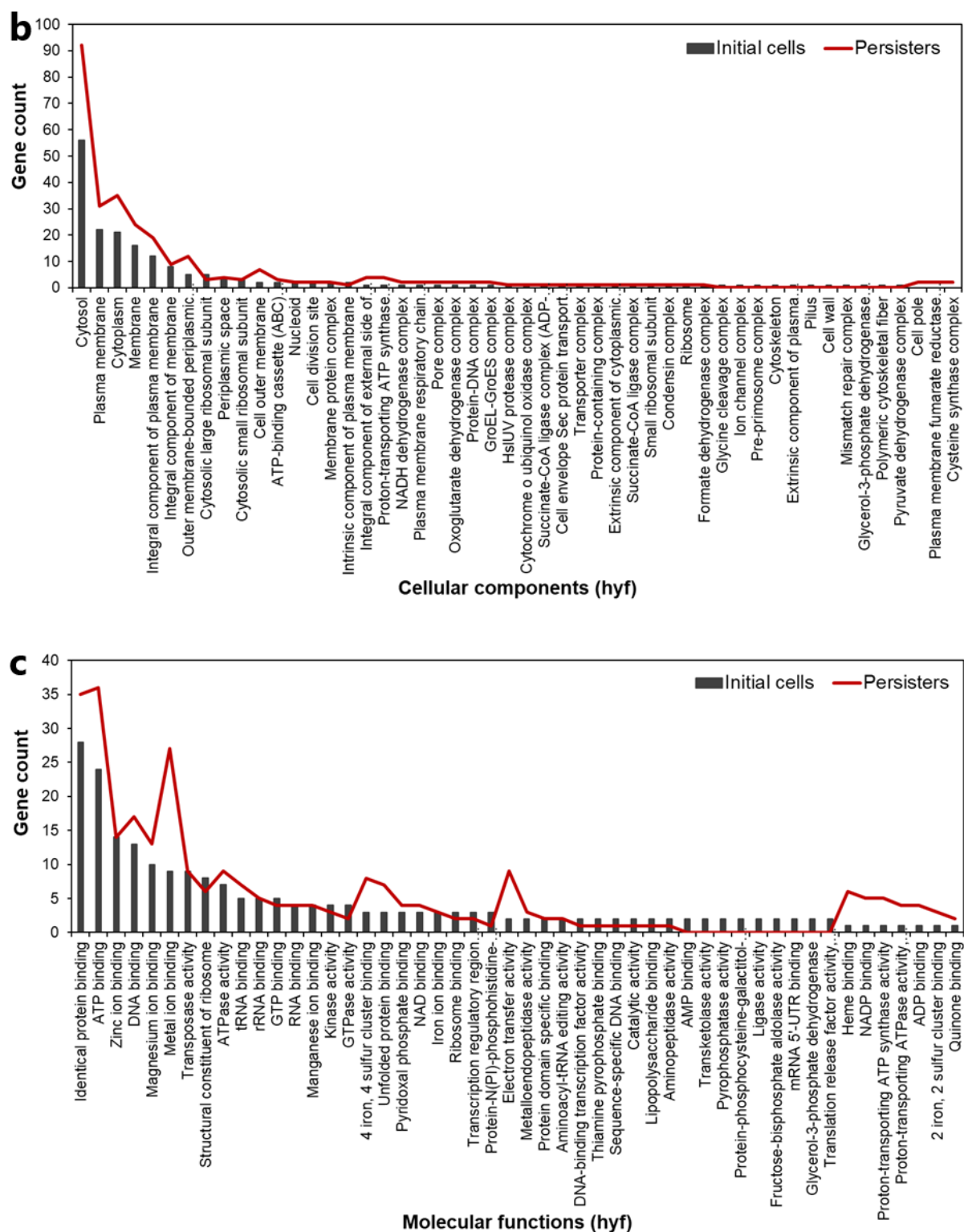


**Figure 4. 9** GO enrichment analysis of differentially expressed genes from initial cells and persisters of the *hyf* operon mutant for biological processes (a), cellular components (b), and molecular functions (c).

Only the top 50 terms are presented. The data from the mutant strains were normalized with that of the PS.

As result, the translation, large ribosomal subunit, cellular response to DNA damage stimulus, carbohydrate metabolic process, protein folding and transport, cell division and cycle, response to the antibiotic, tricarboxylic acid cycle, and phosphoenol pyruvate-dependent sugar phosphotransferase system were found most altered BPs in persisters of all mutant cells (Figure 4.6a, 4.7a, 4.8a, 4.9a). In the category of CC, cytosol, and cytoplasm, membrane and plasma membrane, integral component of membrane and plasma membrane, large and small ribosomal subunits, outer cell membrane, periplasmic space, pore complex, proton-transporting ATP synthase complex, ATP-binding cassette transporter complex, plasma membrane respiratory chain complex I or NADH dehydrogenase complex were obtained as significantly altered CCs in persisters of all mutant cells (Figure 4.6b, 4.7b, 4.8b, 4.9b). Whereas the common MFs observed in all persister cells include, ATP and NAD binding, DNA and RNA binding, structural constituent of ribosome, metal ion binding, magnesium, and zinc ion binding, ATPase activity, tRNA and rRNA binding, 4 iron-4 sulfur cluster binding, electron transfer activity, proton-transporting ATP synthase activity, and oxidoreductase activity (Figure 4.6c, 4.7c, 4.8c, 4.9c). This analysis demonstrates the significant role of hydrogenases in persistence mediated via multiple metabolic factors and phenomena.

#### **4.4. Discussion**

To investigate the significance of hydrogenase in persistence, four hydrogenases operon deletion mutants were exposed to a dose of antibiotic at their mid-exponential phase to get persister cells. Ampicillin was chosen as it is widely used for persister isolation (Wang, 2017; Lewis, 2019). The initial cells and the persisters were then evaluated for their growth, cellular viability, and transcriptomics.

*E. coli* hydrogenases were mainly studied under anaerobic conditions (Vardar-Schara, 2008; Trchounian, 2012). Therefore, both oxygen-deprived (micro-aerobic) and anaerobic cultural conditions were employed to investigate persistence with hydrogenases. As reported,

the survival of persisters requires a small (20%) drop in DO saturation, and at high DO concentration levels, the persister population is killed over time (Grant, 2012). A near zero oxygen concentration cultural conditions found in this study (Figure 4.1b), may indicate the presence of a persister subpopulation. Additionally, since the persister population gets killed overtime at high levels of oxygen, and their survival requires a drop in DO (Grant, 2012), the micro-aerobic conditions appear feasible for the growth of persisters, in this study.

The increased cellular viabilities of the persisters of hydrogenase (large subunit gene and operon) mutants, revealed the significance of hydrogenases on persistence (Figure 4.2a and b). Comparable affected viabilities of operon persisters than the single gene persisters pointed to a more deleterious nature of operon deletion, which is supported by our previous studies on hydrogen metabolism (chapter 3) (Shekhar, 2021). Hyd-2 and Hyd-3 indicated their more significance in the viabilities of persisters. Hydrogenases were never extensively studied for their effects on drug metabolism, however, the uptake-hydrogenases have been reported for showing significance in some bacteria (Zbell, 2008). Our previous studies demonstrated that all four hydrogenases of *E. coli* have uptake activity (Shekhar, 2021), which may support the enhanced cell viability of the persisters of mutants. Purified Hyd-1 of *Clostridium pasteurianum* was found able to reduce several 2-, 4- and 5-nitroimidazole compounds via an electron carrier-coupled mechanism that activities of hydrogenases in drug metabolism (Church, 1990).

Hydrogenases have shown their activity under aerobic or micro-aerobic conditions also (Olson, 2002; Cordero, 2019), however, *E. coli* hydrogenases were mainly reported from anaerobic conditions (Maeda, 2018; Vardar-Schara, 2008; Trchounian, 2012), therefore, this was interesting to find that the expression of hydrogenases was relatively elevated in persisters, under both the conditions (Figure 4.3a and b). As previous reports say that the expression of Hyd-1 and Hyd-2 was found to be maximum under anaerobic conditions (Richard, 1999; Maeda, 2018); Hyd-3, repressed by oxygen (Pecher, 1983); and Hyd-4, normally does not

transcribe or shows very low transcription (Trchounian, 2012). These reports support the low or almost no expressions, as in our study.

As reported by Kohanski et al. (2010), in the primary drug-target interaction, NADH-coupled electron transport is a key upregulated pathway that induces a surge in NADH consumption upon exposure to bactericidal antibiotics. This catabolic depletion of NADH likely induces a burst in superoxide ( $O_2^{\cdot-}$ ) generation via ETC. These  $O_2^{\cdot-}$  damages Fe-S clusters and facilitate the formation of hydroxyl ( $\cdot OH$ ) radicals via the Fenton reaction. These  $\cdot OH$  radicals contribute to cell death through cellular damage. The electrons are transferred to ETC via the Fe-S clusters harbored in the subunit proteins of hydrogenases, therefore considered as redox-sensitive proteins to implicate in the mechanism for antibiotic-induced cell death or persistence (Stiebritz, 2012). Since ROS is identified as a critical antibiotic-induced cellular stress, tolerance to antibiotics is the ability of the cell to defend itself against it (Kohanski, 2010). Contrary to this, according to a few reports, ROS can provide a protective effect against antibiotics by inducing persistence (Dwyer, 2014; Brynildsen, 2013). A relative decrease in ROS levels in antibiotic-treated mutant cells in comparison with PS may indicate their ROS scavenging activity (Figure 4.4), where *hyb* mutant seems to be able in ROS detoxification and persistence since bacterial survival against antibiotics is also reported to be mediated by such an activity (Grant, 2012; Lewis, 2019).

In general, the central metabolism of the cell yields metabolites, ATP, and reduced cofactors (NADH,  $FADH_2$ ) (Wilmaerts, 2019). The electron transport chain (ETC) consists of NADH dehydrogenases, and terminal oxidases and is recognized as strongly branched, which allows the cells to respond to changing environments (Borisov, 2011; Efremov, 2012). In aerobic conditions, ubiquinone accepts electrons from NADH dehydrogenase I and transports them to one of the terminal oxidases (Wilmaerts, 2019; Efremov, 2012). In this, protons are transported across the membrane, creating an electrochemical proton gradient, which drives

ATP synthesis (Unden, 1997). Furthermore, the catabolism generates NADH, which is then oxidized by enzymes in the ETC and contributes to PMF. The elevated PMF facilitates the uptake of bactericidal antibiotics and the killing of persisters (Allison, 2011; Kohanski, 2007). At the exponential phase, persisters were found characteristically as the least redox-active subpopulation, indicating low metabolic activity is the key to the survival of persister cells (Wood, 2013; Mehmet, 2015). Since the formation of persister cells is inversely correlated with metabolic activity and energy production (Lewis, 2019), metabolism is recognized as a general cause of tolerance since most bactericidal antibiotics kill by corrupting metabolic activity and energy-dependent targets (Shan, 2017). Persister survival has been attributed to the inhibition of essential cell functions during antibiotic stress, therefore; metabolism plays a critical role in this process (Amato, 2014; Liu, 2020; Cabral, 2018). Amino acid biosynthesis and degradation (Liu, 2020b), carbohydrate biosynthesis and degradation (Agamennone, 2019), cell wall biogenesis (Costerton, 1975), and energy metabolism (Shan, 2017; Cabral, 2018; Mohiuddin, 2020; Shan, 2017), glycolysis (Murima, 2014), lipid metabolism (Cañas-Duarte, 2020), metabolic intermediate biosynthesis (Murima, 2014), oxidative phosphorylation (Amato, 2014; Mohiuddin, 2020), and TCA cycle (Wang, 2018), are reported to be significantly involved in persistence and thereby found to be contributory persisters of all four hydrogenase operon mutants (Figure 4.5).

As previously identified and crucial in persistence, the translation (Cho, 2015), large ribosomal subunit (Maisonneuve, 2011), cellular response to DNA damage stimulus (Mok, 2018), carbohydrate metabolic process (Agamennone, 2019), protein folding and transport (Scheuplein, 2020; May, 2018; Holland 2004), cell division and cycle (Aakre, 2012; Sass, 2013), response to antibiotic (Lewis, 2019), TCA cycle (Wang, 2018), and phosphoenol pyruvate-dependent sugar phosphotransferase system (Postma, 1989) were also found most commonly altered biological processes in all four hydrogenase persisters (4.6a-c, 4.7a-c, 4.8a-

c, 4.9a-c). Similarly, cytosol, and cytoplasm (Reyes-Fernández, 2020), membrane and plasma membrane (May, 2018), integral components of membrane and plasma membrane (May et al. 2018), large and small ribosomal subunits (Wood, 2019; Maisonneuve, 2011; Romilly, 2014), cell outer membrane (May, 2018), periplasmic space (Costerton, 1975), pore complex (Brito, 2019), proton-transporting ATP synthase complex (Shan et al. 2017), ATP-binding cassette transporter complex (Lewis, 2012), plasma membrane respiratory chain complex I or NADH dehydrogenase complex, cytochrome complex (Allison, 2011), as identified key cellular components were also obtained altered in all four hydrogenase persisters (Figure 4.6a, 4.7a, 4.8a, 4.9a). Finally, in the same way, the observed key molecular functions reported crucial in persistence such as ATP and NAD binding (Lewis 2012; Pu, 2019; Mohiuddin, 2020), DNA and RNA binding (Zeinert, 2018; Mohiuddin, 2020; Maisonneuve, 2011; Romilly, 2014), structural constituent of ribosome (Wood, 2019; Cho, 2015), metal ion binding (Falcón García, 2020), magnesium and zinc ion binding (Xu, 2020), ATPase activity (Shan, 2017), tRNA and rRNA binding (Romilly, 2014), 4 iron-4 sulfur cluster binding (Kohanski, 2010), electron transfer activity (Allison, 2011; Tuchscher, 2020), proton-transporting ATP synthase activity (Mohiuddin, 2020), and oxidoreductase activity (Amato, 2014; Mohiuddin, 2020) were also found notably influenced in all hydrogenase persisters (Figure 4.6b, 4.7b, 4.8b, 4.9b). These results demonstrate the influential and significant roles of hydrogenases on metabolism and therefore, on persistence.

#### **4.5. Conclusion**

Hydrogenases of *E.coli* were found to have influencing roles in persistence via their effects on metabolism. Hydrogenases specifically Hyd-2 and Hyd-3 seem to be relatively more significant. The transcriptomic analysis further revealed wide genomic connectivity of hydrogenases to influence persistence. This study also showed that the hydrogenases may have

a potential ability to influence cellular physiology and thereby cellular metabolism, a deeper investigation further is therefore recommended.

## CHAPTER 5

# ELUCIDATING THE SIGNIFICANCE OF HYDROGENASES IN CELLULAR VIABILITY AND ACID RESISTANCE OF *ESCHERICHIA COLI*

### 5.1. Introduction

The extraordinary ability of *Escherichia coli* to survive and resist extreme acid stress makes it a model for this research (Hayes, 2006; Tsakalidou, 2011). Along with well-studied *E. coli* strains (such as O157:H7 and K-12) (King, 2010; Maurer, 2005) other bacteria, for instance, *Salmonella enterica* (Spector, 2012), *Shigella flexneri* (McNorton, 2012), *Helicobacter pylori* (Ansari, 2017), and, most popularly known, lactic acid bacteria (Tsakalidou, 2011), are known to be resistant to low pH and survive in the acidic conditions of the mammalian stomach up to an approximate pH of 2.0 (Kanjee, 2013).

Microorganisms have developed various effective mechanisms to survive in acidic environments including actively expelling protons out of the cell and modifying the proton permeability of the cellular membrane (Lund, 2014). The basic action of acid resistance is the direct consumption of intracellular protons to counteract acid stress (Kanjee, 2013). Hydrogenases are complex metalloenzymes that catalyze the reversible conversion between hydrogen, and protons and may have a potent role in acid resistance (Hayes, 2006; Tsakalidou, 2011). It has been suggested that these enzymes in *E. coli* decrease cytoplasmic acid stress and contribute to its acid resistance systems (Hayes, 2006). Hydrogenases of *E. coli* respond to pH and oxygen levels and showed higher expression in acid than in base (Hayes, 2006; Noguchi, 2010). Their activity may be important at low pH for their contribution to the expulsion of excess protons from the cytoplasm (Lund, 2014; Trchounian, 2012).

*E. coli* can adapt to changing oxygen levels since it is a facultative anaerobe found as a commensal in the gastrointestinal tract (GIT) (Pedraz, 2020). Despite aerobic and anaerobic

abilities, the oxygen-deprived (micro-aerobic) atmosphere is significantly less well characterized (Bettenbrock, 2014). Therefore, considerable information on bacterial extreme-acid survival in such an environment is lacking (Riggins, 2013). However, the GIT provides a variety of environmental challenges to any bacterium seeking to successfully colonize in the host, including extreme acidic pH (Marteyn, 2011), yet several are still able to adapt and combat the immune system such as *S. enterica* (Spector, 2012), *S. flexneri* (McNorton, 2012), and *H. pylori* (Ansari, 2017). The GIT has traditionally been reported as an anaerobic environment (Bäckhed, 2005), although it is now described to consist of physiologically low oxygen levels since there is a significant microaerobiosis due to oxygen diffusion from vascularised tissue (Partridge, 2007). The dissolved oxygen (DO) concentration in the GIT is reported to be in the range of 0–100  $\mu\text{M}$  (Riggins, 2013) and is present in varying degrees in the gut environment (decreasing from the stomach towards the distal colon) (Jubelin, 2018). A unique oxygen gradient exists within the human GIT (Singhal, 2020) due to fluctuations in perfusion facilitated by oxygen uptake through swallowing food, digestion-dependent blood flow and oxygenation of the intestinal mucosa, and oxygen consumption by the epithelium and microbiota (Marteyn, 2011). Pathogens in the GIT are therefore clearly exposed to fluctuating oxygen conditions (Marteyn, 2011), not a strict anaerobic environment.

Bacterial cultures after a definite growth show a reduction in DO, even to an undetectable level (Stolper, 2010). Bacteria such as *H. pylori* showed successful growth under near-zero oxygen conditions and combat acid stress (Ansari, 2017; Bhattacharyya, 2000; Olson, 2002). Active hydrogenase enzymes are essentially required to survive under such acidic conditions (Bhattacharyya, 2000) since molecular hydrogen is their source of energy (Olson, 2002). Therefore, this gastric pathogen grows under such reduced oxygen conditions and utilizes protons provided by hydrogenases as terminal electron acceptors facilitating acid resistance (Bhattacharyya, 2000; Olson, 2002). Since *E. coli* hydrogenases have never been

studied under oxygen-deprived cultural conditions, this study investigates their influential role in acid resistance under such conditions. The four-hydrogenase operon deleted mutants were evaluated by using their initial and acid-resistant cells. Despite the differences, all the hydrogenases were found to influence bacterial survival in an acidic environment by possessing acid resistance. Moreover, elevated hydrogenase expressions, enhanced cellular viabilities, and affected pH homeostasis were also observed in all acid-resistant cells. Comparing all the hydrogenases, Hyd-2 was found to have a relatively more significant role in acid resistance under such oxygen-deprived (micro-aerobic) conditions. Additionally, transcriptomic analysis validated the affected acid resistance systems in the acid-resistant hydrogenase mutants.

## 5.2. Materials and Methods

### 5.2.1. Bacterial strains and media

*E. coli* K-12 BW25113 was used as the wild-type (WT) strain in this study. All the strains used in this study, including operon mutants, are listed in Table 5.1. A medium containing 10 g/L Bacto Tryptone, 5 g/L yeast extract, and 5 g/L NaCl was used to grow the strains. The final concentrations of each antibiotic used in LB-ampicillin, LB-chloramphenicol, and LB-kanamycin media or plates were 50 µg/mL ampicillin, 30 µg/mL chloramphenicol, and 50 µg/mL kanamycin, respectively. Carbenicillin (10 µg/mL) was used in place of ampicillin whenever necessary. All experiments were conducted and repeated using at least three biological replicates.

**Table 5. 1 *E. coli* strains used in this study**

Strains	Genotype/relevant characteristics	Reference
<i>E. coli</i> BW25113	F <sup>+</sup> Δ( <i>araD-araB</i> )567Δ <i>lacZ</i> 4787 (::rrnB-3)λ <sup>-</sup> <i>rph-1</i> Δ( <i>rhaD-rhaB</i> ) 568 <i>hsdR</i> 514; parental strain for the KEIO collection	Yale Coli Genetic Stock Center
<i>E. coli</i> BW25113 Δ <sup>a</sup> <i>hyaA</i> - F <sup>c</sup> :: <sup>b</sup> <i>kan</i> <sup>d</sup>	Hydrogenase 1 operon deleted mutant	(Shekhar, 2021)

<i>E. coli</i> BW25113 $\Delta hybO-F::kan$	Hydrogenase 2 operon deleted mutant	(Shekhar, 2021)
<i>E. coli</i> BW25113 $\Delta hycA-I::kan$	Hydrogenase 3 operon deleted mutant	(Shekhar, 2021)
<i>E. coli</i> BW25113 $\Delta hyfA-R::kan$	Hydrogenase 4 operon deleted mutant	(Shekhar, 2021)
<i>E. coli</i> BW25113 $\Delta gadE::kan$	<i>gadE</i> gene deleted mutant	(Baba, 2006)

a and b:  $\Delta$  and  $::$  represents “deletion” and “replaced by gene,” respectively.

c: A-F, O-F, A-I, and A-R represents the “from and to” deleted segment of *hya*, *hyb*, *hyc*, and *hyf* operons, respectively.

d: *kan* denotes the kanamycin resistance gene.

### 5.2.2. The hydrogenase operon and *gadE* mutants

Each hydrogenase operon mutant investigated in this study was constructed in our previous study (Shekhar, 2021). The  $\Delta gadE$  mutant KEIO strains were provided by the KEIO library (National Institute of Genetics, Japan) (Baba, 2006). The *gadE* mutation was verified by three PCR reactions to evaluate the structure of the mutant’s loci, as previously explained (Baba, 2006). The primers used in this work are listed in Table 5.2.

**Table 5. 2 List of primers used in this study**

Primer	Significance	Sequence (5’-3’)	Reference
<b>Primers used in confirmation of mutations</b>			
k1	Confirmation of kanamycin	CAGTCATAGCCGAATAGCCT	(Shekhar, 2021)
k2	resistance gene	CGGTGCCCTGAATGAACTGC	
<i>gadE</i> -F	To confirm <i>gadE</i> gene mutation	ACAAGCTGATAACAACCAG	This study
		GAA	
<i>gadE</i> -R		AGTGATCGACATGGTGAGGT	This study
<b>Primers used in qRT-PCR</b>			
<i>hyaB</i> -F	Expressing large subunit gene of	CACGGCGGACTTCATTAACA	This study
<i>hyaB</i> -R	Hyd-1	CCGTAGCTGAGAACGCATTT	
		AT	
<i>hybC</i> -F	Expressing large subunit gene of	CAAAGTGAAGCGACTTTGTTG	This study
	Hyd-2	AG	
<i>hybC</i> -R		GGTAGTTCACCGCACCTTTA	
<i>hycE</i> -F	Expressing large subunit gene of	CCATTCTGCTGGAGGTAGAA	This study
	Hyd-3	C	

<i>hycE</i> -R		ACGCGGAAGAACTGCATAA	
<i>hyfG</i> -F	Expressing large subunit gene of Hyd-4	CTGCATATCACCTCCGATGA	This study
		A	
<i>hyfG</i> -R		TGCCGCGATGGACATAAA	
<i>rrsG</i> -F	Housekeeping gene for expression	TATTGCACAATGGGCGCAAG	(Shekhar,
<i>rrsG</i> -R	data	ACTTAACAAACCGCCTGCGT	2022)

---

F and R represent forward and reverse primers, respectively.

### 5.2.3. Acid resistance assay

The acid resistance assay was performed as previously described (Wu, 2014). Overnight cultures were prepared aerobically at 37 °C with shaking at 180 rpm with antibiotics (for mutants) or without antibiotics (for WT). The 50 mL fresh LB medium was then inoculated with 50 µL overnight culture (1:1000 ratio) and grown aerobically to the mid-exponential phase ( $OD_{600\text{ nm}} \approx 0.8\text{--}1.0$ ) without antibiotic. Cells were then challenged to nearly pH 2.5 by adjusting the pH with HCl using 37% HCl and incubated for 2 hrs at 37 °C with shaking at 180 rpm. To measure cell viability, samples were taken before and after pH adjustment, washed, and serially diluted in 0.85% (w/v) NaCl solution, plated on LB agar and grown overnight at 37 °C to determine CFU/mL. Cell populations before pH adjustment are termed initial cells. Acid-resistant cells are obtained from the initial cells after certain growth under acidic pH.

### 5.2.4. Total RNA extraction and quantitative reverse transcription PCR (qRT-PCR)

The initial and acid-resistant cell populations were grown as explained above and removed from the cultures to collect the pellets for RNA extraction as previously described (Shekhar, 2022). Housekeeping gene *rrsG* (16S rRNA) was used to normalize the expression data. RNA extracted from the WT was used as the reference template. All the primers used for this transcription analysis are listed in Table 5.2.

### 5.2.5. DNA library preparation and high-throughput sequencing

The DNA library preparation was performed using Illumina's Nextera XT DNA Library Prep Kit, following the manufacturer's recommended protocol. The raw sequence data have

been contributed to the National Center for Biotechnology Information (NCBI) under the Short Reads Archive, accession number PRJNA671558.

### **5.2.6. RNA Seq data analysis**

The transcriptomic data analysis was performed as previously described (McClure, 2013). FastQ formatted raw reads were subjected to quality assessment to determine whether the raw reads were qualified for mapping by FastQC and trimmed using cutadapt tool based on the Phred quality score cutoff  $\geq 30$ . The trimmed good-quality reads were mapped to the reference genome of *E. coli* str. K-12 substr. MG1655 (NC\_000913.3). The Rockhopper software was employed to map the reference genome (McClure, 2013). Gene expression was normalized by calculating reads per kilobase per million mapped reads. The edgeR tool was used to perform the differential gene expression analysis. The functional annotations were retrieved from the EcoCyc database.

### **5.2.7 Dissolved-Oxygen measurements**

DO levels within culture flasks were determined using Custom's DO sensor (DO-1000PE) according to the manufacturer's instructions. The 50 mL cultures of initial and acid-resistant cell populations were prepared as above and DO was monitored before and after pH adjustment. The oxygen sensor was calibrated to media at 37 °C.

### **5.2.8. Intracellular pH measurement**

Intracellular pH (pHi) was measured by the methodology previously described (Olsen, 2002b). Two separate cultures of the strains containing pGFPratiometric, with and without 10  $\mu$ M carbonyl cyanide-m-chlorophenylhydrazone (CCCP), were prepared in LB (chloramphenicol, 30 mg/ml) and grown for 16 hrs with incubation at 37°C with shaking at 120 rpm. The cultures containing CCCP were used to make a calibration curve. Pellets from 1 mL cultures were collected in several tubes as per the number of extracellular pHs tested (5.8, 6.2, 6.6, 7.0, 7.4, 7.8) and washed twice with a potassium phosphate buffer (pH 7.5) containing

glucose (10 mM). The pellets were then separately resuspended in a potassium phosphate buffer (containing 10 mM glucose) of a different pH and incubated for 30 min at RT. Then, 200 µl of the bacterial suspension was transferred to a 96-well plate, and fluorescence was recorded at excitation (nm)/emission (nm) wavelength combinations 410/430 using a plate reader.

### **5.2.9. Statistical analysis**

Statistical significance was evaluated with the Student t-test or ANOVA and Tukey's test. P values of <0.05, <0.01, and <0.001 were considered significant (\*), very significant (\*\*), and highly significant (\*\*\*) respectively. For transcriptomic analysis, significant genes were filtered with a p-value  $\leq 0.05$ . Upregulated and downregulated genes were filtered using fold change  $\geq 0.8$  and  $\leq -0.8$ , respectively.

## **5.3. Results**

### **5.3.1. Oxygen-deprived state of the mutant cultures**

Hydrogenases were mostly studied and reported to be maximally expressed under anaerobic conditions (Vardar-Schara, 2008). As previously indicated, the growing bacteria in cultures consume oxygen faster (Stolper, 2010) until it reaches zero or a deprived state. Therefore, in the case of hydrogenase, it was required to anticipate the DO concentration in the cultures during the growth (Fig. 5.1a and b) of mutant cells. DO levels were found to drop to near-zero in the cultures at their mid-exponential phase, i.e., the point at which the pH of the culture was adjusted to ~2.5. This result indicates that DO concentrations declined to zero under the test conditions, where hydrogenase activity was presumed to be feasible.

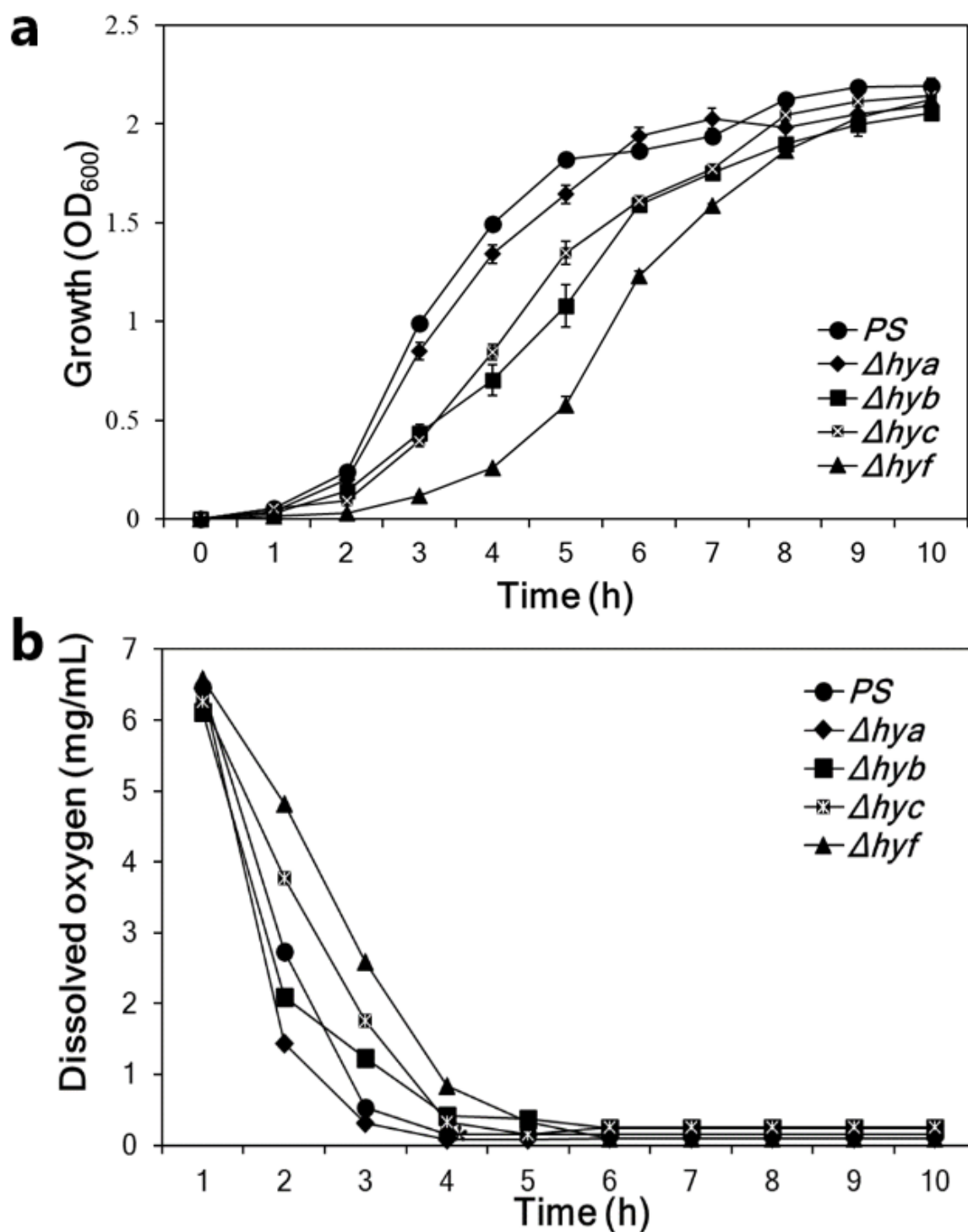


**Figure 5. 1** Growth and dissolved oxygen (DO) concentrations of the hydrogenase mutants. (a) Growth curves of the operon mutants and comparison with the wild type. (b) DO concentrations in the cultures of the strains at different time points of the growth. Data represent the average of three replicates. The error bars indicate the standard deviation.

### 5.3.2. Elevated hydrogenase expressions

Transcriptomic studies of pH stress mainly focused on aerated cultures (Maurer, 2005; Tucker, 2002), demonstrating hydrogenase activity under aerobic or micro-aerobic conditions (Olson, 2002a). Therefore, the expression of each hydrogenase was elucidated in acid-stressed under oxygen-deprived cultural conditions, where an expression of the gene encoding the large subunit protein of each hydrogenase was evaluated (Fig. 5.2). A diminished expression of hydrogenases in the cells from the cultures of the initial cells was observed, which was expected as the initial exposure to a micro-aerobic cultural environment may reduce hydrogenase functioning and expression. Interestingly, hydrogenase expression was found significantly elevated in all acid-resistant cells compared to the WT strain. In contrast to the *hyc* mutant, the *hya*, *hyb*, and *hyf* mutants showed relatively more expression in acid-resistant cells, which might signal the more influential role of Hyd-3. As presumed, these elevated hydrogen expressions from the acid-resistant cells may indicate a significant role in the acid resistance under an oxygen-deprived cultural state.

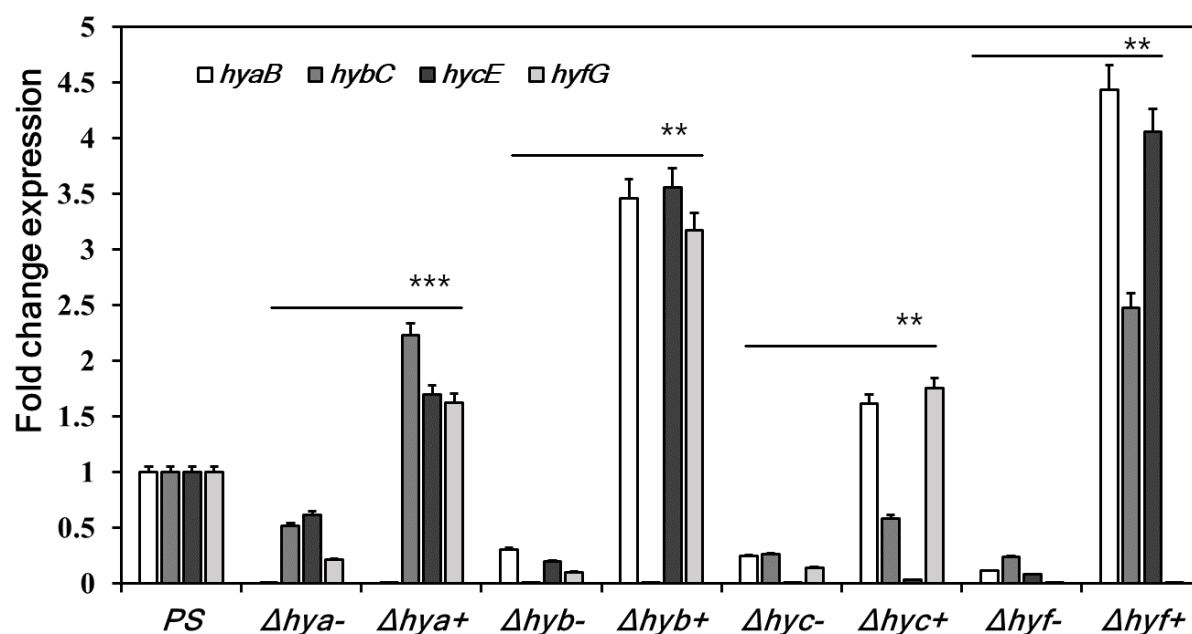
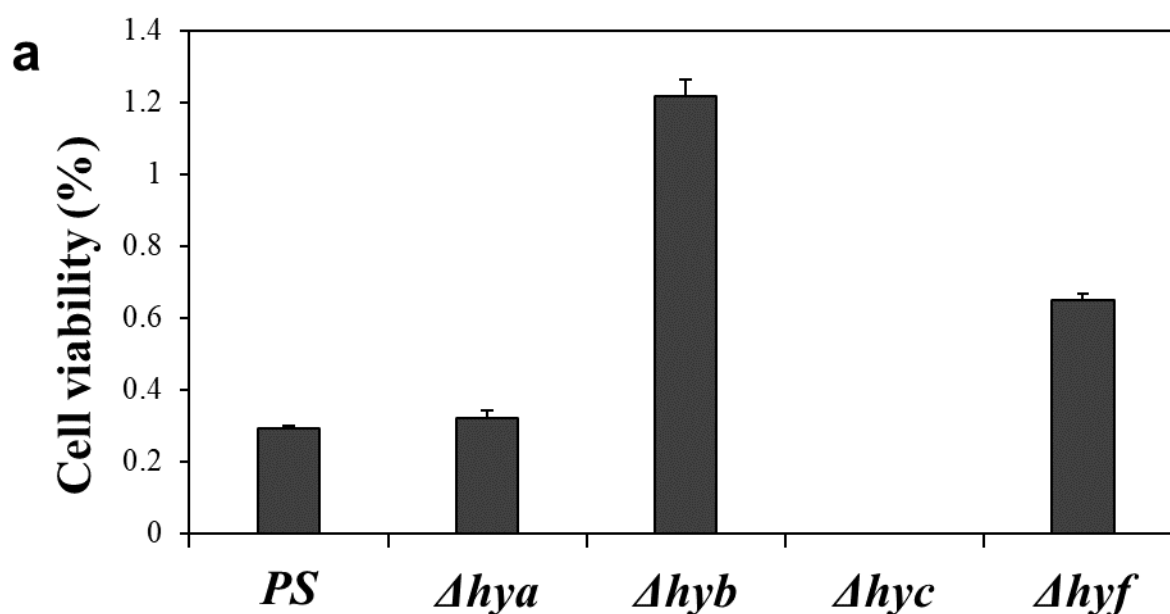


**Figure 5. 2** Elevated hydrogenase expressions in the acid-resistant hydrogenase mutant cells. The fold change expression levels of hydrogenases (genes encoding large subunit) in the initial (-) and acid resistant (+) cells of the four hydrogenase operon mutants. The relative expression

level was normalized with a housekeeping gene, *rrsG* (16S rRNA). Data are presented as means and SEM (n = 5; \*\*, P < 0.01; \*\*\*, P < 0.001).

### 5.3.3. Viabilities of the hydrogenase operon mutants in acid resistance

Cellular viability is the most frequently observed phenotype of acid-tolerant cells in acid stress (Tsakalidou, 2011). To evaluate the hydrogenase-based variation in the cell viability, CFU was estimated from initial and acid-resistant cells. A group of the same strains was also grown anaerobically for comparative analysis. As a result, under both conditions, the cellular viabilities of all the mutants were found to be influenced compared to the WT (Fig. 5.3a and b). In comparison with anaerobic conditions, micro-aerobic cultural conditions were found to be relatively more threatening to survival due to comparatively low viabilities. Under both conditions, the *hyb* mutation was noted to be most significant for survival since the viabilities were found relatively higher than other mutations. Unlike the *hyb* mutant, the *hyc* mutant was found to be struggling to survive under both conditions due to significantly reduced viabilities. The *hya* and *hyf* deletions showed nearly similar viabilities with more from micro-aerobic states by later one.



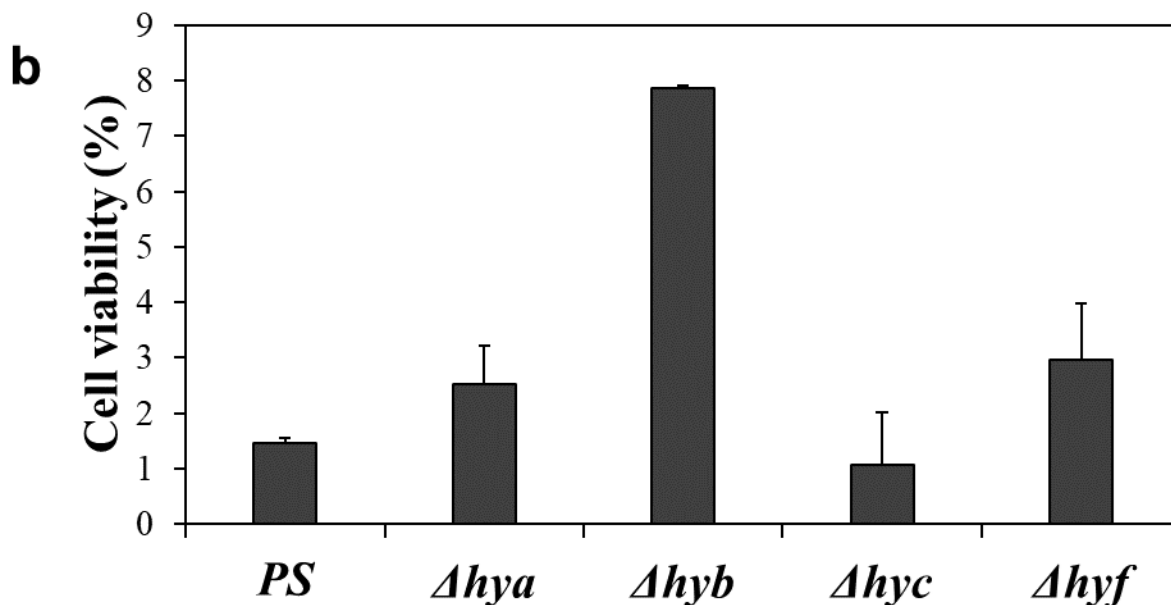


**Figure 5. 3** Influenced cellular viability of the hydrogenase operon mutants at low pH. Cellular viability of the initial and acid-resistant cells of hydrogenase operon mutants under (a) micro-aerobic cultural conditions, and (b) anaerobic conditions. Cell viability was calculated by dividing the CFU/mL obtained from the acid-stressed culture by the CFU/mL obtained from the initial cells. Data are the mean of three independent assays with triplicates; the error bars indicate standard deviation.

#### 5.3.4. The Effect of extracellular pH (pHex) on intracellular pH (pHi)

The bacterial ability to actively counteract drops in cytoplasmic pH by the direct export or consumption of intracellular protons to counteract the acid stress indicates the involvement of cellular components or metabolic functions in bacterial survival (Kanjee, 2013). Since hydrogenases are essential membrane protein complexes involved in proton metabolism (Vardar-Schara, 2008), they are presumed to be influential in cytoplasmic pH in response to external pH change. A mutant of the *gadE* gene was also included in the study for comparative analysis as a positive control as it is well known for the maintenance of pH homeostasis (Hommais, 2004). As expected, the *gadE* mutant showed a significantly affected pH homeostasis (Fig. 5.4). In contrast to that, all the strains were found to be unable to maintain a constant pHi when pHex was changed, except the WT. Interestingly, the *hyb* mutant was found to be relatively closer to the WT in this activity, which might indicate its ability to balance its cytoplasmic pH upon external acidification. The other mutants, *hya*, *hyc*, and *hyf*, showed

relatively more affected pH homeostasis. When compared with the *gadE*, these results verified that the hydrogenases are also vital for pHi maintenance.

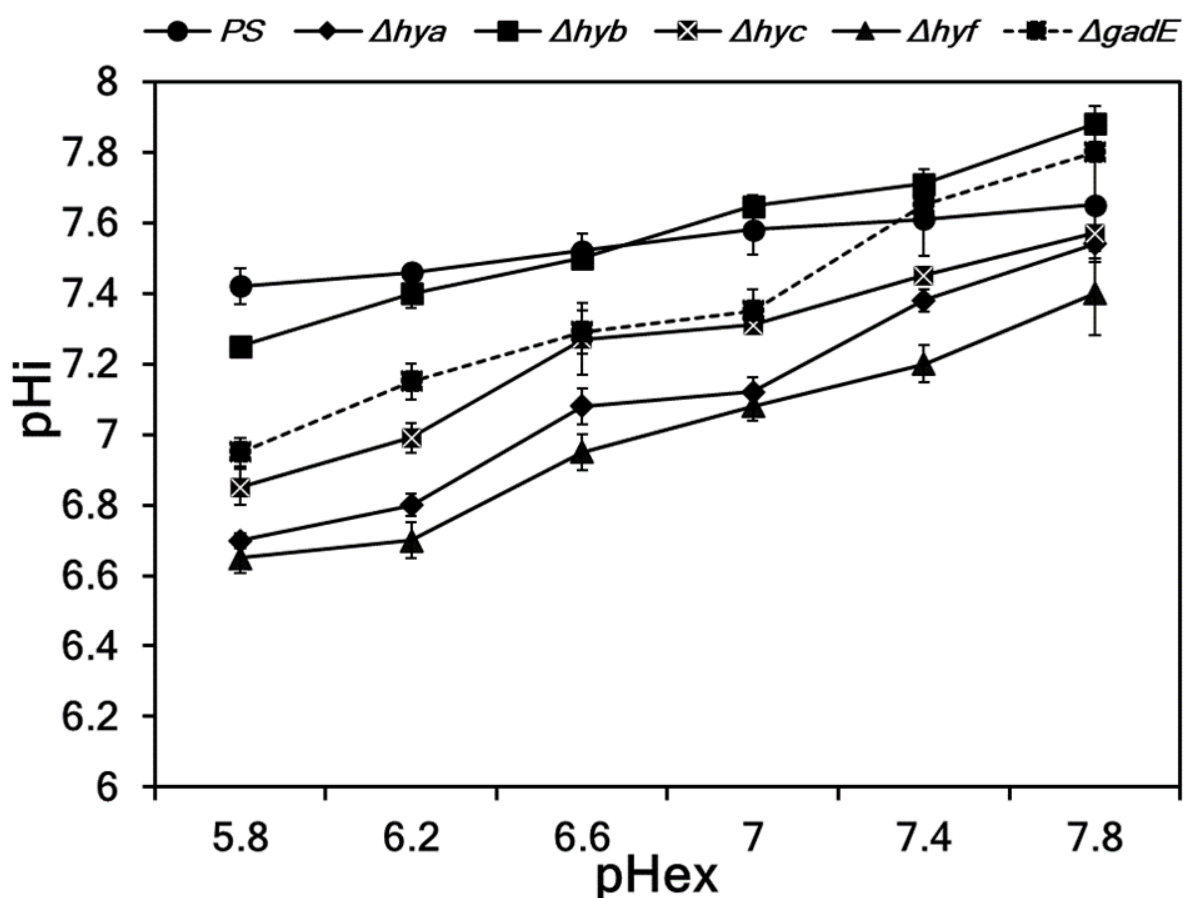


**Figure 5. 4** The hydrogenase operon mutants are not able to maintain their internal pH when external pH changes.

The relationship between intracellular pH (pHi) and extracellular pH (pHex) was estimated using the cultures of the hydrogenase operon mutants containing pGFPPratiometric resuspended in a potassium phosphate buffer of a different pH. Error bars indicate standard deviation in biological triplicates.

### 5.3.5. Affected acid resistance systems in the acid-resistant cells

It is reported from previous studies that the bacteria generally show a transcriptional and translational response to a drop in pH, and if this response is prevented or reduced, then the growth and survival of these bacteria are impaired at a lower pH (Lund, 2014). To assess a transcriptional change, the differential expression of several key acid-resistance associated genes was examined from transcriptional data (Fig. 5.5). The fold change expression data was normalized using the data of WT and only significantly ( $p$ -value  $\leq 0.05$ ) upregulated or

Chandra SHEKHAR (Maeda Lab.)

downregulated genes were appraised for further consideration. As a result, the *rpoS* gene was commonly found to be repressed in all acid-resistant cells. The *hyb* mutant showed relatively more repression than others, although this difference was considerably small. The genes associated with the glutamate decarboxylase (GAD) system were also commonly observed as repressed genes in almost all the acid-resistant cells, except the *hyc* mutant, where these genes were found to be affected but not significantly. The genes *cfa* and *hdeD* in the *hyc* and *hyf* mutants, respectively, were also found to be significantly repressed. Interestingly, the *adiA* gene was observed to be relatively more upregulated in the acid-stressed *hyf* mutant cells. These results may indicate that the influence of hydrogenases on acid resistance might be regulated or associated with the key genes of acid-resistant metabolism.

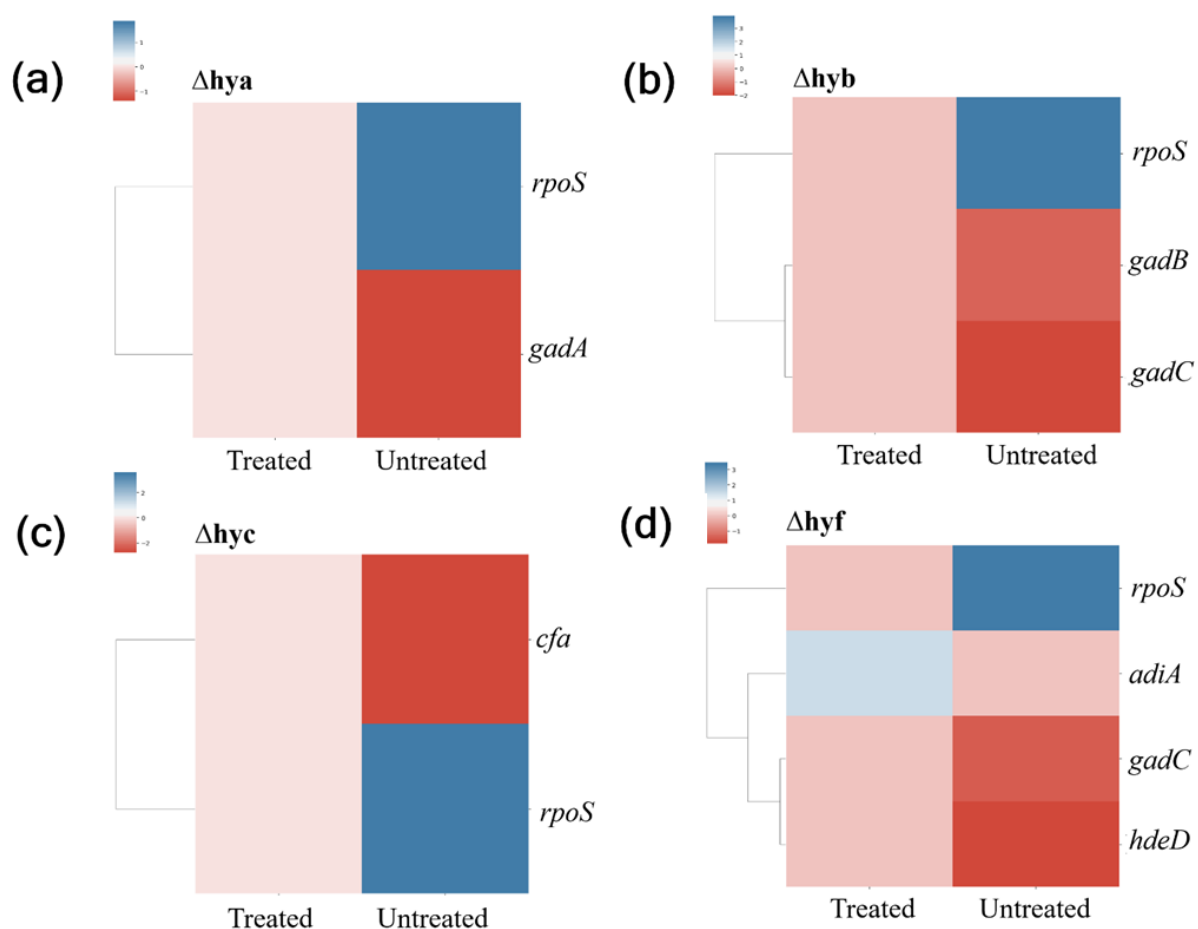


**Figure 5. 5** Downregulated expression of the genes associated with acid resistance systems.

Heat map diagram of the relative gene expression levels of some of the key genes of *E. coli*. acid resistance systems. The map represents the acid-resistant cells of (a) the *hya* operon mutant, (b) the *hyb* operon mutant, (c) the *hyc* operon mutant, and (d) the *hyf* operon mutant in comparison with their respective initial cells. The fold change expression was normalized using the data of the wild type and only significant expressions ( $p\text{-value} \leq 0.05$ ) were considered. The raw sequence data is available at NCBI under the SRA accession number PRJNA671558.

#### 5.4. Discussion

Our previous studies on hydrogen metabolism have shown that hydrogenases operon deletions have more impacts on metabolism, growth, and survival than single-gene (largest subunit genes of hydrogenases) deletions in *E. coli* (Shekhar, 2021). Until now, most of the previous studies have been conducted using single-gene mutants (Shekhar, 2021), despite the possibility of cross-talk or complementarity due to the existence of homology among them (Trchounian, 2012; Vardar-Schara, 2008). The well-known hydrogenases of some bacteria such as *H. pylori*, a native of the human GIT, are recognized as significant for their crucial contribution to energy and acid resistance (Ansari, 2017; Spector, 2012; McNorton, 2012). The environment in the GIT is characterized by varying levels of oxygen with concentrations decreasing from the stomach to the colon (Jubelin, 2018), therefore, pathogens in the tract are exposed to fluctuating oxygen levels (Marteyn, 2011). Information about the influence of hydrogenase on acid resistance at an undetectable, near-zero, or deprived DO concentration is not available since most of the current studies characterized aerobic and anaerobic conditions significantly (Bettenbrock, 2014). This study evaluated hydrogenases by complete removal of their operon segments from the genome and subsequently investigated them in micro-aerobic cultural conditions. The initial and acid-resistant cells were evaluated for various metabolic phenomena that have been reported relevant to the acid resistance of *E. coli*.

For *E. coli* hydrogenases, anaerobic conditions are the most appropriate for their maximum function in cellular, physiologic, and metabolic activities (Vardar-Schara, 2008; Trchounian, 2012). During the bacterial growth (Fig. 5.1a), cultures showed the growing

bacterial population consumed oxygen at a faster rate (Stolper, 2010), which led to zero or a deprived state of DO, and this was further verified in the study (Fig. 5.1b). In terms of the oxygenic environment, this condition may resemble the environment of the GIT, where DO levels fluctuate near zero (Riggins, 2013; Jubelin, 2018). The points at which the cultures were imparted with the acidic stress (pH ~ 2.5) and the collection of the acid resistance cells were also observed to have zero oxygen levels (Fig. 5.1b). Although the mutants were observed with varying oxygen consumption rates, hydrogenase activity was presumed to be achievable as indicated by a few studies conducted under aerobic or micro-aerobic conditions (Olson, 2002a). When the expression of the respective largest subunit genes was elucidated in each acid-resistant cell, their expressions were found to be significantly elevated than that of the initial cells (Fig. 5.2). As previously reported, the expression of Hyd-1 and Hyd-2 was found to be maximum under anaerobic conditions (Trchounian, 2012; Sargent, 2016), Hyd-3 was found to be repressed by oxygen (Trchounian, 2012; Sargent, 2016), and Hyd-4 does not normally transcribe or expresses a very low transcription (Trchounian, 2012; Sargent, 2016). Acid and anaerobiosis co-induce the hydrogenases of Hyd-1 (Trchounian et al., 2012; King et al., 1999), and formate-lyase complex FHL (Noguchi, 2010). Furthermore, the importance of hydrogenase expression for pH stress was confirmed by the loss of acid resistance in a defective strain of *hyp* (Hayes, 2006). The elevated hydrogenase expression may also turn up due to the oxygen-deprived state of the culture at that point of bacterial growth as verified by DO measurement (Fig. 5.1b). Therefore, these results and observations can confirm that hydrogenases fulfill a prominent and influential role in bacterial acid resistance under oxygen-deprived cultural conditions.

Cellular viability, as the best-observed phenotype of the acid-tolerant cells (Tsakalidou, 2011), demonstrated a further distinction among the mutant cells in terms of acid resistance (Fig. 5.3a–b). The oxygen-deprived cultural condition was found to be relatively more

threatening to cellular viability due to the low viabilities observed. Compared to the *hya* and *hyf*, the *hyb* and *hyc* mutants were found to be crucial for survival, since their viabilities were found to improve and reduced, respectively, under both conditions. Previous reports indicated a significant relevance of hydrogenases in acid resistance, specifically Hyd-1 and Hyd-2 under aerobic conditions, and Hyd-3 under anaerobic conditions (McNorton, 2012; Noguchi, 2010). Therefore, hydrogenase uptake under aerobic conditions and hydrogenase production under anaerobic conditions are presumed to function prominently in the survival of bacteria under different stresses, including the presence of antibiotics in addition to acid (Spector, 2012). Since Hyd-2 and Hyd-3 are uptake and production hydrogenases in *E. coli*, respectively, they produced contrasting phenotypes under similar conditions of acid resistance (Fig. 5.3a–b).

Intracellular pH falls very rapidly to a level roughly the same as that outside the cell when the external medium is acidified (Lund, 2014). The bacterial ability to actively counteract drops in cytoplasmic pH by the direct export or consumption of intracellular protons to counteract the acid stress point out the involvement of cellular components or metabolic functions in bacterial survival (Kanjee, 2013). With hydrogenases being essential membrane protein complexes involved in proton metabolism (Sargent, 2016), this study presumed and proved them to be influential in cytoplasmic pH in response to external pH change, since all the mutants were found to be unable to maintain a constant  $pH_i$  when  $pH_{ex}$  was changed (Fig. 5.4). As previously reported, the  $pH_i$  of *E. coli* only changes from 7.2 to 7.8 over a  $pH_{ex}$  range of 5.5 to 9 (Slonczewski, 1981), which matches this study's estimated values. A relatively smaller deviation in  $pH_i$  change in the *hyb* mutant demonstrated its comparable ability to balance cytoplasmic pH upon external acidification. The pH dependence of gene expression, as previously analyzed (Hayes, 2006), in oxygen-limited cultures of the *E. coli* K-12 strain, revealed pH-dependent expressions of hydrogenases. Under oxygen limitation, each hydrogenase showed higher expression in acid than in base, indicating that extreme-acid

resistance requires hydrogenase production (Hayes, 2006). This might be the reason why the mutants, *hya*, *hyc*, and *hyf* showed relatively more affected pH homeostasis upon external acidification.

As previously reported, the bacteria generally showed a transcriptional and translational response to a drop in pH where multiple genes, such as the *rpoS*, *gadA*, *gadB*, *gadC*, *cfa*, *adiA*, and *hdeD*, etc., were significantly associated (Lund, 2014). The *rpoS* encodes a sigma factor ( $\sigma^S$ ), a subunit of RNA polymerase that acts as the master regulator of the general stress response in *E. coli* (Hengge-Aronis, 2002). The *gadA*, *gadB*, and *gadC* encode glutamate decarboxylase enzymes, which are part of the glutamate-dependent acid resistance system 2 and confer resistance to extreme acid conditions (Moreau, 2007; Hersh, 1996). A  $\Delta cfa$  mutant showed reduced resistance to acid shock and extreme acid conditions (Chang, 1999) compared to the WT (Riggins, 2013). The *adiA* plays a role in pH homeostasis by consuming protons and neutralizing the acidic by-products. An *adiA* mutant was defective in arginine-dependent acid resistance (Gong, 2003). The *hdeD* is required for the acid resistance phenotype since a strain containing an *hdeD* null mutation appeared to have no defect in the acid response (Tucker, 2002). The repressed expression of the mentioned genes in the acid resistance cells of all the mutants showed an affected acid resistance system and thereby, supports the connectivity of hydrogenases in the pH homeostasis of *E. coli* (Fig. 5.5). Notably, the *hyb* mutant showed a relatively higher downregulation of genes in the acid resistant cells, which further demonstrated its high potential for survival under acidic stress. Moreover, the *adiA* gene was also found to be relatively more upregulated in the acid-stressed *hyf* mutant cells, which might associate it with the arginine-dependent acid resistance system. This diverse gene connectivity of the hydrogenases demonstrates that the influence of hydrogenases on acid resistance might be regulated or associated with the key genes of acid-resistant metabolism.

## **5.5. Conclusion**

Hydrogenases are found to possess acid resistance functions under oxygen-deprived cultural (micro-aerobic) conditions also, although their cellular viability is relatively higher under anaerobic conditions. Among all, Hyd-2 is found relatively more significant for survival if all tested activities are considered, however, remaining hydrogenases also showed a notable contribution to bacterial acid resistance.

## CHAPTER 6

# INVESTIGATION OF THE HYDROGEN METABOLISM BY A NEW APPROACH OF RANDOM GENOMIC DELETIONS USING AMBIGUOUS SEQUENCES IN THE *ESCHERICHIA COLI* GENOME

### 6.1. Introduction

*Escherichia coli* (*E. coli*), the most completely characterized single-cell life form, is a preferred model organism in bacterial genetic engineering research because of the available whole genome sequence and described molecular genetics (Blattner, 1997; Jeong, 2013). There are several methods available for genome-based engineering and to generate large mutant sets through both random and directed approaches (Osterman, 2008; Suzuki, 2006). Among all the reported approaches, homology-dependent, recombination-mediated, genetic engineering is considered as most efficient that allows engineering genes and segments of the bacterial chromosome directly by using polymerase chain reaction (PCR) products or synthetic oligonucleotides (Court, 2002; Kang, 2004). The *E. coli* KEIO mutant library is the best example of a directed homologous recombination application to evaluate the importance of each nonlethal gene rapidly (Baba, 2006). On the other hand, the random mutagenesis method has been developed to introduce random mutations and produce significant numbers of mutants (Fujii, 2006; Murakami, 2002).

Numerous studies have highlighted the importance of genomic deletions such as understanding protein evolution (Kim, 2010), and improving the function of nucleic acid aptamers, ribozymes, and deoxyribozymes generated by *in vitro* selection (Suzuki, 2008; Court, 2002). Although conventional random mutagenesis also proved to be a versatile strategy for improving protein functions or creating artificial enzymes (Stemmer, 1994; Petrounia, 2000), these methods are technically difficult (Fujii, 2006). Large genomic segment deletion methods are also popular to minimize and engineer microbial genomes (Suzuki, 2006), where

transposons-mediated ones are most efficient (Fujii, 2006; Goryshin, 2003; Morelli, 2017). Some of the homologous recombination-based approaches were also reported successful such as using insertion sequences along with Cre/loxP system (Tsuge, 2007), FLP-FRT sites (Leprince, 2012), recognition sites (Murakami, 2002), and Tn5 transposons along with recognition sites (Kang, 2004). However, the mentioned methods are laborious and impose difficulty in identifying the insertion sites as well as isolating mutants of every respective gene (Osterman, 2008; Morelli, 2017).

In sequences, the ambiguous base represents unspecified nucleotide (N) signifying any possible nucleotide (Wright, 2016), which were demonstrated as noteworthy constructs in genomics (Pezo, 2014). A completely “ambiguous” base (capable of pairing with the canonical bases A, T, G, C, and U) has been coined the term “universal base” (Berger, 2000; Nichols, 1994). As suggested earlier, the generation of unique random genetic sequences of ATGC can be generated by ambiguous sequences indicated by the capability of heterocycles to be incorporated into the four canonical bases through ambiguous pairing (Pezo, 2014). The indexed primers used in DNA sequencing consist of 3bp ambiguities (NNN) to increase diversity during sequencing cycles and improve the identification of clusters on the sequencing substrate and thus enhancing the number of reads per run (O'Donnell, 2016; Wang, 2012). Moreover, site-directed mutagenesis was also performed by employing oligonucleotides containing NNN ambiguous nucleotides corresponding to the randomized codon at the frameshift site (Curran, 1993). Codon randomization can generate a randomized gene library of mutants by replacing a section of DNA from the parental gene with a synthetic DNA cassette in which specific codons are randomized using NNN (Hughes, 2003). Employing primers designed based on ambiguous sequence information is advantageous when using PCR-based applications such as diagnosis or cloning (Nichols, 1994; Rossolini, 1994).

The importance of genomic insertion/deletions and their applications in understanding genomic evolution and designing a simple genetic engineering strategy demands a new easy, efficient, minimum number steps, and less laborious approach. We present a method to generate bacterial mutants with random genomic insertion and deletions (Figure 6.1). Our approach utilizes PCR products flanking ambiguous NNN-sequence extensions, which randomly recombine at multiple locations on the *E. coli* genome and generate various insertions-deletion mutants varying in the number of insertions. This strategy enables the deletion of multiple random genomic locations, and at the same time, insertion of the randomized ambiguous sequences along with the selectable marker into the same position. The results demonstrated the efficiency of this simple approach to generating fully functional bacterial mutants. Moreover, the strategy also recommended being efficient to insert any desired insert into the genome randomly.

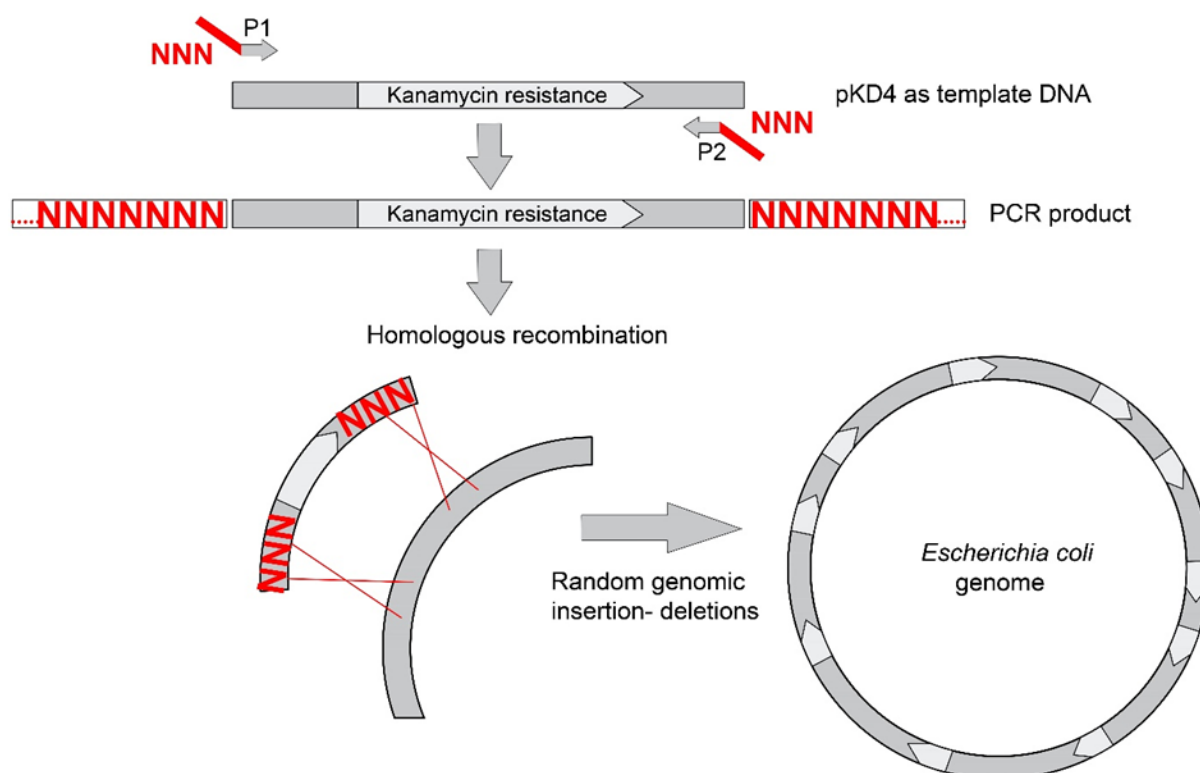


**Figure 6. 1** Illustration of the random genomic deletion strategy.

This study examines the oligonucleotides containing an effective length of ambiguous (NNN) sequence-based primers that may recombine at multiple random genomic locations of *E. coli*. PCR products were prepared using primers (P1 and P2) containing the flanking sequence of

ambiguous (30-nt NNN) nucleotides using pKD4 as template DNA since it consists of kanamycin resistance gene (KmR) which would be a selectable marker for the identification of positive recombinants (clones). The PCR products were then electroporated into the *E. coli* cell which was supposed to recombine at (multiple) random positions in the genome.

## 6.1. Materials and Methods

### 6.2.1. Bacterial strains, media, and growth conditions

*E. coli* K-12 BW25113 was used as the parent strain (abbreviated as PS) in the study. All the strains and plasmids of this study are listed in Table 6.1. The strains were initially streaked from  $-70^{\circ}\text{C}$  glycerol stocks on Luria-Bertani (LB) (Maeda, 2008) agar plates and a single colony was used to inoculate to grow at  $37^{\circ}\text{C}$  for overnight (in the presence of kanamycin,  $50\text{ }\mu\text{g/mL}$ , in case of mutants). A fresh culture was prepared in 250 mL flask (Iwaki, Japan) containing 50 mL LB at  $37^{\circ}\text{C}$  with shaking at 120 rpm using a bioshaker (BR-180LF, Taitec). All experiments were conducted using at least three biological replicates. The medium containing 10 g/L Bacto Tryptone, 5 g/L yeast extract, and 5 g/L NaCl was used to grow the strains. The final concentrations of each antibiotic used in LB-ampicillin and LB-kanamycin media, or plates were  $50\text{ }\mu\text{g/mL}$  ampicillin and  $50\text{ }\mu\text{g/mL}$  kanamycin, respectively. Carbenicillin ( $10\text{ }\mu\text{g/mL}$ ) was used in place of ampicillin whenever necessary.

**Table 6. 1 *E. coli* strains, mutants, and plasmids used in this study**

Strains/plasmids	Genotype/relevant characteristics	Reference
<i>E. coli</i> BW25113	F $\Delta$ ( <i>araD-araB</i> )567 $\Delta$ lacZ4787	Yale Coli Genetic Stock
	(::rrnB-3) $\lambda$ <sup>-</sup> <i>rph-1</i> $\Delta$ ( <i>rhaD-rhaB</i> ) 568	Center
	<i>hsdR</i> 514; parental strain for the Keio collection	
pKD4	PCR template containing FRT-kanamycin-FRT cassette	Yale Coli Genetic Stock Center
pKD46	Red recombinase expression system	Yale Coli Genetic Stock Center
<i>E. coli</i> BW25113 $\Delta$ <i>hybC</i> :: <i>Kan</i>	Hyd-2 large subunit gene deleted mutant	(This study)

<i>E. coli</i> BW25113	Hyd-3 large subunit gene deleted	(This study)
$\Delta hycE::Kan$	mutant	

### 6.2.2. Designing the primers for test gene deletion and random genomic deletion

Primers for constructing gene deletions were designed as explained by Datsenko and Wanner (Datsenko, 2000). These primers consist of homologous (to the adjacent upstream or downstream regions of the target gene) and kanamycin resistance gene (KmR) specific regions (Figure 6.1). Four different versions of these primers were designed by including three different sizes of flanking homologous sequences i.e., 50-nt, 40-nt, 30-nt, and 20-nt. *hycE* and *hybC* genes were selected as test genes to evaluate the minimum primer length required to efficiently construct the mutants. N-terminal deletion primers had a 50-nt (40-nt, 30-nt, or 20-nt) long 5' extensions and the 20-nt sequence 5'-GTGTAGGCTGGAGCTGCTTC-3' (primer P1). C-terminal deletion primers consisted of 50-nt (40-nt, 30-nt, or 20-nt) long homologous extension and the 20-nt 5'-CATATGAATATCCTCCTTAG-3' sequence (primer P2). A similar approach was followed to design the primers containing 30-nt ambiguous NNN-extension sequences. Therefore, the N-terminal of these deletion primers had a 30-nt-long 5' extension that includes an NNN-sequence and the 20-nt sequence of 5'-GTGTAGGCTGGAGCTGCTTC-3' (P1). C-terminal deletion primers consisted of 30-nt downstream NNN-sequence and the 20-nt 5'-CATATGAATATCCTCCTTAG-3' sequence (P2). All primers used in this study are listed in Table 6.2.

**Table 6. 2 List of primers used in this study**

Primer	Significance	Sequence (5'-3')	Reference
<b>Primers used to evaluate the primer efficiency and accuracy</b>			
k1	To confirm the presence of KmR gene	CAGTCATAGCCGAATAGCCT	(Datsenko, 2000)
k2	To confirm the presence of KmR gene	CGGTGCCCTGAATGAACTGC	

hybC-50-F <sup>a</sup>	Primer containing 50- nt extension	CTTCCTCCTTTAAAACAAAACGAT CATAATCGTCATGAGGCGAGCAA AGCGTGTAGGCTGGAGCTGCTTC	This study
hybC-50-R <sup>b</sup>	homologous to <i>hybC</i> gene flanking region	GGCTTCATCGGTCAGCAAAATATT GCCGACCCCTAAGACTAAAATAC GCACATATGAATATCCTCCTTAG	
hybC-40-F	Primer containing 40- nt extension	TAAAACAAAACGATCATAATCGT CATGAGGCGAGCAAAGCGTGTAG GCTGGAGCTGCTTC	This study
hybC-40-R	homologous to <i>hybC</i> gene flanking region	GTCAGCAAAATATTGCCGACCCCT AAGACTAAAATACGCACATATGA ATATCCTCCTTAG	
hybC-30-F	Primer containing 30- nt extension	CGATCATAATCGTCATGAGGCGA GCAAAGCGTGTAGGCTGGAGCTG CTTC	This study
hybC-30-R	homologous to <i>hybC</i> gene flanking region	TATTGCCGACCCCTAAGACTAAAA TACGCACATATGAATATCCTCCTT AG	
hybC-20-F	Primer containing 20- nt extension	CGTCATGAGG CGAGCAAAGCGTGTAGGCTGGAG CTGCTTC	This study
hybC-20-R	homologous to <i>hybC</i> gene flanking region	CCCTAAGACTAAAATACGCACAT ATGAATATCCTCCTTAG	
hycE-50-F	Primer containing 50- nt extension	TTTTTAGCGTTCGTCTCCTTGCTGG CGGCGTGATTAAAGAGAGTTTGA GCGTGTAGGCTGGAGCTGCTTC	This study
hycE-50-R	homologous to <i>hycE</i> gene flanking region	GCCGTGCCGGTTTTGATGACTTTT TTGATAAAGGTAAACATGGCGAT TCCCATATGAATATCCTCCTTAG	
hycE-40-F	Primer containing 40- nt extension	TCGTCTCCTTGCTGGCGGCGTGAT TAAAGAGAGTTTGAGCGTGTAGG CTGGAGCTGCTTC	This study
hycE-40-R	homologous to <i>hycE</i> gene flanking region	TTTTGATGACTTTTTTGATAAAGG TAAACATGGCGATTCCCATATGAA TATCCTCCTTAG	

hycE-30-F	Primer containing 30-nt extension	GCTGGCGGCGTGATTAAAGAGAG	This study
	homologous to <i>hycE</i>	TTTGAGCGTGTAGGCTGGAGCTGC	
hycE-30-R	gene flanking region	TTC	
		TTTTTTGATAAAGGTAAACATGGC	
		GATTCCCATATGAATATCCTCCTT	
		AG	
hycE-20-F	Primer containing 20-nt extension	TGATTAAAGAGAGTTTGAGCGTGT	This study
		AGGCTGGAGCTGCTTC	
hycE-20-R	homologous to <i>hycE</i>	AAGGTAAACATGGCGATTCCCAT	
	gene flanking region	ATGAATATCCTCCTTAG	
NNN-30-F	Primer containing 30-nt ambiguous (NNN)	NNNNNNNNNNNNNNNNNNNNNNNN	This study
	extension sequence	NNNNNNNNGTGTAGGCTGGAGCT	
		GCTTC	
NNN-30-R		NNNNNNNNNNNNNNNNNNNNNNNN	
		NNNNNNNNCATATGAATATCCTCC	
		TTAG	

---

**Primers used in the confirmation of genomic insertion-deletion**

---

<i>hybC</i> -Cf <sup>c</sup>	To confirm <i>hybC</i> gene	TCCCGACCTGGGAAGAACTG	(Vardar-
<i>hybC</i> -Cr <sup>d</sup>	deletion	GTGCCGCCATCGAGGATCTC	Schara, 2008)
<i>hycE</i> -Cf	To confirm <i>hycE</i> gene	GTGGTCGGCGTCCTGGTTATCG	(Vardar-
<i>hycE</i> -Cr	deletion	CTGCTCTGGCTTACCACGGAAG	Schara, 2008)

---

**Primers used in RT-PCR**

---

<i>rrsG</i> -F	Housekeeping gene	TATTGCACAATGGGCGCAAG	(Yusoff, 2012)
<i>rrsG</i> -R		ACTTAACAAACCGCCTGCGT	
KmR-F	To know kanamycin	AGGCTATTCGGCTATGACTG	This study
KmR-R	resistance gene	GCAGTTCATTGAGGGCACCG	
	expression level		

---

a and b: F and R represent forward and reverse primers, respectively.

c and d: Cf and Cr represent forward and reverse primers, respectively, used for mutation confirmation.

### 6.2.3. Preparation of PCR product and genomic deletions

The methodology for constructing test gene deletion mutant and random genomic deletions was based on the procedure explained by Datsenko and Wanner (Datsenko, 2000), with some modifications (Figure 6.1). The PCR product (nearly 1.4kb in size) enclosing the sequence of selectable marker flanking by homologous of the ambiguous sequence was

prepared by using the above-mentioned primers and pKD4 as a template DNA since it contains the KmR gene. The remaining procedures were also conducted according to the original literature (Baba, 2006; Datsenko, 2000). Since, for the recombination, *exo*, *bet*, and *gam* gene products are required for efficient recombination (Court, 2002; Baba, 2006; Datsenko, 2000), PS strain harboring pKD46 was used. Electroporation was done through 0.1 cm cuvette at 1.8 V and 200 ohm according to the manufacturer's instructions (Bio-Rad) using 50 µL of the electrocompetent cells and different concentrations (50-400ng/µl) of the purified PCR products. The shocked cells were added to 1 mL LB medium and incubated for 1 h at 37°C, and then, one half was spread onto an LB agar plate containing kanamycin to select kanamycin-resistant transformants (mutants).

#### **6.2.4. Evaluation of the accuracy of the primers: mutation verification**

Three PCRs were conducted to evaluate the structure of gene deletion mutants as explained previously (Baba, 2006; Datsenko, 2000). Two KmR gene-specific primers (k1 and k2) were used to confirm the insertion to the target gene locations. Two reactions were performed using upstream and downstream region-specific primers of the targeted gene with k1 or k2 to confirm for both new junction fragments. The third reaction was carried out with the flanking upstream and downstream region-specific primers only to verify the simultaneous loss of the parental gene fragment and gain of the new mutant-specific fragment. A fresh colony of each mutant was suspended in 20 µL water, from which 2 µL were used in the PCR mixture after boiling the cells at 100°C for 5 min. The colony PCR was carried out using Quick Taq® HS DyeMix reagent (Toyobo Co., Ltd.). The PCR mixture consisted of 12.5 µL of 2× Quick Taq® HS DyeMix buffer and 0.75 µL of each primer (20 mM). The total volume was adjusted up to 25 µL by sterilized water, and the products were amplified for 30 cycles (initial denaturation at 95°C for 2 min, denaturation at 95°C for 30 s, annealing at 54°C for 30 s,

elongation at 68°C for 1 min, and final extension at 68°C for 10 min). PS colonies were always included for comparative verification. All primers used in this study are listed in Table 6.2.

For the calculation, the accuracy was defined as the fraction of the total colonies in which inserted PCR product was confirmed (Motohashi, 2017), represented as:

$$\text{Accuracy} = \frac{\text{Number of correct mutants confirmed by colony} - \text{PCR}}{\text{Total number of mutants assayed in colony} - \text{PCR assay}}$$

### 6.2.5. Evaluation of the efficiency of the primers: phenotype verification

The efficiency of the primers was estimated by evaluating the affected phenotype after the mutation. *hycE* and *hybC* since their crucial role in *E. coli* hydrogen metabolism were selected as test genes (Maeda, 2008). Screening Chemochromic membranes (GVD, Cambridge, MA, USA; (Maeda, 2008) were used to identify correct mutants based on their hydrogen productivity (Maeda, 2008). By the functions of the selected genes, the activity of hydrogen production will be lost and somehow maintained after the deletion of *hycE* and *hybC*, respectively (Maeda, 2008). The colonies of the transformants obtained above were transferred to square agar plates (100×100×15 mm) containing LB-agar supplemented with glucose (100mM), and the plates were incubated anaerobically at 37°C for 14 h using a Gas-Pak anaerobic system. In the presence of oxygen, Whatman filter paper was placed firmly on top of the colonies on each plate, and the glass plates coated with the chemochromic membrane were placed on top of the Whatman paper. The colonies grown from the *hycE* gene deleted mutant must not be able to develop a deep blue color indicating the lost hydrogen productivity and will indicate an accurate gene deletion mutant. Unlike *hycE* mutant, *hybC* mutant would not show a significant change in hydrogen productivity as its reversible nature of hydrogen utilization and production (Shekhar, 2021). The positive control (PS) was included since it will show deep blue color on the membrane indicating its hydrogen productivity.

For the calculation, the efficiency (Motohashi, 2017) was defined as the fraction of the total

number of colonies with lost (in case of *hycE*) hydrogen productivity, represented as:

$$\text{Efficiency} = \frac{\text{Number of colonies confirmed with no hydrogen productivity}}{\text{Total number of colonies assessed for hydrogen productivity}}$$

#### **6.2.6. Total RNA extraction and quantitative reverse transcription-PCR (qRT-PCR)**

Aerobic cultures using the colonies of the mutants and PS were prepared in LB medium and grown at 37°C with shaking 120rpm. The cultures incubated overnight were used for collecting cell pellets for RNA extraction using 100 µL RNALater Solution (Applied Biosystems, Foster City, CA) in 2 mL screw-cap tubes after centrifugation at 13krpm for 1 min. The tubes containing cell pellets were immersed in 100 mL dissolved dry ice in ethanol (95%) for 10 s and stored at –70°C before RNA extraction. Total RNA was extracted using a bead beater model 3011b (Wakenyaku Co. Ltd., Japan) and the RNeasy Mini Kit (Qiagen, Inc., Valencia, CA) as explained previously (Mustapha, 2018). StepOne Real-Time PCR System and Power SYBR Green® RNA-to-CT™ 1-Step Kit (Applied Biosystems) were used for the transcription analysis of the KmR gene. Housekeeping gene *rrsG* (16S rRNA) and *hyfG* were used to normalize the expression data and as a positive control, respectively. RNA extracted from the PS was used as the reference template. All primers used for this transcription analysis are listed in Table 2. Three technical replicate samples were performed. The expression of the listed genes was analyzed using 50 ng total RNA, and the collected data were analyzed through the relative quantification for qRT-PCR ( $2^{-\Delta\Delta CT}$ ) (Pfaffl, 2001).

#### **6.2.7. Phenotypic evaluations of random genomic deletion mutants: Hydrogen productivity and growth**

The overnight aerobic culture of all the strains (18 confirmed mutants and PS) was adjusted to OD<sub>600</sub> of 0.05 in fresh LB medium (25 mL) in the crimp top vial (65 mL) supplemented with 100mM glucose inside the anaerobic system (Forma Anaerobic System 1025, Thermo Scientific). The cultures were sparged with nitrogen for 5 min to remove oxygen after sealing

the vials with rubber and an aluminum cap. These culture vials were then incubated at 37°C, 120 rpm. The amount of hydrogen generated in the headspace was measured by gas chromatography (GC) using a 6890 gas chromatograph equipped with an AT 19095P-NS5 column (Agilent Technologies, Inc., Santa Clara, CA) as described previously (Shekhar, 2021). Total protein was calculated as 0.22 mg/mL/OD<sub>600</sub>. The amount of hydrogen generated was calculated using the following equation (Shekhar, 2021):

Hydrogen production (μmol) =

Peak area × Standard hydrogen curve × 65,000 μL (headspace)/100 μL (injection)

Three independent fresh cultures were prepared to have OD less than 0.05 using overnight aerobically grown strains. The cell turbidity of the strains was recorded at 600 nm wavelength at the interval of 30 min on growing aerobically at 37°C. Only the values belonging to the exponential part of growth were taken to calculate the specific growth rate (μ) (Donner, 2017).

### 6.3. Results

#### 6.3.1. Determining the effective minimum length of homology extension to generate gene deletion mutants:

Initially, primers of different homology extension lengths (50, 40, 30, 20-nt) were used to formulate the highest efficiency and accuracy by deleting *hycE* and *hybC* genes (test genes) from *E. coli* genome and evaluating the affected phenotype (hydrogen productivity). As a result, the maximum number of mutant bacterial colonies of transformants (*hycE* and *hybC* gene deleted mutants) were observed when PCR products prepared by the primers containing 50-nt homology extension were used, for both the genes (Figure 6.2a). An appreciable number of colonies were also observed from the 40-nt and 30-nt homology extension primers (although colony number size was small with 30-nt extension). Interestingly, 20-nt homology extension primers were also found able to produce a significantly smaller number of colonies (data not

shown, because the results with these primers were not consistent in this and later assays). The PCR product concentration of 50ng/  $\mu$ L used in this work demonstrated not only the efficiency of these primers but also indicated a possibility to get a comparable size of colonies with primers of 30-nt homology extension with its high concentrations. Therefore, when higher concentrations (100, 150, 200ng/ $\mu$ L) of the PCR product prepared from this primer were then used to evaluate its efficiency, an increased number of colonies were found in a concentration dependency manner (Figure 6.2b).

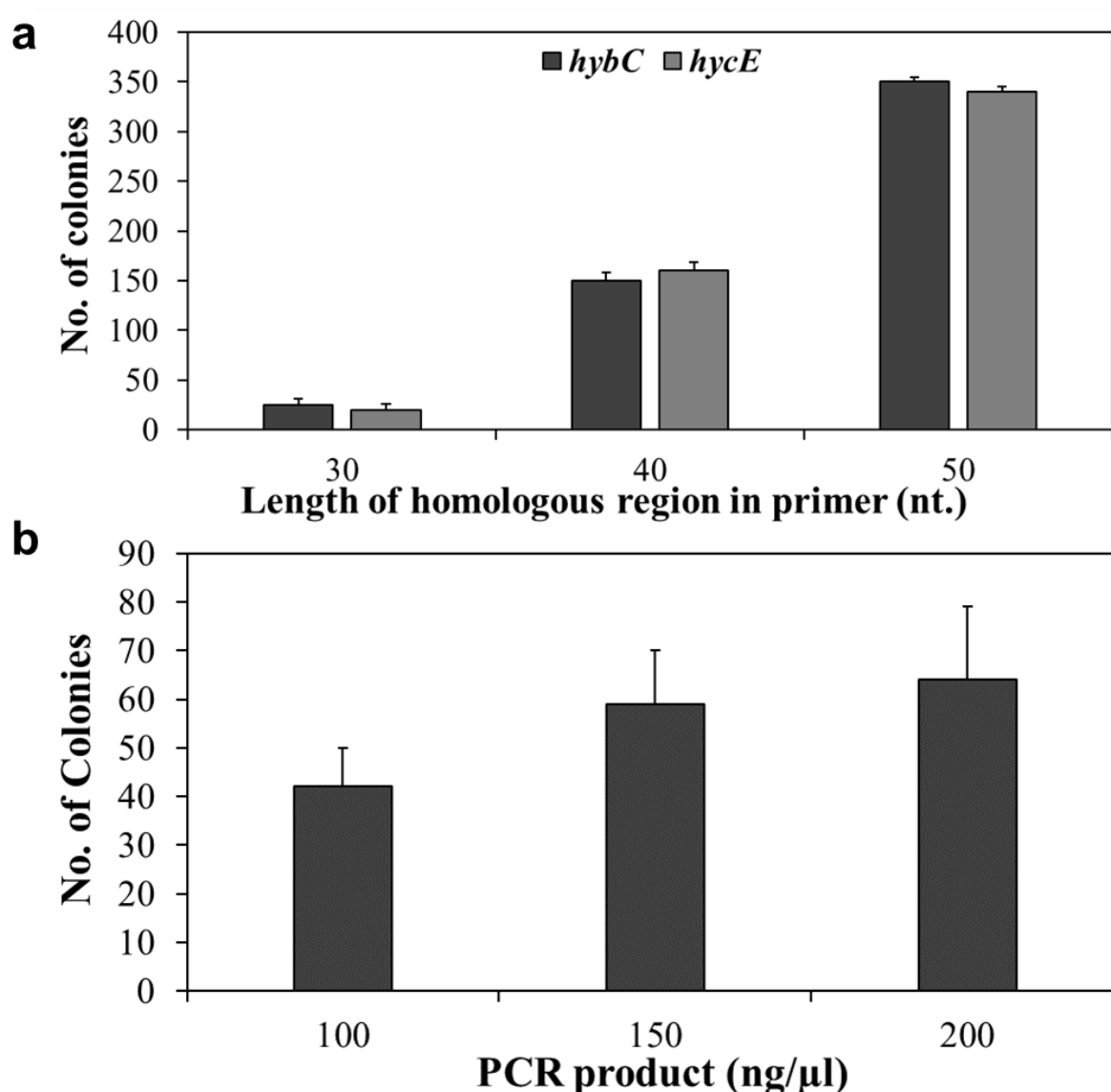


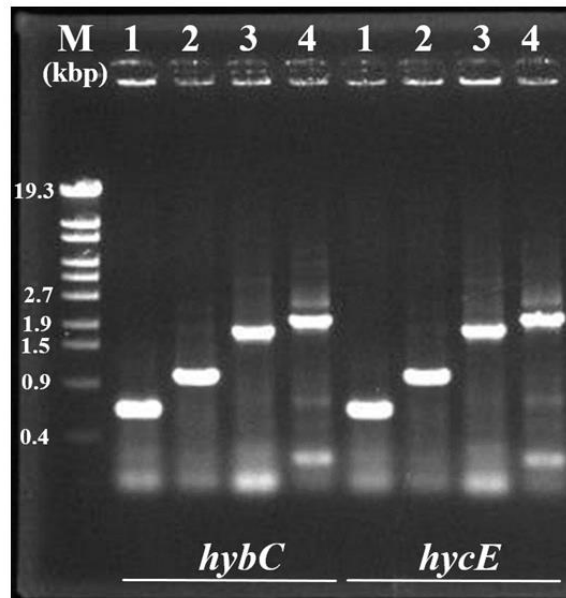
**Figure 6. 2** Determining the effective minimum length of homology extension to generate gene deletion mutants.

Evaluation of the efficiency of the three different lengths of homology extensions in terms of the number of colonies of the recombinants. (a) *hybC* and *hycE* genes were tested to delete with PCR product flanking with 50, 40, 30-nt long homology extensions separately at 50ng/μl concentration. (b) PCR product with 30-nt long homology extension evaluated at higher concentrations such as 100, 150, 200ng/μl concentrations to test the *hycE* gene deletion. The data indicated is the mean from three independent experiments and error bars represent stdev.

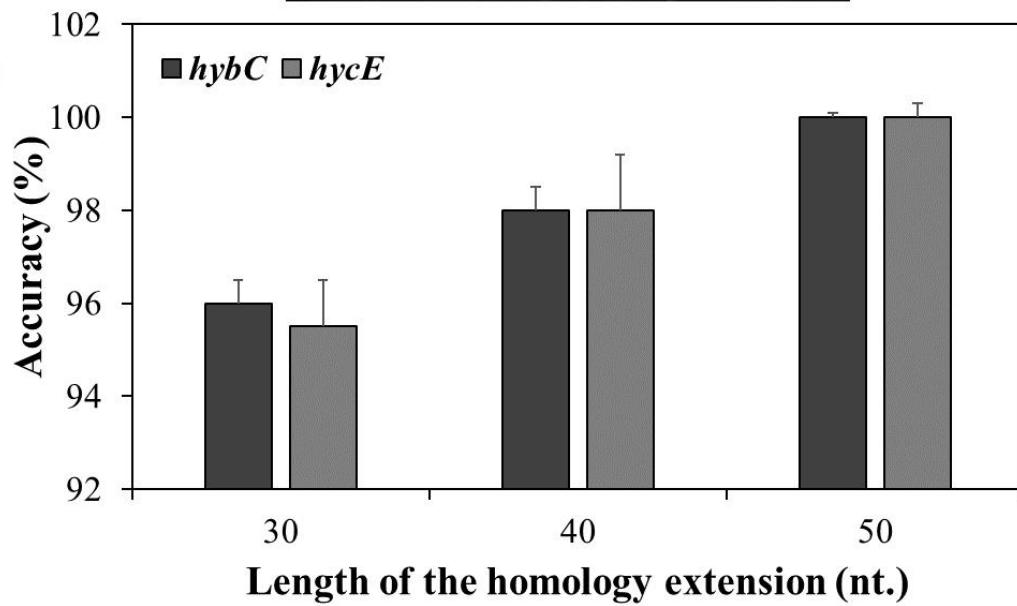
**Figure 6. 3** Evaluating the efficiency and accuracy of the homology extension (below).

The primer efficiency and accuracy were investigated by evaluating their phenotype and genotype, respectively. (a) Verification of target genes (*hybC* and *hycE*) mutation by colony-PCR. Three PCRs were performed to confirm each deletion mutation (Baba, 2006; Datsenko, 2000). (1) forward primer specific for the upstream locus of target gene (Cf) + KmR specific reverse primer (k1), (2) KmR specific forward primer (k1) + reverse primer specific for the downstream locus of target gene (Cr), (3) Cf + Cr. (1), (2), and (3) were performed for mutants. (4) Cf + Cr using PS cells. M indicates marker 6 (OneSTEP; Nippon Gene, Japan). The amplified fragments in (1), (2), and (3) PCR reactions are nearly 0.6, 1.1, and 1.6kbp respectively, whereas (4) is nearly 1.7kbp. In the case of *hybC*, gene and PCR amplicon lengths are 1704 bp, 1804 bp, respectively. Whereas, in case of *hycE* gene and PCR amplicon lengths are 1710 bp, 1810 bp, respectively. (b) Accuracy of the primers flanking with 30, 40, and 50-nt homology extensions used for *hybC* and *hycE* gene deletions based on the results obtained in (a). The accuracy is defined as the fraction of the total colonies with confirmed inserted PCR product. (c) Efficiency of the primers, flanking with 30, 40, and 50-nt homology extensions used for *hybC* and *hycE* gene deletions, to impart the desired phenotypic effect on hydrogen metabolism. The mutant with deleted *hycE* gene would not be able to produce hydrogen, whereas the deletion of *hybC* would not produce a significant change in hydrogen productivity (Maeda, 2008). The efficiency is defined as the fraction of the total number of colonies with lost (in case of *hycE*) hydrogen productivity. Colonies in the range of 15-35 were obtained in three independent experiments. Almost all the colonies able to regrow were tested. The data indicating estimated efficiency and accuracy is the mean of the three experiments. The error bars represent stdev.

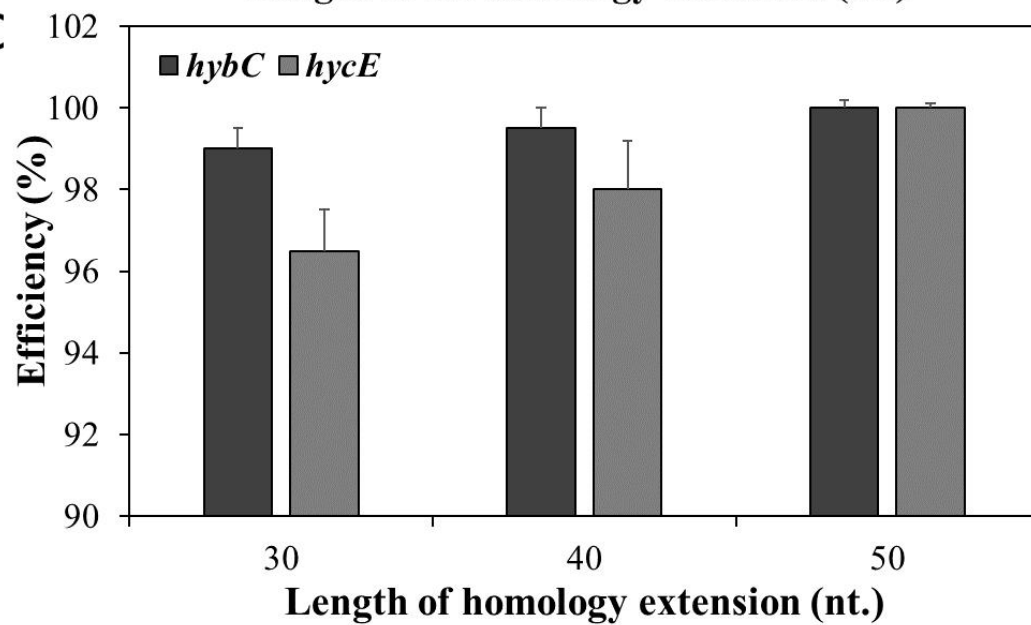
**a**



**b**



**c**



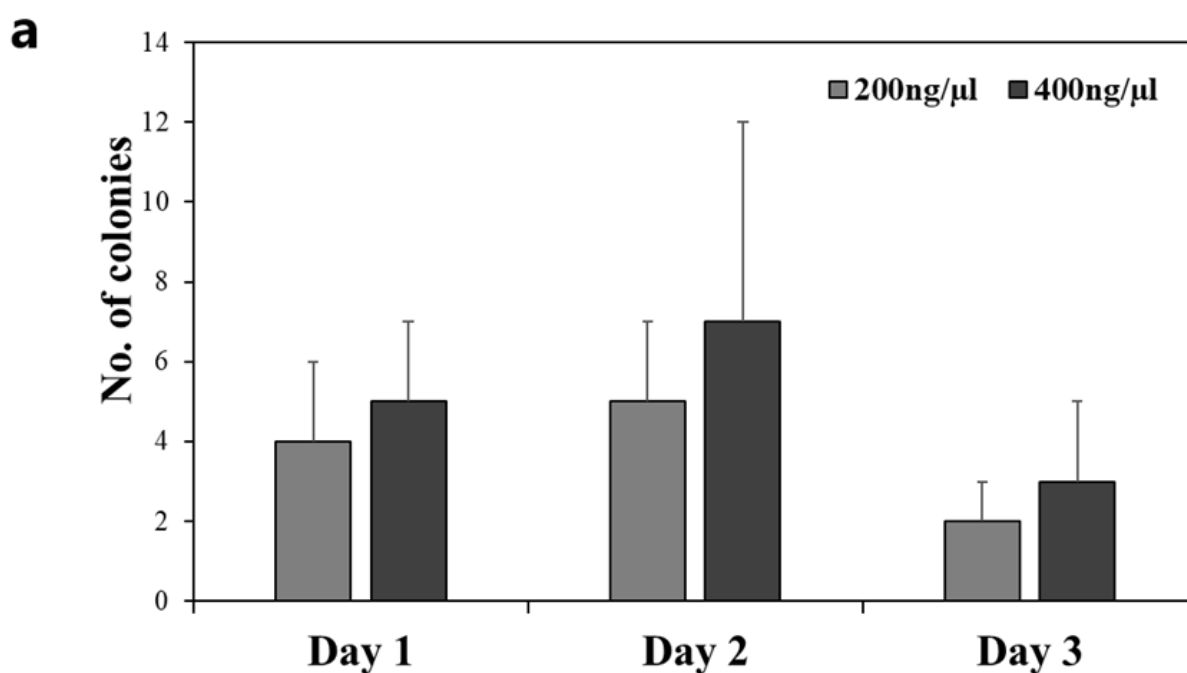
### **6.3.2. Evaluating the efficiency and accuracy of the homology extension:**

To estimate the efficiency further and accuracy of the primers, the phenotype and genotype were investigated, respectively (Figure 6.3). For the accuracy evaluation (genotype), colony PCR reactions were conducted as explained earlier. The primer was considered accurate if the created mutation was correct on all three reactions of PCR (Figure 6.3a). As a result, PCR product prepared from 50-nt homology extension was found 100% accurate for both the test gene deletions (Figure 6.3b) and also with *hybC* gene. With *hycE* gene, in some experiments and homology extension length, accuracy was found compromised. Although it was not a big difference, the primers with extension lengths of 40 and 30-nts designed for *hycE* showed an affected accuracy. All the colonies which were able to regrow were investigated for phenotypic variation as a criterion to evaluate the efficiency of the primers. The abilities of hydrogen productivity were assessed from both the mutant colonies (*hycE* and *hybC*) using chemochromic plates as these plates provide a surface for the hydrogen metabolic reaction and produce a blue color indicating hydrogen production (Maeda, 2008). The PS was taken as a positive control. As expected, a significant efficiency was observed from *hybC* mutant and with all the three types of lengths of homology extensions (Figure 6.3c). Whereas, in the case of *hycE* mutation, it was found best effective with 50-nt length, as efficiency was found compromised with 30-nt long homology extension.

### **6.3.3. Genomic deletions using randomly targeting primers and confirmation:**

Based on the results so far, the primers with an extension of 30-nt containing NNN sequence were designed to test their recombination (insertion) at random places in the genome to produce deletion mutants. After the recombination, the bacterial colonies were observed to grow very slowly when PCR products prepared using primers containing 30-nt NNN extension were used. This might indicate the disruption or gene inactivation of some lethal or essential genomic region that could produce a slow growth of bacteria (Ryan, 1949). Therefore, the agar

plates were kept at incubation for 72 hours to monitor the growth of colonies (Figure 6.4a). Interestingly, at both the PCR product concentrations (200ng/ $\mu$ l and 400 ng/ $\mu$ l) colonies successfully could be obtained. As indicated earlier also, more colonies were observed at higher concentrations. It was observed that 24 hrs incubation could produce more colonies than 12 and 72 hrs incubation. Nearly 25-40 colonies were obtained after 72 hours of incubation each time, which were allowed to grow again on fresh media. Finally, 19 colonies were randomly selected showing good growth to verify the insertions of the PCR products using colony PCR. As result, from all 19 colonies, 18 colonies (clones) were found positive insertion-deletion mutants indicating the PCR product containing NNN-extension was successfully recombined into their genomes (Figure 6.4b).



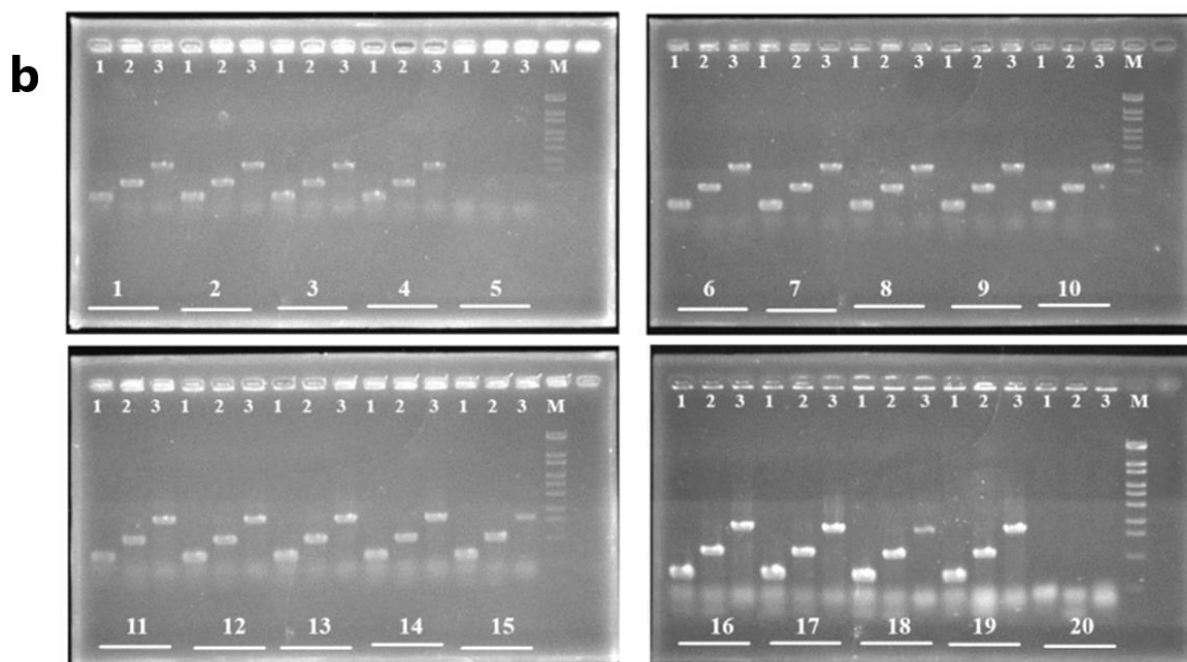


**Figure 6. 4** Genomic deletions using randomly targeting primers and confirmation. Evaluation of the efficiency of the primers with 30-nt ambiguous (NNN) sequences to recombine in the genome, in terms of the number of recombinant colonies (clones) (a). Two different concentrations (200ng/ $\mu$ l and 400ng/ $\mu$ l) of the PCR product were used, and colonies were allowed to grow for 72 hours. The data indicated is the mean from two independent experiments and error bars represent stdev. (b) The confirmation of insertion-deletion of the PCR product containing 30-nt ambiguous (NNN) sequences into the genome using colony-PCR. As explained in Figure 3A, three PCR reactions were performed on 19 recombinant colonies (clones). These clones are indicated by numbers 1-19. Colony number 20 indicates PS. No bands from clone number 5 indicate the confirmation of unsuccessful recombination. M indicates marker 6 (OneSTEP; Nippon Gene, Japan). The sizes of the corresponding bands are the same as indicated in Figure 6.3a.

#### 6.3.4. Estimating the number of insertions in a single genome:

The results so far demonstrated that the PCR product prepared using primers possessing ambiguous NNN-sequence extension could successfully be recombined in the genome. It was supposed to be interesting to know whether it was a single point insertion or multiple insertions were there in the genome. To investigate this, we decided to estimate the expression level of the KmR gene, which was enclosed in between the flanking NNN extensions of the PCR product. All the 18 clones verified in the previous step were included in this investigation. As a positive control, a KEIO mutant,  $\Delta hyfG$ , and negative control, PS strain were included in the study for the comparative analysis. Surprisingly, the fold change expression levels in all the 18

clones were found significantly increased (Figure 6.5). This result demonstrated the multiple insertions of the PCR product containing NNN-extension in the *E. coli* genome.

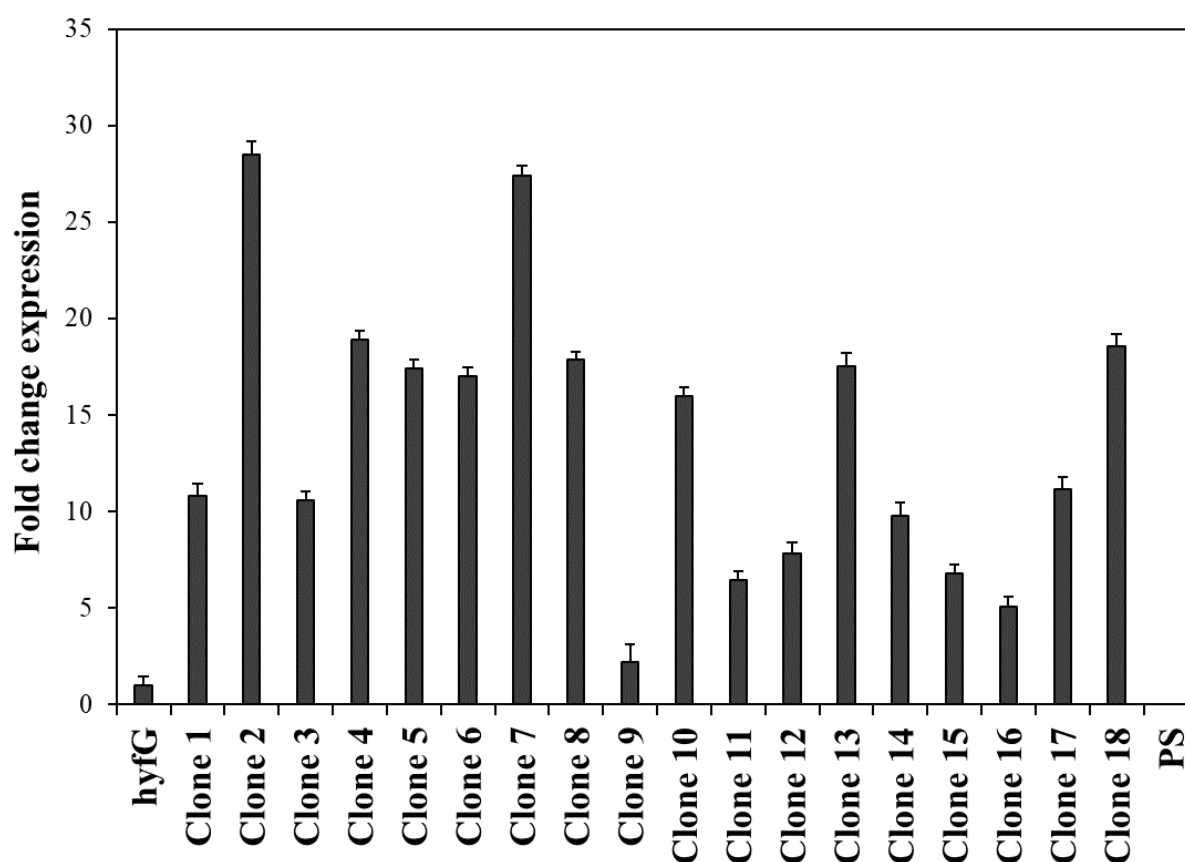


**Figure 6. 5:** Estimation of the number of insertions in a single genome.

The fold change expression of KmR gene in 18 PCR verified clones. The KEIO mutant *hyfG*, since it carries a single copy of KmR gene, was taken as a reference to estimate the relative expression levels of KmR gene. The data was normalized by the housekeeping gene (*rrsG*). PS indicates parent strain. The data indicated is the mean from the run of triplicates on the 96-well plate and error bars represent stdev.

### 6.3.5. Evaluation of the phenotype of the multiple random insertions containing mutants:

Hydrogen productivity was evaluated as a phenotypic trait to estimate any metabolic change in the hydrogen metabolism. Anaerobic cultures of all the clones with multiple insertions were prepared as explained previously (Shekhar, 2021) supplemented with 100mM glucose. After 24 h growth, all the clones were evaluated for their hydrogen productivities (Figure 6.6a). As a result, there was no significant change observed in all 18 clones compared to the PS. Similar to that, the growths were also monitored to estimate their specific growth

rates under aerobic conditions (Shekhar, 2021) (Figure 6.6b). The results showed the growth was not affected significantly, although, the rates were observed relatively reduced as compared to PS. These results might be reflecting the multiple random insertion positions were not either coding or essential regions of the genome.

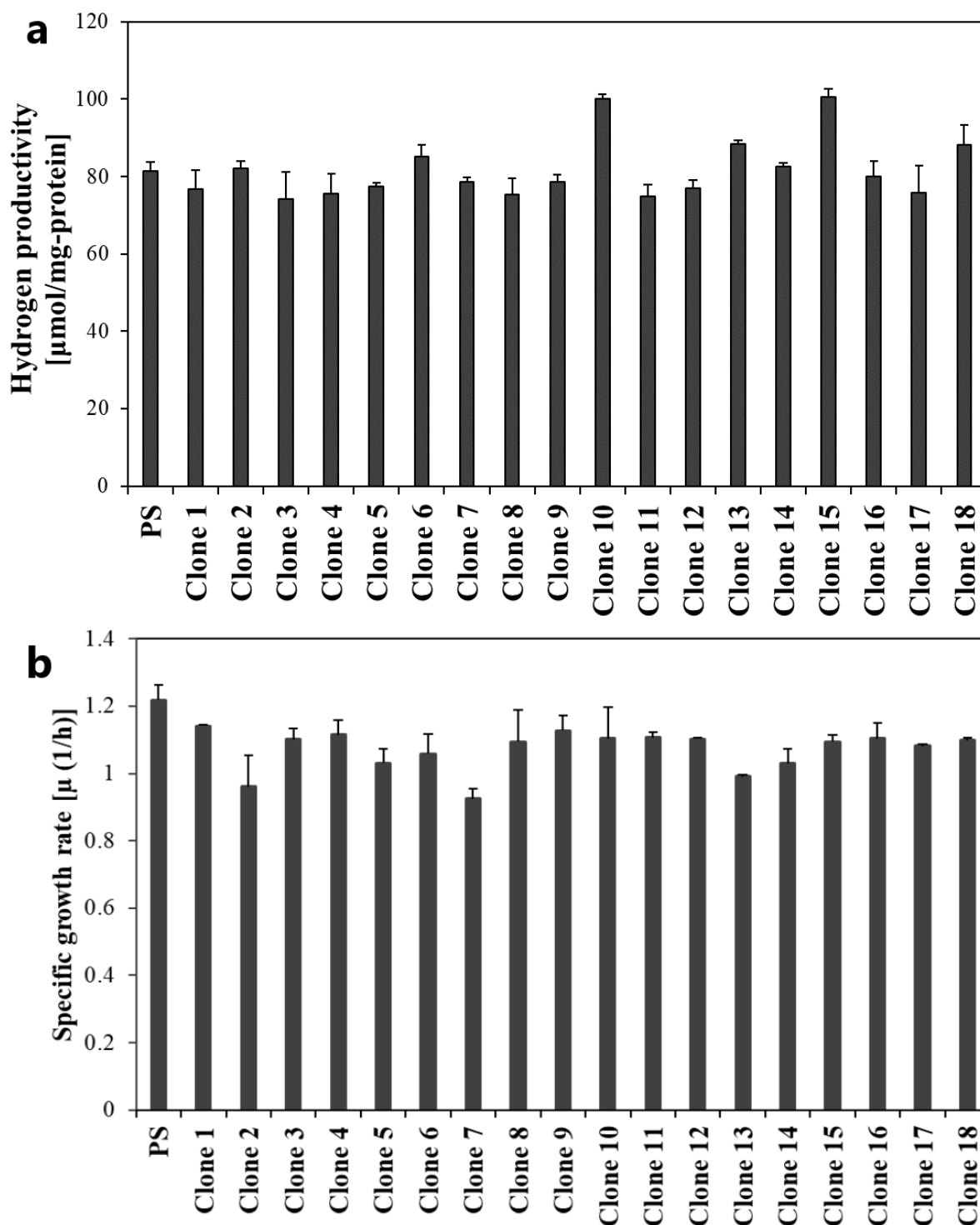


**Figure 6. 6** Evaluation of the phenotype of the multiple random insertions containing mutants.

(a) Hydrogen productivity of the 18 clones was evaluated to investigate a phenotypic alteration in metabolism due to the multiple random genomic insertion-deletions. The assay was performed under anaerobic conditions (Shekhar, 2021) and hydrogen was recorded after 24 hrs shown here. (b) The same 18 clones were further investigated for their specific growth rates under aerobic conditions. The data indicated is the mean of biological triplicates and error bars represent stdev. PS indicates parent strain.

#### 6.4. Discussion

Random and targeted genomic deletions are important to understand gene, protein, or genome evolution (Kim, 2010; Hosseini, 2018), and to improve the functions of some important biological entities (Suzuki, 2008; Court, 2002). Homologous recombination-based genetic engineering is considered as most versatile and precise one (Court, 2002) since it allows engineering genes and segments of the bacterial chromosome directly by using PCR products or synthetic oligonucleotides (Court, 2002; Kang, 2004; Datsenko, 2000). Through homologous recombination, a targeting gene and a homologous DNA fragment on a chromosome can be integrated with the aid of three genes *gam*, *bet*, and *exo* accomplished by Red-recombination in these flanking homologies (Datsenko, 2000). The plasmid expressing Red system (pKD46) was employed in the study since its ability to yield an enhanced number of recombinants (Datsenko, 2000). The Gam protein is capable of inhibiting the Exonuclease V activity of RecBCD allowing for the transformation of linear DNA (Datsenko, 2000; Unger, 1972), whereas the *bet* and *exo* gene products are capable of promoting homologous recombination at short regions of homology between the PCR product and the chromosome (Ellermeier, 2002). As the degenerate oligonucleotides target multiple regions due to their ability to match multiple conserved regions in the genome (Girgis, 1988; Maki, 1991; Snijders, 1991), we hypothesized that an ambiguous base (also known as universal base) sequence should be capable of pairing with a sequence of canonical bases A, T, G, and C. We found that codon randomization, using NNN, can generate a gene library of mutants by replacing a genomic region (Hughes, 2003), which further strengthened our hypothesis.

Homologous recombination-based targeted genomic deletions were mainly reported by using 50-nt homology extension (Court, 2002; Baba, 2006; Datsenko, 2000; Posfai, 1994), although a range of (30-100 bp) end homology regions were also reported (Court, 2002; Motohashi, 2017; Kanca, 2019). The length between 20 and 30 bp were reported less efficient in cloning-related work (Motohashi, 2017; Hua, 1997). A length of 9 bp was reported as a minimum but efficiency was found compromised up to 50% (Fujimoto, 2009). From various studies incorporating homology extensions, an appropriate minimum homology length with significant efficiency and accuracy is still unclear. To employ ambiguous primers for this approach, it was requisite to formulate the minimum primer length with high efficiency and accuracy for the genomic deletions. Therefore, in this study, initially, several primers of the most studied homology extension lengths (50, 40, 30, 20-nt) were designed to target the deletion of *hycE* and *hybC* (test) genes (Table 6.2). The PCR product containing KmR gene (selectable marker) flanking desired homology extension facilitated getting only insertion-deletion mutant (Court, 2002; Datsenko, 2000). The highest homology length (50-40-nt) generated the highest number of mutants; however, lower lengths (30-20-nt) were also found effective (Figure 6.2a), as mentioned, an oligo length of 30-nt generates recombinants but a large increase is obtained with 40-nt long oligos (Court, 2002; Ellis, 2001). The lengths of 30 and 20-nt long homology extensions showed increased efficiency at a higher concentration of PCR products (such as 200ng/μL) (Figure 6.2a, b). It was also reported that targeting efficiency increases in a linear relationship with increasing concentration of the donor DNA (Yu, 2000). Therefore, a higher concentration of the PCR products seems appropriate to enhance the recombination rate. Further, phenotype and genotype of the test gene mutants were evaluated to estimate the efficiency and accuracy of the investigated primer lengths, which showed 50-nt extension-based primers as the highest (almost near to 100%) accurate and efficient (Figure 6.3b, c), supporting previous reports (Court, 2002; Datsenko, 2000). As indicated by a few studies

(Kang, 2004), our study further verifies that to efficiently execute the homologous recombination, the recombinase system requires a 30 bp homology on both ends of the insert. The efficiency and accuracy from the primers containing 20-nt extension were observed not to be consistent (data not shown) which might be because of non-specific recombinations of the PCR products (Bell, 1991), also, 20 bp homology length was reported to produce a few recombinants only, whereas, with homology length, more than 20 bp (20-40bp), the magnitude of homologous recombination found increased four-fold (Yu, 2000). Therefore, based on these results supported by previously reported data, primers with 30-nt homology extensions were considered the most effective, whereas primers of 20-nt extension length were omitted for the next objectives in the study.

Next, the ambiguous sequence (NNN) flanking PCR products (prepared using primers containing 30-nt NNN-extensions) were investigated for their efficiency in random insertions in the genome via homologous recombination, as per the hypothesis. Interestingly, some colonies (25-40 in different experiments) were observed in 72 hours of incubation (Figure 6.4a) using higher concentrations (200ng/μl and 400 ng/μl) of the PCR products as their higher efficiency indicated previously (Figure 6.2b). As mentioned previously, diminution in the number of colonies after genetic modifications or genomic deletions is a frequently observed phenomenon in bacteria (Kim, 2014; Kurokawa, 2016), the 19 colonies showed good growths further evaluated to confirm insertion-deletions through colony-PCR. Surprisingly, the results demonstrated the recombination of ambiguous sequence-based PCR products in the *E. coli* genome (Figure 6.4b). Further, it was interesting to know the number of recombinations (insertions) per genome. Based on the expression of the KmR gene, all 18 clones were evaluated through RT-PCR (Figure 6.1, Figure 6.5).  $\Delta hyfG$ , a KEIO mutant, containing a single copy of KmR gene, was selected as a positive control, and PS was considered as a negative control. It was surprising to find that the recombination was at multiple locations on the genome since the

expression of the KmR was found to be increased significantly in all recombinant colony strains as compared to the *hyfG* mutant (Figure 6.5). In bacterial cells, chromosomes are highly compacted to fit and organized such that they can be efficiently replicated, and each part is accessible for transcription (Le, 2013). As explained by Garmendia et al. (Garmendia, 2021), the local three-dimensional structure of the DNA is a major determining factor for successful recombination. The bacterial chromosome is not homogenous about homologous recombination and the three-dimensional structure of the nucleoid creates regions that are more or less accessible for recombination and therefore, may be the major factor influencing the recombinational accessibility of each chromosomal site (Garmendia, 2021). The orientation of the recombination cassettes and genes also shows a significant impact on recombination and affects recombination rates (Garmendia, 2021). Moreover, the variable length of the segment of the chromosome replaced by the PCR product may also be a factor in variable integrations (Kolisnychenko, 2002). Therefore, each region of the chromosome, position, and orientation of sequences influences the rate of recombination independently of the location of the homologous copy (Garmendia, 2021). Previous reports indicate that the recombination frequency depends on the size of the insert (Ublinskaya, 2012; Gu, 2015). The insertions were found one when 7.3-kb and two when 11.3-kb DNA fragments were employed in the homologous recombination strategy (Mizoguchi, 2008). Moreover, some recent approaches such as the chemically inducible chromosomal evolution (CICHe) system and chromosomal integration of genes with multiple copies (CIGMC) could integrate 40-60 and 15 copies, respectively, of the target gene in the bacterial chromosome via homologous recombination (Gu, 2015; St-Pierre, 2013). There are several studies employing the homologous recombination approaches (using lambda-phage and the Red recombination system) for genomic deletions and reported variable genomic insertions or integrations (Datsenko, 2000; Garmendia, 2021; Kolisnychenko, 2002; Kato, 2007; Mau, 2006]. These reports support the applicability of PCR products derived from

oligonucleotides containing NNN ambiguous sequences to recombine at multiple random positions via homologous recombination, as demonstrated by this study (Figure 6.5).

Finally, the phenotype of all the multiple insertion-deletions mutants (clones) was evaluated to find any major metabolic implications of this approach by assessing their specific growth rates under aerobic and ability of hydrogen production under anaerobic conditions. As result, no significant change in the growth and hydrogen productivity was observed, although the growth rates were found relatively reduced as compared to PS (Figure 6.6a, b). Contrary to the slow growth of development of the recombinant colonies just after recombination, growth rates at this time indicated not being affected critically (Figure 6.6b). Reports also revealed that some strains even after many genomic deletions exhibited normal growth (Mizoguchi, 2008). Since the metabolic network in *E. coli* is robust and can adjust to the loss of a major metabolic gene in alternative ways (St-Pierre, 2013), recombinants were supposed to adapt to the loss of major metabolic genes. The specific growth rates of the mutants might indicate a normal functioning metabolism and good adaptative capabilities with altered genotypes. The unaltered hydrogen metabolism of the mutants might point to at least one (out of four) still functioning hydrogenase gene (Maeda, 2008; Shekhar, 2021). Moreover, the results might also be reflecting the positions of multiple random genomic insertion-deletions were not either coding or metabolically essential or not associated with the region encoding metabolically important proteins.

## **6.5. Conclusion**

In conclusion, in this study, 30-nt as the minimum length for effective homologous recombination and the most efficient and accurate in generating deletion mutations was further verified. Based on this, 30-nt long extensions of ambiguous NNN-sequence were investigated for their efficient ability to recombine in the genome. The PCR products containing KmR gene flanking NNN-sequence were demonstrated to be able to recombine at random genomic

positions via homologous recombination and generate multiple insertion-deletion mutants. An effect on phenotype due to changed genotype was further evaluated by assessing several random insertion-deletion mutant clones for their hydrogen productivities and growth rates, which were found unaffected. The results indicated a normal metabolism or unaffected coding or essential region of the genome due to this approach. This study presents the efficiency of ambiguous sequences in random genomic deletions along with their potential abilities in the insertion of required gene inserts into the genome.



## CHAPTER 7

### CONCLUDING REMARKS AND SUGGESTIONS FOR THE FUTURE

More significant functions and phenotypic effects could be evaluated from hydrogenases than expected based on previous studies. This study demonstrated that hydrogenases and hydrogen metabolism have much more applications, other than hydrogen production. The novel hydrogenase operon mutants constructed in this study showed Hyd-2 and Hyd-3 as the most significant hydrogenases in *E. coli*, although the other two also showed considerable regulating properties in the test conditions. Almost all the studies in this research recognized them as distinctive from the others. Both are observed as the main hydrogen-producing hydrogenases in *E. coli*. Since all the hydrogenases are solely able for hydrogen uptake activity, Hyd-2, confirms its unique bi-functional nature and is therefore hypothesized to possess highly significant characteristic features exhibited in diverse metabolic activities. Hydrogenases, specifically Hyd-2 as most, along with hydrogen productivity, are marked as crucial for growth and central carbon (glucose) metabolism, persistence, and acid resistance. Moreover, hydrogenases have shown regulating roles in bacterial survival under stresses such as antibiotics and acid due to their significant ability to maintain energy and metabolic balance, combat ROS, cellular pH homeostasis, and wide transcriptomic connectivity.

The hydrogenases appeared significant in the maintenance of proton gradient across the membrane which might be by reducing protons released through metabolism to hydrogen. As reported previously, hydrogenases act as electron valves and are involved in the quinone pool, where electrons are used for  $\text{NAD}^+$  reduction activity, and their functioning is dependent on the FOF1-ATPase activity; hydrogenases were expected to contribute distinctively (among one another) gradients and therefore shown an effect on ATP synthesis and NADH content in the cell. Global transcriptomic analysis demonstrated a regulating role of the hydrogenases in the

diverse and critical metabolic activities, which further indicates their crucial roles in bacterial healthy metabolism and survival. The altered levels of hydrogenases and associated gene expressions under test conditions provide clear evidence in favor of such widespread metabolic activity.

Most studies on microbial hydrogen metabolism focus on only hydrogenase enzymatic activities. Hydrogenase-based gene surveys indicated their comprehensive genomic connectivity to other metabolic pathways at the global genomic scale. Through the significant advances made in understanding the roles, structure, mechanism, and biosynthesis, it is becoming clear that the different [NiFe]-hydrogenase isoenzymes in *E. coli* contribute in distinctly different ways to the anaerobic physiology of the organism. Despite the previous extensive research progress, there remains much to be discovered about microbial hydrogen metabolism on the genomic level. Based on their comprehensive genomic connectivity, found in this study, more research on hydrogenases is explicitly encouraged for their in-depth bacterial metabolic roles. New advances in biology, especially next-generation high-throughput technologies, will be significantly helpful in advancing knowledge in all these areas.

## REFERENCES

- Aakre** CD, Laub MT. Asymmetric cell division: a persistent issue? *Dev Cell*. 2012 Feb 14;22(2):235-6. doi: 10.1016/j.devcel.2012.01.016. PMID: 22340488; PMCID: PMC3295579.
- Agamennone** V, Le NG, van Straalen NM, Brouwer A, Roelofs D. Antimicrobial activity and carbohydrate metabolism in the bacterial metagenome of the soil-living invertebrate *Folsomia candida*. *Sci Rep*. 2019 May 13;9(1):7308. doi: 10.1038/s41598-019-43828-w. PMID: 31086216; PMCID: PMC6513849.
- Alberts** B, Johnson A, Lewis J, et al. *Molecular Biology of the Cell*. 4th ed. New York: Garland Science; 2002.
- Allison** KR, Brynildsen MP, Collins JJ. Metabolite-enabled eradication of bacterial persisters by aminoglycosides. *Nature*. 2011 May 12;473(7346):216-20. doi: 10.1038/nature10069. PMID: 21562562; PMCID: PMC3145328.
- Amato** SM, Fazen CH, Henry TC, Mok WW, Orman MA, Sandvik EL, Volzing KG, Brynildsen MP. The role of metabolism in bacterial persistence. *Front Microbiol*. 2014 Mar 3;5:70. doi: 10.3389/fmicb.2014.00070. PMID: 24624123; PMCID: PMC3939429.
- Andrews** S. 2010. Fastqc A Quality Control Tool For High Throughput Sequence Data. Available from <http://www.bioinformatics.babraham.ac.uk/projects/fastqc> [accessed August 27, 2020].
- Andrews** SC, Berks BC, McClay J, Ambler A, Quail MA, Golby P, Guest JR. A 12-cistron *Escherichia coli* operon (hyf) encoding a putative proton-translocating formate hydrogenlyase system. *Microbiology (Reading)*. 1997 Nov;143 ( Pt 11):3633-3647. doi: 10.1099/00221287-143-11-3633. PMID: 9387241.

- Ansari S**, Yamaoka Y. Survival of *Helicobacter pylori* in gastric acidic territory. *Helicobacter*. 2017 Aug;22(4):10.1111/hel.12386. doi: 10.1111/hel.12386. Epub 2017 Apr 12. PMID: 28402047; PMCID: PMC5851894.
- Baba T**, Ara T, Hasegawa M, Takai Y, Okumura Y, Baba M, Datsenko KA, Tomita M, Wanner BL, Mori H. Construction of *Escherichia coli* K-12 in-frame, single-gene knockout mutants: the Keio collection. *Mol Syst Biol*. 2006;2:2006.0008. doi: 10.1038/msb4100050. Epub 2006 Feb 21. PMID: 16738554; PMCID: PMC1681482.
- Bäckhed F**, Ley RE, Sonnenburg JL, Peterson DA, Gordon JI. Host-bacterial mutualism in the human intestine. *Science*. 2005 Mar 25;307(5717):1915-20. doi: 10.1126/science.1104816. PMID: 15790844.
- Bagramyan K**, Mnatsakanyan N, Poladian A, Vassilian A, Trchounian A. The roles of hydrogenases 3 and 4, and the F<sub>0</sub>F<sub>1</sub>-ATPase, in H<sub>2</sub> production by *Escherichia coli* at alkaline and acidic pH. *FEBS Lett*. 2002 Apr 10;516(1-3):172-8. doi: 10.1016/s0014-5793(02)02555-3. PMID: 11959127.
- Ballantine SP**, Boxer DH. Isolation and characterisation of a soluble active fragment of hydrogenase isoenzyme 2 from the membranes of anaerobically grown *Escherichia coli*. *Eur J Biochem*. 1986 Apr 15;156(2):277-84. doi: 10.1111/j.1432-1033.1986.tb09578.x. PMID: 3516690.
- Ballantine SP**, Boxer DH. Nickel-containing hydrogenase isoenzymes from anaerobically grown *Escherichia coli* K-12. *J Bacteriol*. 1985 Aug;163(2):454-9. doi: 10.1128/jb.163.2.454-459.1985. PMID: 3894325; PMCID: PMC219143.
- Batista AP**, Marreiros BC, Pereira MM. The antiporter-like subunit constituent of the universal adaptor of complex I, group 4 membrane-bound [NiFe]-hydrogenases and related complexes. *Biol Chem*. 2013 May;394(5):659-66. doi: 10.1515/hsz-2012-0342. PMID: 23509215.

- Bell DA, DeMarini DM.** Excessive cycling converts PCR products to random-length higher molecular weight fragments. *Nucleic Acids Res.* 1991 Sep 25;19(18):5079. doi: 10.1093/nar/19.18.5079. PMID: 1923779; PMCID: PMC328818.
- Benoit SL, Schmalstig AA, Glushka J, Maier SE, Edison AS, Maier RJ.** Nickel chelation therapy as an approach to combat multi-drug resistant enteric pathogens. *Sci Rep.* 2019 Sep 25;9(1):13851. doi: 10.1038/s41598-019-50027-0. Erratum in: *Sci Rep.* 2019 Nov 25;9(1):17813. PMID: 31554822; PMCID: PMC6761267.
- Berger M, Wu Y, Ogawa AK, McMinn DL, Schultz PG, Romesberg FE.** Universal bases for hybridization, replication and chain termination. *Nucleic Acids Res.* 2000 Aug 1;28(15):2911-4. doi: 10.1093/nar/28.15.2911. PMID: 10908353; PMCID: PMC102677.
- Bettenbrock K, Bai H, Ederer M, Green J, Hellingwerf KJ, Holcombe M, Kunz S, Rolfe MD, Sanguinetti G, Sawodny O, Sharma P, Steinsiek S, Poole RK.** Towards a systems level understanding of the oxygen response of *Escherichia coli*. *Adv Microb Physiol.* 2014;64:65-114. doi: 10.1016/B978-0-12-800143-1.00002-6. PMID: 24797925.
- Bhattacharyya S, Krishnarnurthy P, Shaker R, Vakil N, Phadnis SH, Dunn BE.** *Helicobacter pylori* requires active hydrogenase enzyme to survive under acidic conditions. *Gastroenterology* 2000; 118:A729. doi: 10.1016/S0016-5085(00)85046-5.
- Blattner FR, Plunkett G 3rd, Bloch CA, Perna NT, Burland V, Riley M, Collado-Vides J, Glasner JD, Rode CK, Mayhew GF, Gregor J, Davis NW, Kirkpatrick HA, Goeden MA, Rose DJ, Mau B, Shao Y.** The complete genome sequence of *Escherichia coli* K-12. *Science.* 1997 Sep 5;277(5331):1453-62. doi: 10.1126/science.277.5331.1453. PMID: 9278503.
- Blokesch M, Böck A.** Properties of the [NiFe]-hydrogenase maturation protein HypD. *FEBS Lett.* 2006 Jul 24;580(17):4065-8. doi: 10.1016/j.febslet.2006.06.045. Epub 2006 Jun 27. PMID: 16814778.

- Blokesch** M, Magalon A, Böck A. Interplay between the specific chaperone-like proteins HybG and HypC in maturation of hydrogenases 1, 2, and 3 from *Escherichia coli*. J Bacteriol. 2001 May;183(9):2817-22. doi: 10.1128/JB.183.9.2817-2822.2001. PMID: 11292801; PMCID: PMC99498.
- Böhm** R, Sauter M, Böck A. Nucleotide sequence and expression of an operon in *Escherichia coli* coding for formate hydrogenlyase components. Mol Microbiol. 1990 Feb;4(2):231-43. doi: 10.1111/j.1365-2958.1990.tb00590.x. PMID: 2187144.
- Bommer** GT, Van Schaftingen E, Veiga-da-Cunha M. Metabolite Repair Enzymes Control Metabolic Damage in Glycolysis. Trends Biochem Sci. 2020 Mar;45(3):228-243. doi: 10.1016/j.tibs.2019.07.004. Epub 2019 Aug 28. PMID: 31473074.
- Borisov** VB, Gennis RB, Hemp J, Verkhovsky MI. The cytochrome bd respiratory oxygen reductases. Biochim Biophys Acta. 2011 Nov;1807(11):1398-413. doi: 10.1016/j.bbabi.2011.06.016. Epub 2011 Jul 1. PMID: 21756872; PMCID: PMC3171616.
- Bowles** LK, Ellefson WL. Effects of butanol on *Clostridium acetobutylicum*. Appl Environ Microbiol. 1985 Nov;50(5):1165-70. doi: 10.1128/aem.50.5.1165-1170.1985. PMID: 2868690; PMCID: PMC238718.
- Brito** C, Cabanes D, Sarmiento Mesquita F, Sousa S. Mechanisms protecting host cells against bacterial pore-forming toxins. Cell Mol Life Sci. 2019 Apr;76(7):1319-1339. doi: 10.1007/s00018-018-2992-8. Epub 2018 Dec 27. PMID: 30591958; PMCID: PMC6420883.
- Brøndsted** L, Atlung T. Effect of growth conditions on expression of the acid phosphatase (cyx-appA) operon and the appY gene, which encodes a transcriptional activator of *Escherichia coli*. J Bacteriol. 1996 Mar;178(6):1556-64. doi: 10.1128/jb.178.6.1556-1564.1996. PMID: 8626281; PMCID: PMC177838.

- Brynildsen MP**, Winkler JA, Spina CS, MacDonald IC, Collins JJ. Potentiating antibacterial activity by predictably enhancing endogenous microbial ROS production. *Nat Biotechnol.* 2013 Feb;31(2):160-5. doi: 10.1038/nbt.2458. Epub 2013 Jan 6. PMID: 23292609; PMCID: PMC3568245.
- Cabral DJ**, Wurster JI, Belenky P. Antibiotic Persistence as a Metabolic Adaptation: Stress, Metabolism, the Host, and New Directions. *Pharmaceuticals (Basel).* 2018 Feb 1;11(1):14. doi: 10.3390/ph11010014. PMID: 29389876; PMCID: PMC5874710.
- Cañas-Duarte S**, Perez-Lopez M, Herrfurth C, Sun L, Contreras L, Feussner I. et al. 2020. An integrative approach points to membrane composition as a key factor in *E. coli* persistence. *bioRxiv*, 2020.08.28.271171. doi: 10.1101/2020.08.28.271171.
- Carlson R**, Sreenc F. Fundamental *Escherichia coli* biochemical pathways for biomass and energy production: identification of reactions. *Biotechnol Bioeng.* 2004 Jan 5;85(1):1-19. doi: 10.1002/bit.10812. PMID: 14705007.
- Chang YY**, Cronan JE Jr. Membrane cyclopropane fatty acid content is a major factor in acid resistance of *Escherichia coli*. *Mol Microbiol.* 1999 Jul;33(2):249-59. doi: 10.1046/j.1365-2958.1999.01456.x. PMID: 10411742.
- Cherepanov PP**, Wackernagel W. Gene disruption in *Escherichia coli*: TcR and KmR cassettes with the option of Flp-catalyzed excision of the antibiotic-resistance determinant. *Gene.* 1995 May 26;158(1):9-14. doi: 10.1016/0378-1119(95)00193-a. PMID: 7789817.
- Cho J**, Rogers J, Kearns M, Leslie M, Hartson SD, Wilson KS. *Escherichia coli* persister cells suppress translation by selectively disassembling and degrading their ribosomes. *Mol Microbiol.* 2015 Jan;95(2):352-64. doi: 10.1111/mmi.12884. Epub 2014 Dec 19. PMID: 25425348.
- Chowdhury N**, Kwan BW, Wood TK. Persistence Increases in the Absence of the Alarmones Guanosine Tetraphosphate by Reducing Cell Growth. *Sci Rep.* 2016 Feb 3;6:20519. doi:

10.1038/srep20519. PMID: 26837570; PMCID: PMC4738310.

- Christensen** CE, Karlsson M, Winther JR, Jensen PR, Lerche MH. Non-invasive in-cell determination of free cytosolic [NAD<sup>+</sup>]/[NADH] ratios using hyperpolarized glucose show large variations in metabolic phenotypes. *J Biol Chem*. 2014 Jan 24;289(4):2344-52. doi: 10.1074/jbc.M113.498626. Epub 2013 Dec 3. PMID: 24302737; PMCID: PMC3900977.
- Church** DL, Rabin HR, Laishley EJ. Reduction of 2-, 4- and 5-nitroimidazole drugs by hydrogenase 1 in *Clostridium pasteurianum*. *J Antimicrob Chemother*. 1990 Jan;25(1):15-23. doi: 10.1093/jac/25.1.15. PMID: 2180890.
- Cordero** PRF, Grinter R, Hards K, Cryle MJ, Warr CG, Cook GM, Greening C. Two uptake hydrogenases differentially interact with the aerobic respiratory chain during mycobacterial growth and persistence. *J Biol Chem*. 2019 Dec 13;294(50):18980-18991. doi: 10.1074/jbc.RA119.011076. Epub 2019 Oct 17. PMID: 31624148; PMCID: PMC6916507.
- Costerton** JW, Cheng KJ. The role of the bacterial cell envelope in antibiotic resistance. *J Antimicrob Chemother*. 1975 Dec;1(4):363-77. doi: 10.1093/jac/1.4.363. PMID: 1107294.
- Court** DL, Sawitzke JA, Thomason LC. Genetic engineering using homologous recombination. *Annu Rev Genet*. 2002;36:361-88. doi: 10.1146/annurev.genet.36.061102.093104. Epub 2002 Jun 11. PMID: 12429697.
- Curran** TP, Shapiro R, Riordan JF. Alteration of the enzymatic specificity of human angiogenin by site-directed mutagenesis. *Biochemistry*. 1993 Mar 9;32(9):2307-13. doi: 10.1021/bi00060a023. PMID: 8095159.
- Datsenko** KA, Wanner BL. One-step inactivation of chromosomal genes in *Escherichia coli* K-12 using PCR products. *Proc Natl Acad Sci U S A*. 2000 Jun 6;97(12):6640-5. doi: 10.1073/pnas.120163297. PMID: 10829079; PMCID: PMC18686.
- Donner** J, Reck M, Bunk B, Jarek M, App CB, Meier-Kolthoff JP, Overmann J, Müller R, Kirschning A, Wagner-Döbler I. The Biofilm Inhibitor Carolacton Enters Gram-Negative

Cells: Studies Using a TolC-Deficient Strain of *Escherichia coli*. mSphere. 2017 Sep 27;2(5):e00375-17. doi: 10.1128/mSphereDirect.00375-17. PMID: 28959742; PMCID: PMC5615136.

**Dwyer DJ**, Belenky PA, Yang JH, MacDonald IC, Martell JD, Takahashi N, Chan CT, Lobritz MA, Braff D, Schwarz EG, Ye JD, Pati M, Vercruysse M, Ralifo PS, Allison KR, Khalil AS, Ting AY, Walker GC, Collins JJ. Antibiotics induce redox-related physiological alterations as part of their lethality. Proc Natl Acad Sci U S A. 2014 May 20;111(20):E2100-9. doi: 10.1073/pnas.1401876111. Epub 2014 May 6. PMID: 24803433; PMCID: PMC4034191.

**Efremov RG**, Sazanov LA. The coupling mechanism of respiratory complex I - a structural and evolutionary perspective. Biochim Biophys Acta. 2012 Oct;1817(10):1785-95. doi: 10.1016/j.bbabi.2012.02.015. Epub 2012 Feb 22. PMID: 22386882.

**Ellermeier CD**, Janakiraman A, Slauch JM. Construction of targeted single copy lac fusions using lambda Red and FLP-mediated site-specific recombination in bacteria. Gene. 2002 May 15;290(1-2):153-61. doi: 10.1016/s0378-1119(02)00551-6. PMID: 12062810.

**Ellis HM**, Yu D, DiTizio T, Court DL. High efficiency mutagenesis, repair, and engineering of chromosomal DNA using single-stranded oligonucleotides. Proc Natl Acad Sci U S A. 2001 Jun 5;98(12):6742-6. doi: 10.1073/pnas.121164898. Epub 2001 May 29. PMID: 11381128; PMCID: PMC34423.

**Fang HH**, Liu H. Effect of pH on hydrogen production from glucose by a mixed culture. Bioresour Technol. 2002 Mar;82(1):87-93. doi: 10.1016/s0960-8524(01)00110-9. PMID: 11858207.

**Fujii R**, Kitaoka M, Hayashi K. RAISE: a simple and novel method of generating random insertion and deletion mutations. Nucleic Acids Res. 2006 Feb 21;34(4):e30. doi: 10.1093/nar/gnj032. PMID: 16493137; PMCID: PMC1380258.

- Fujimoto R**, Osakabe T, Saito M, Kurosawa N, Isobe M. Minimum length of homology arms required for effective Red/ET recombination. *Biosci Biotechnol Biochem*. 2009 Dec;73(12):2783-6. doi: 10.1271/bbb.90584. Epub 2009 Dec 7. PMID: 19966478.
- Garmendia E**, Brandis G, Guy L, Cao S, Hughes D. Chromosomal Location Determines the Rate of Intrachromosomal Homologous Recombination in *Salmonella*. *mBio*. 2021 Jun 29;12(3):e0115121. doi: 10.1128/mBio.01151-21. Epub 2021 Jun 1. PMID: 34061591; PMCID: PMC8262849.
- Girgis SI**, Alevizaki M, Denny P, Ferrier GJ, Legon S. Generation of DNA probes for peptides with highly degenerate codons using mixed primer PCR. *Nucleic Acids Res*. 1988 Nov 11;16(21):10371. doi: 10.1093/nar/16.21.10371. PMID: 3194210; PMCID: PMC338873.
- Gong S**, Richard H, Foster JW. YjdE (AdiC) is the arginine:agmatine antiporter essential for arginine-dependent acid resistance in *Escherichia coli*. *J Bacteriol*. 2003 Aug;185(15):4402-9. doi: 10.1128/JB.185.15.4402-4409.2003. PMID: 12867448; PMCID: PMC165756.
- Goodall ECA**, Robinson A, Johnston IG, Jabbari S, Turner KA, Cunningham AF, Lund PA, Cole JA, Henderson IR. The Essential Genome of *Escherichia coli* K-12. *mBio*. 2018 Feb 20;9(1):e02096-17. doi: 10.1128/mBio.02096-17. PMID: 29463657; PMCID: PMC5821084.
- Goryshin IY**, Naumann TA, Apodaca J, Reznikoff WS. Chromosomal deletion formation system based on Tn5 double transposition: use for making minimal genomes and essential gene analysis. *Genome Res*. 2003 Apr;13(4):644-53. doi: 10.1101/gr.611403. Epub 2003 Mar 12. PMID: 12654720; PMCID: PMC430159.
- Grant SS**, Kaufmann BB, Chand NS, Haseley N, Hung DT. Eradication of bacterial persisters with antibiotic-generated hydroxyl radicals. *Proc Natl Acad Sci U S A*. 2012 Jul 24;109(30):12147-52. doi: 10.1073/pnas.1203735109. Epub 2012 Jul 9. PMID: 22778419;

PMCID: PMC3409745.

**Gu P**, Yang F, Su T, Wang Q, Liang Q, Qi Q. A rapid and reliable strategy for chromosomal integration of gene(s) with multiple copies. *Sci Rep*. 2015 Apr 8;5:9684. doi: 10.1038/srep09684. PMID: 25851494; PMCID: PMC4389210.

**Guerrero-Mendiola C**, García-Trejo JJ, Encalada R, Saavedra E, Ramírez-Silva L. The contribution of two isozymes to the pyruvate kinase activity of *Vibrio cholerae*: One K<sup>+</sup>-dependent constitutively active and another K<sup>+</sup>-independent with essential allosteric activation. *PLoS One*. 2017 Jul 7;12(7):e0178673. doi: 10.1371/journal.pone.0178673. PMID: 28686591; PMCID: PMC5501398.

**Hada T**, Yamamoto T, Yamamoto A, Ohkura K, Yamazaki N, Takiguchi Y, Shinohara Y. Comparison of the catalytic activities of three isozymes of carnitine palmitoyltransferase 1 expressed in COS7 cells. *Appl Biochem Biotechnol*. 2014 Feb;172(3):1486-96. doi: 10.1007/s12010-013-0619-y. Epub 2013 Nov 13. PMID: 24222496.

**Hakobyan M**, Sargsyan H, Bagramyan K. Proton translocation coupled to formate oxidation in anaerobically grown fermenting *Escherichia coli*. *Biophys Chem*. 2005 May 1;115(1):55-61. doi: 10.1016/j.bpc.2005.01.002. Epub 2005 Jan 26. Erratum in: *Biophys Chem*. 2005 Dec 1;118(2-3):135. PMID: 15848284.

**Hallenbeck PC**, Benemann JR. Biological hydrogen production: Fundamentals and limiting processes. *Int J Hydrog Energy* 2002; 27:1185–1193. doi: 10.1016/S0360-3199(02)00131-3.

**Hallenbeck PC**. Microbial paths to renewable hydrogen production. *Biofuels* 2014; 2:285–302. doi: 10.4155/bfs.11.6.

**Hayes ET**, Wilks JC, Sanfilippo P, Yohannes E, Tate DP, Jones BD, Radmacher MD, BonDurant SS, Slonczewski JL. Oxygen limitation modulates pH regulation of catabolism and hydrogenases, multidrug transporters, and envelope composition in *Escherichia coli*

- K-12. BMC Microbiol. 2006 Oct 6;6:89. doi: 10.1186/1471-2180-6-89. PMID: 17026754; PMCID: PMC1626474.
- Hengge-Aronis R.** Signal transduction and regulatory mechanisms involved in control of the sigma(S) (RpoS) subunit of RNA polymerase. Microbiol Mol Biol Rev. 2002 Sep;66(3):373-95, table of contents. doi: 10.1128/MMBR.66.3.373-395.2002. PMID: 12208995; PMCID: PMC120795.
- Hersh BM, Farooq FT, Barstad DN, Blankenhorn DL, Slonczewski JL.** A glutamate-dependent acid resistance gene in *Escherichia coli*. J Bacteriol. 1996 Jul;178(13):3978-81. doi: 10.1128/jb.178.13.3978-3981.1996. PMID: 8682809; PMCID: PMC232665.
- Holland IB.** Translocation of bacterial proteins--an overview. Biochim Biophys Acta. 2004 Nov 11;1694(1-3):5-16. doi: 10.1016/j.bbamcr.2004.02.007. PMID: 15546654.
- Holm AK, Blank LM, Oldiges M, Schmid A, Solem C, Jensen PR, Vemuri GN.** Metabolic and transcriptional response to cofactor perturbations in *Escherichia coli*. J Biol Chem. 2010 Jun 4;285(23):17498-506. doi: 10.1074/jbc.M109.095570. Epub 2010 Mar 18. PMID: 20299454; PMCID: PMC2878514.
- Hommais F, Krin E, Coppée JY, Lacroix C, Yeramian E, Danchin A, Bertin P.** GadE (YhiE): a novel activator involved in the response to acid environment in *Escherichia coli*. Microbiology (Reading). 2004 Jan;150(Pt 1):61-72. doi: 10.1099/mic.0.26659-0. PMID: 14702398.
- Hong SH, Wang X, O'Connor HF, Benedik MJ, Wood TK.** Bacterial persistence increases as environmental fitness decreases. Microb Biotechnol. 2012 Jul;5(4):509-22. doi: 10.1111/j.1751-7915.2011.00327.x. Epub 2012 Jan 6. PMID: 22221537; PMCID: PMC3323757.
- Hosseini SR, Wagner A.** Genomic organization underlying deletional robustness in bacterial metabolic systems. Proc Natl Acad Sci U S A. 2018 Jul 3;115(27):7075-7080. doi:

- 10.1073/pnas.1717243115. Epub 2018 Jun 18. PMID: 29915048; PMCID: PMC6142276.
- Hua** SB, Qiu M, Chan E, Zhu L, Luo Y. Minimum length of sequence homology required for in vivo cloning by homologous recombination in yeast. *Plasmid*. 1997;38(2):91-6. doi: 10.1006/plas.1997.1305. PMID: 9339466.
- Hughes** MD, Nagel DA, Santos AF, Sutherland AJ, Hine AV. Removing the redundancy from randomised gene libraries. *J Mol Biol*. 2003 Aug 29;331(5):973-9. doi: 10.1016/s0022-2836(03)00833-7. PMID: 12927534.
- Jeong** J, Cho N, Jung D, Bang D. Genome-scale genetic engineering in *Escherichia coli*. *Biotechnol Adv*. 2013 Nov;31(6):804-10. doi: 10.1016/j.biotechadv.2013.04.003. Epub 2013 Apr 24. PMID: 23624241.
- Jiang** GR, Nikolova S, Clark DP. Regulation of the *ldhA* gene, encoding the fermentative lactate dehydrogenase of *Escherichia coli*. *Microbiology (Reading)*. 2001 Sep;147(Pt 9):2437-2446. doi: 10.1099/00221287-147-9-2437. PMID: 11535784.
- Jo** BH, Cha HJ. Activation of formate hydrogen-lyase via expression of uptake [NiFe]-hydrogenase in *Escherichia coli* BL21(DE3). *Microb Cell Fact*. 2015 Sep 22;14:151. doi: 10.1186/s12934-015-0343-0. PMID: 26395073; PMCID: PMC4578252.
- Jubelin** G, Desvaux M, Schüller S, Etienne-Mesmin L, Muniesa M, Blanquet-Diot S. Modulation of Enterohaemorrhagic *Escherichia coli* Survival and Virulence in the Human Gastrointestinal Tract. *Microorganisms*. 2018 Nov 19;6(4):115. doi: 10.3390/microorganisms6040115. PMID: 30463258; PMCID: PMC6313751.
- Kajfasz** JK, Quivey RG. Responses of Lactic Acid Bacteria to Acid Stress. In: Tsakalidou E, Papadimitriou K (ed.). *Stress Responses of Lactic Acid Bacteria*. Food Microbiology and Food Safety. 2011. Springer, Boston, MA. doi: 10.1007/978-0-387-92771-8\_2.
- Kanca** O, Zirin J, Garcia-Marques J, Knight SM, Yang-Zhou D, Amador G, Chung H, Zuo Z, Ma L, He Y, Lin WW, Fang Y, Ge M, Yamamoto S, Schulze KL, Hu Y, Spradling AC,

- Mohr SE, Perrimon N, Bellen HJ. An efficient CRISPR-based strategy to insert small and large fragments of DNA using short homology arms. *Elife*. 2019 Nov 1;8:e51539. doi: 10.7554/eLife.51539. PMID: 31674908; PMCID: PMC6855806.
- Kanehisa M**, Goto S. KEGG: kyoto encyclopedia of genes and genomes. *Nucleic Acids Res*. 2000 Jan 1;28(1):27-30. doi: 10.1093/nar/28.1.27. PMID: 10592173; PMCID: PMC102409.
- Kang Y**, Durfee T, Glasner JD, Qiu Y, Frisch D, Winterberg KM, Blattner FR. Systematic mutagenesis of the *Escherichia coli* genome. *J Bacteriol*. 2004 Aug;186(15):4921-30. doi: 10.1128/JB.186.15.4921-4930.2004. Erratum in: *J Bacteriol*. 2004 Dec;186(24):8548. PMID: 15262929; PMCID: PMC451658.
- Kanjee U**, Houry WA. Mechanisms of acid resistance in *Escherichia coli*. *Annu Rev Microbiol*. 2013;67:65-81. doi: 10.1146/annurev-micro-092412-155708. Epub 2013 May 20. PMID: 23701194.
- Kargeti M**, Venkatesh KV. The effect of global transcriptional regulators on the anaerobic fermentative metabolism of *Escherichia coli*. *Mol Biosyst*. 2017 Jun 27;13(7):1388-1398. doi: 10.1039/c6mb00721j. PMID: 28573283.
- Kato J**, Hashimoto M. Construction of consecutive deletions of the *Escherichia coli* chromosome. *Mol Syst Biol*. 2007;3:132. doi: 10.1038/msb4100174. Epub 2007 Aug 14. PMID: 17700540; PMCID: PMC1964801.
- Keren I**, Kaldalu N, Spoering A, Wang Y, Lewis K. Persister cells and tolerance to antimicrobials. *FEMS Microbiol Lett*. 2004 Jan 15;230(1):13-8. doi: 10.1016/S0378-1097(03)00856-5. Erratum in: *FEMS Microbiol Lett*. 2004 May 1;234(1):187. PMID: 14734160.
- Kim J**, Webb AM, Kershner JP, Blaskowski S, Copley SD. A versatile and highly efficient method for scarless genome editing in *Escherichia coli* and *Salmonella enterica*. *BMC*

- Biotechnol. 2014 Sep 25;14:84. doi: 10.1186/1472-6750-14-84. PMID: 25255806; PMCID: PMC4236582.
- Kim M**, Rai N, Zorraquino V, Tagkopoulos I. Multi-omics integration accurately predicts cellular state in unexplored conditions for *Escherichia coli*. Nat Commun. 2016 Oct 7;7:13090. doi: 10.1038/ncomms13090. PMID: 27713404; PMCID: PMC5059772.
- Kim R**, Guo JT. Systematic analysis of short internal indels and their impact on protein folding. BMC Struct Biol. 2010 Aug 4;10:24. doi: 10.1186/1472-6807-10-24. PMID: 20684774; PMCID: PMC2924343.
- King PW**, Przybyla AE. Response of *hya* expression to external pH in *Escherichia coli*. J Bacteriol. 1999 Sep;181(17):5250-6. doi: 10.1128/JB.181.17.5250-5256.1999. PMID: 10464194; PMCID: PMC94029.
- King PW**, Przybyla AE. Response of *hya* expression to external pH in *Escherichia coli*. J Bacteriol. 1999 Sep;181(17):5250-6. doi: 10.1128/JB.181.17.5250-5256.1999. PMID: 10464194; PMCID: PMC94029.
- King T**, Lucchini S, Hinton JC, Gobius K. Transcriptomic analysis of *Escherichia coli* O157:H7 and K-12 cultures exposed to inorganic and organic acids in stationary phase reveals acidulant- and strain-specific acid tolerance responses. Appl Environ Microbiol. 2010 Oct;76(19):6514-28. doi: 10.1128/AEM.02392-09. Epub 2010 Aug 13. PMID: 20709847; PMCID: PMC2950450.
- Kohanski MA**, Dwyer DJ, Hayete B, Lawrence CA, Collins JJ. A common mechanism of cellular death induced by bactericidal antibiotics. Cell. 2007 Sep 7;130(5):797-810. doi: 10.1016/j.cell.2007.06.049. PMID: 17803904.
- Kolisnychenko V**, Plunkett G 3rd, Herring CD, Fehér T, Pósfai J, Blattner FR, Pósfai G. Engineering a reduced *Escherichia coli* genome. Genome Res. 2002 Apr;12(4):640-7. doi: 10.1101/gr.217202. PMID: 11932248; PMCID: PMC187512.

- Kurokawa M**, Seno S, Matsuda H, Ying BW. Correlation between genome reduction and bacterial growth. *DNA Res.* 2016 Dec;23(6):517-525. doi: 10.1093/dnares/dsw035. Epub 2016 Jul 3. PMID: 27374613; PMCID: PMC5144675.
- Langmead B**, Salzberg SL. Fast gapped-read alignment with Bowtie 2. *Nat Methods.* 2012 Mar 4;9(4):357-9. doi: 10.1038/nmeth.1923. PMID: 22388286; PMCID: PMC3322381.
- Laurinavichene TV**, Tsygankov AA. H<sub>2</sub> consumption by *Escherichia coli* coupled via hydrogenase 1 or hydrogenase 2 to different terminal electron acceptors. *FEMS Microbiol Lett.* 2001 Aug 7;202(1):121-4. doi: 10.1111/j.1574-6968.2001.tb10790.x. PMID: 11506918.
- Le TB**, Imakaev MV, Mirny LA, Laub MT. High-resolution mapping of the spatial organization of a bacterial chromosome. *Science.* 2013 Nov 8;342(6159):731-4. doi: 10.1126/science.1242059. Epub 2013 Oct 24. PMID: 24158908; PMCID: PMC3927313.
- Leonhartsberger S**, Korsa I, Böck A. The molecular biology of formate metabolism in enterobacteria. *J Mol Microbiol Biotechnol.* 2002 May;4(3):269-76. PMID: 11931558.
- Leprince A**, de Lorenzo V, Völler P, van Passel MW, Martins dos Santos VA. Random and cyclical deletion of large DNA segments in the genome of *Pseudomonas putida*. *Environ Microbiol.* 2012 Jun;14(6):1444-53. doi: 10.1111/j.1462-2920.2012.02730.x. Epub 2012 Mar 19. PMID: 22429517; PMCID: PMC3429869.
- Lewis K.** *Persister Cells and Infectious Disease.* Springer International Publishing. 2019.
- Lewis VG**, Ween MP, McDevitt CA. The role of ATP-binding cassette transporters in bacterial pathogenicity. *Protoplasma.* 2012 Oct;249(4):919-42. doi: 10.1007/s00709-011-0360-8. Epub 2012 Jan 13. PMID: 22246051.
- Liu Q**, Chen N, Chen H, Huang Y. RNA-Seq analysis of differentially expressed genes of *Staphylococcus epidermidis* isolated from postoperative endophthalmitis and the healthy

conjunctiva. Sci Rep. 2020 Aug 28;10(1):14234. doi: 10.1038/s41598-020-71050-6. PMID: 32859978; PMCID: PMC7455711.

**Liu Y**, Yang K, Zhang H, Jia Y, Wang Z. Combating Antibiotic Tolerance Through Activating Bacterial Metabolism. Front Microbiol. 2020 Oct 22;11:577564. doi: 10.3389/fmicb.2020.577564. PMID: 33193198; PMCID: PMC7642520.

**Lund P**, Tramonti A, De Biase D. Coping with low pH: molecular strategies in neutralophilic bacteria. FEMS Microbiol Rev. 2014 Nov;38(6):1091-125. doi: 10.1111/1574-6976.12076. Epub 2014 Jul 2. PMID: 24898062.

**Maeda T**, Sanchez-Torres V, Wood TK. Enhanced hydrogen production from glucose by metabolically engineered *Escherichia coli*. Appl Microbiol Biotechnol. 2007 Dec;77(4):879-90. doi: 10.1007/s00253-007-1217-0. Epub 2007 Oct 16. PMID: 17938909.

**Maeda T**, Sanchez-Torres V, Wood TK. *Escherichia coli* hydrogenase 3 is a reversible enzyme possessing hydrogen uptake and synthesis activities. Appl Microbiol Biotechnol. 2007 Oct;76(5):1035-42. doi: 10.1007/s00253-007-1086-6. Epub 2007 Aug 1. PMID: 17668201.

**Maeda T**, Sanchez-Torres V, Wood TK. Metabolic engineering to enhance bacterial hydrogen production. Microb Biotechnol. 2008 Jan;1(1):30-9. doi: 10.1111/j.1751-7915.2007.00003.x. PMID: 21261819; PMCID: PMC3864429.

**Maeda T**, Sanchez-Torres V, Wood TK. Protein engineering of hydrogenase 3 to enhance hydrogen production. Appl Microbiol Biotechnol. 2008 May;79(1):77-86. doi: 10.1007/s00253-008-1416-3. Epub 2008 Mar 12. PMID: 18335216.

**Maeda T**, Tran KT, Yamasaki R, Wood TK. Current state and perspectives in hydrogen production by *Escherichia coli*: roles of hydrogenases in glucose or glycerol metabolism. Appl Microbiol Biotechnol. 2018 Mar;102(5):2041-2050. doi: 10.1007/s00253-018-8752-8. Epub 2018 Jan 24. PMID: 29368215.

- Maeda T**, Vardar G, Self WT, Wood TK. Inhibition of hydrogen uptake in *Escherichia coli* by expressing the hydrogenase from the cyanobacterium *Synechocystis* sp. PCC 6803. *BMC Biotechnol.* 2007 May 23;7:25. doi: 10.1186/1472-6750-7-25. PMID: 17521447; PMCID: PMC1904212.
- Maeda T**, Yoshimura T, Shimazu T, Shirai Y, Ogawa HI. Enhanced production of lactic acid with reducing excess sludge by lactate fermentation. *J Hazard Mater.* 2009 Sep 15;168(2-3):656-63. doi: 10.1016/j.jhazmat.2009.02.067. Epub 2009 Feb 23. PMID: 19286312.
- Magoc T**, Wood D, Salzberg SL. EDGE-pro: Estimated Degree of Gene Expression in Prokaryotic Genomes. *Evol Bioinform Online.* 2013;9:127-36. doi: 10.4137/EBO.S11250. Epub 2013 Mar 10. PMID: 23531787; PMCID: PMC3603529.
- Maier L**, Barthel M, Stecher B, Maier RJ, Gunn JS, Hardt WD. Salmonella Typhimurium strain ATCC14028 requires H<sub>2</sub>-hydrogenases for growth in the gut, but not at systemic sites. *PLoS One.* 2014 Oct 10;9(10):e110187. doi: 10.1371/journal.pone.0110187. PMID: 25303479; PMCID: PMC4193879.
- Maisonneuve E**, Gerdes K. Molecular mechanisms underlying bacterial persisters. *Cell.* 2014 Apr 24;157(3):539-48. doi: 10.1016/j.cell.2014.02.050. PMID: 24766804.
- Maisonneuve E**, Shakespeare LJ, Jørgensen MG, Gerdes K. Bacterial persistence by RNA endonucleases. *Proc Natl Acad Sci U S A.* 2011 Aug 9;108(32):13206-11. doi: 10.1073/pnas.1100186108. Epub 2011 Jul 25. Retraction in: *Proc Natl Acad Sci U S A.* 2018 Mar 12;: PMID: 21788497; PMCID: PMC3156201.
- Maki H**, Saito S, Ibaraki T, Ichijo M, Yoshie O. Use of universal and type-specific primers in the polymerase chain reaction for the detection and typing of genital human papillomaviruses. *Jpn J Cancer Res.* 1991 Apr;82(4):411-9. doi: 10.1111/j.1349-7006.1991.tb01864.x. PMID: 1646198; PMCID: PMC5918436.
- Malcovati M**, Kornberg HL. Two types of pyruvate kinase in *Escherichia coli* K12. *Biochim*

Biophys Acta. 1969 Apr 22;178(2):420-3. doi: 10.1016/0005-2744(69)90417-3. PMID: 4890755.

**Marreiros** BC, Batista AP, Duarte AM, Pereira MM. A missing link between complex I and group 4 membrane-bound [NiFe] hydrogenases. Biochim Biophys Acta. 2013 Feb;1827(2):198-209. doi: 10.1016/j.bbabi.2012.09.012. Epub 2012 Sep 20. PMID: 23000657.

**Marteyn** B, Scorza FB, Sansonetti PJ, Tang C. Breathing life into pathogens: the influence of oxygen on bacterial virulence and host responses in the gastrointestinal tract. Cell Microbiol. 2011 Feb;13(2):171-6. doi: 10.1111/j.1462-5822.2010.01549.x. Epub 2010 Dec 19. PMID: 21166974.

**Martin** M. Cutadapt removes adapter sequences from high-throughput sequencing reads. EMBnet.journal, 2011; 17(1):10-12. doi: 10.14806/ej.17.1.200.

**Mau** B, Glasner JD, Darling AE, Perna NT. Genome-wide detection and analysis of homologous recombination among sequenced strains of *Escherichia coli*. Genome Biol. 2006;7(5):R44. doi: 10.1186/gb-2006-7-5-r44. Epub 2006 May 31. PMID: 16737554; PMCID: PMC1779527.

**Maurer** LM, Yohannes E, Bondurant SS, Radmacher M, Slonczewski JL. pH regulates genes for flagellar motility, catabolism, and oxidative stress in *Escherichia coli* K-12. J Bacteriol. 2005 Jan;187(1):304-19. doi: 10.1128/JB.187.1.304-319.2005. PMID: 15601715; PMCID: PMC538838.

**May** KL, Grabowicz M. The bacterial outer membrane is an evolving antibiotic barrier. Proc Natl Acad Sci U S A. 2018 Sep 4;115(36):8852-8854. doi: 10.1073/pnas.1812779115. Epub 2018 Aug 23. PMID: 30139916; PMCID: PMC6130387.

**McClure** R, Balasubramanian D, Sun Y, Bobrovskyy M, Sumby P, Genco CA, Vanderpool CK, Tjaden B. Computational analysis of bacterial RNA-Seq data. Nucleic Acids Res.

- 2013 Aug;41(14):e140. doi: 10.1093/nar/gkt444. Epub 2013 May 28. PMID: 23716638; PMCID: PMC3737546.
- McNorton MM**, Maier RJ. Roles of H<sub>2</sub> uptake hydrogenases in *Shigella flexneri* acid tolerance. Microbiology (Reading). 2012 Aug;158(Pt 8):2204-2212. doi: 10.1099/mic.0.058248-0. Epub 2012 May 24. PMID: 22628482; PMCID: PMC3542139.
- Menon NK**, Chatelus CY, Dervartanian M, Wendt JC, Shanmugam KT, Peck HD Jr, Przybyla AE. Cloning, sequencing, and mutational analysis of the *hyb* operon encoding *Escherichia coli* hydrogenase 2. J Bacteriol. 1994 Jul;176(14):4416-23. doi: 10.1128/jb.176.14.4416-4423.1994. PMID: 8021226; PMCID: PMC205655.
- Menon NK**, Robbins J, Wendt JC, Shanmugam KT, Przybyla AE. Mutational analysis and characterization of the *Escherichia coli hya* operon, which encodes [NiFe] hydrogenase 1. J Bacteriol. 1991 Aug;173(15):4851-61. doi: 10.1128/jb.173.15.4851-4861.1991. PMID: 1856178; PMCID: PMC208165.
- Millard CS**, Chao YP, Liao JC, Donnelly MI. Enhanced production of succinic acid by overexpression of phosphoenolpyruvate carboxylase in *Escherichia coli*. Appl Environ Microbiol. 1996 May;62(5):1808-10. doi: 10.1128/aem.62.5.1808-1810.1996. PMID: 8633880; PMCID: PMC167956.
- Mirzoyan S**, Romero-Pareja PM, Coello MD, Trchounian A, Trchounian K. Evidence for hydrogenase-4 catalyzed biohydrogen production in *Escherichia coli*. Int J Hydrog Energy 2017; 42:21697-703. doi: 10.1016/j.ijhydene.2017.07.126.
- Mirzoyan S**, Trchounian A, Trchounian K. Role of hydrogenases 3 and 4 in *Escherichia coli* growth and H<sub>2</sub> producing hydrogenase activity during anaerobic utilization of lactose. Int J Hydrog Energy 2018; 43:18151-18159. doi: 10.1016/j.ijhydene.2018.08.032.
- Mizoguchi H**, Sawano Y, Kato J, Mori H. Superpositioning of deletions promotes growth of *Escherichia coli* with a reduced genome. DNA Res. 2008 Oct;15(5):277-84. doi:

- 10.1093/dnares/dsn019. Epub 2008 Aug 27. PMID: 18753290; PMCID: PMC2575892.
- Mohiuddin** SG, Hoang T, Saba A, Karki P, Orman MA. Identifying Metabolic Inhibitors to Reduce Bacterial Persistence. *Front Microbiol.* 2020 Mar 27;11:472. doi: 10.3389/fmicb.2020.00472. PMID: 32292393; PMCID: PMC7118205.
- Mok** WWK, Brynildsen MP. Timing of DNA damage responses impacts persistence to fluoroquinolones. *Proc Natl Acad Sci U S A.* 2018 Jul 3;115(27):E6301-E6309. doi: 10.1073/pnas.1804218115. Epub 2018 Jun 18. PMID: 29915065; PMCID: PMC6142227.
- Moreau** PL. The lysine decarboxylase CadA protects *Escherichia coli* starved of phosphate against fermentation acids. *J Bacteriol.* 2007 Mar;189(6):2249-61. doi: 10.1128/JB.01306-06. Epub 2007 Jan 5. PMID: 17209032; PMCID: PMC1899392.
- Morelli** A, Cabezas Y, Mills LJ, Seelig B. Extensive libraries of gene truncation variants generated by in vitro transposition. *Nucleic Acids Res.* 2017 Jun 2;45(10):e78. doi: 10.1093/nar/gkx030. PMID: 28130425; PMCID: PMC5449547.
- Morita** T, El-Kazzaz W, Tanaka Y, Inada T, Aiba H. Accumulation of glucose 6-phosphate or fructose 6-phosphate is responsible for destabilization of glucose transporter mRNA in *Escherichia coli*. *J Biol Chem.* 2003 May 2;278(18):15608-14. doi: 10.1074/jbc.M300177200. Epub 2003 Feb 10. PMID: 12578824.
- Motohashi** K. Evaluation of the efficiency and utility of recombinant enzyme-free seamless DNA cloning methods. *Biochem Biophys Rep.* 2017 Jan 26;9:310-315. doi: 10.1016/j.bbrep.2017.01.010. PMID: 28956018; PMCID: PMC5614619.
- Murakami** H, Hohsaka T, Sisido M. Random insertion and deletion of arbitrary number of bases for codon-based random mutation of DNAs. *Nat Biotechnol.* 2002 Jan;20(1):76-81. doi: 10.1038/nbt0102-76. PMID: 11753366.

- Murima** P, McKinney JD, Pethe K. Targeting bacterial central metabolism for drug development. *Chem Biol.* 2014 Nov 20;21(11):1423-32. doi: 10.1016/j.chembiol.2014.08.020. Epub 2014 Oct 16. PMID: 25442374.
- Mustapha** NA, Hu A, Yu CP, Sharuddin SS, Ramli N, Shirai Y, Maeda T. Seeking key microorganisms for enhancing methane production in anaerobic digestion of waste sewage sludge. *Appl Microbiol Biotechnol.* 2018 Jun;102(12):5323-5334. doi: 10.1007/s00253-018-9003-8. Epub 2018 Apr 25. PMID: 29696331.
- Nakamura** Y, Fukami K. Regulation and physiological functions of mammalian phospholipase C. *J Biochem.* 2017 Apr 1;161(4):315-321. doi: 10.1093/jb/mvw094. PMID: 28130414.
- Nath** K, Kumar A, Das D. Effect of some environmental parameters on fermentative hydrogen production by *Enterobacter cloacae* DM11. *Can J Microbiol.* 2006 Jun;52(6):525-32. doi: 10.1139/w06-005. PMID: 16788720.
- Nichols** R, Andrews PC, Zhang P, Bergstrom DE. A universal nucleoside for use at ambiguous sites in DNA primers. *Nature.* 1994 Jun 9;369(6480):492-3. doi: 10.1038/369492a0. PMID: 8202140.
- Nie** W, Tang H, Fang Z, Chen J, Chen H, Xiu Q. Hydrogenase: the next antibiotic target? *Clin Sci (Lond).* 2012 Jun;122(12):575-80. doi: 10.1042/CS20110396. PMID: 22390199.
- Noguchi** K, Riggins DP, Eldahan KC, Kitko RD, Slonczewski JL. Hydrogenase-3 contributes to anaerobic acid resistance of *Escherichia coli*. *PLoS One.* 2010 Apr 12;5(4):e10132. doi: 10.1371/journal.pone.0010132. PMID: 20405029; PMCID: PMC2853565.
- O'Donnell** JL, Kelly RP, Lowell NC, Port JA. Indexed PCR Primers Induce Template-Specific Bias in Large-Scale DNA Sequencing Studies. *PLoS One.* 2016 Mar 7;11(3):e0148698. doi: 10.1371/journal.pone.0148698. PMID: 26950069; PMCID: PMC4780811.
- Ohsawa** I, Ishikawa M, Takahashi K, Watanabe M, Nishimaki K, Yamagata K, Katsura K, Katayama Y, Asoh S, Ohta S. Hydrogen acts as a therapeutic antioxidant by selectively

- reducing cytotoxic oxygen radicals. *Nat Med*. 2007 Jun;13(6):688-94. doi: 10.1038/nm1577. Epub 2007 May 7. PMID: 17486089.
- Olsen** KN, Budde BB, Siegumfeldt H, Rechinger KB, Jakobsen M, Ingmer H. Noninvasive measurement of bacterial intracellular pH on a single-cell level with green fluorescent protein and fluorescence ratio imaging microscopy. *Appl Environ Microbiol*. 2002 Aug;68(8):4145-7. doi: 10.1128/AEM.68.8.4145-4147.2002. PMID: 12147523; PMCID: PMC123996.
- Olson** JW, Maier RJ. Molecular hydrogen as an energy source for *Helicobacter pylori*. *Science*. 2002 Nov 29;298(5599):1788-90. doi: 10.1126/science.1077123. PMID: 12459589.
- Orman** MA, Brynildsen MP. Inhibition of stationary phase respiration impairs persister formation in *E. coli*. *Nat Commun*. 2015 Aug 6;6:7983. doi: 10.1038/ncomms8983. Erratum in: *Nat Commun*. 2016;7:10756. PMID: 26246187; PMCID: PMC4530465.
- Osterman** AL, Gerdes SY. *Microbial Gene Essentiality: Protocols and Bioinformatics*. Humana Press. 2008.
- Pandey** A, Chang, JS, Hallenbeck P, Larroche C (2013) *Biohydrogen*. Elsevier, Oxford.
- Partridge** JD, Sanguinetti G, Dibden DP, Roberts RE, Poole RK, Green J. Transition of *Escherichia coli* from aerobic to micro-aerobic conditions involves fast and slow reacting regulatory components. *J Biol Chem*. 2007 Apr 13;282(15):11230-7. doi: 10.1074/jbc.M700728200. Epub 2007 Feb 16. PMID: 17307737.
- Payot** S, Guedon E, Cailliez C, Gelhaye E, Petitdemange H. Metabolism of cellobiose by *Clostridium cellulolyticum* growing in continuous culture: evidence for decreased NADH reoxidation as a factor limiting growth. *Microbiology (Reading)*. 1998 Feb;144(2):375-384. doi: 10.1099/00221287-144-2-375. PMID: 33757226.

- Pecher** A, Zinoni F, Jatisatienr C, Wirth R, Hennecke H, Böck A. On the redox control of synthesis of anaerobically induced enzymes in enterobacteriaceae. Arch Microbiol. 1983 Nov;136(2):131-6. doi: 10.1007/BF00404787. PMID: 6360066.
- Pedraz** L, Blanco-Cabra N, Torrents E. Gradual adaptation of facultative anaerobic pathogens to microaerobic and anaerobic conditions. FASEB J. 2020 Feb;34(2):2912-2928. doi: 10.1096/fj.201902861R. Epub 2019 Dec 27. PMID: 31908067.
- Penfold** DW, Forster CF, Macaskie LE. Increased hydrogen production by *Escherichia coli* strain HD701 in comparison with the wild-type parent strain MC4100. Enzyme Microb Technol. 2003; 33:185-189. doi: 10.1016/S0141-0229(03)00115-7.
- Petrounia** IP, Arnold FH. Designed evolution of enzymatic properties. Curr Opin Biotechnol. 2000 Aug;11(4):325-30. doi: 10.1016/s0958-1669(00)00107-5. PMID: 10975451.
- Pezo** V, Schepers G, Lambertucci C, Marlière P, Herdewijn P. Probing ambiguous base-pairs by genetic transformation with XNA templates. Chembiochem. 2014 Oct 13;15(15):2255-8. doi: 10.1002/cbic.201402226. Epub 2014 Aug 26. PMID: 25158283.
- Pfaffl** MW. A new mathematical model for relative quantification in real-time RT-PCR. Nucleic Acids Res. 2001 May 1;29(9):e45. doi: 10.1093/nar/29.9.e45. PMID: 11328886; PMCID: PMC55695.
- Pinske** C, Jaroschinsky M, Linek S, Kelly CL, Sargent F, Sawers RG. Physiology and bioenergetics of [NiFe]-hydrogenase 2-catalyzed H<sub>2</sub>-consuming and H<sub>2</sub>-producing reactions in *Escherichia coli*. J Bacteriol. 2015 Jan;197(2):296-306. doi: 10.1128/JB.02335-14. Epub 2014 Nov 3. PMID: 25368299; PMCID: PMC4272588.
- Pinske** C, Sawers RG. Anaerobic Formate and Hydrogen Metabolism. EcoSal Plus. 2016 Oct;7(1). doi: 10.1128/ecosalplus.ESP-0011-2016. PMID: 27735784.
- Plumbridge** J. Regulation of gene expression in the PTS in *Escherichia coli*: the role and interactions of Mlc. Curr Opin Microbiol. 2002 Apr;5(2):187-93. doi: 10.1016/s1369-

5274(02)00296-5. PMID: 11934616.

**Pósfai** G, Koob M, Hradecná Z, Hasan N, Filutowicz M, Szybalski W. In vivo excision and amplification of large segments of the *Escherichia coli* genome. Nucleic Acids Res. 1994 Jun 25;22(12):2392-8. doi: 10.1093/nar/22.12.2392. PMID: 8036169; PMCID: PMC523700.

**Postma** PW, Broekhuizen CP, Geerse RH. The role of the PEP: carbohydrate phosphotransferase system in the regulation of bacterial metabolism. FEMS Microbiol Rev. 1989 Jun;5(1-2):69-80. doi: 10.1016/0168-6445(89)90010-7. PMID: 2699253.

**Pu** Y, Li Y, Jin X, Tian T, Ma Q, Zhao Z, Lin SY, Chen Z, Li B, Yao G, Leake MC, Lo CJ, Bai F. ATP-Dependent Dynamic Protein Aggregation Regulates Bacterial Dormancy Depth Critical for Antibiotic Tolerance. Mol Cell. 2019 Jan 3;73(1):143-156.e4. doi: 10.1016/j.molcel.2018.10.022. Epub 2018 Nov 21. PMID: 30472191.

**Rasmussen** LJ, Møller PL, Atlung T. Carbon metabolism regulates expression of the pfl (pyruvate formate-lyase) gene in *Escherichia coli*. J Bacteriol. 1991 Oct;173(20):6390-7. doi: 10.1128/jb.173.20.6390-6397.1991. PMID: 1917868; PMCID: PMC208971.

**Redwood** MD, Mikheenko IP, Sargent F, Macaskie LE. Dissecting the roles of *Escherichia coli* hydrogenases in biohydrogen production. FEMS Microbiol Lett. 2008 Jan;278(1):48-55. doi: 10.1111/j.1574-6968.2007.00966.x. Epub 2007 Nov 6. PMID: 17995952.

**Reyes-Fernández** EZ, Schuldiner S. Acidification of Cytoplasm in *Escherichia coli* Provides a Strategy to Cope with Stress and Facilitates Development of Antibiotic Resistance. Sci Rep. 2020 Jun 19;10(1):9954. doi: 10.1038/s41598-020-66890-1. PMID: 32561799; PMCID: PMC7305162.

**Richard** DJ, Sawers G, Sargent F, McWalter L, Boxer DH. Transcriptional regulation in response to oxygen and nitrate of the operons encoding the [NiFe] hydrogenases 1 and 2 of *Escherichia coli*. Microbiology (Reading). 1999 Oct;145 ( Pt 10):2903-12. doi:

10.1099/00221287-145-10-2903. PMID: 10537212.

**Riggins DP**, Narvaez MJ, Martinez KA, Harden MM, Slonczewski JL. *Escherichia coli* K-12 survives anaerobic exposure at pH 2 without RpoS, Gad, or hydrogenases, but shows sensitivity to autoclaved broth products. PLoS One. 2013;8(3):e56796. doi: 10.1371/journal.pone.0056796. Epub 2013 Mar 8. PMID: 23520457; PMCID: PMC3592846.

**Robinson MD**, McCarthy DJ, Smyth GK. edgeR: a Bioconductor package for differential expression analysis of digital gene expression data. Bioinformatics. 2010 Jan 1;26(1):139-40. doi: 10.1093/bioinformatics/btp616. Epub 2009 Nov 11. PMID: 19910308; PMCID: PMC2796818.

**Romilly C**, Lays C, Tomasini A, Caldelari I, Benito Y, Hammann P, Geissmann T, Boisset S, Romby P, Vandenesch F. A non-coding RNA promotes bacterial persistence and decreases virulence by regulating a regulator in *Staphylococcus aureus*. PLoS Pathog. 2014 Mar 20;10(3):e1003979. doi: 10.1371/journal.ppat.1003979. PMID: 24651379; PMCID: PMC3961350.

**Rossolini GM**, Cresti S, Ingianni A, Cattani P, Riccio ML, Satta G. Use of deoxyinosine-containing primers vs degenerate primers for polymerase chain reaction based on ambiguous sequence information. Mol Cell Probes. 1994 Apr;8(2):91-8. doi: 10.1006/mcpr.1994.1013. PMID: 7935517.

**Russell JB**, Diez-Gonzalez F. The effects of fermentation acids on bacterial growth. Adv Microb Physiol. 1998;39:205-34. doi: 10.1016/s0065-2911(08)60017-x. PMID: 9328648.

**Ryan FJ**, Schneider LK. The consequences of mutation during the growth of biochemical mutants of *Escherichia coli* IV. : The Mechanism of inhibition of Histidine-independent Bacteria by Histidineless Bacteria. J Bacteriol. 1949 Aug;58(2):201-13. PMID: 16561773; PMCID: PMC385611.

- Sambrook J**, Fritsch EF, Maniatis T. Molecular Cloning: A Laboratory Manual. 2nd ed. 1989. Cold Spring Harbor, NY: Cold Spring Harbor Laboratory Press.
- Sanchez-Torres V**, Maeda T, Wood TK. Protein engineering of the transcriptional activator FhlA To enhance hydrogen production in *Escherichia coli*. Appl Environ Microbiol. 2009 Sep;75(17):5639-46. doi: 10.1128/AEM.00638-09. Epub 2009 Jul 6. PMID: 19581479; PMCID: PMC2737898.
- Sanchez-Torres V**, Mohd Yusoff MZ, Nakano C, Maeda T, Ogawa HI, Wood TK. Influence of *Escherichia coli* hydrogenases on hydrogen fermentation from glycerol. Int J Hydrogen Energy 2013;38:3905-12. doi: 10.1016/j.ijhydene.2013.01.031.
- Sapra R**, Bagramyan K, Adams MW. A simple energy-conserving system: proton reduction coupled to proton translocation. Proc Natl Acad Sci U S A. 2003 Jun 24;100(13):7545-50. doi: 10.1073/pnas.1331436100. Epub 2003 Jun 5. PMID: 12792025; PMCID: PMC164623.
- Saragliadis A**, Trunk T, Leo JC. Producing Gene Deletions in *Escherichia coli* by P1 Transduction with Excisable Antibiotic Resistance Cassettes. J Vis Exp. 2018 Sep 1;(139):58267. doi: 10.3791/58267. PMID: 30222159; PMCID: PMC6235078.
- Sargent F**. The Model [NiFe]-Hydrogenases of *Escherichia coli*. Adv Microb Physiol. 2016;68:433-507. doi: 10.1016/bs.ampbs.2016.02.008. Epub 2016 Mar 23. PMID: 27134027.
- Sass P**, Brötz-Oesterhelt H. Bacterial cell division as a target for new antibiotics. Curr Opin Microbiol. 2013 Oct;16(5):522-30. doi: 10.1016/j.mib.2013.07.006. Epub 2013 Aug 8. PMID: 23932516.
- Sauter M**, Böhm R, Böck A. Mutational analysis of the operon (hyc) determining hydrogenase 3 formation in *Escherichia coli*. Mol Microbiol. 1992 Jun;6(11):1523-32. doi: 10.1111/j.1365-2958.1992.tb00873.x. PMID: 1625581.

- Sawers G.** The hydrogenases and formate dehydrogenases of *Escherichia coli*. *Antonie Van Leeuwenhoek*. 1994;66(1-3):57-88. doi: 10.1007/BF00871633. PMID: 7747941.
- Sawers RG, Ballantine SP, Boxer DH.** Differential expression of hydrogenase isoenzymes in *Escherichia coli* K-12: evidence for a third isoenzyme. *J Bacteriol*. 1985 Dec;164(3):1324-31. doi: 10.1128/jb.164.3.1324-1331.1985. PMID: 3905769; PMCID: PMC219333.
- Sawers RG, Boxer DH.** Purification and properties of membrane-bound hydrogenase isoenzyme 1 from anaerobically grown *Escherichia coli* K12. *Eur J Biochem*. 1986 Apr 15;156(2):265-75. doi: 10.1111/j.1432-1033.1986.tb09577.x. PMID: 3516689.
- Sawers RG, Jamieson DJ, Higgins CF, Boxer DH.** Characterization and physiological roles of membrane-bound hydrogenase isoenzymes from *Salmonella typhimurium*. *J Bacteriol*. 1986 Oct;168(1):398-404. doi: 10.1128/jb.168.1.398-404.1986. PMID: 3531177; PMCID: PMC213464.
- Scheuplein NJ, Bzdyl NM, Kibble EA, Lohr T, Holzgrabe U, Sarkar-Tyson M.** Targeting Protein Folding: A Novel Approach for the Treatment of Pathogenic Bacteria. *J Med Chem*. 2020 Nov 25;63(22):13355-13388. doi: 10.1021/acs.jmedchem.0c00911. Epub 2020 Aug 28. PMID: 32786507.
- Schlensog V, Böck A.** Identification and sequence analysis of the gene encoding the transcriptional activator of the formate hydrogenlyase system of *Escherichia coli*. *Mol Microbiol*. 1990 Aug;4(8):1319-27. doi: 10.1111/j.1365-2958.1990.tb00711.x. PMID: 2280686.
- Self WT, Hasona A, Shanmugam KT.** Expression and regulation of a silent operon, *hyf*, coding for hydrogenase 4 isoenzyme in *Escherichia coli*. *J Bacteriol*. 2004 Jan;186(2):580-7. doi: 10.1128/JB.186.2.580-587.2004. PMID: 14702328; PMCID: PMC305750.
- Shan Y, Brown Gandt A, Rowe SE, Deisinger JP, Conlon BP, Lewis K.** ATP-Dependent Persister Formation in *Escherichia coli*. *mBio*. 2017 Feb 7;8(1):e02267-16. doi:

10.1128/mBio.02267-16. PMID: 28174313; PMCID: PMC5296605.

**Shan Y**, Lai Y, Yan A. Metabolic reprogramming under microaerobic and anaerobic conditions in bacteria. *Subcell Biochem.* 2012;64:159-79. doi: 10.1007/978-94-007-5055-5\_8. PMID: 23080250.

**Shekhar C**, Kai T, Garcia-Contreras R, Sanchez-Torres V, Maeda T. Evaluation of Hydrogen Metabolism by *Escherichia coli* Strains Possessing Only the Single Hydrogenase in the Genome. *Int J Hydrog Energy.* 2021;46:1728-39. doi:10.1016/j.ijhydene.2020.10.070.

**Shekhar C**, Maeda T. A simple approach for random genomic insertion-deletions using ambiguous sequences in *Escherichia coli*. *J Basic Microbiol.* 2022 Aug;62(8):948-962. doi: 10.1002/jobm.202100636. Epub 2022 Jun 23. PMID: 35739617.

**Shimada T**, Fujita N, Yamamoto K, Ishihama A. Novel roles of cAMP receptor protein (CRP) in regulation of transport and metabolism of carbon sources. *PLoS One.* 2011;6(6):e20081. doi: 10.1371/journal.pone.0020081. Epub 2011 Jun 1. PMID: 21673794; PMCID: PMC3105977.

**Siddiquee KA**, Arauzo-Bravo MJ, Shimizu K. Effect of a pyruvate kinase (*pykF*-gene) knockout mutation on the control of gene expression and metabolic fluxes in *Escherichia coli*. *FEMS Microbiol Lett.* 2004 Jun 1;235(1):25-33. doi: 10.1016/j.femsle.2004.04.004. PMID: 15158258.

**Silhavy TJ**, Berman ML, Enquist LW. Experiments with gene fusions. 1st ed. Cold Spring Harbor Laboratories, NY: Cold Spring Harbor Laboratory Press; 1984.

**Singh A**, Lynch MD, Gill RT. Genes restoring redox balance in fermentation-deficient *E. coli* NZN111. *Metab Eng.* 2009 Nov;11(6):347-54. doi: 10.1016/j.ymben.2009.07.002. Epub 2009 Jul 21. PMID: 19628049.

**Singhal R**, Shah YM. Oxygen battle in the gut: Hypoxia and hypoxia-inducible factors in metabolic and inflammatory responses in the intestine. *J Biol Chem.* 2020 Jul

24;295(30):10493-10505. doi: 10.1074/jbc.REV120.011188. Epub 2020 Jun 5. PMID: 32503843; PMCID: PMC7383395.

**Skibinski** DA, Golby P, Chang YS, Sargent F, Hoffman R, Harper R, Guest JR, Attwood MM, Berks BC, Andrews SC. Regulation of the hydrogenase-4 operon of *Escherichia coli* by the sigma(54)-dependent transcriptional activators FhlA and HyfR. J Bacteriol. 2002 Dec;184(23):6642-53. doi: 10.1128/JB.184.23.6642-6653.2002. PMID: 12426353; PMCID: PMC135417.

**Slonczewski** JL, Rosen BP, Alger JR, Macnab RM. pH homeostasis in *Escherichia coli*: measurement by <sup>31</sup>P nuclear magnetic resonance of methylphosphonate and phosphate. Proc Natl Acad Sci U S A. 1981 Oct;78(10):6271-5. doi: 10.1073/pnas.78.10.6271. PMID: 7031646; PMCID: PMC349020.

**Snijders** PJ, Meijer CJ, Walboomers JM. Degenerate primers based on highly conserved regions of amino acid sequence in papillomaviruses can be used in a generalized polymerase chain reaction to detect productive human papillomavirus infection. J Gen Virol. 1991 Nov;72 (Pt 11):2781-6. doi: 10.1099/0022-1317-72-11-2781. PMID: 1658205.

**Spector** MP, Kenyon WJ. Resistance and survival strategies of *Salmonella enterica* to environmental stresses. Food Res Int 2012; 45:455–481. doi: 10.1016/j.foodres.2011.06.056.

**Srikanth** S, Venkata Mohan S, Lalit Babu V, Sarma PN. Metabolic shift and electron discharge pattern of anaerobic consortia as a function of pretreatment method applied during fermentative hydrogen Production. Int J Hydrog Energy 2010; 35:10693–10700. doi: 10.1016/j.ijhydene.2010.02.055.

**Stemmer** WP. Rapid evolution of a protein in vitro by DNA shuffling. Nature. 1994 Aug 4;370(6488):389-91. doi: 10.1038/370389a0. PMID: 8047147.

- Stiebritz** MT, Reiher M. Hydrogenases and oxygen. *Chem Sci* 2012; 3:1739-1751. doi:10.1039/C2SC01112C.
- Stolper** DA, Revsbech NP, Canfield DE. Aerobic growth at nanomolar oxygen concentrations. *Proc Natl Acad Sci U S A*. 2010 Nov 2;107(44):18755-60. doi: 10.1073/pnas.1013435107. Epub 2010 Oct 25. PMID: 20974919; PMCID: PMC2973883.
- St-Pierre** F, Cui L, Priest DG, Endy D, Dodd IB, Shearwin KE. One-step cloning and chromosomal integration of DNA. *ACS Synth Biol*. 2013 Sep 20;2(9):537-41. doi: 10.1021/sb400021j. Epub 2013 May 20. PMID: 24050148.
- Sun** Y, Fukamachi T, Saito H, Kobayashi H. ATP requirement for acidic resistance in *Escherichia coli*. *J Bacteriol*. 2011 Jun;193(12):3072-7. doi: 10.1128/JB.00091-11. Epub 2011 Apr 8. PMID: 21478347; PMCID: PMC3133219.
- Suzuki** N, Inui M, Yukawa H. Random genome deletion methods applicable to prokaryotes. *Appl Microbiol Biotechnol*. 2008 Jun;79(4):519-26. doi: 10.1007/s00253-008-1512-4. Epub 2008 May 20. PMID: 18491037.
- Suzuki** N, Okai N, Nonaka H, Tsuge Y, Inui M, Yukawa H. High-throughput transposon mutagenesis of *Corynebacterium glutamicum* and construction of a single-gene disruptant mutant library. *Appl Environ Microbiol*. 2006 May;72(5):3750-5. doi: 10.1128/AEM.72.5.3750-3755.2006. PMID: 16672528; PMCID: PMC1472376.
- Szenk** M, Dill KA, de Graff AMR. Why Do Fast-Growing Bacteria Enter Overflow Metabolism? Testing the Membrane Real Estate Hypothesis. *Cell Syst*. 2017 Aug 23;5(2):95-104. doi: 10.1016/j.cels.2017.06.005. Epub 2017 Jul 26. PMID: 28755958.
- Tran** KT, Maeda T, Wood TK. Metabolic engineering of *Escherichia coli* to enhance hydrogen production from glycerol. *Appl Microbiol Biotechnol*. 2014 May;98(10):4757-70. doi: 10.1007/s00253-014-5600-3. Epub 2014 Mar 11. PMID: 24615384.
- Trchounian** K, Blbulyan S, Trchounian A. Hydrogenase activity and proton-motive force

- generation by *Escherichia coli* during glycerol fermentation. J Bioenerg Biomembr. 2013 Jun;45(3):253-60. doi: 10.1007/s10863-012-9498-0. Epub 2012 Dec 28. PMID: 23271421.
- Trchounian K**, Pinske C, Sawers RG, Trchounian A. Dependence on the F0F1-ATP synthase for the activities of the hydrogen-oxidizing hydrogenases 1 and 2 during glucose and glycerol fermentation at high and low pH in *Escherichia coli*. J Bioenerg Biomembr. 2011 Dec;43(6):645-50. doi: 10.1007/s10863-011-9397-9. Epub 2011 Nov 12. PMID: 22081210.
- Trchounian K**, Poladyan A, Vassilian A, Trchounian A. Multiple and reversible hydrogenases for hydrogen production by *Escherichia coli*: dependence on fermentation substrate, pH and the F(0)F(1)-ATPase. Crit Rev Biochem Mol Biol. 2012 May-Jun;47(3):236-49. doi: 10.3109/10409238.2012.655375. Epub 2012 Feb 7. PMID: 22313414.
- Trchounian K**, Sanchez-Torres V, Wood TK, Trchounian A. *Escherichia coli* hydrogenase activity and H<sub>2</sub> production under glycerol fermentation at a low pH. Int J Hydrog Energy 2011;36:4323-31. doi: 10.1016/j.ijhydene.2010.12.128.
- Trchounian K**, Sargsyan H, Trchounian A. Hydrogen production by *Escherichia coli* depends on glucose concentration and its combination with glycerol at different pHs. Int J Hydrog Energy 2014; 39:6419-6423. doi: 10.1016/j.ijhydene.2014.02.050.
- Trchounian K**, Soboh B, Sawers RG, Trchounian A. Contribution of hydrogenase 2 to stationary phase H<sub>2</sub> production by *Escherichia coli* during fermentation of glycerol. Cell Biochem Biophys. 2013 May;66(1):103-8. doi: 10.1007/s12013-012-9458-7. PMID: 23090790.
- Trchounian K**, Trchounian A. Hydrogen producing activity by *Escherichia coli* hydrogenase 4 (hyf) depends on glucose concentration. Int J Hydrog Energy 2014;39:16914-18. doi: 10.1016/j.ijhydene.2014.08.059.
- Trchounian K**, Trchounian A. Hydrogenase 2 is most and hydrogenase 1 is less responsible for H<sub>2</sub> production by *Escherichia coli* under glycerol fermentation at neutral and slightly

- alkaline pH. Int J Hydrog Energy 2009;34:8839-8845. doi: 10.1016/j.ijhydene.2009.08.056.
- Tsakalidou** E, Papadimitriou K. Stress Responses of Lactic Acid Bacteria. Food Microbiology and Food Safety. 2011. Springer, Boston, MA.
- Tsuge** Y, Suzuki N, Inui M, Yukawa H. Random segment deletion based on IS31831 and Cre/loxP excision system in *Corynebacterium glutamicum*. Appl Microbiol Biotechnol. 2007 Apr;74(6):1333-41. doi: 10.1007/s00253-006-0788-5. Epub 2007 Jan 13. PMID: 17221197.
- Tuschherr** L, Löffler B, Proctor RA. Persistence of *Staphylococcus aureus*: Multiple Metabolic Pathways Impact the Expression of Virulence Factors in Small-Colony Variants (SCVs). Front Microbiol. 2020 May 21;11:1028. doi: 10.3389/fmicb.2020.01028. PMID: 32508801; PMCID: PMC7253646.
- Tucker** DL, Tucker N, Conway T. Gene expression profiling of the pH response in *Escherichia coli*. J Bacteriol. 2002 Dec;184(23):6551-8. doi: 10.1128/JB.184.23.6551-6558.2002. PMID: 12426343; PMCID: PMC135413.
- Ublinskaya** AA, Samsonov VV, Mashko SV, Stoyanova NV. A PCR-free cloning method for the targeted  $\phi 80$  Int-mediated integration of any long DNA fragment, bracketed with meganuclease recognition sites, into the *Escherichia coli* chromosome. J Microbiol Methods. 2012 Jun;89(3):167-73. doi: 10.1016/j.mimet.2012.03.013. Epub 2012 Mar 29. PMID: 22484061.
- Unden** G, Bongaerts J. Alternative respiratory pathways of *Escherichia coli*: energetics and transcriptional regulation in response to electron acceptors. Biochim Biophys Acta. 1997 Jul 4;1320(3):217-34. doi: 10.1016/s0005-2728(97)00034-0. PMID: 9230919.
- Unger** RC, Echols H, Clark AJ. Interaction of the recombination pathways of bacteriophage lambda and host *Escherichia coli*: effects on lambda recombination. J Mol Biol. 1972;70:531-7.

- Vanyan L**, Trchounian K. HyfF subunit of hydrogenase 4 is crucial for regulating FOF1 dependent proton/potassium fluxes during fermentation of various concentrations of glucose. *J Bioenerg Biomembr.* 2022 Apr;54(2):69-79. doi: 10.1007/s10863-022-09930-x. Epub 2022 Feb 2. PMID: 35106641.
- Vardar-Schara G**, Maeda T, Wood TK. Metabolically engineered bacteria for producing hydrogen via fermentation. *Microb Biotechnol.* 2008 Mar;1(2):107-25. doi: 10.1111/j.1751-7915.2007.00009.x. PMID: 21261829; PMCID: PMC3864445.
- Wang S**, Meyer E, McKay JK, Matz MV. 2b-RAD: a simple and flexible method for genome-wide genotyping. *Nat Methods.* 2012 May 20;9(8):808-10. doi: 10.1038/nmeth.2023. PMID: 22609625.
- Wang T**, El Meouche I, Dunlop MJ. Bacterial persistence induced by salicylate via reactive oxygen species. *Sci Rep.* 2017 Mar 10;7:43839. doi: 10.1038/srep43839. PMID: 28281556; PMCID: PMC5345018.
- Wang Y**, Bojer MS, George SE, Wang Z, Jensen PR, Wolz C, Ingmer H. Inactivation of TCA cycle enhances *Staphylococcus aureus* persister cell formation in stationary phase. *Sci Rep.* 2018 Jul 18;8(1):10849. doi: 10.1038/s41598-018-29123-0. PMID: 30022089; PMCID: PMC6052003.
- Wilmaerts D**, Windels EM, Verstraeten N, Michiels J. General Mechanisms Leading to Persister Formation and Awakening. *Trends Genet.* 2019 Jun;35(6):401-411. doi: 10.1016/j.tig.2019.03.007. Epub 2019 Apr 27. PMID: 31036343.
- Windle BE**, Hays JB. A phage P1 function that stimulates homologous recombination of the *Escherichia coli* chromosome. *Proc Natl Acad Sci U S A.* 1986 Jun;83(11):3885-9. doi: 10.1073/pnas.83.11.3885. PMID: 3012538; PMCID: PMC323629.
- Wood TK**, Knabel SJ, Kwan BW. Bacterial persister cell formation and dormancy. *Appl Environ Microbiol.* 2013 Dec;79(23):7116-21. doi: 10.1128/AEM.02636-13. Epub 2013

Sep 13. PMID: 24038684; PMCID: PMC3837759.

**Wood TK**, Song S, Yamasaki R. Ribosome dependence of persister cell formation and resuscitation. *J Microbiol.* 2019 Mar;57(3):213-219. doi: 10.1007/s12275-019-8629-2. Epub 2019 Feb 26. PMID: 30806978.

**Wood TK**. Combatting bacterial persister cells. *Biotechnol Bioeng.* 2016 Mar;113(3):476-83. doi: 10.1002/bit.25721. Epub 2015 Sep 3. PMID: 26264116.

**Wright ES**. Using DECIPHER v2.0 to Analyze Big Biological Sequence Data in R PDF download. *The R Journal.* 2016;8:352-59.

**Wu J**, Li Y, Cai Z, Jin Y. Pyruvate-associated acid resistance in bacteria. *Appl Environ Microbiol.* 2014 Jul;80(14):4108-13. doi: 10.1128/AEM.01001-14. Epub 2014 May 2. PMID: 24795365; PMCID: PMC4068671.

**Xu T**, Wang X, Meng L, Zhu M, Wu J, Xu Y, Zhang Y, Zhang W. Magnesium Links Starvation-Mediated Antibiotic Persistence to ATP. *mSphere.* 2020 Jan 8;5(1):e00862-19. doi: 10.1128/mSphere.00862-19. PMID: 31915231; PMCID: PMC6952205.

**Yoshida A**, Nishimura T, Kawaguchi H, Inui M, Yukawa H. Enhanced hydrogen production from glucose using ldh- and frd-inactivated *Escherichia coli* strains. *Appl Microbiol Biotechnol.* 2006 Nov;73(1):67-72. doi: 10.1007/s00253-006-0456-9. Epub 2006 May 9. PMID: 16683133.

**Young MD**, Wakefield MJ, Smyth GK, Oshlack A. Gene ontology analysis for RNA-seq: accounting for selection bias. *Genome Biol.* 2010;11(2):R14. doi: 10.1186/gb-2010-11-2-r14. Epub 2010 Feb 4. PMID: 20132535; PMCID: PMC2872874.

**Yu D**, Ellis HM, Lee EC, Jenkins NA, Copeland NG, Court DL. An efficient recombination system for chromosome engineering in *Escherichia coli*. *Proc Natl Acad Sci U S A.* 2000 May 23;97(11):5978-83. doi: 10.1073/pnas.100127597. PMID: 10811905; PMCID: PMC18544.

- Yusoff** MZ, Maeda T, Sanchez-Torres V, Ogawa HI, Shirai Y, Hassan MA, et al. Uncharacterized *Escherichia coli* proteins YdjA and YhjY are related to biohydrogen production. *Int J Hydrog Energy*. 2012;37:17778-87.
- Zbell** AL, Maier SE, Maier RJ. Salmonella enterica serovar Typhimurium NiFe uptake-type hydrogenases are differentially expressed in vivo. *Infect Immun*. 2008 Oct;76(10):4445-54. doi: 10.1128/IAI.00741-08. Epub 2008 Jul 14. PMID: 18625729; PMCID: PMC2546827.
- Zeinert** RD, Liu J, Yang Q, Du Y, Haynes CM, Chien P. A legacy role for DNA binding of Lon protects against genotoxic stress. *bioRxiv*, 2018;317677. doi: 10.1101/317677.
- Zhang** X, Jantama K, Shanmugam KT, Ingram LO. Reengineering *Escherichia coli* for Succinate Production in Mineral Salts Medium. *Appl Environ Microbiol*. 2009 Dec;75(24):7807-13. doi: 10.1128/AEM.01758-09. Epub 2009 Oct 16. PMID: 19837840; PMCID: PMC2794101.
- Zhao** C, Zhang Y, Li Y. Production of fuels and chemicals from renewable resources using engineered *Escherichia coli*. *Biotechnol Adv*. 2019; 37 (7): 107402. doi: 10.1016/j.biotechadv.2019.06.001.

## PUBLICATION AND CONFERENCE ATTENDED

### Publication

1. **Chandra Shekhar**, Tomonori Kai, Rodolfo Garcia-Contreras, Viviana Sanchez-Torres, Toshinari Maeda. Evaluation of hydrogen metabolism by *Escherichia coli* strains possessing only a single hydrogenase in the genome. *Int. J. Hydrog. Energy*. 2021;46(2):1728-39. (PUBLISHED)
2. **Chandra Shekhar** and Toshinari Maeda. A simple approach for random genomic insertion deletions using ambiguous sequence-based primers in *Escherichia coli*. *J. Basic Microbiol.* 2022;1-15. (PUBLISHED)
3. **Chandra Shekhar** and Toshinari Maeda. Impaired glucose metabolism by deleting the operon of hydrogenase 2 in *Escherichia coli*. *Arch. Microbiol.* 2022;204:627. (PUBLISHED)
4. **Chandra Shekhar**, Tomonori Kai, Thomas K. Wood, Toshinari Maeda. Hydrogenase 2 is significant for cellular viability and acid resistance of *Escherichia coli* under oxygen-deprived cultural conditions. (Under review, *Antonie van Leeuwenhoek*).
5. **Chandra Shekhar**, Tomonori Kai, Thomas K. Wood, Toshinari Maeda. Evaluation of *Escherichia coli* hydrogenases in persistence. (Under review, preprint: DOI: 10.21203/rs.3.rs-1402538/v1).

### Seminar and symposium presented

1. International Symposium on Applied Engineering and Sciences, Dec. 2018, Japan (Poster)
2. **Shekhar C**, Imabayashi A, Maeda T. Operon Mutant Library of *Escherichia coli* Hydrogenases to Understand the True Function of Hydrogen Metabolism. Japan Society for Bioscience, Biotechnology, and Agrochemistry West 1st Student Forum, Nov. 2018, Japan (Oral)
3. Japan-Korea Joint Symposium on Bio-microsensing Technology, Japan (participant)



## **ACKNOWLEDGEMENT**

First, I would like to express my deepest gratitude to my supervisor, Dr. Toshinari Maeda, for his vital supervision all the time. I was entirely inspired by his working attitude and strong determination. Those qualities will bring many benefits for me on the way to becoming an independent researcher. I also would like to take this opportunity to thank Prof. Rodolfo Garcia-Contreras from UNAM University, Mexico, and Prof. Viviana Sanchez-Torres from Universidad Industrial de Santander, Bucaramanga, Colombia, for their valuable suggestions, comments, and assistance during my study. Also, Prof. Thomas K Wood from Pennsylvania State University, USA, for providing some essential research protocols.

My sincere thanks also go to Imabayashi Ayaka and Tomonori Kai for their kind help in the study. Big thanks to all Maeda lab members, especially Tomonori Kai, Xiao Shui, Yijing Xu, and Sakura Taira, to help me in the lab, administrative, documentation work, and troubles living in Japan. Extreme gratitude to Yamada Michio, one of the most inspiring persons I met in Japan and the owner of my part-time job restaurant. I would also like to thank Shiraishi Yukiko for her helps in hard times. I will never forget the support and friendship of all these people.

In the end, I would like to thank my father, my mother, my sister, and my brothers for their unconditional support and motivation. A very special thanks to Jyoti for her unconditional love and support in this journey. Finally, I thank Lord Vishnu, ‘the source and the consciousness of life on earth, for guiding me at every moment in my life.